Deposition of organic thin films by plasma and photochemical techniques

Graham Robert Eyre

DEPOSITION OF ORGANIC THIN FILMS BY PLASMA AND PHOTOCHEMICAL TECHNIQUES

by

Graham Robert Eyre, B.Sc.(Hons.), MRSC, C.Chem.
(St. Cuthbert's Society)

A thesis submitted
for the Degree of Doctor of Philosophy
to the University of Durham

1990

MEMORANDUM

The work described in this thesis was carried out in the University of Durham between October 1985 and December 1988. It has not been submitted for any other degree, and is the original work of the author except where acknowledged by reference.

EXPERIMENTAL NOTE

The majority of the conclusions reached in this thesis are based on a series of experiments involving single point results - individual experiments were not routinely repeated, for a particular set of conditions. The justification for this is twofold.

Firstly, using the apparatus available it was difficult to exactly reproduce experimental conditions with respect to power input/photon flux versus flow rate. The trends shown by the results were therefore felt to be more important than individual results.

Secondly, where experiments were repeated, and the deposited films subjected to analysis by ESCA / XPS, the individual values achieved for both elemental stoichiometries and other numerical results were typically within $\pm$ 10% - 15% of the mean (taken to be experimental error), and the overall trends were found to be unaffected by the actual spread of results.

This conclusion was previously reached by HS Munro and H Grunwald (J.Polym.Sci., Polym.Chem.Ed., 23, 479 (1985)) for plasma polymers deposited using acrylonitrile, and has been used as the precedent for this work. The repeatability of results for films deposited from fluoroethylenes is dealt with in Chapter Two.

ACKNOWLEDGEMENTS

I would like to gratefully acknowledge the help and encouragement given to me both during my studies at Durham, and afterwards whilst I was still writing up the results. Clare, Clive, Rob (Anyone for Tennis?) Short, Ian, Sonia and Alex (Oh no! I'm skint again!) Shard all provided in-lab entertainment, whilst George, Ray and Gordon kept the whole show on the road. My deepest thanks must go to Vince and Mike for running all those mass spectra for me - often at short notice when they could easily have declined - whilst I'm still not sure how Dr Hugh Munro managed to put up with my antics for so long. A special mention must go to Lynn Williams, who took over as my supervisor after Hugh's departure - a sincere "Thanks" for all your patience!

The money was kindly funded by S.E.R.C. in the form of an I.T. award, at least some of which was spent researching the offerings in the New Inn across the road. Who said beer and bench don't mix!!

ACKNOWLEDGEMENTS

I would like to gratefully acknowledge the help and encouragement given to me both during my studies at Durham, and afterwards whilst I was still writing up the results. Clare, Clive, Rob (Anyone for Tennis?) Short, Ian, Sonia and Alex (Oh no! I'm skint again!) Shard all provided in-lab entertainment, whilst George, Ray and Gordon kept the whole show on the road. My deepest thanks must go to Vince and Mike for running all those mass spectra for me - often at short notice when they could easily have declined - whilst I'm still not sure how Dr Hugh Munro managed to put up with my antics for so long. A special mention must go to Lynn Williams, who took over as my supervisor after Hugh's departure - a sincere "Thanks" for all your patience!

The money was kindly funded by S.E.R.C. in the form of an I.T. award, at least some of which was spent researching the offerings in the New Inn across the road. Who said beer and bench don't mix!!

DEPOSITION OF ORGANIC THIN FILMS BY PLASMA AND PHOTOCHEMICAL TECHNIQUES

by

GRAHAM EYRE

ABSTRACT

The work detailed in this thesis concerns organic thin films synthesised either using R.F. inductively coupled plasmas excited in unsaturated monomers containing either fluorine or a nitrile group, or else irradiating the said monomers in vacuo using ultraviolet light.

The effect of the following parameters on the composition and structure of the resultant films was determined using ESCA/XPS : a) power input to the R.F. plasma system, b) photon flux during UV irradiation, c) monomer type (including structural isomerism), and d) monomer flow rate. Relative system deposition rates were rationalised in terms of Yasuda's parameter, W/FM, which was found to hold true qualitatively, if not quantitatively.

Introduction of halogen vapour to the plasma system in the presence of nitrile monomers physically decreased the glow volume. Analysis by ESCA and UV absorption spectroscopy revealed the presence of ionic halogen species in the resultant films. An overall decrease in deposition rate of the system was also observed. A similar result for the latter was seen for UV irradiation in the presence of iodine. The results were rationalised by assigning a free radical mechanism for both plasma and photochemical film deposition which is inhibited by halogens.

Films formed by irradiation at >200 nm were found to have differing chemical compositions compared to those obtained in the vacuum ultraviolet (<200 nm). This result was attributed to the differing photochemistries occurring in the two wavelength regions. Reference to the gas-phase photochemical literature enabled identification of the likely intermediates and term states involved, including 1,1 and 1,2 molecular elimination from ethylenic monomers in the vacuum UV to give the respective ethynes, together with secondary photolysis products. Consequently a mechanism for surface photopolymerisation was outlined which was compared with that proposed for plasma polymerisation, both of which involve vibrationally excited ground states for the monomers studied.

CONTENTS

CHAPTER ONE

AN INTRODUCTION TO PLASMA POLYMERIZATION

1.1 Introduction

A plasma, by definition, refers to the partially ionised gaseous state consisting of molecules, atoms and ions in both ground and excited (including metastable) states together with electrons, the whole being in overall electrical neutrality.

Historically dating back to the work of Crookes (1879) and Thomson (1897) on the properties of cathode rays emitted from discharge tubes, gas discharges have been studied by scientists ever since. It was Langmuir[1] (1928) who coined the word plasma to denote the state of ionised gases formed in an electrical discharge. Plasma polymerization has since come to mean the process by which (thin) polymeric materials are deposited from the gas phase under the influence of a plasma.

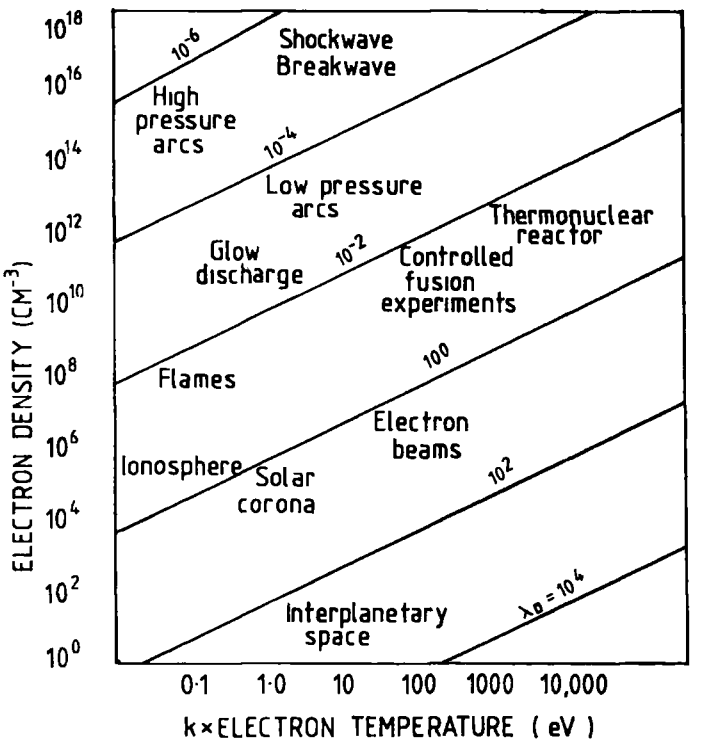

FIGURE 1.1 Plasmas Found in Nature and the Laboratory, Characterised by Their Electron Temperatures and Electron Densities

Numerous types of plasmas exist in nature and/or can be created in the laboratory, each able to be characterised using the criteria of electron temperature and also electron density[2].

Figure 1.1 illustrates a variety of known plasmas. Divided into "cool", non-equilibrium and hot, equilibrium plasmas, it is the former range which encompasses the realm of "polymerising" plasmas (or glow discharges) whilst the latter, characterised by a very high gas temperature which is equated approximately to electron temperature, find uses in the compositional analysis of materials, for example in inductively coupled Plasma-Optical Emission Spectrophotometry (ICP-OES)[3] or inductively coupled Plasma Mass Spectrometry (ICP-MS).

1.2 Fundamental Aspects of Plasmas

A plasma is electrically neutral when the dimensions of the discharge column are significantly greater than the Debye length[2] λ_D.

$$\lambda_D = \left(\frac{E_o kTe}{ne^2}\right)^{1/2}$$

which defines the distance over which a charge imbalance may exist, where

E_o is the permitivity of free space

k is the Boltzmann constant

Te is the electron temperature

n is the electron density

e is the charge on the electron

Ionisation, essential if the discharge is to be initiated and maintained, is caused by collisions between electrons and gas molecules. If the collision is inelastic - i.e. results in the transfer of usable energy from the electron to the molecule - the latter will be ionised or, if insufficient energy is transferred, then a higher energy state of the molecule results in which the excess energy can be stored in rotational, vibrational, and/or electronic excitation, as well as in translational energy. Meanwhile the impacted electron gains its lost kinetic energy from the electric field that exists in the plasma, which accelerates it until the next collision. If the pressure in the system is too high then the distance between collisions (mean free path) is too short, resulting in insufficient energy gain by the electron between collisions to ionise the gas molecules. Conversely, too low a pressure results in too long a mean free path such that few collisions occur and hence they are no longer important. Balancing these two extremes results in a typical operating pressure for plasma polymerization systems of 0.05-10 torr. At charge densities of ca. 10^{10} cm^{-3} this gives a calculated average lifetime of an electron against recombination of about a millisecond[5], with average electron velocities, c, between collisions given by:[6]

$$\bar{c} = \left(\frac{Me^2 E \lambda}{m^3} \right)^{1/4}$$

where M is the mass of the heavier particle

e is the electron charge

E is the electric field

λ is the electron mean free path

m is the electronic mass

The electron energy distribution described in terms of energy input, discharge dimensions and gas pressure lead to the Maxwellian distribution[7] shown in Figure 1.2

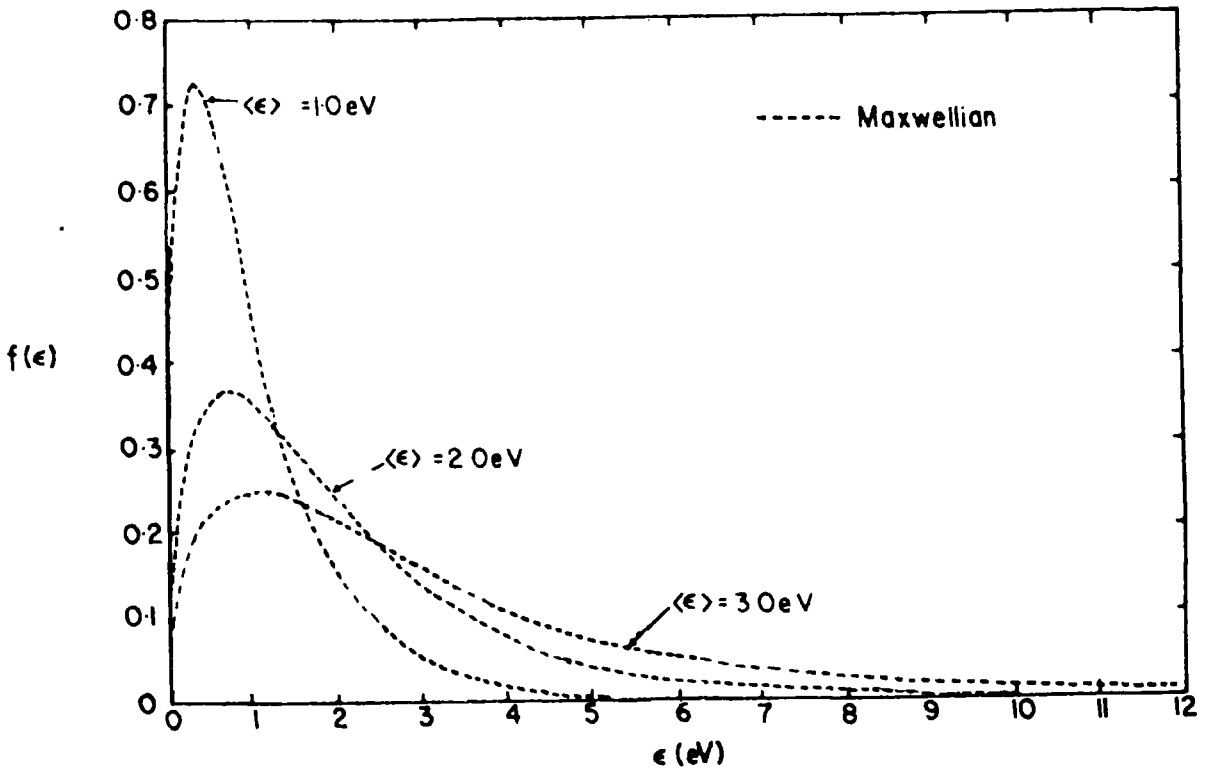

FIGURE 1.2 Maxwellian energy distributions of electrons in an inert gas

Numerical solutions are only possible for simple systems, but can be replaced in practice by experimental analyses using probe measurements[8] and electron sampling[9] (see below). Suffice to say that the electron energy distribution is such that, though extremely high energies can be reached by a few electrons, the average energy is 2-3ev[4], i.e. below the ionisation threshold of most organic molecules, since these are typically $\geq$10+ev. Much of the chemistry involved in plasma chemistry - in particular plasma polymerization - is therefore

likely to be connected with excitation, rather than ionisation, of the molecule and resulting fragmentation mechanisms. However, it is also possible that some molecules undergo excitation and dissociation due to the vacuum ultraviolet (VUV) emission of the gas - e.g. for an argon plasma[10]. Such emissions can be used as the incident radiation in surface modification or photopolymerization.

TABLE 1.1 Energies associated with a glow discharge and some typical bond energies

Energies (eV) associated with a glow discharge:			
Electrons	0-20		
Ions	0-2		
Metastables	0-20		
Visible/UV	3-40		
Bond energies (eV):			
C-H	4.3	C=O	8.0
C-F	4.4	C-N	2.9
C-C	3.4	C=C	6.1

1.2.1 Plasma Diagnostics

As mentioned above, numerical solutions to find the electron temperature - and density - of a plasma can only be applied to simple systems. More complicated situations can only be solved by practical means, i.e. by the use of plasma diagnostic tools and techniques. A short review of various diagnostic techniques has been presented by Till[11]. Briefly, they can be divided into three main groups dependent upon the position of, and interference caused by, the analytical probe; i.e. in situ non-intrusive, in situ intrusive and ex situ[11]. Some of the more popular in situ techniques used over the years have been (Langmuir) probe methods,[8,12] whilst optical analysis of the spectral output of a plasma[13] is perhaps the most non-intrusive method, together with laser/laser fluorescence[14], infrared[15] and other spectroscopic techniques.[16,17,18] Of these latter, the use of a matrix (eg a solid Argon matrix) to trap out and isolate the reactive plasma species before spectroscopic (eg IR) analysis[17] requires a physical sampling of the plasma effluent, as do most mass spectrometric techniques.[18a,b] This sampling is usually achieved by placing a small orifice immediately downstream of the discharge region to create as little disturbance to the plasma as possible. Obviously, this situation is not ideal, for, in addition, the species which are actually sampled will not be exactly those which are generated in the heart of the glow discharge region. Rather, they are more likely to be the related products of the excited state species produced "in glow". This in itself raises an important point with respect to all plasmas, and in particular depositing/polymerising systems - the natures of the excited species produced on the actual glow region ("in glow") are different

from those produced in the non-discharge (or "out of glow") regions. The main reason for this lies in the differences in density, temperature and distribution of energies of the electrons in the two regions; since these in turn cause differences in the degree and nature, of ionisation and other excitation processes. Hence the relaxation processes and - for a plasma depositing/polymerizing system - the molecule fragmentation processes are altered, modifying the deposition mechanism(s). Thus the nature of the polymer films produced is related to, and affected by, the electron energy and density distribution functions. Since both quantities are affected by parameters such as the shape of the plasma reactor, the nature of the discharge means (electrodes, microwave, inductively or capacitively coupled etc), which in their turn affect the nature of the excited species formed and the deposition/polymerization mechanism, it follows that the nature of the polymer films formed - including chemical composition and properties - should also be dependent on these parameters. Any diagnostic insight gained into the true nature of the excited species, in situ and undisturbed, is therefore important in giving the plasma chemist some idea as to the nature of the species actually causing the deposition process - i.e. the polymerization mechanism. The less the diagnostic technique used interferes with the actual plasma and plasma processes, the more accurate the picture gained. Thus techniques such as quadrupolar mass spectrometry[18c], and optical/spectrometric methods are useful since they do not disturb the plasma, whilst more novel methods, such as the use of sound waves,[19a] and wave guides[19b] have also been employed. Theoretical investigation of (less complicated) systems continues.[20]

1.3 Plasma Techniques

There are various separate components which make up a plasma system. Chiefly, these comprise the actual chamber or reaction vessel, together with a suitable pumping system to achieve the required base and operating pressures (these can be as low as 10^{-6} torr up to 10^{-10} torr); a source of electrical power and the means to couple this power to the vacuum system. This is illustrated schematically in Figure 1.3

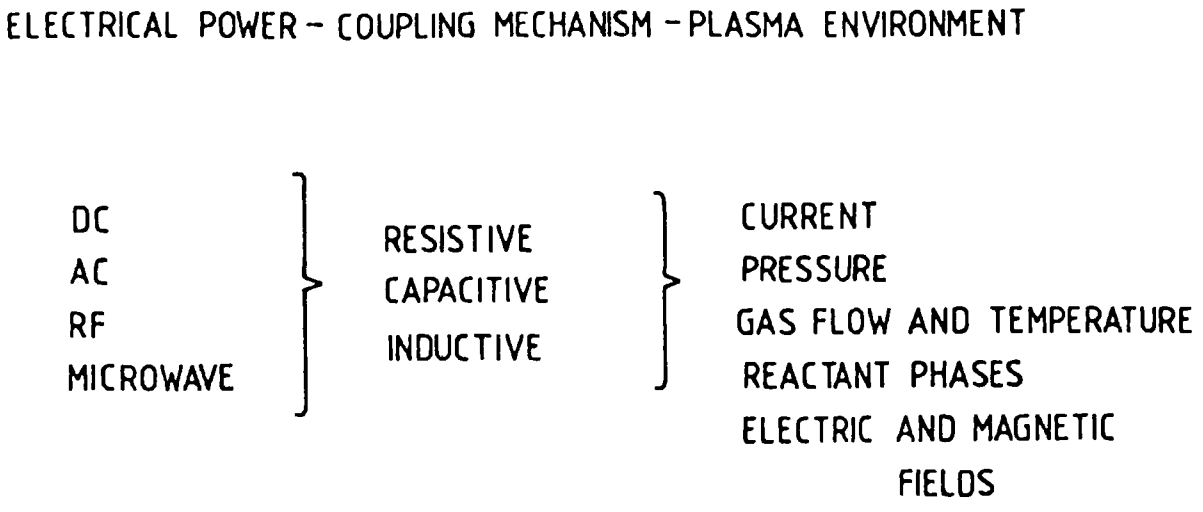

FIGURE 1.3 Elements of a Glow Discharge System

Note that whilst resistive coupling mechanisms, used in dc glow discharges, are examples of direct coupling, capacitive and inductive techniques are examples of indirect coupling means.[21] It is the last of these methods - the inductively coupled plasma - which is used throughout this work, obviating the need for electrodes within the

system (the presence of these disturbs the electron density distribution in the reactor chamber that might otherwise be found if an external power source is used, due to both the physical presence of the electrodes altering the shape of the deposition chamber, and also the creation of a plasma sheath at the interface between the electrode surface and the plasma). Use of an ICP results in deposition occurring throughout the reactor under appropriate plasma conditions (as opposed to on the electrodes in a DC resistively coupled system), with high controllability of the plasma operating parameters. However, indirect coupling mechanisms can only be used with frequencies higher than 1MHz[22]; any lower and direct contact of the electrodes with the plasma is necessary for sufficient energy transfer to take place to sustain the plasma. Many frequencies have been used, from 60Hz (AC) to 13.56MHz (RF)[23], though few studies have been carried out to determine the nature of the product/s of a given plasma with exciting frequency[24]. This is in marked contrast to the investigation of various other parameters, such as (electrical) power, flow rate of monomer, pressure-and-shape-of system etc., and their effect on the plasma sustained and the nature of any product (polymer) formed. Typical operating parameters are given in Table 1.2.

	Power Input	Pressure/torr	Frequency/Hz
DC	10-100V / 1A	0.001-760	-
RF	0.1-150	0.01-1	60Hz-13.56MHz

TABLE 1.2 Typical Discharge Operating Parameters

Attention has so far been focused on DC and ICP discharges; in comparison, microwave discharges are less stable at low pressures. Since an increase in pressure generally leads to an increase in the (monomer) gas temperature, which in its turn can cause decomposition of organic species, microwave techniques are less common in plasma polymerization work. However, all three techniques are commonly used in plasma chemistry - and physics - as a whole.

1.4 Reactive Species in a Plasma

Since a plasma is sustained principally by electron impact excitation, resulting in ionisation and excitation processes, the reactive species found in the plasma state will include ions, neutral species, atoms, metastables and free radicals (all in either their ground or excited states). The latter two species are produced by fragmentation of gas molecules ("monomer" molecules if it is a depositing/polymerising system) in either the ionised, or an excited, state, whilst the concentration of neutrals is quite large (typically $10^{16} cm^{-3}$ at 1 torr[22]). The total numbers of positive and negative species are the same to effect overall neutrality, and are typically some 4-6 orders of magnitude less than the number of neutrals[25].

The above situation is further complicated by the presence of accelerated electrons, forming a highly energetic "soup" capable of achieving reaction activation energies not normally achievable by conventional (thermal). The resulting reaction mechanisms enable organic compounds not normally thought of as monomers for polymerization (eg benzene and other aromatic compounds) to be plasma

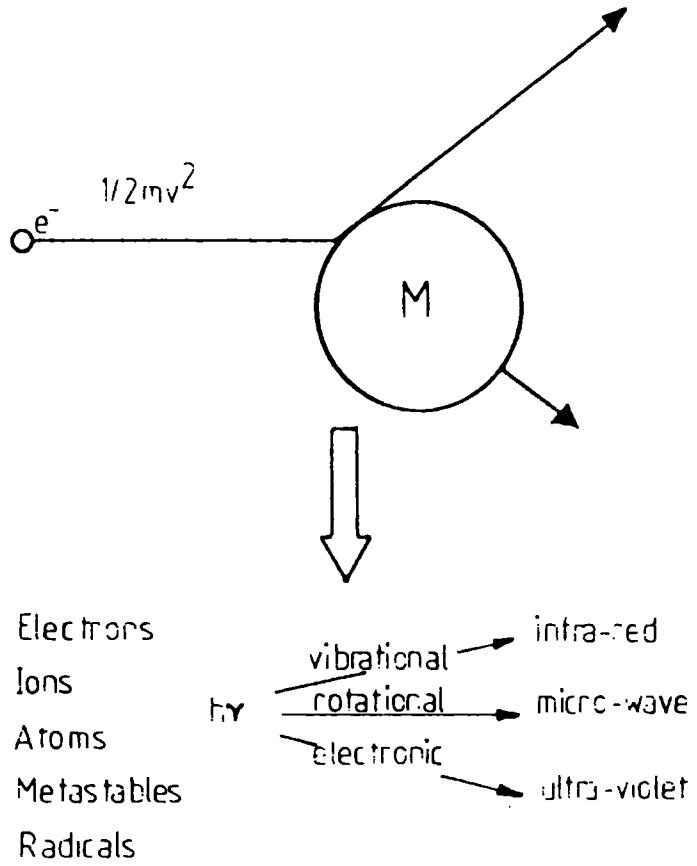

FIGURE 1.4 Collision Processes in a Plasma

deposited as organic thin films. These films - alias plasma polymers - are a product of the highly reactive intermediates formed in the plasma gaseous state, though the actual mechanisms of deposition can be quite complex, often involving extensive molecular rearrangements such as those shown in perfluoroaromatic compounds.[26] Overall, the resultant films can have structures very similar to conventional polymers obtained from, for example, vinylic compounds (conventional monomers) but are more likely to be highly crosslinked due to free radical reactions. The actual nature of the film will depend on the nature of

the monomer used together with the reactor system and the experimental parameters selected. An example of this occurs with fluoroethylenes which, as shown in Chapter 2, possess a number of CF_3 and CF_2 functionalities together with quaternary carbon hydrocarbon environments even when the original compounds contained none of these.

1.4.1 Plasma Reactions

In general terms, typical reactions which occur in a plasma involve the following:[27]

(a) Generation of reactive species

(b) Isomerization

(c) Oligermerization and dimerization

(d) Elimination

Study of these reactions falls within the realm of plasma diagnostics described earlier. In general, most plasma reactions can be described as:-

$$M \xrightarrow{\text{Excitation}} M^* \xrightarrow{\text{Bond Breakage}} I \xrightarrow{\text{Stabilization}} \text{Product}$$

Where M* is the excited neutral or ionic species and I is the neutral or ionic intermediate.[28]

1.5 Plasma Applications

Concentrating on the "cool" (as opposed to "hot") plasma, there are two main areas in which applications have been developed - surface modification of surfaces (especially polymers), and plasma synthesis techniques (again, mainly of polymers).

1.5.1 Surface Modification

(a) Direct Modification

Direct modification of surfaces using a plasma generally utilises a non-polymerizable gas (such as fluorine or oxygen) in order to alter the properties of the surface. The first technique of any note is that of surface grafting,[29] in which the polymer surface is exposed to a plasma such that activation of the surface creates radical sites. This in turn initiates a conventional (free radical) polymerization process at the surface when the graft monomer is introduced into the reactor in the absence of a plasma. Alternatively, a technique known as CASING - crosslinking by activated species of inert gases - has been used to improve adhesive bonding,[30] wettability[31] and printing of polymers. Here the modification is effected by direct and radiative energy transfer from plasmas excited in inert gases.

Surface modification by plasma etching has been suggested to be of great importance, particularly in the microelectronics industry[32-38]. Fluorocarbon gases are used to fluorinate surfaces[32-33] (possibly thought to be via gas phase formation of highly reactive fluoride ions), whilst plasma oxidation can be used to create low energy, hydrophilic surfaces on, for example, contact lenses, thus making them more comfortable to wear.[39] This occurs by introducing carbon-oxygen functionalities into the surface which being hydrophilic themselves, gives the surface its overall "water-loving" property. Other functionalities and hence properties, can be introduced into similar or other surfaces simply by replacing the oxygen in the oxidation chamber by any suitable etchant desired, such as sulphur dioxide, SO_2[40] or even other organic compounds.[41] The area continues

to attract interest, eg in review form,[42] whilst expanding to include modification of "unconventional" polymer surfaces, such as fluororesin composites,[43] amorphous carbon, diamond and graphite films,[44] and liquids.[45]

(b) Indirect Modification

In addition to the above techniques of direct surface modification, the intrinsic properties and characteristics of plasma polymers have been used in order to modify the overall behaviour of a surface by coating it with a thin plasma polymer film. These properties derive from the fact that film deposition is a gas-phase process without the need for solvent evaporation - which leads, in general, to a "pinhole-free", three-dimensional network that is usually highly crosslinked and has no distinct repeat unit as found in conventional polymers. Hence possible uses have included, amongst others[35], as protective coatings[49,50], whilst other applications are dealt with later on - including surface modification of carbon fibres and composites, both of which are becoming increasingly important in industry (modification often improves the physical properties of the material). Thus, for example, deposition of an acrylonitrile plasma polymer on a carbon fibre surface was found by Dagli and Sung[46] to give a substantial improvement in both interlaminar shear and flexual strength. Other work has continued on blocks[48] as well as fibres.[47]

1.5.2 Polymer Synthesis

This has been a particularly active area of interest, especially with regard to organic and organometallic compounds, since the

processes offer advantages over conventional polymer synthesis. These can be in the form of the type of "monomer" used - for example benzene, of no practical importance for conventional polymerization techniques and reactions due to the aromatic nature of its unsaturated carbon - carbon bonds, is just as easily "polymerised" in a plasma as is the more conventional monomer ethylene - to the incorporation of other functionalities (such as fluorine groups of organometallics) to alter the physical (especially electrical) and chemical properties of the film/polymer deposited/formed. It is this area of synthesis and applications that is explored in a major part of this work and which is therefore considered next.

1.6 Plasma Polymerization

As stated at the beginning of this Chapter, a plasma is a gaseous state consisting of ions and excited states together with electrons, the whole being in overall electrical neutrality.

If a plasma is induced in the pure vapour of a compound then the formation of ions and other excited species of that compound results. These and other species formed from various fragmentation pathways may lead to deposition of thin films from the gas phase, commonly known as plasma polymers. Note that, (i) though most often deposited as thin film coverings on substrates, such as gold or aluminium, this need not always be the case - experimental conditions may result in the formation of "free standing" polymer that is not attached to the substrate (this has been noted by both Yasuda and Till and was also observed by the author for the plasma polymerization of 1,1-difluoroethylene, in which "strands" of polymer were deposited

throughout the reactor and not just on the reactor walls and substrates placed within the plasma chamber) or even oils rather than solids; (ii) though called a "polymer", the structure of the deposited material may bear little resemblance to any polymer synthesised by so called conventional techniques (such as radical, cationic and anionic solution-state polymerization) - many plasma polymers are in fact highly cross-linked networks with no distinct repeat unit such as would be found in polyethylene or polystyrene; hence the term plasma deposition can be, and often is, substituted for plasma polymerization; (iii) the range of materials that can be deposited can range from organic, through organometallic to inorganic compounds, with systems giving rise to deposition from many compounds not normally regarded as conventional monomers (for example benzene, tetramethyltin and silanes). The realm of inorganic depositions, though of increasing importance in industry is outside the scope of this work, which concentrates on plasma polymeric films deposited from vinylic systems containing cyano functional groups, in particular 2-chloroacrylonitrile and allyl cyanide. First, though it is useful to survey the field of organic plasma polymerization as a whole.

1.6.1 Organometallic Systems

Until 1986, much of the work in this area had been dominated by Suhr[22] and his co-workers. Overall, successful depositing systems were achieved by avoiding high electron temperatures and elevated temperatures, since these cause damage to the organometallic molecule. Further, by controlling and varying the metal content of the resultant films, substantial changes in conductivity could be achieved.

This is particularly true for films deposited from tetramethyltin,[51,52] which have been found to have a reaction time of only a few seconds to changes in electrical resistance, and hence conductivity. This can be induced by exposure to propane, thus enabling their use as gas sensors.[53] The converse behaviour is true of organo-gold compounds, where it is the electrical resistivity which is the important controllable property.[53] Interest in this particular area has blossomed,[54,59] with optical emission spectroscopy being used as a diagnostic tool to monitor the plasma.[60,61] Indeed, interest has increased in general,[62,65] with other metals incorporated including mercury,[66] iron, (both in the form of ferrocene[67] and also iron carbonyl[68]), palladium and nickel.[65] Potential use of such compounds include the idea of using Bu_3Sn methacrylate as an antifouling pesticidal coating.[69]

It should be noted that, for the majority of these polymer films, the metal atoms can be incorporated as grains dispersed in a "matrix" of organic polymer.[70] This could result in a substantial amount of metal incorporation uniformly distributed throughout the film, depending on experimental conditions. An alternative, non-uniform case is aggregation of metal at the surface such that the top layers of film are no longer representative of the bulk.[59] This affects the application here of some analytical techniques - eg IR spectroscopy would probably not pick up such an imbalance in metal distribution in the film, especially if the overall metal content remains more or less constant, whereas a surface sensitive tool such as XPS/ESCA should be ideal in these circumstances. Further ways in which the metal atoms are incorporated into the polymer films are as metal clusters,[54,68] or

else by actually being bonded into the film by a metal-carbon bond, rather than by simple physical incorporation (Till obtained some evidence from mass spectrometry studies to suggest that this was the case for the incorporation of mercury into PFB films).[71]

1.6.2 Organic Systems

The remaining organic polymerizing systems can be split into the following subject areas, namely pure hydrocarbons, hydrocarbons with functionalities other than fluorine, and fluorocarbons :

(a) Hydrocarbons

Earlier reviews in this area, and of plasma polymers in general, have been presented by Yasuda,[72-75] Shen and Bell[76,77] et al[35,78-82] whilst the topic continues to attract attention[83-85]. Areas of interest include biomedical applications,[86] vacuum lithography,[87] and catalysis in plasma polymerization.[88] Many of these works attempt to explain the possible mechanisms of plasma deposition, whilst others concentrate more on the characterisation and characteristics of the polymers formed, with a view to potential applications. Whilst some authors have concentrated on more conventional "monomers",[89-97] others have branched out into the field of aromatic compounds.[98-103] In addition, work has focused on trying to elucidate and understand the influence of the various experimental parameters (such as the role of the elemental composition of the starting monomer,[104] the influence of different reactor designs[105] and energy coupling mechanisms[96,106] - including the effect of this on the power input to the system,[107] - and the role of different gases in the system, whether polymerizable in

their own right, or non-polymerizable such as argon).[108,109] Other studies have investigated the effect of outside influences on the system, such as the effect of externally induced magnetic fields,[110] and of ion bombardment of the substrate.[111] All these works have investigated aspects of both the nature of the polymer films deposited (both in terms of physical properties, such as conductivity of the surface, and chemical structure and bonding) and the deposition/polymerization species and mechanisms.

(b) Hydrocarbons with Functionalities other than Fluorine

There is a scarcity of literature in this particular branch of potential monomers, the majority of work being carried out using either compounds with oxygen functionalities already in situ (such as methyl methacrylate[112] or allyl alcohol[113]), or else nitrogen. The latter has been shown to be incorporated into thin films by polymerising a monomer such as ethylene, in the presence of nitrogen gas.[115] Though at first sight this might seem surprising, it is no more so than the incorporation of gold or mercury atoms in a film surface when they are introduced to a plasma system in their atomic vapour form. The resultant incorporation can alter physical properties of the film, such as the dielectric constant and breakdown strength.[115] An alternative to merely physical incorporation of nitrogen is the existence of nitrogen functionalities within the monomer leading to chemical incorporation of nitrogen in the plasma polymer films. Thus allylamine has been used to synthesise reverse osmosis membranes[115] and other films,[113] as have pyrrole and benzylamine.[116] However, the incorporation of such specific functionalities into a plasma polymer is

generally considered to be difficult - eg acid fuctionalities have a tendency to eliminate as CO_2. The important factors here are the operating conditions and the nature of the monomer. However, a number of studies have concentrated on organic compounds containing cyano/nitrile groups[116-122] - including acrylonitrile - and it is to this family of potential monomers that this work is mainly devoted.

Finally in this section, it should be noted that there is no reason why any other functionality should not be directly incorporated into a plasma polymer system, providing that a suitable choice of starting material is made. Thus, for example, thiophene,[116] iodomethane[123] and allyl iodide[124] have all been studied.

(c) Fluorocarbons

Study of these compounds in a plasma and their resultant polymers account for a large proportion of the current literature. Subdivided according to monomer type, saturated fluorocarbons - especially fluoromethanes - are perhaps more useful as etchants and for surface fluorinating processes (see earlier section on surface modification) rather than as monomers for plasma polymerization.[125-132] This is in marked contrast to the fluoroethylenes[133] - especially tetrafluoroethylene[134] - which have attracted a high degree of interest, combining as they do the functionality of carbon-fluorine bonds together with unsaturation. The third class of fluorocarbons are the fluoroaromatics, which - perhaps unlike their pure hydrocarbon analogues - have also been extensively investigated, especially by Munro and Till.[135] For a fuller description of fluorocarbon plasma polymers as a whole, and of perfluorobenzenes in particular, references

135 and 136 which give a view of the field in general and of perfluoroaromatics in particular.[135]

1.7 Plasma Deposition Mechanisms

Although the formation of polymers and other thin films by plasma techniques has been known for years,[137] the detailed mechanisms involved are still not fully understood. Classified by Yasuda into 'plasma-induced' polymerization and 'plasma-state' polymerization,[138] the plasma processes in the first case involve initiation of a conventional polymerization mechanism in compounds containing polymerizable structures - such as vinylic bonds - (e.g. by creation in the plasma state of free radicals which then initiate a conventional, chain growth radical mechanism on the substrate surface); whilst in the second, the processes - and excited species - involved in the polymerization/deposition of the (polymer) film are anything but conventional, possibly involving a variety of excited states, radicals (including diradicals) and possibly even ions. Note that both sets of processes can occur simultaneously in any given plasma system.[139] The final product is determined by the competing deposition processes, together with polymer ablation.

The overall schematic mechanism of plasma polymerization has been termed CAP - Competitive Ablation and Polymerization[139] (see Figure 1.5). Thus, in plasma etching, it is the ablation processes which dominate, whereas in depositing systems it is the polymerization processes. This can be illustrated practically in the case of carbon tetrafluoride, CF_4, which is believed to have an abundance of highly reactive fluoride species created in its plasma, and hence is of use as

an etchant,[140] whereas in fluoroethylenes the vinylic nature of the compound might be expected to dominate. This seems to be the case, such that plasma polymerised films deposit rapidly, the analysis of which by ESCA (Electron Spectroscopy for Chemical Analysis) reveals a stoichiometry consistent with the elimination of hydrogen fluoride.[141]

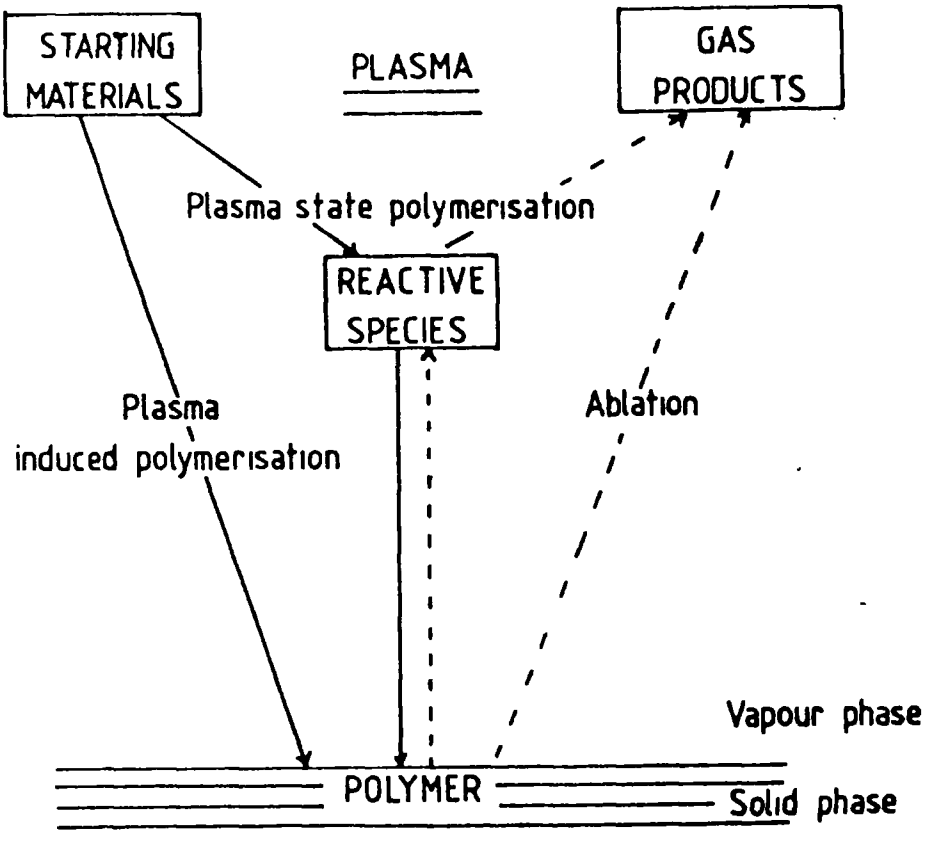

FIGURE 1.5 Competitive ablation and polymerization in glow discharge polymerization

This was found, by the author, for the three monomers vinylidene fluoride (CH_2=CHF), 1,1-difluoroethylene (CH_2=CF_2) and trifluoroethylene, 1,1-difluoroethylene in particular depositing so rapidly that strand-like samples of the polymer were physically collectable in addition to the usual thin film deposited on a substrate (aluminium foil). This suggests that the dominant species in the plasma are <u>not</u> fluoride ions, but rather that the fluorine is perhaps eliminated molecularly, either by 1,1 or 1,2 molecular elimination of a combination of H_2, HF and F_2. If this is so, then it would suggest the utilisation of Rydberg states as well as valence shell orbitals in the excited states. Both can also result in scission of the carbon - fluorine bond, and hence the possibility of (etching) fluoride ions dominating in the gas phase (NB the C-F bond has an dissociation energy of 4.4ev;[142] many of the electrons available for impact excitation have somewhat larger energies than this (see Figure 1.2)).

Thus, possible mechanisms for dissociation of vinylic compounds in general are via 1) electron impact excitation of a π electron into a π^* or Rydberg orbital, 2) the capture of an incident electron into a low lying orbital. Both will tend to give rise to unimolecular decomposition of the excited states/radical ions formed.[143,144] In the case of electron capture, if the carbon-carbon double bond is substituted - as is the case in both chloro[143] and fluoroethylenes[144] -then chloride and fluoride ions respectively will be formed. At first sight, this might seem to rule this process out as a possible route to plasma deposition of fluoroethylenes, since an abundance of fluoride ions will give rise to an etching rather than a polymerising system. However, for chlorine-containing molecules, it is known that the

chloride ion yield is highest when the carbon-chloride bond lies out of the nodal plane of the ii system, since the temporary anion formed by electron attachment is then found to be in a repulsive state such that chloride ion appears with a very large kinetic energy.[143] However, in chloroethylenes (and chlorobenzenes), the C-Cl bond does lie on the nodal plane. Thus, symmetry of the ground states of the potential fragments of dissociation from the repulsive state no longer permit their formation adiabatically by direct dissociation of the initial anion. Instead, the ground state fragment symmetry necessitates a predissociation mechanism which distorts the anion from its original $^{1}\pi^{*}$) symmetry.[143] Any excess energy of the system is channelled primarily into the various vibrational modes of the organic moiety such that the resulting fragment is released with less kinetic energy than if direct dissociation had taken place. This is similarly so with fluoroethylenes,[144] where the formation of fluoride ion is formed, but not usually as the dominant channel; rather the formation is preferred of species such as $C{=}CH_2^-$, $C{=}CHF^-$, $C{=}CF_2^-$ and FHF^-, all five resulting from dissociation from the resonance. Note that this is equivalent to 1,1 molecular elimination - had the dissociation process involved 1,2 elimination (either molecularly or its step-wise equivalent) then the resultant biradical would be of the form $^{\cdot}C{=}C^{\cdot}$, which would preferentially rearrange to form the acetylenic compound rather than undergo radical recombination reactions. Indeed, Yasuda et al[139] have often observed such acetylenes as by-products of polymerizing systems, and consider their formation to be an integral and important part of the overall plasma deposition mechanism.

Overall, such mechanisms - whether unimolecular dissociation from excited states or radical anions - could certainly account for at least part of the fluorine loss observed in the fluoroethylenes, even if they may not perhaps be the dominant pathways. This contrasts with the observations for electron capture in acrylonitrile and benzonitrile, where it was found for both compounds that the energetically most favourable dissociation channel is cleavage of the C-CN carbon carbon bond to give $R^{\cdot} + CN^{-}$ [145]. The electron capture again occurs into a molecular orbital with π^{*} character. However, this also appears to be true for saturated nitriles, which similarly dissociate to give the cyanide ion.[145] In all the nitrile compounds studied, the electron cross-sections were unusually low; further, since there was virtually no kinetic energy release in the resultant fragments which, apart from CN^{-}, were observed to include (M-H) and ($M-H_2$) anions. This would tend to support the idea that a predissociation, rather than direct dissociation mechanism occurs.

The above discussion illustrates the possible role of symmetry control in bond cleavage processes in unsaturated compounds - although there is no reason why this cannot be extended to organic molecules in general. Similarly, though the above studies were carried out under non-plasma conditions, there is no reason why symmetry could not play a role in plasma chemistry, and in plasma polymerization in particular, since most dissociation mechanisms in the excited state are influenced by the symmetry of the excited state concerned as well as thermochemical considerations (for example activation energy of the transition state involved, bond dissociation energies etc). This concept of symmetry control is, therefore, bound up not only in

dissociative electron attachment mechanisms, but also in other fragmentation mechanisms involving excited states - including those accessed by electron impact excitation in the plasma state, and by photonic excitation in photochemistry. Further, since symmetry is dependent on the excited state involved,[143] it is therefore dependent on the nature of the excited molecule - i.e. whether they are Rydberg or valence-bond in character. This aspect is particularly true in photochemical systems, which have been extensively studied in the literature (see Chapter 5). Since it is known that organic thin films can be deposited using ultra-violet photochemical techniques, and that these films can be very similar in nature to those deposited in a plasma system,[125] we can conclude that the mechanisms and excited states involved in both processes are not dissimilar. Hence, if symmetry aspects and the nature of the (excited state) orbitals occupied is important in photochemical deposition, there is no reason to suppose that they might not be in plasma polymerization mechanisms as well.

The idea of a reaction mechanism - or pathway - including not only the transition state(s) involved but also the fragmentation paths to produce the species actually responsible for film deposition is not new. Yasuda[139], amongst others, has suggested the importance of biradicals in the actual polymerization growth mechanism. It is therefore worth noting that dissociative electron attachment and molecular eliminations from both valence and Rydberg orbitals[147] can give rise to the formation of biradicals, as well as successive (free radical) fragmentation of two bonds on the same carbon atom (e.g. CH_4 --> CH_2+2H) and so cannot be entirely ruled out as dissociation

mechanisms in the plasma. That free radicals are important in plasma polymerization (although not essential for a plasma itself to exist) has been shown by numerous workers, among them Munro and Grunwald,[121] who demonstrated that the introduction of iodine - a known free radical scavenger - into a depositing acrylonitrile plasma system caused an immediate and large drop in the observable glow discharge volume. On analysis, the substrates which were placed outside of the glow volume were found to have little or no film deposition on them, whilst those placed inside were found to be rich in iodine (which was also found to have effectively "doped" the system and altered its conductivity from that of an insulator almost to that of a semiconductor).

Further evidence for the role of radicals can be obtained by ESCA analysis of fluoropolymers[109] which reveal that, even for those systems which do not contain fluorine other than singly bonded to carbon, it is possible to obtain CF_2 and CF_3 functionalities. The latter are particularly to be found in plasma polymerised fluoroethylenes and perfluoroaromatics, and must involve free radical combination of fluorine with, say, CF_2 biradicals. Such biradicals are therefore important as building blocks in the growth of plasma polymer films. Whilst it is possible that plasma-induced polymerization may, in fact, be a cause of plasma deposition[139] one might also suggest that a direct step growth (rather than a chain growth) mechanism is responsible for plasma deposition. In theory, the latter requires only one activated species to cause 100% conversion of monomer to polymer - although, in practice, somewhat more than a single initiating species is required due to the possibility of termination steps. Nevertheless, the majority of molecules present under this mechanism will <u>not</u> have been activated.

In a typical plasma, the electron density is sufficiently high to ensure that most molecules <u>will</u> undergo collisional activation of some sort. Thus, a primary requirement of step-growth polymerization - the separate initiation of each step of polymerization - is satisfied. A way in which biradicals promote step-growth, whereas "single" radicals such as CH_3 cannot, has been suggested schematically by Yasuda[148] (see Figure 1.6) a simplified version of which was first proposed by Yasuda and Tsu[149] in 1978 (a fuller discussion can be found in reference 139).

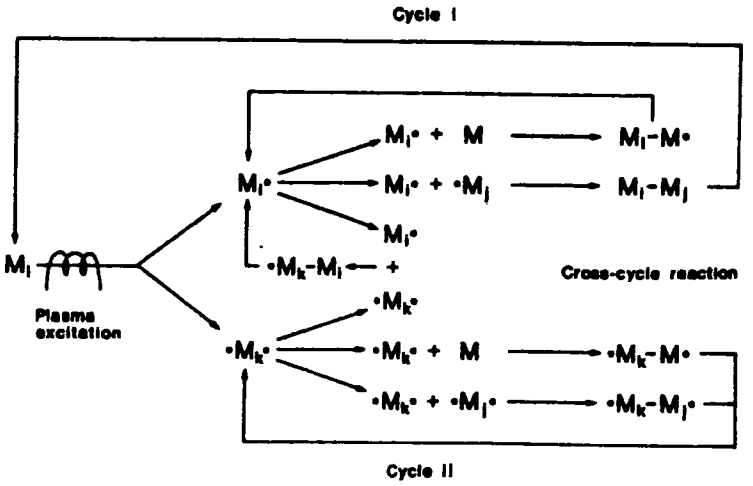

<u>FIGURE 1.6</u> Proposed Rapid Step Growth Mechanism For Plasma Polymerization

Figure 1.6 shows that after initial excitation of the species M, either to form the excited species M* or more particularly to generate the biradical $:M_k$, the propagation mechanism is postulated to be mainly free radical in nature (M:* itself becomes the analogous free radical M). The role of the biradicals can easily be seen - note that, unlike single radical recombination, the addition of a biradical does not quench the radical nature of the resultant product species. If a termination step occurs then further polymer growth can only occur by subsequent excitation of the newly formed (and quenched) species by the plasma. However, biradicals need not be limited to merely propagating chain length, since processing two active sizes makes them ideal for bridging chains. This could equally be true of any species M:.

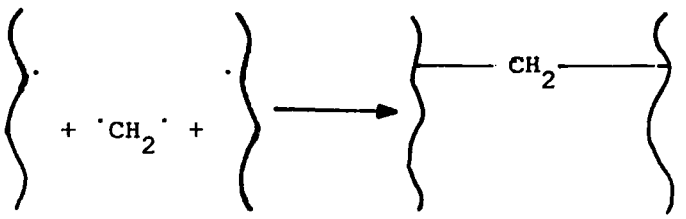

An important bulk property of plasma polymers is that of a large quantity of free radicals trapped within the polymer matrix during film formation. This is due to a steady state concentration of activated species not being reached in the plasma, such that those quenched in film formation are not balanced by the quantity formed. Thus the growing film incorporates one part of the activated radical (or diradical) so rapidly that it can be trapped within the cross-linked matrix before its active site has a chance to be quenched by another incoming radical. Being reactive in nature, the presence of large

numbers of such trapped species in the film may affect the performance in particular applications, especially as any subsequent quenching (for example by atmospheric oxygen molecules) will tend to modify the film's properties, possibly even nullifying its usefulness. Evidence for the presence of radicals in the film surface comes from Electron Spin Resonance Spectroscopy (ESR) which has shown that the quantity of free radicals present is related to the chemical structure of the film (saturated aliphatic hydrocarbons yield the lowest, highly unsaturated monomers the highest, level of trapped free radicals within polymer films[149]).

Throughout the above discussion, reference has been made mainly to radicals, rarely to anions, and not at all to cations. Yet, by definition, these latter exist in sufficient abundance to affect the chemistry occurring both in the gas phase and also on the polymer surface. Clark et al proposed that radical cations were responsible for polymer formation, particularly in the case of the fluoro-ethylenes.[141] However, the formation of organic thin films by irradiation with ultra-violet light in similar vacuum systems[146] has shown that it is possible to obtain chemical compositions akin to those obtained by plasma polymerization methods for the same starting compound,[146,151] even if the deposition rates of the photochemical process (known as surface photopolymerization) are markedly slower. The absence of electrons in such a photochemical system, apart from the few, low energy electrons that might be produced by photoelectric means from the aluminium substrates used, means that energy is imparted to the system by incident photons rather than by highly energetic electron impact excitation. At the wavelengths used (principally 174 nm and

254 nm)[146] there was insufficient energy available to photoionize the monomers (many organic molecules typically have ionization energies in excess of 8-10ev[152], an equivalent photon energy to which is only achieved below 150 nm); hence radical cations were not present in the system and do not have to be invoked in the surface photopolymerization mechanism. In view of this evidence, it is quite possible that radical cations play little role in plasma polymerization either, although important to maintaining the plasma state. Furthermore, a recent study has shown that, far from acting as polymerising species, incident ions at a polymerising surface can actually act in favour of the ablative part of the CAP mechanism,[153] a situation somewhat similar to the effect of fluoride ion on fluorocarbon etching systems.[140]

The above view is somewhat counterbalanced by the work of Kobayashi and co-workers, who claim that, in the plasma polymerization of a mixture of methane, ethylene and hydrogen gas ionic species <u>are</u> important for film formation, whilst the role of single (methyl) radicals appears to be promotion of the growth of diamond particles in the film. This idea of nucleation, or cluster, growth has also been noted in other plasma systems, including organometallics.

Overall, current thinking emphasises the role of all activated species in sustaining the plasma state, but the importance of radicals - especially biradicals - in plasma polymerization in particular, with the emphasis on a step growth, rather than chain growth, mechanism.

1.8 SUMMARY

This chapter has attempted to introduce the reader to the concept of a plasma, and to the reactive species that exist in it. In particular, plasma technology - whether used for surface modification or plasma synthesis - is increasing in importance. Where organic thin films are produced by plasma polymerization techniques, it has been shown that the nature of the film - both physical and chemical - depends on the type of starting material and reactor system used, as well as experimental parameters such as the power (W) and flow rate (F) of monomer delivered to the system. The latter are often expressed in terms of Yasuda's parameter W/FM,[139] where M is the molecular weight of the monomer used, in an attempt to correlate the processes occurring within a glow discharge system. Such attempts are a part of an overall aim to understand the deposition processes - and hence mechanisms - involved. If the "how" and "why" of the process can be understood then perhaps it can be more accurately controlled. The latter would be of interest to industry in general - and to electronics in particular. Therefore this work is devoted to the problem of probing the processes that occur in thin film deposition by the study of organic thin films deposited under different experimental conditions.

CHAPTER 2

PLASMA POLYMERISATION OF SOME FLUOROETHYLENES

2.1 Introduction

The range of organic compounds deposited by plasma or glow discharge means is considerable, varying from "traditional" monomers such as ethylene or styrene, which can be polymerized by conventional (i.e. non-plasma) techniques - to non-aromatic,[1] and aromatic hydrocarbons,[2] heteromatics,[3] organometallics [4] and fluorocarbons.[5] The deposited films are usually highly cross-linked networks lacking basic repeat units found in eg polystyrene or polyethylene, but can often have superior physical and chemical properties compared to thin films formed by other methods.[6] In particular, since the process involves deposition directly from the gas phase onto (normally) a substrate, with no solvent involvement, the result is a thin, pinhole free, film typically hundreds of Angstroms thick. The high degree of crosslinking usually means that it is insoluble in most conventional solvents. However, one possible drawback is that such polymers can exhibit stress cracking properties - especially if the film is very thick - when exposed to oxygen or moisture uptake from the atmosphere. Despite this, plasma polymerization - as well as plasma etching - techniques have become of increasing importance in such areas of industry as electronics. Surveys of the current chemical literature usually reveal increasing uses of plasma polymer films, whether as membranes for osmosis or gas separation,[7] in protective coatings[8] or biomedical applications,[9] or as conducting or other films within electronics.[10] However, of all the potential monomers studied, fluorocarbons have attracted perhaps the most attention,[5] whilst the area of nitrile containing compounds - including acrylonitrile[11] - has shown an increase in recent years.

2.2 Plasma Fluoropolymers

The first practical and industrial application of fluorinated organic compounds was the introduction of fluoroderivatives such as methane and ethane into refrigerants.[12] Since then the increasing ease of fluorocarbon synthesis has meant that such materials have spread into many diverse areas of application such as lubricants, water and oil repellants, together with use in textile finishes, adhesives, fire extinguishers, anaesthetics and anti-inflammatory drugs, though all these later areas are of lesser importance than the original. Many such applications result from the surface properties exhibited by fluoropolymers, i.e. their very low surface free energy and low coefficients of friction. This can be seen, for example, by the use of polytetra-fluoroethylene (PTFE) as non-stick coatings in saucepans.

Since plasma fluoropolymers also exhibit the well known feature of being pinhole free uniformly thin films exhibiting superior physical, chemical, electrical and mechanical properties,[13] the glow discharge synthesis of such materials has been a particularly active area of research, especially with regard to applications as membranes.[7] However, the highly cross-linked nature of many of the resultant films - and in particular their insolubility in the usual range of organic solvents - has meant that bulk sample analytical techniques are difficult. Rather, surface-sensitive techniques such as SIMS[5b] and - in particular - ESCA have increasingly come into use, the latter proving to be an ideal spectroscopic tool for investigating structure and bonding in plasma polymerization in general.[14]

The use of ESCA to study fluorocarbon plasma polymers allows compositional information to be obtained from the C1s spectrum which

can then be cross-referenced to the atomic ratios of carbon to fluorine obtained as a whole.[15] Hence, the accuracy of the assignments made in the C1s envelope can be checked. A fuller account of the general application of ESCA to structure and bonding in plasma polymer surfaces, including fluoropolymers, has been presented by Shuttleworth,[15] who, in conjunction with Clark,[16] helped pioneer the application of ESCA to the study of fluoroethylenes in general, and difluoroethylene in particular. It is this work that has been used as a basis for the first part of this chapter, the range of fluoroethylenes being extended to include trifluoroethylene, $CHF=CF_2$, and vinylidene fluoride, $CH_2=CHF$ as well as the 1,1-difluoroethylene previously studied. The results form a part of the basis of discussion on plasma polymerization mechanisms found in Chapter One.

2.3 Experimental

2.3.1 Plasma Polymerisation

Plasma polymerization was carried out in a tubular reactor, Figure 2.1. Aluminium substrates were placed at various distances along a glass slide, which was then inserted down the length of the reactor such that the latter was roughly split it into an upper and a lower half. The reactor comprised the central part of a glass vacuum system. Flanged joints and the cold trap were sealed with Viton O rings whilst all other connections were made with Cajon ultra torr couplings on ground glass. Vacuum taps were sealed with PTFE stoppers.

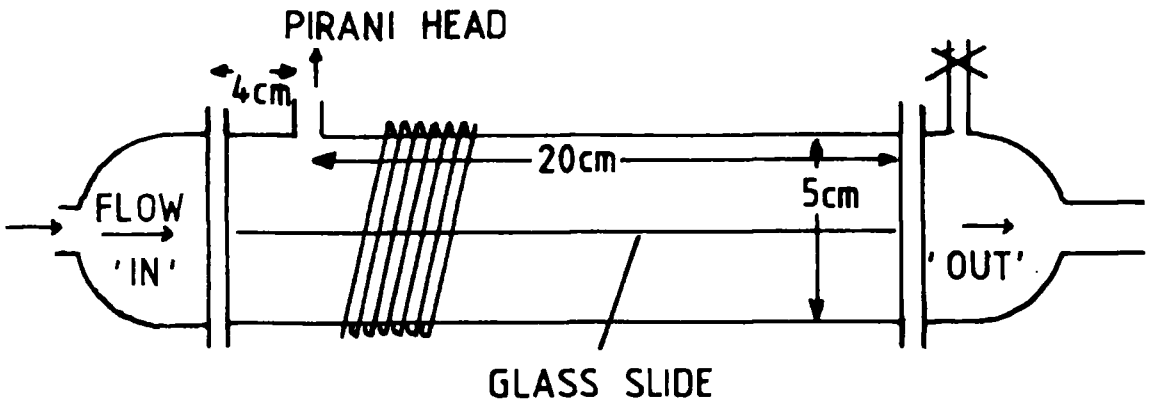

FIGURE 2.1 Deposition Chamber

Figure 2.2 schematically illustrates the experimental configuration, which was evacuated using an Edwards ED2M2 $2ls^{-1}$ or $8ls^{-1}$ mechanical rotary pump. The cold trap was filled with liquid nitrogen in order to trap out any reactive/waste products before they reached the pump and prevent any back-streaming of pump oil into the reaction chamber. In addition, it acted as a pump in its own right, the whole apparatus giving typical base pressures of circa 10^{-2}mb. Pressure measurements were made using a Pirani thermocouple gauge.

The reaction chamber was cleaned out before each set of experiments, and was thoroughly scrubbed with a hard nylon brush using acetone, detergent and Ajax powder, washed thoroughly with both water and acetone and then baked in an oven to dry. The needle valve assembly was similarly thoroughly cleaned before the use of a different monomer, to prevent contamination between monomer systems.

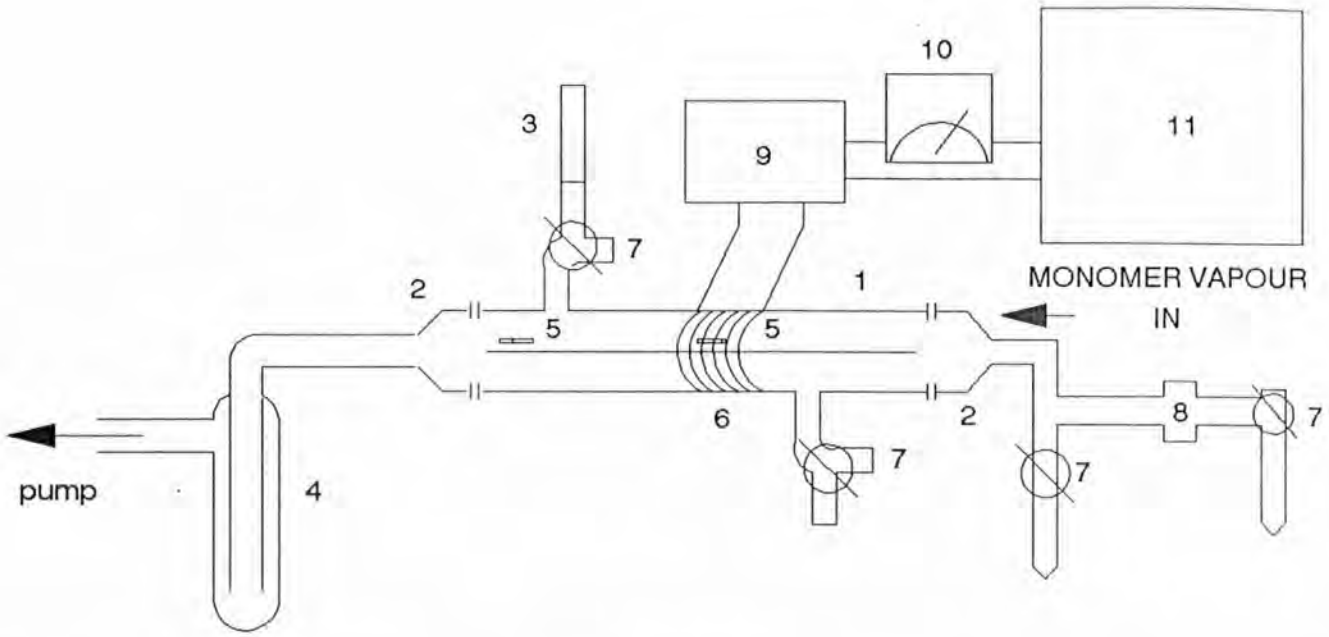

KEY :

1 REACTOR	5 SUBSTRATE	9 MATCHING LC NETWORK
2 END CAP	6 COIL	10 POWER METER
3 PIRANI HEAD	7 YOUNG'S TAP	11 R.F. GENERATOR
4 COLD TRAP	8 NEEDLE VALVE	

FIGURE 2.2a Experimental Configuration of Vacuum Line

RF Generator & Associated Equipment

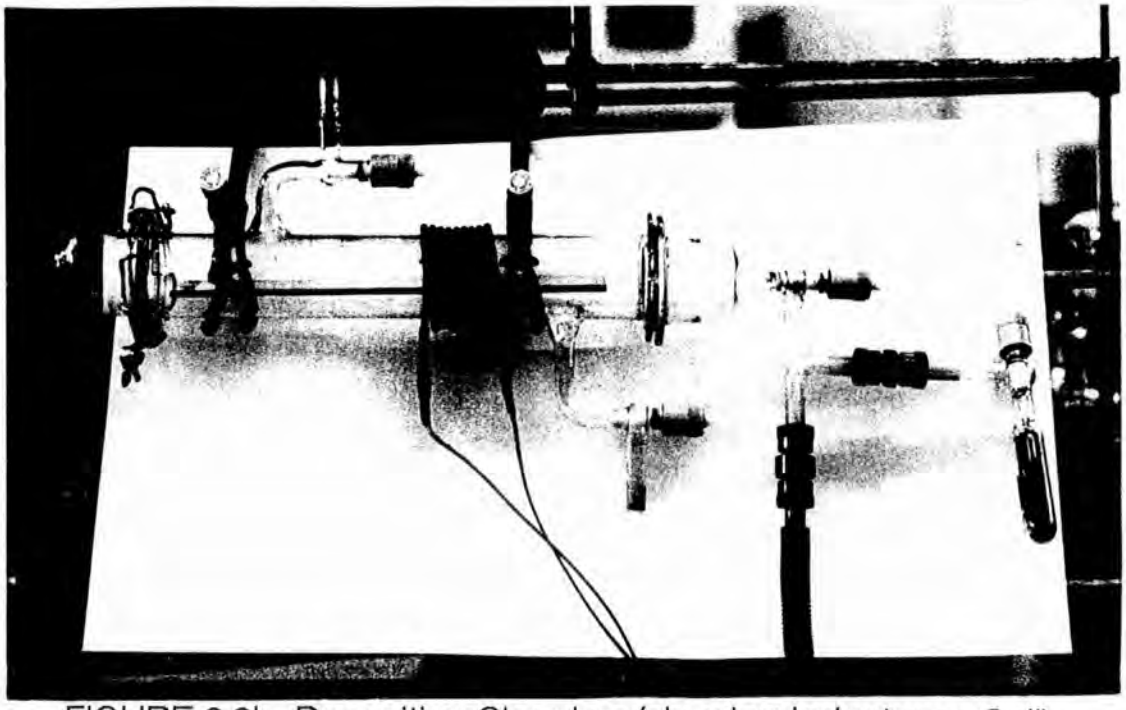

FIGURE 2.2b Deposition Chamber (showing Inductance Coil)

The reactor walls and sealing O rings were all found to contain absorbed moisture and air from the atmosphere if left exposed for any length of time. The vacuum system was therefore left to pump down overnight at the start of each series of experiments in order to achieve a base pressure as near to 10^{-2} mb as possible. The overall leak rate of the vacuum system was tested at the start of each experiment by closing the system off from the rotary pump and measuring the rise of pressure on the reactor over a period of time. The experiment proceeded only if the leak rate was very small, since an unacceptably high amount of oxygen and/or nitrogen would otherwise have been incorporated into the polymer film during polymerization (some oxygen uptake will always occur unless the reactor walls are truly desorbed and the leak rate zero).

In the case of the gaseous fluoroethylenes, which were supplied by Aldrich in cylinder form, the cylinder head was attached to an Edwards vacuum needle valve using pressure tubing. This was first evacuated and then the whole system purged with the monomer in use prior to the start of the experiment. All polymerizations were carried out under dynamic flow conditions - i.e. with the Young's tap to the pump open - rather than in a static system, i.e. with the tap closed.

The r.f. power was supplied by a 13.56 MHZ r.f. generator inductively coupled to the reactor via an externally wound 9 turn copper coil, and capable of delivering between 0.1-150 watts. The inductive (coil) load was matched to the generator via an LC matching network. A DIAWA SW110A meter was used to measure standing wave ratio (SWR) and rf power (Figure 2.2). Maximum power transfer to the coil occurred when the SWR was at a minimum, the optimum value being 1.

After each deposition period, typically 5-10 minutes, the reactor was let up to atmosphere. Initially, this was done under nitrogen or argon, before transfer of the substrate and film to the spectrometer under an inert gas blanket. Once early results had established that there was no observable difference between the oxygen content of samples analysed using this procedure and those which had been let up to atmosphere and exposed to air during transfer, the latter practice was exclusively used. However, the whole process was carried out as quickly as possible to minimise the chance of oxygen uptake.

2.3.2 ESCA Analysis

The films were deposited onto aluminium foil substrates. Once the plasma chamber had been let up to atmosphere, these were removed and mounted onto a three sided probe tip using double sided Scotch adhesive tape. The tip was then mounted onto the end of a probe and inserted into the spectrometer. Analyses were carried out on either a Kratos ES300 or ES200 spectrometer. All irradiation utilised Mg $Ka_{1,2}$ X-Rays, having an energy of 1253.6ev. The take off angle normally used was 35^{o} unless an angle dependence study was undertaken, in which case spectra were run at 70^{o} as well.

The ES300 spectrometer was controlled by the Kratos DS300 system based on an LSI-11 minicomputer running under RT-11. Data acquired was stored on floppy disc, the repeated scanning of up to 10 regions being allowed. A data analysis package was available, allowing a full peak synthesis and filing routine. On occasion the ES300 had to be run in analogue, rather than digital mode. In this instance the output was recorded on paper using an X-Y chart recorder as scanning of the

spectrum progressed, and peak fitted using a Du Pont 310 curve resolver. Peak areas were then calculated using a microcomputer programme on an Apple.

In contrast, the ES200 spectrometer, initially equipped to run in analogue mode only, was "home converted" to digital control using a BBC microcomputer and home-written software. The spectra recorded were stored on floppy discs, and could be peak fitted to the same standard as those analysed using the DS300 system, again using a locally written programme. For both machines, component analyses were achieved following linear background subtraction, using gaussian peaks with a constant full width at half height. C1s component peak positions were assigned by reference to the experimentally determined binding energies of the various functionalities in known standard samples[15] and were constant to within $\pm$ 0.3ev. The height of each peak component was found that gave the best chemical fit.

2.3.3 Calculation of Flow Rate

The ideal gas law is considered to operate in the vacuum ranges used for plasma polymerization, since, at these pressures, gases and vapours can be considered as ideal. Thus:

$$PV = nRT \qquad (1)$$

where n = no. of moles of gas

R = gas constant

T = absolute temperature (K)

P = pressure (torr)

V = volume of the system (m^3)

Differentiating (1) with respect to time, t, and rearranging :

$$\frac{dn}{dt} = \frac{dP}{dt}\,\frac{V}{RT} = \text{flow rate in mols}^{-1}, x$$

now, $1cm^3_{STP} = \frac{1}{22,414}$ mol $= 4.46 \times 10^{-5}$ mol

Therefore, the flow rate in $cm^3_{STP}\ min^{-1}$ is given by :

$$\text{flow rate} = \frac{x \times 60}{4.46 \times 10^{-5}}$$

Similarly, the leak rate, y, can be calculated. dP and dt in each case are taken to be the increase in pressure, dP, with respect to a measured time period, dt.

Now, since $R = 8.31434\ JK^{-1}\ mol^{-1} = 6.24 \times 10^4\ \frac{torr.cm^3}{mol\ k}$

and 1 torr = 1.33 mb

then $R = 6.24 \times 10^4 \times 1.33$

$= 8.3 \times 10^4\ mbcm^3\ mol^{-1}k^{-1}$

The experiments were carried out at a temperature of 288^oK (15^oC - room temperature in the laboratory). The reactor had a volume, V = 1000 cm^3.

Therefore, the actual flow rate, F, is given by

$$F = \frac{10^3}{8.3\times10^4} \times \frac{273}{288^2} \times \frac{dP}{dt} \times \frac{60}{4.46\times10^{-5}}$$

$$= 53.35 \frac{dP}{dt} \quad cm^3_{STP} min^{-1}$$

NOTE: In the later photochemical experiments (see Chapter 5) the volume of the reactor used changed. The flow rates were calculated simply by measuring dP and dt as usual, but altering the volume, V, in the above equation.

The overall flow rate for the experiment is obtained by subtracting the observed leak rate from the flow rate. Usually the former was so small that it could effectively be ignored.

2.4 Results and Discussion

Typical examples of the C1s and F1s core level spectra obtained for plasma polymerized perfluoroethylenes are shown in Figure 2.3. As has been noted for plasma polymers of perfluorobenzene, the overall band profiles of each of the levels studied, and their relative area ratios, remained more or less constant over the range of operation parameters used, so no mention is made here of the specific experimental conditions used; in general, however, the typical system operating pressure was in the region of 0.01-1.0 mb, power delivered to the inductance coil being in the range 3-70W.

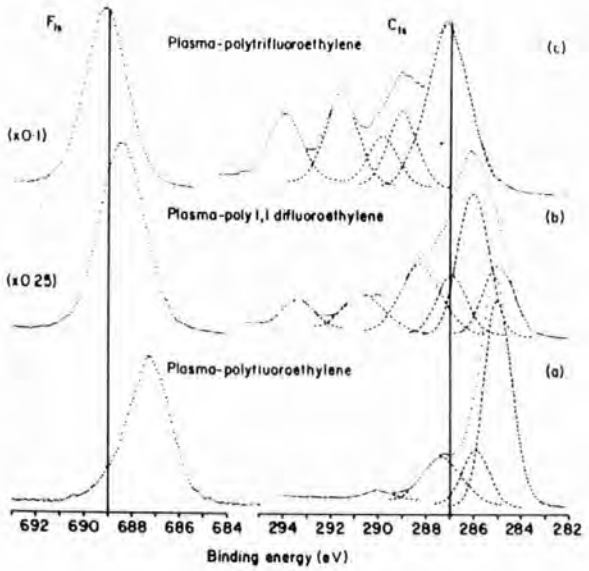

FIGURE 2.3(i) Typical C1s and F1s Core Level Spectra for Plasma Polymers of (a) Vinylidene Fluoride / Fluoroethylene, (b) 1,1-difluoroethylene, (c) Trifluoroethylene.

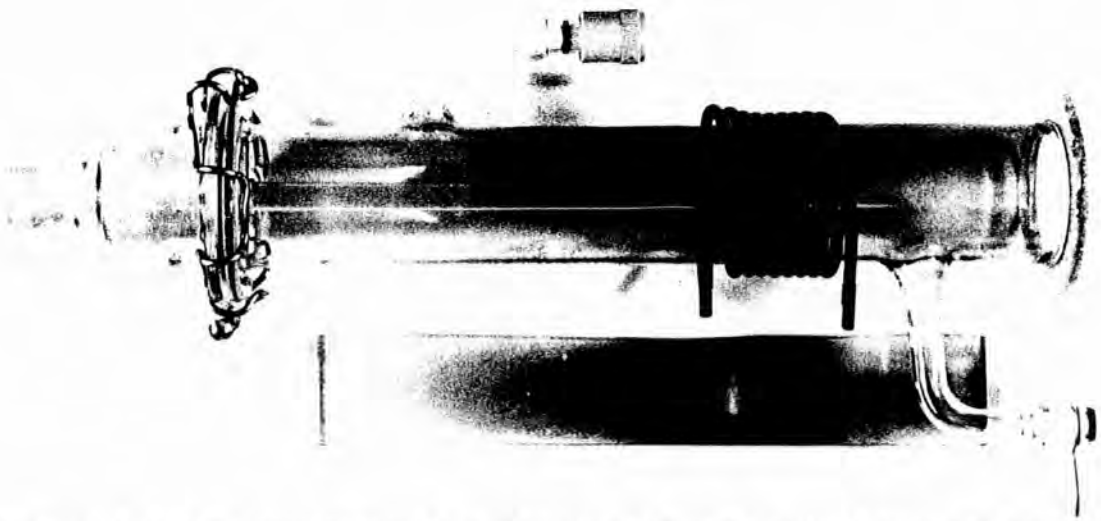

FIGURE 2.3(ii) Deposition Chamber, Showing the Typical Deposition Pattern with Respect to the Position of the Coil.

Before considering the results for all three monomers, it is worth noting the problems associated with the ESCA analysis of the samples. These lie principally in 1) accurate deconvolution of the spectra (or "envelope") observed, 2) allowance for the contamination of the film surface (since ESCA is essentially a surface sensitive tool, any such contamination will be exhibited in the spectra observed).

Surface contamination essentially comes from two sources:

A. The presence of oxygen in the sample - as shown by the O1s core level present in all the plasma polymers studied, and centred at approximately 533.5ev. Usually broad, complex and made up of at least two components due to C-O and C=O functionalities, the presence of $-CO_2$ and $-CO_3$ is also possible in more highly oxygenated systems. As mentioned in the experimental section the reactor walls were desorbed of oxygen by pumping down the reactor chamber overnight prior to each series of experiments. However, this will never be 100% effective; further, any leak in the vacuum system, however small, will result in the uptake of oxygen, especially by the highly reactive free radicals trapped in the cross-linked matrix during deposition[17] (see Chapter One). As oxygen incorporation is typically in the ratio of only one oxygen atom for every ten or twenty carbon atoms, and it has been shown that oxygen incorporation will occur even if the reaction chamber is bolted onto the spectrometer such that transfer between the two takes place in vacuo, no special precautions were thought necessary. This was confirmed when films let up to nitrogen or argon, and then transferred to the spectrometer whilst still under an inert gas blanket, showed little (if any) difference to those let up to, and transferred in, atmosphere.

B. The second source of contamination is evidenced by the presence of a hydrocarbon peak in the C1s spectrum, arising from three effects: (i) a thin layer being deposited on top of hydrocarbon contamination in the substrate,[14a] (ii) the deposition of hydrocarbon onto the polymer whilst it is being transferred to the spectrometer,[14] or (iii) the formation of a hydrocarbon overlayer during analysis in the spectrometer.[14d] Clark and AbRahman have shown evidence that (ii) is responsible for the hydrocarbon contamination of perfluorobenzene,[18] and it is thought that this equally applies to the fluoroethylenes. However, it is also known that there is an appreciable build up of hydrocarbon on the film surface during analysis in the spectrometer, due to "boiling off" of contaminant from the X-ray cap and window.[19] It should be noted that both hydrocarbon and oxygen contamination were present for <u>all</u> plasma polymer samples studied in this work.

Deconvolution of the spectra was not carried out in the case of the O1s envelope, since a detailed knowledge of the oxygen structure and bonding was not required - only the overall content. The F1s core level is a symmetrically shaped peak centred at around 689.0ev, corresponding to the range of fluorine environments found in the C1s spectrum. Since the respective binding energies of these are very close in value for the thick films deposited, a single symmetrical peak resulted. Note that if the amount of film deposited is insufficient to fully cover the substrate (such that a signal due to the Al2p core level is visible), then a second peak can appear in the F1s envelope to a lower binding energy than the original. This is observed for perfluorobenzene,[5b] and also for the Cl2p peak in chloroacrylonitrile. Since the amount by which the peak is shifted in the respective F1s and

Cl2p peaks is about 2ev, compared to the 4ev expected if metal-fluorine bonding occurs, the lower binding energy is probably due to the interaction of the adsorbed monomer with the substrate surface. This idea has been pursued by Till,[5b] as has the idea of the presence of small $\pi \rightarrow \pi^*$ shake-up satellites some 7 to 8ev removed to higher binding energy due to transitions accompanying core ionisation of vinylic $C\text{-}F_x$ groups (x=1 or 2), and indicative of unsaturation in the plasma polymer. This shake-up was not clearly observed for the fluoroethylenes studied, but has been noted by Dilks.[20]

Detailed analysis of the (very broad and complex) C1s envelope reveals a variety of component functionalities. These have been detailed elsewhere for fluoroethylenes in particular,[15.16] but essentially consist of the following: C (representing carbon atoms not bonded to any fluorine functionalities), C-CF (carbon atoms bonded to a CF functionality etc), CF, $CF\text{-}CF_n$, CF_2, CF_3 and a small satellite - the latter exhibiting, along with the presence of a step-function, evidence for unsaturation in the polymer film (see Figure 2.4). The typical energy separation between the primary photoionization peak and the shake-up satellite is about 7-8ev removed to higher binding energy, depending on the degree of fluorination of the parent monomer (7ev corresponding to a hydrocarbon system and 8ev to a fully fluorinated aromatic compound). The spectrum is further complicated by the insulating nature of the film, which shifts the binding energies of the peaks observed to a higher energy, and also due to satellite peaks removed some 8 to 10ev to lower binding energy. The former is overcome to the hydrocarbon peak, which was taken to occur at a standard, unshifted 285.0ev, and calibrated accordingly; the latter,

satellite peaks are the result of using unmonochromatic radiation and were not analysed further. Both the above are standard practices throughout this work.

Injected Material	Binding Energies (eV)							
	CF_3	CF_2	CF_a	CF_b	C_a	C_b	CH	F
CH_2CH_2							285.0	
CH_2CHF		290.0		287.4		285.9	285.0	687.3
cis CHFCHF	292.9	290.0		287.7	287.0	285.8	285.0	687.6
trans CHFCHF	292.7	290.0		287.8	286.8	285.8	285.0	687.5
CF_2CH_2	293.4	290.6		288.2	287.0	286.0	285.0	688.4
CF_2CHF	294.0	291.6	289.9	289.0	287.2		285.0	689.1
CF_2CF_2	294.1	291.9	289.7		287.6		285.0	689.5

TABLE 2.1a C1s and F1s Peak Assignments for the Plasma Polymers Derived From Fluorinated Ethylenes

MONOMER	Stoichiometry (F/C)	
	From F1s/C1s	From C1s Envelope
CH_2CHF	0.15	0.20
CF_2CH_2	0.51	0.56
CF_2CHF	0.99	0.99

TABLE 2.1b Fluorine/Carbon Stoichiometries Derived From the ESCA Data for the Plasma Polymers Studied

Elemental stoichiometry is obtained by a ratio of the appropriate peak areas multiplied by a sensitivity factor, the latter taking into account the sensitivity of the spectrometer for a particular core level, and includes such factors as electron mean free path and analyser response to the electron energy. The sensitivity factors used throughout this work can be determined either experimentally and/or theoretically - a list of values employed are to be found in Appendix 1. Cross-referencing of the stoichiometry obtained (as mentioned earlier in this Chapter) can be carried out using the contributions of

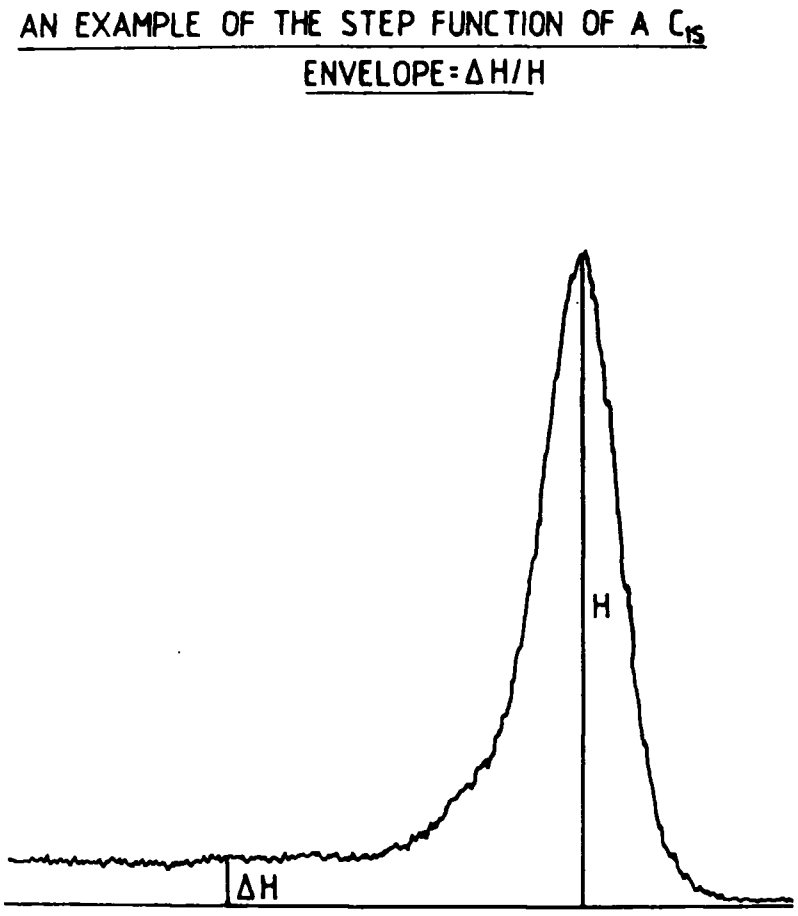

FIGURE 2.4 The Step Function as Seen in the C1s Envelope

each component peak in the C1s envelope which has one or more fluorines directly attached to a carbon atom. These are summed such that:-

$$C:F = \frac{[\%CF] + [\%CF\text{-}CF] + 2[\%CF_2] + 3[\%CF_3]}{100}$$

Agreement in all cases was found to be within a few %, confirming that the C1s envelope had been correctly deconvoluted using a good chemical fit. The differences can be attributed to the contribution to the overall C1s envelope of any signal due to both hydrocarbon contamination and also the shake-up satellite, if present (see below), as manual error in controlling the peak-fitting routine.

The results for all three monomer gases studied are shown in Table 2.1b. Effectively, the overall carbon to fluorine ratios are 1:1 for trifluoroethylene and 2:1 for 1,1-difluoroethylene, whilst the vinyl fluoride F1s core level shows that there is very little retention of fluorine in the respective plasma polymer. Since the starting C:F ratios were 2:3, 2:2 and 2:1 respectively, this is strongly indicative of the overall elimination of HF from the monomer. This can be checked by examination of the C1s envelopes - whilst both tri- and 1,1-difluoroethylene have a significant amount of $\underline{C}F$, $\underline{C}F_2$ and even $\underline{C}F_3$ environments, those for vinyl fluoride show very little evidence for the latter environment at all (Figure 2.3.i). It was not possible to precisely check that the C:H ratio had decreased as expected (i.e. dropping from 2:1, 1:1 and 2:3 for $CF_2{=}CFH$, $CF_2{=}CH_2$ and $CFH{=}CH_2$ to no H content, 2:1 and 1:1 respectively) since (i) ESCA is unable to analyse hydrogen H1s envelopes. (ii) In the C1s envelopes, the peak component

at 285.0ev is due not only to true hydrocarbon C-H due to the film, but also any quaternary carbon species (ie any carbon atoms bonded to four other C atoms rather than either H or F) as well as extraneous hydrocarbon contamination. However, the 285.0ev components are suitably very low for trifluoroethylene and very high for vinyl fluoride respectively, whilst difluoroethylene falls between the two. (iii) as noted by Dilks,[20] the existence of vinylic CH in the polymer leads to the presence of a small shake-up satellite removed by about 7ev from the 285.0 ev reference. This peak will contribute to the overall C1s signal used in the F1s/C1s ratio calculation, whereas on peak-fitting the C1s spectrum alone it can be discounted. The latter approach can thus lead to a higher calculated F/C ratio than the former.

Furthermore, the number of CF_2 and CF_3 groups in evidence in the C1s spectrum which are indicative of rearrangement in the monomers and films, increase in a similar order - i.e. $CHF=CH_2 < CF_2=CH_2 < CF_2=CFH$, corresponding not only to the amount of fluorine in the plasma polymerized films, but to the structure of the monomer as well (both di and trifluoroethylene already have CF_2 groups in their structure, hence making formation of the CF_3 moiety somewhat easier compared to vinyl fluoride). It should be noted that there is a high proportion of CF_3 groups in plasma polymerized trifluoroethylene as well.

Supporting evidence for the above results is provided by Shuttleworth[15] and by Clark[16] and Dilks,[20] who similarly studied fluoroethylene monomers other than $CF_2=CF_2$, and also found that, for an inductively coupled plasma, the resultant stoichiometry is consistent with the elimination of HF. These workers also considered the possible

nature of the activated species involved in the plasma chemistry. Thus Shuttleworth suggested that plasma of 1,1- difluoroethylene, together with cis- and trans-1,2- difluoroethylene, eliminate HF to form fluoroacetylene - a suggestion supported by microanalysis of the plasma polymer formed, which revealed a fluorine to hydrogen ratio of approximately 1:1 (and hence a carbon to hydrogen ratio of 2:1).[15,16] Based on this evidence Shuttleworth argued that the deposition mechanism utilised radical cations as the excited species involved in the polymerization process, rather than molecules which are found in electronically excited states, both species able to result from electron impact excitation. Indeed, for a (fluoro)ethylenic system such excitation can lead to occupation of both the singlet and triplet states following a $\pi \rightarrow \pi^*$ transition, as well as ionisation. The corresponding excitations are thought to be close to $\sim$7.5ev and $\sim$4.4ev for the respective states. Similarly, the ionisation energy of the fluoroethylenes is close to that of ethylene (ethylene 10.51ev, 1,1-difluoroethylene 10.48ev).[21] It is therefore easier to access the electronically excited π^* - or, indeed, Rydberg 3s states, than to achieve ionisation. However, thermochemical and entropy considerations have shown that, for the fluoroethylenes, elimination of HF^- to produce the triplet state is energetically expensive (e.g. 38 kcal $mole^{-1}$ for the 1,1-substituted derivative).[15,16] The argument in favour of radical cations compared to electronically excited states therefore lies in a consideration of the thermochemistry of the reactions involved, as well as the view that a Maxwellian distribution of the electron energies present in the plasma would tend to favour more electrons with sufficient energy to cause ionisation, rather than

merely excitation. However, the resultant scheme suggested for the initial stages of the plasma polymerization process does not hold up in view of more recent evidence. In particular there has been increasing indication in the literature that plasma polymerization involves free radicals - in particular biradicals - as the major depositing species.[6] This is not to say that ions - including radical cations - are not involved in the deposition process or, perhaps more likely, as ablative or cross-linking species due to their impact with the surface; rather, two pieces of evidence in particular show that radical cations are unlikely to be a major depositing species in ethylenic systems :

(i) the addition of iodine vapour - a known effective, free radical scavenger - drastically reduces the flow volume of various systems to which it has been added, principally cyano containing compounds such as acrylonitrile and its derivatives 2-chloro- and methacrylonitrile.[22] Furthermore, it was found that there was effectively no deposition outside of the glow region - which was restricted to the region of the inductance coil only (i.e. the region of highest energy input to the system and hence, presumably, electron energy distribution) - and that, in the film that was deposited, a high degree of iodine uptake had occurred. This is presumably via free radical recombination, and hence strongly suggests a free radical film growth mechanism.

(ii) it has been demonstrated, both in this work for trifluoro-ethylene and elsewhere for tetrafluoroethylene that organic thin films can be deposited photochemically using vacuum ultra-violet (<200 nm) or conventional ultra-violet (>200 nm) light.[23] The former films, known as surface photopolymers, proved to be almost identical in chemical

composition (as studied by ESCA) to corresponding films produced by plasma techniques, whilst the latter were found by infra-red spectroscopy to contain CF_3 moieties (see chapter 5). Hence, since the wavelengths used were well below the photoionization threshold, radical cations do not have to be invoked in the deposition mechanism. Also, as was suggested in Chapter 1, since it is thought to be free radicals that are actually responsible for the bulk of thin film formation, it seems reasonable to assume that they must have been formed from an electronically excited state - especially the biradicals - since there are innumerable examples of this in the photochemical literature (see chapter 5). In addition, even if (as suggested by Shuttleworth) thermochemical considerations do weigh against the formation of triplet states then the possibility still exists that the electronically excited state is in fact Rydberg in nature, from which molecular elimination of HF or F- is entirely possible, the first resulting in the biradicals :C=C and X-$\dot{C}$=C$\dot{}$-Y (the latter of which instantaneously rearranges to the corresponding ethyne), or else electron capture might occur to form the radical anion. The excited state here was shown in Chapter One to have $^2\Pi$ symmetry and to follow a predissociation mechanism, again involving molecular elimination as one of the fragmentation pathways, again with biradicals as a result.[24]

Finally, although, for the experimental conditions used both in this work and that done by Shuttleworth, the overall stoichiometry suggests elimination of HF from the molecule, this will not be the only dissociation pathway involved; analogy with the mass spectrometric studies undertaken for chlorine substituted olefins would suggest that although the major dissociation pathway from excited states and radical

ions alike is indeed molecular elimination, other dissociation channels - and hence products - are possible.[25] For example, direct (bond) dissociations may occur to give rise to other positive and negative ions in the plasma besides radical anions and cations. These too, may play a role in the overall competitive ablation and polymerization mechanism. This does not detract from the idea that free radicals are currently considered to be the prominent depositing species responsible for film growth.

CHAPTER 3

PLASMA POLYMERIZATION OF ORGANIC COMPOUNDS CONTAINING A CYANO OR NITRILE GROUP

3.1 Introduction

Organic nitriles (organic compounds containing a pendant cyano group) are of potential interest in plasma chemistry since they are a source of nitrogen and (in the carbon-nitrogen triple bond) contain unsaturation. Hence, saturated hydrocarbons containing C-CN, such as acetonitrile, Me_3CN, also contain unsaturation within Yasuda's classification of monomers,[1] whilst acrylonitrile, CH_2=CHCN, contains unsaturation due to both the carbon-carbon double bond and also the nitrile group. This latter compound has received attention in the literature in recent years,[2-6] studies centring on the properties of its plasma polymers - and their dependence on the characteristics of the plasma systems - together with their potential applications (eg for use in the surface modification of polymers, graphite blocks and fibres to alter the overall strength and tensile properties of the substrate).[1,3] Studies of other nitriles are less common, but include the related compounds metha- and 2-chloroacrylonitrile,[7] which were found to eliminate HCN and ClCN, respectively, to give the corresponding acetylenes. Allyl cyanide provides a contrast to acrylonitrile itself, since the cyano group is no longer 1,2 to the carbon-carbon double bond, being removed by one methylene unit, CH_2. The molecule thus possesses both allylic and nitrile character, and so was chosen as a monomer for this work, together with metha- and (in particular) 2-chloroacrylonitrile. A contrast is thus provided between different cyano containing compounds, and also between 2-chloroacrylonitrile and vinylidene fluoride, both of which have a halogen atom directly attached to an unsaturated carbon atom.

3.2 Aim

The work of Yasuda and co-workers has shown the importance of various components that affect the plasma polymerization process; namely, flow rate (F), power (W) and the molecular weight of the precursor (M).[1] All three parameters are encompassed in the composite discharge parameter W/FM, and have been shown to be important in the description and control of experimental conditions of the plasma polymerization process. Most emphasis has been on the effect of W, F and M on rates of deposition and, to a lesser extent, chemical composition. This Chapter therefore investigates the chemical composition of various organic monomers deposited by plasma polymerization techniques, as studied by ESCA. It was hoped that the results might shed light on some aspects of the deposition mechanisms.

3.3 Experimental

3.3.1 Plasma Polymerization

The experimental set up was identical to that in Chapter Two with regard to the vacuum line and rf generator. The monomers used were:

Acrylonitrile)
2-Chloroacrylonitrile) supplied by Aldrich
Methacrylonitrile)
Allyl cyanide)

Acrylonitrile was principally used to "test" the system. Its behaviour was found to agree with that observed by Munro and Grunwald,[6] and will not be considered further except in discussion.

All the monomer compounds exist in the liquid state at room temperature and pressure. Prior to use, each compound was transferred

from its stock bottle to a monomer tube, the latter sealed with a Young's tap. The monomer was degassed by alternate freeze-thaw cycles in vacuo prior to being attached to the reaction chamber. Monomer vapour was bled into the chamber using an Edwards needle valve; leak and flow rates were measured using an XY recorder wired up to a Pirani pressure head. A new flow rate was calculated for each experiment.

3.3.2 ESCA Analysis

ESCA spectra were run on either a Kratos ES200 or ES300 spectrometer in digital mode and peak-fitted using the Kratos Data Handling Package (ES300) or locally written computer software (ES200). All peak assignments were referenced to that of C-H occurring at a binding energy of 285.0 eV. Two model compounds were run - polyacrylonitrile and polychloroacrylonitrile, both of which were commercially supplied. Polyacrylonitrile gave rise to the C1s and N1s spectra shown in Figure 3.3.1. Theses were resolved as follows :

a) C1s Two peaks were found, centred at 285.0 eV and 286.6 eV in the ratio of 2:1. The latter was assigned to carbon directly bonded to nitrogen in the nitrile group, with the remaining two carbon atoms giving chemical shifts of 285.0 eV.

b) N1s One peak was seen, centred at 399.3 eV and corresponding to nitrogen triply bonded to carbon.

Poly(alpha)chloroacrylonitrile spectra are shown in Figure 3.3.2.

a) C1s Initial interpretation proved difficult, since the expected result had been either three peaks in the ratio 1:1:1, or else two peaks in the ratio 2:1. The spectrum shown was resolved into three peaks centred at 285.0 eV, initially assigned as $\underline{C}H_2=C$; 286.6 eV,

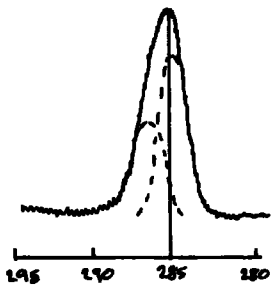

C1s Envelope

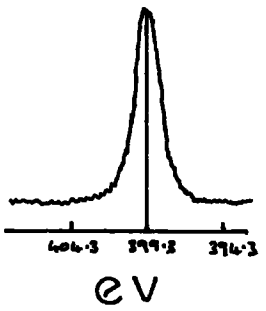

N1s Envelope

FIGURE 3.3.1 C1s and N1s Spectra for Polyacrylonitrile

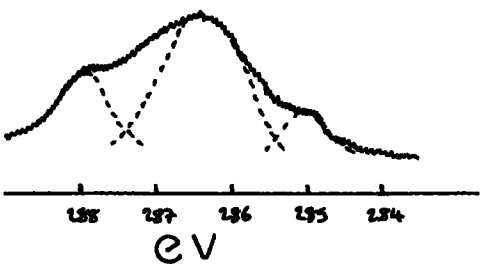

C1s Envelope

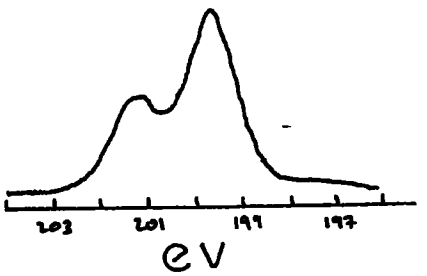

Cl2p Envelope

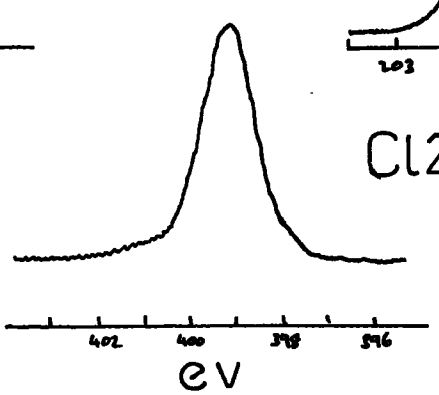

N1s Envelope

FIGURE 3.3.2 C1s, Cl2p, N1s Spectra for Poly(alpha)chloroacrylonitrile

assigned to nitrogen triply bonded to carbon; and 288.1 eV, attributed to carbon bonded to chlorine and to the nitrile group. However, the 29:53:18 ratio of peak areas found did not fit the molecular formula. Since the sample was run in powder form, rather than as a cast film, peak 1 was assumed to be due to intergranular hydrocarbon contamination - a reasonable assumption, since the adjacent CClCN moiety was also thought likely to give rise to a binding energy higher than 285.0 eV due to an inductive effect. Subtracting out this contamination gave new atomic values as follows :

C	Cl	N
1	0.33	0.34

ie the revised C1s envelope not only gave the 2:1 ratio anticipated, but also gave the correct elemental ratios as well. The binding energies were thus assigned as follows :

CH_2 = CCl - CN

286.6 288.0 286.5 (all binding energies in eV)

Assignment using the hydrocarbon contamination as reference at 285.0 eV was cross-checked using the $Cl2p^{3/2}$ peak, known to occur at 200.4 eV.[8]

b) The N1s envelope again revealed a single peak, centred at 399.3 eV.

Using the above data, the C1s spectra obtained for the plasma polymers of both monomers were fitted with four peaks, centred at 1) 285.0 eV 2) 286.6 eV 3) 287.8 eV 4) 289.0 eV. Since resolution was deemed to be accurate to $\pm$ 0.3 eV, these peak assignments also encompassed the following chemical environments : CCl, C-N, C=N, C-O (286.6 eV), C=O (287.8 eV), $-CO_2-$ (289.0 eV). Whilst it is acknowledged that the above list was not exhaustive with respect to the

possible number of different carbon environments formed in the plasma polymer films, it was felt that the assignments covered a sufficient majority to enable quantitative analysis of the films to be carried out. Due to the large number of environments occurring at each binding energy, trends are presented in terms of peak contributions to the overall C1s spectrum, rather than individual chemical environments.

b) The N1s spectra were fitted using two peaks - that at 399.3 eV, corresponding to nitrogen triply bonded to carbon, was found to be accompanied by a second peak centred at 400.8 eV, assigned to nitrogen singly or doubly bonded to carbon (see below for explanation).

Methacrylonitrile and allyl cyanide plasma polymers were also peak fitted using the above assignments.

3.3.3 Mass Spectrometric Investigations

These were carried out on the Departmental spectrometer, a VG Analytical machine equipped with a Winchester Disk Drive System.
The fragmentation patterns for each monomer were studied with respect to increasing energy of the bombarding electrons. Accelerating voltages used were : 8,10,12,14,16,18,20,70 eV. Low resolution was initially used throughout. However, the m/e peak observed at 26 for acrylonitrile was found to be of ambiguous origin; this was resolved to be due to $HCCH^{+\cdot}$ rather than $CN^{+\cdot}$ using high resolution.

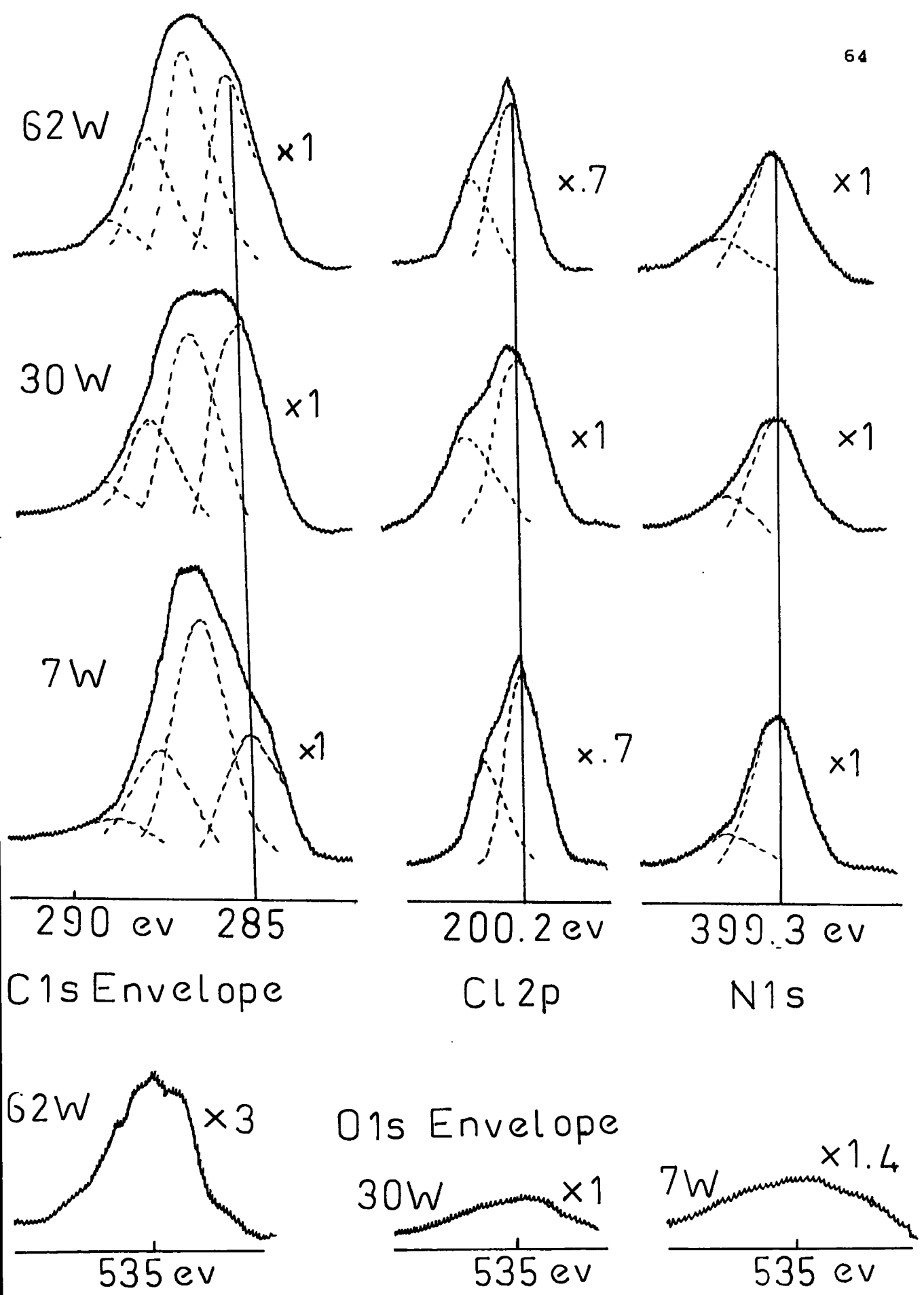

FIGURE 3.1 C1s, Cl2p, N1s and O1s Core Levels Corresponding to Plasma Polymers run at RF Input Powers of 7, 30 and 62 Watts.

CHLOROACRYLONITRILE

3.4 Results and Discussion

3.4.1 2-Chloroacrylonitrile

The core-level spectra in Figure 3.1 show typical C1s, C12p, N1s and O1s spectra corresponding to rf input power of 30W at an operating pressure of 0.1mbar (equivalent to a flow rate of $10.3cm^3_{stp}\ min^{-1}$). The O1s envelopes are very similar to those found for fluoroethylene films, and will not be considered further except for the calculation of the C:O stoichiometry. The C1s envelope, as discussed in section 3.3.2, consists of four main peaks - that centred at 285.0 eV representing hydrocarbon or quaternary carbon environments, together with three further components at 286.6, 288.0 and 289.2 eV.

For all the polymers studied in this Chapter there was evidence for at least two nitrogen environments, the second being centred at about 400.8 eV, or 1.5 eV removed to a higher binding energy. This was first observed by Hiraoka and Lee for poly (alpha-chloroacrylonitrile) on heating, and was attributed to opening of the carbon-nitrogen triple bonds of three neighbouring nitrile units to form a six membered heterocyclic ring, thus giving rise to both single and double carbon-nitrogen bonds :

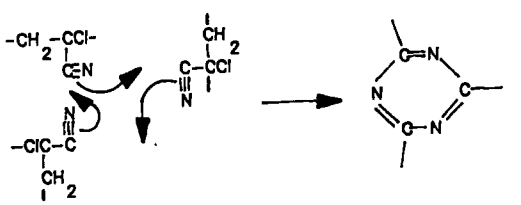

The latter were consequently thought to be responsible for the 1.5 eV shift observed.

Although there is no direct evidence for the presence of such six-membered rings in the polymer films studied in this work, the plasma contains electrons of sufficient energy to break at least one of the bonds in the cyano group. The presence of the second peak at 400.8 eV is thus taken as evidence that this does occur.

Two main series of experiments were performed in order to test Yasuda's W/FM parameter - 1) varying the inductive power supplied to the system for a given, fixed flow rate; 2) increasing the flow rate for a given power. The plasma deposition process falls into two categories. Firstly, for a low flow rate and high power (high W/F) the system is monomer deficient - i.e. there is a high power input into the system in comparison to the availability of monomer. The second region is the reverse of this, and hence is power deficient (low W/F) If a graph is drawn of deposition rate against W/FM Figure 3.2), then an increase in the deposition rate will occur up to the point at which the amount of power being put into the system becomes the limiting factor; thereafter as W/FM further increases the deposition rate will decrease.

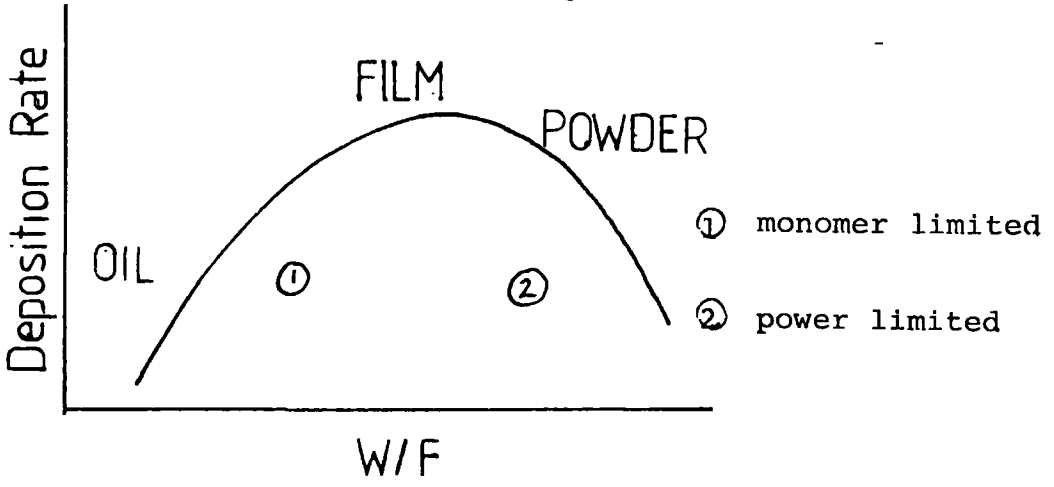

FIGURE 3.2 Deposition Rate versus W/FM

Thus, restriction of either monomer or power availability should affect the chemical composition of the plasma polymer formed. The experiments carried out aimed to test this idea. Table 3.1 and Figure 3.3 illustrate the atomic ratios of chlorine, nitrogen and oxygen versus carbon with respect to increasing power for the IN COIL (as opposed to tail, or OUT OF COIL) region for films deposited from chloroacrylonitrile. Initially, both chlorine and nitrogen content decreased with respect to carbon as W increased from 10 to 40 watts. This higher power was a minimum for nitrogen, the content of the film with respect to carbon increasing thereafter. In contrast, the chlorine content, although behaving similarly up to 40W, then remained fairly constant at about 18 or 19 chlorine atoms per 100 carbon atoms. A comparison of the relative amounts of nitrogen and chlorine via the ratio N/Cl showed that, initially, there was only a slight rise between 7 and 20W and effectively no further increase until 50W, at which point more nitrogen was present in the film than chlorine. The oxygen content of the films rose throughout the series.

The above results can be explained in terms of the ease of elimination of both Cl and N from chloroacrylonitrile - at low W/F, there is little elimination of chlorine moieties and only some elimination of nitrogen ones; as the power increases (such that W/F increases) then a larger availability of power with respect to monomer enables more excitation of monomer to occur - and hence more elimination and dissociation, both of which reduce both the nitrogen and chlorine content of the film. As W was further increased chlorine appeared to be preferentially eliminated, since the nitrogen content of the film increased. The oxygen content probably rises due to reaction

CHLOROACRYLONITRILE

Plasma Polymers - IN COIL vs TAIL Region

FIGURE 3.3

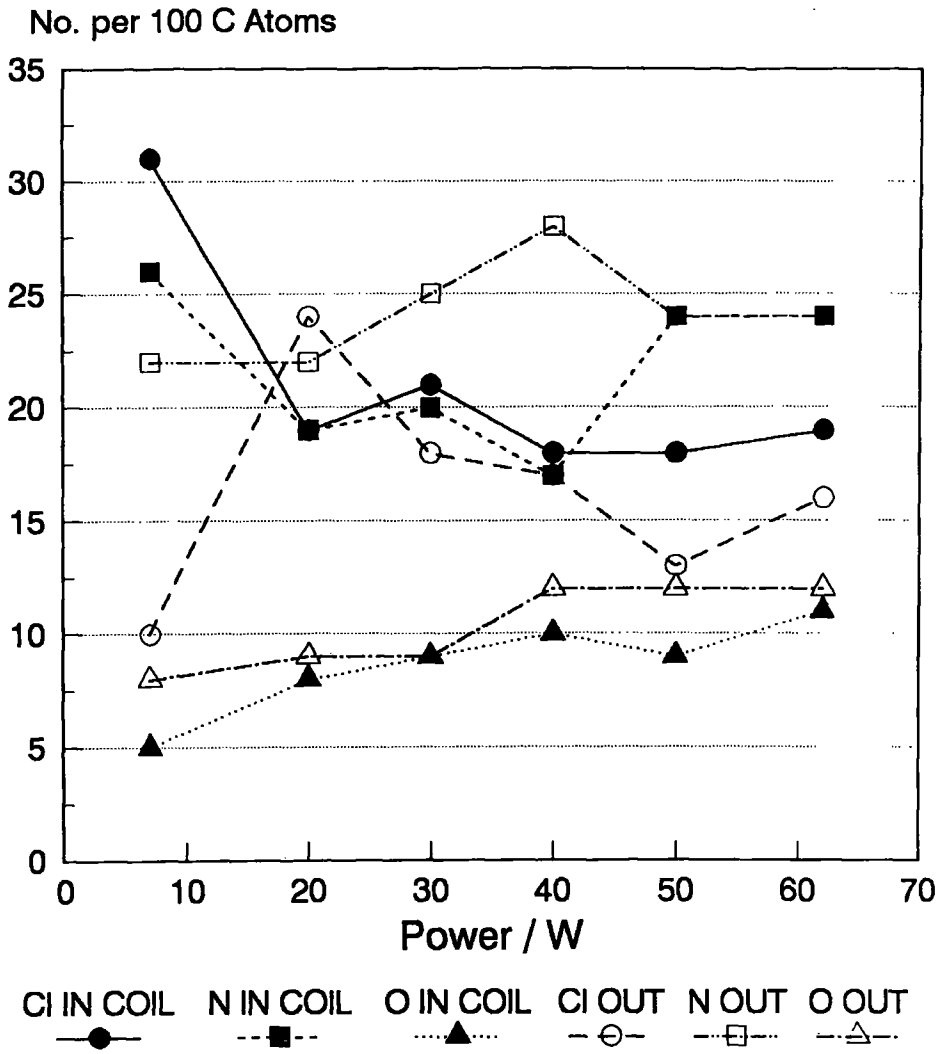

SUBSTRATE POSITION	POWER / W 7	20	30	40	50	60
IN COIL	0.85	0.94	0.95	0.98	1.32	1.28
OUT OF COIL	1.54	0.89	1.37	1.59	1.82	1.56

TABLE 3.1 Chloroacrylonitrile Plasma Polymers
N / Cl Ratio wrt Power

with a larger number of free radical species in the film surface as the power increases. Evidence that uptake occurs during the deposition process was gained by the use of an inert gas blanket over the sample during transfer to the ESCA spectrometer. Comparison of results with those obtained in the absence of a nitrogen blanket showed little difference (if any) within experimental error, suggesting uptake effectively does not occur during transfer to the spectrometer.

The stoichiometry results can be compared to those obtained for the various C1s (Figure 3.4a) and N1s envelopes (Figure 3.5). The former shows that, for low W/F in coil, there is a low hydrocarbon content, but a high number of environments occurring at about 286.6 eV. Since the oxygen content at 7W is very low (See Table 3.1 and Graph 3.3), this suggests either that (i) there are a large number of CH_2-$\underline{C}$Cl(CN) environments in the plasma polymer, together with intact nitrile groups, or (ii) a large number of nitrile groups "opened up" to give -C=N-C- instead of -C≡N, and hence the contribution of the former environments to the 286.6 eV peak in the polymer has dramatically increased (there are now two carbon-nitrogen environments for every one previously). This can be checked by reference to the N1s envelopes, which duly showed that some nitrile groups have undergone reārrangement (Figure 3.5). However, although the overall trend shows an increasing amount of such rearrangement with respect to increasing power (similar to the behaviour of acrylonitrile as seen by Munro and Grunwald), -C-N and -C=N environments account for less than 30% of the total, hence probably only some 15-20% of the original number of nitrile groups underwent reaction. This cause alone is therefore insufficient to account for the significant decrease in the number of environments

CHLOROACRYLONITRILE PLASMA POLYMER

C1s Envelope wrt Power

FIGURE 3.4a - IN COIL

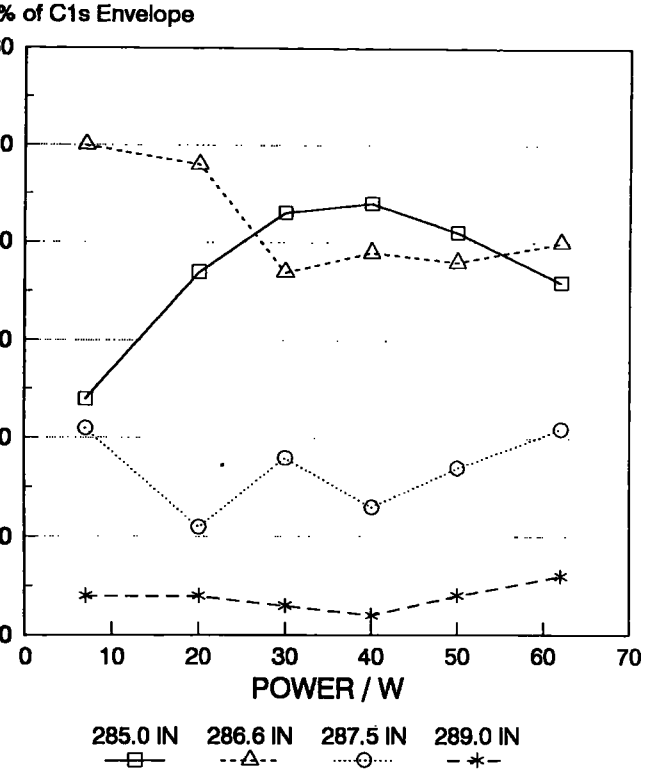

CHLOROACRYLONITRILE PLASMA POLYMER

C1s Envelope wrt Power

FIGURE 3.4B - OUT OF COIL

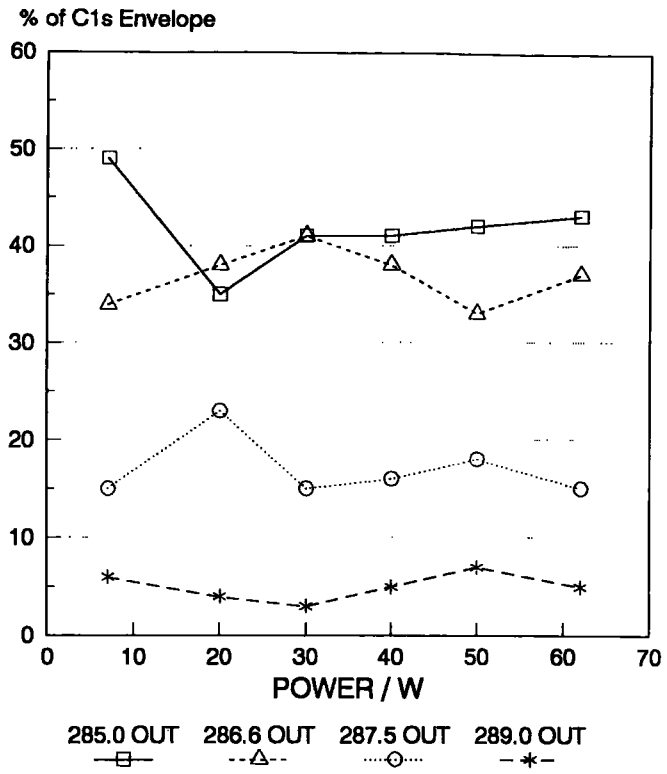

CHLOROACRYLONITRILE PLASMA POLYMER

N1s Envelope

FIGURE3.5

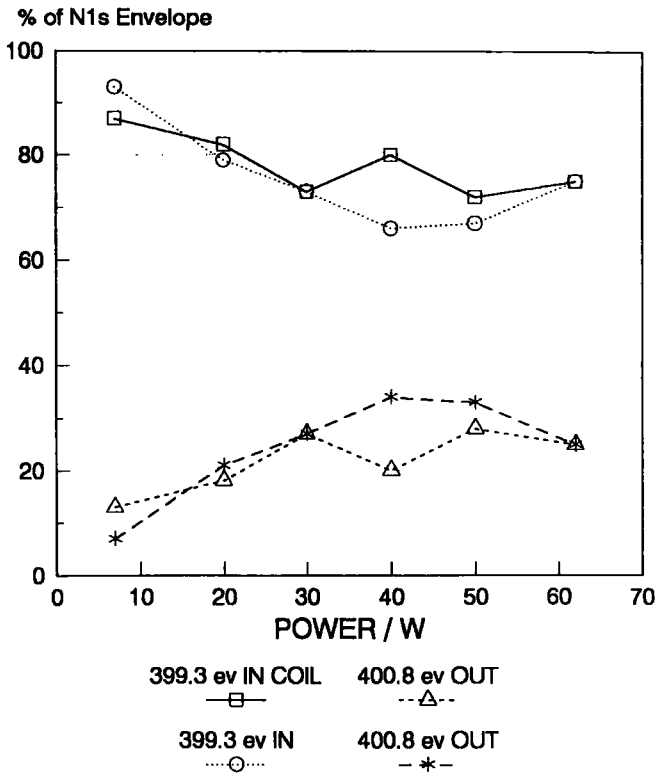

found at 286.6 eV between 7 and 40W. Rather the answer may be that, at lower power - such that the system is power deficient - the polymerization mechanism includes a significant amount of fresh monomer reacting with free radicals or other activated species on the film surface. The fact that the amount of hydrocarbon present at 285.0 eV passes through a maximum at 40W could be taken as evidence that (a) the $-\underline{C}H_2-CCl(CN)$ environments present at lower powers give way to other hydrocarbon environments at 40W, (b) elimination of chlorine and nitrogen environments occurs from the monomer in the gas phase prior to film deposition. Option (b) is supported by the fact that the 40W hydrocarbon maximum also corresponds to the nitrogen and chlorine content minima. Obviously, any elimination of either N, as $CN^{\cdot}$ or HCN, or Cl as $Cl^{\cdot}$ or HCl, will cause a marked reduction in the secondary shifts seen not only by adjacent methylene groups (previously to be found at 286.6 eV) but also the quaternary carbon to which both the chlorine and nitrile groups were originally attached (previously found at 288.0 eV). Possible mechanisms of such eliminations have already been mentioned in Chapter One and are reviewed later in the section.

The peak centred at 288.0 eV exhibited apparently erratic behaviour. Since this peak is indicative of carbonyl environments, an overall slight increase in their contribution might be expected as the power increases. However, it is believed to be the =CCl(CN) environments which are mainly responsible for this peak; the erratic behaviour therefore suggests that the number of such environments remaining intact is also erratic - an unexpected result since the chlorine and nitrogen contents go through minima, such that the number of carbon-nitrogen and carbon-chlorine environments might be expected

to show similar behaviour. However, since shifts in ESCA are additive, the presence of adjacent C-Cl, C-CN, CCl-CN or even CCl_2 and CCl_3 groups in the polymer film could cause a number of environments to appear at this higher binding energy. However, in general there is a rough correlation between the carbon-chlorine stoichiometry and the C1s environment at 288.0 eV observed in the plasma polymer films.

For all the films analysed the Cl2p region was run before the carbon C1s since the C-Cl bond proved to be labile - if the Cl2p spectrum was run second, this resulted in degradation of the chlorine signal by some 10-20%, even though the extra exposure time to the incident X-rays involved was only 6 minutes.

Analysis of the Cl2p envelope revealed that, in general, there was only one organic chlorine environment present, centred at 200.4 eV and with two peak components due to $Cl(2p^{1/2})$ and $Cl(2p^{3/2})$. However, on occasion there was evidence of a second environment to a lower binding energy, though very small in intensity. The chemical shift suggests that this environment is in fact ionic in nature, since it is too low to be covalent, such that chloride ions were present in the films. This might be explained by dissociation of the carbon-chlorine bond to give Cl^-, probably via capture of a free electron into a low lying monomer orbital, or else via electron attachment to chlorine atoms, although this is not considered to be the major fragmentation pathway.

The above results and discussion have centred films formed in the coil region of the plasma. Substrates were also placed some 18cm downstream from the coil in the tail region where they were encompassed by the glow volume only at high power input such that it is likely that the plasma polymers deposited did not rely solely on species produced

"in situ" in the glow region, but rather on these active species being swept downstream by the flow rate of the monomer, together with their dissociation products and any other species activated in the tail region itself by electron impact. In general, the highest electron energy distribution function in a plasma - and hence deposition rate - is found in and around the inductance coil itself, since this is where the most rf power is delivered.

A comparison of results for the in coil region with those of the tail region with respect to film stoichiometry showed opposite trends occurring for both nitrogen and, especially, chlorine content, Figure 3.3. Each went through a maximum (Cl at 20W, N at 40W - i.e. where, in coil, it went through a minimum). At low power (7W) the amount of chlorine eliminated from the tail region is very high compared to that in coil, where the films retained virtually all their chlorine content. The N:Cl ratio, effectively the same at 7 and 62W, dropped dramatically at 20W to a minimum, increasing sharply again at 30W to a maximum at 50W. Again, this behaviour is in marked contrast to that found in the coil region. Looking at the hydrocarbon content of the C1s envelope (Figure 3.4b), its behaviour is approximately the opposite to that observed in coil, dropping from a high at 7W to a minimum at 20W (in tune with the maximum in chlorine content) before increasing again to a steady value of about 41%. Similarly, where in coil the 286.6 peak showed a minimum at about 40W, the tail region peak went though a maximum at 30W. However, the 288.0 eV peak was less erratic, showing a maximum at 20W. Thus, both the hydrocarbon and 286.6 eV environment trends appear to be closely linked to that of the chlorine content.

This is again consistent with the arguments outlined above for elimination of chlorine and nitrogen moieties, the former in preference to the latter. Chapter 4 suggests that free radicals are mainly responsible for film deposition, since the introduction of iodine into the system not only largely quenches the glow region, but effectively inhibits plasma polymerization from occurring outside what little glow region remains. This latter information can be interpreted if the plasma polymerization mechanism involves the molecular elimination of HCN and HCl to give the corresponding acetylenes, which in turn give rise to C_2X + H radicals (X = Cl or CN), together with atomic elimination of H, Cl and CN from the monomer. Assuming that these processes occur principally in the gas phase, then film deposition can occur via a free radical mechanism involving conventional polymerization of monomer and acetylenic molecules, together with chain growth both promoted and terminated by the other free radical species present in the plasma (see chapter 5 for a full explanation).

II Variable Flow Rate

Altering the flow rate, F, of the monomer has several effects on a plasma system: (1) increasing F decreases W/FM so that, for high flow rate conditions, the system moves away from being monomer deficient to power deficient; (2) the pressure of the system tends to increase, in turn increasing the number of molecule-molecule and electron-molecule collisions (since the mean free path of the system has been reduced); (3) the average residence time of a given molecule in the coil region, and in the reactor in general, is reduced. Also, since the shorter residence time is the result of an increased average flow velocity,

CHLOROACRYLONITRILE PLASMA POLYMER

Constant W & F, Variable P

FIGURE 3.6 - C1s Envelope

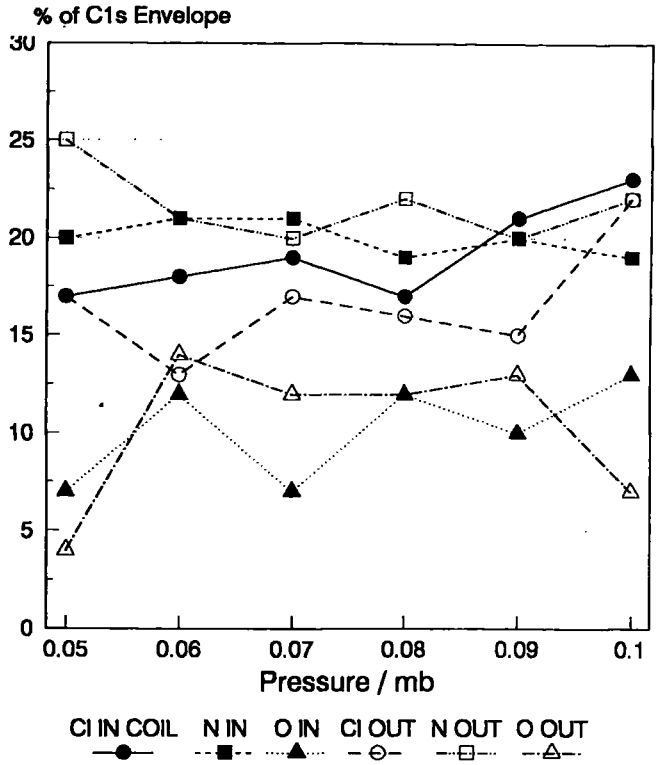

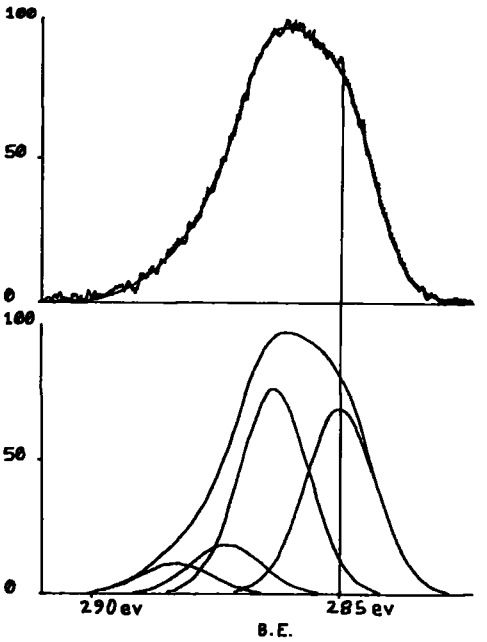

Figure 3.7 C1s Envelope Chloroacrylonitrile Plasma Polymer

CHLOROACRYLONITRILE PLASMA POLYMER

Atomic Ratios - Constant W, Variable F

FIGURE 3.8

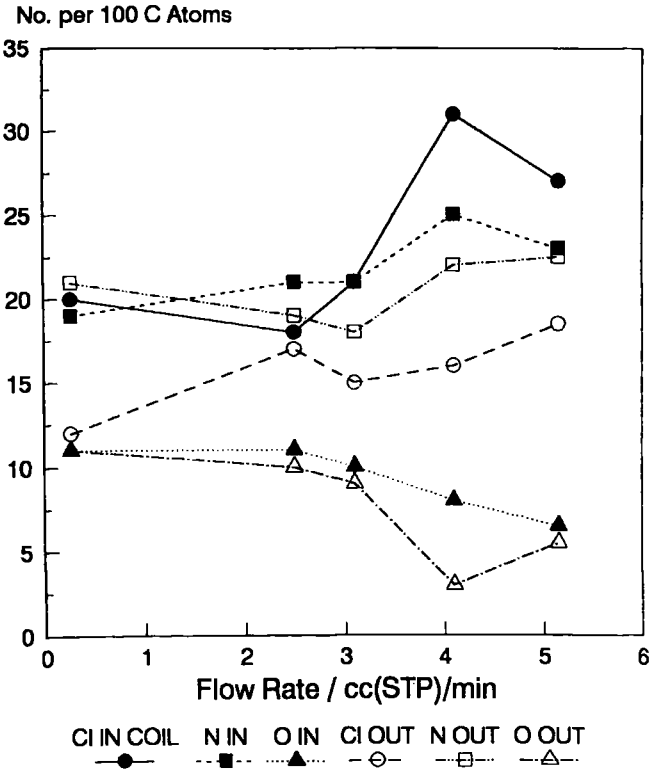

species activated upstream (and in coil in particular) will flow further downstream than previously, since their lifetimes will remain largely unaltered except perhaps by the increased chances of collisional deactivation.

The effect of pressure in the deposition chamber was investigated for a fixed monomer flow input by synthesising a series of films using a constant 6W power and fixed flow rate of monomer throughout. The system pressure was altered from 0.05mb to 0.1mb, in steps of 0.01mb, by altering the pumping efficiency of the system (this was achieved by using the Young's tap between the reactor chamber and cold trap to restrict the flow rate out of the system as necessary, and hence its pressure). The results, Figure 3.6, showed that the overall stoichiometry altered slightly throughout the series. However, the percentage change in atomic ratios was 10-15%, ie within the expected experimental error found for the system. The C1s envelope for the in coil region showed an increase in the contribution from the component centred at 287.5 eV with increasing pressure, likely to result from a higher chlorine content of the film with respect to carbon, and so complementing the slight increase in the latter observed for the Cl / C ratio noted at 0.09 and 0.1 mb. Hence, at least for the in coil region, the chemical composition of the film does appear to be affected by an increase in pressure in the system. A similar trend was not discernible in the C1s envelope for the film deposited out of coil, although a high chlorine content at 0.1 mb was matched by a sudden increase in the 287.5 eV component. Further evidence for such a pressure effect was found in the variation of chemical composition of

plasma polymers deposited using differing monomer flow rates into the system, since an increase in F was found also to increase the pressure.

Overall, the existence of a pressure effect in the film deposition process would suggest a role for collisional deactivation processes in plasma polymerization. This in turn would indicate that the mechanism involves vibrationally excited ground states (which are easily deactivated by collision) caused by initial electron impact excitation of, for example, a singlet state that then undergoes intersystem crossing, Evidence that such vibrationally excited ground states can give rise to thin film formation is found in the fact that plasma polymer-like materials can be obtained via surface photopolymerization. Since the mechanism of thin film formation in the latter is believed to involve such a ground state (see chapter 5), then a similarity in the deposition mechanisms between the two systems can be inferred.

The variation of chlorine and nitrogen content of the plasma polymer films with increasing flow rate can be seen in Figure 3.8, which shows that both contents increase overall with F, both in coil and in the tail region. The oxygen content of the film decreases, probably reflecting the reduced ratio with respect to the number of monomer molecules present in the deposition chamber at higher flow rate, and hence the decreased chance of incorporation into the polymer film as it is formed. The following trends were observed :

(i) both chlorine and nitrogen contents (in and out of coil respectively) appeared to go through a minimum at mid flow rate;

(ii) the chlorine content out of coil was less than that in coil;

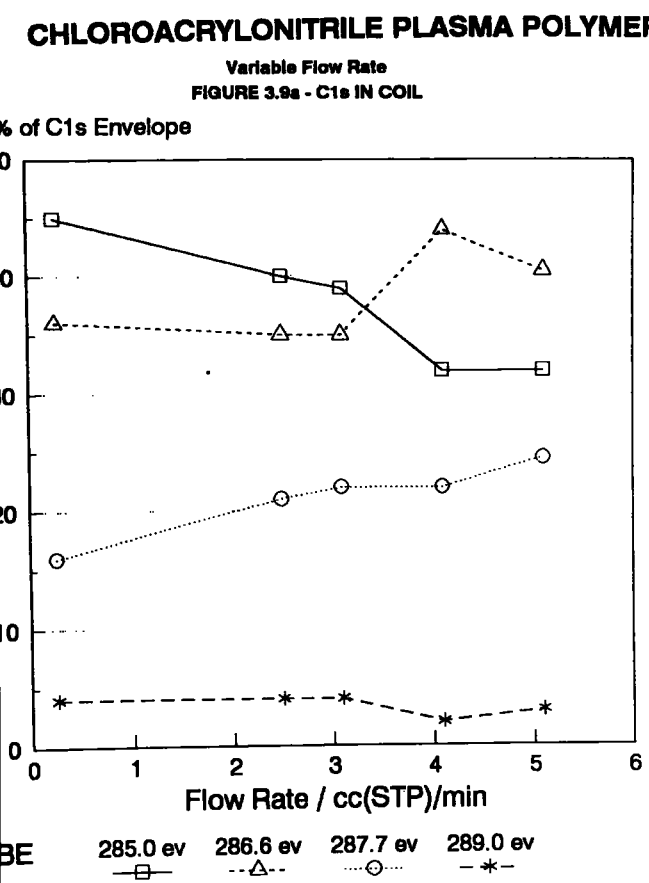

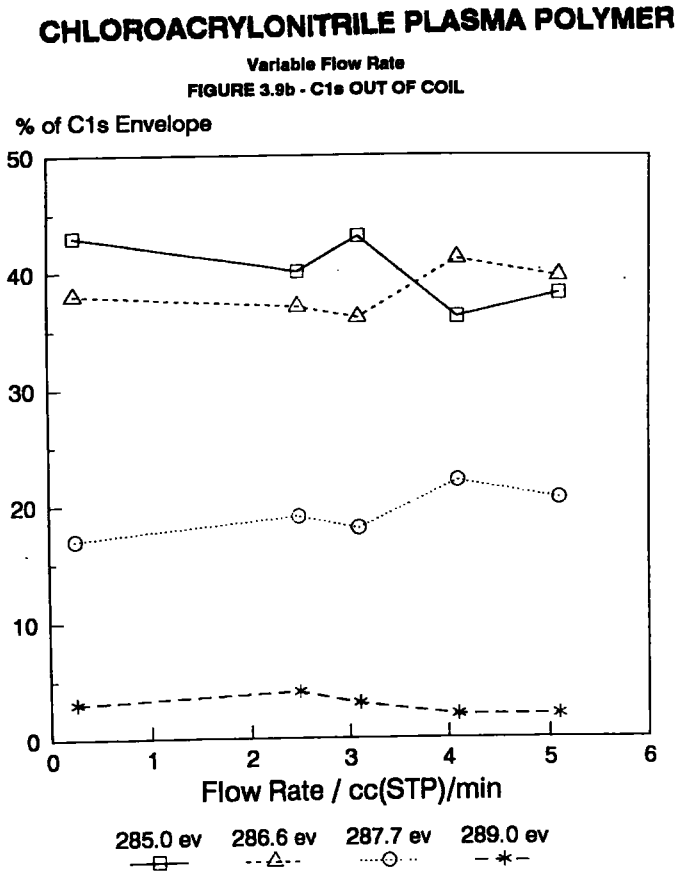

F / cc(STP)/min	0.3	2.1	3.1	4.1	5.1
IN COIL	1.02	0.86	0.99	1.27	1.14
OUT OF COIL	0.57	0.90	0.96	0.71	0.86

TABLE 3.2 N / Cl Ratio - Variable Flow Rate

(iii) at low flow rate there was some evidence for a second (presumably ionic) environment in the Cl2p envelope; this was seen only for the lowest flow rate used;

(iv) a study of the N/Cl ratio (Table 3.2) shows that erratic behaviour occurred in coil, whilst out of coil a maximum was found for a flow rate of some 2-3cm^3 (STP)/min. Although the absolute flow rates measured (using an XY recorder) will have been inaccurate to some extent due to the method used, it is the relative trends which are important. A variation of elemental composition of the film with respect to flow rate is thus shown for chloroacrylonitrile, since the overall percentage changes are either in excess of 50-100% or else hardly at all. Examination of the Cls envelope supports this, particularly for the in coil region, the overall trends being shown in Table 3.3.

Thus, for chloroacrylonitrile at least, there is a dependence of the chemical nature of the plasma polymer films on both the power input to the system and on the flow rate of the monomer. Furthermore, the trend for the nitrogen content in the coil region varies with power in a similar way to that observed in acrylonitrile plasma polymers, suggesting that there may be a structural cause for the observed findings. Of particular interest are the excited species involved in the plasma, and the nature of the depositing species if different from those above.

IN COIL

BE/eV	Trend	% Change Between Extremes
285.0	General Decrease	65
286.6	Maximum	29
288.0	General Increase	83
OUT OF COIL		
285.0	Erratic Behaviour	26
286.6	Little Change	12
288.0	Initial Increase Only	53

TABLE 3.3

Variable Series - C1s Envelopes

Chapter One made reference to several factors that should influence or even control the polymerization process, namely (i) the possible nature of the excited species involved, especially with respect to (ii) the thermochemistry and possibly symmetry control of the dissociation fragments and patterns. A search of the literature reveals that, for electronically excited states (as opposed to ions) of ethylenes, the use of Rydberg, as well as valence shell, orbitals can occur, the dissociation of which can give rise to molecular elimination of HX and to biradicals of the type :C=CXY and X˙C=C˙Y.[9,10] The latter immediately rearranges to the respective ethyne, the former - being a $^3B_2$ triplet - rearranges more slowly (typically requiring collisional deactivation to the ^1A state as an intermediate step)[11] and hence might

be able to undergo typical radical reactions - and hence participate in polymer formation. Both rearrangements could account for the large amount of ethynic compounds which are often seen as by products of the plasma polymerization process.[1] Indeed, Yasuda,[1] and other workers considered that ethyne was an important precursor for polymerization, Clark and Shuttleworth[12] suggesting that elimination of HF from the radical cation $CF_2{=}CH_2^{+\cdot}$ to give $HC{=}CH^{+\cdot}$ was the important step prior to the actual polymerization process. Both Chapters One and Two argued against the importance of the radical cation, but <u>not</u> of the possible importance of ethyne as a precursor to film formation. ESCA data presented so far in this Chapter suggest that elimination of HCl should occur preferentially, and this has indeed been observed for the electrical glow discharge of chloroacrylonitrile to give cyanoethyne, $HC{\equiv}CCN$.[7] However, elimination of HCN was also expected. Since little was known about the actual fragmentation pathways of chloroacrylonitrile ions, an in-house mass spectrometric investigation was undertaken to probe the matter further.

III <u>Mass Spectrometric Investigation</u>

2-chloroacrylonitrile mass spectra were run on a VG Analytical machine equipped with a Winchester Disk Drive System. Output of results was in both graphic and tabular form. Increasing incident electron energies were used to study the (increasingly complex) fragmentation patterns. The energies quoted are approximate, but within $\pm$ 0.5 eV (see Mass Spectra Sequence A).

At the ionisation potential, only the molecular ion peaks due to the two chlorine isotopes are visible (10-11 eV). However, on raising

the electron energy to 12 eV the radical cation fragment C_3H_2N appeared (m/e 52), indicative of C-Cl bond scission (A2). There was no sign of any m/e 26 peak until 14+ eV, together with m/e peaks at 60 and 62. The former was found by a high resolution technique to be due to acetylene, whilst a peak at m/e 27 would be indicative of elimination of HCN. Similarly, a peak at m/e 51 due to C_3HN shows that elimination of HCl also occurs. The question arises as to whether eliminations are stepwise or molecular in nature. The absence of peaks at m/e 61 and 63 at this energy (14 eV) suggests that the fragmentation pathway for loss of HCN is <u>not</u> stepwise, otherwise scheme 1 would occur :

$$\underset{\text{m/e 87, 89}}{[CH_2CCl(CN)]^{+\cdot}} \xrightarrow{-CN^{\cdot}} \underset{\text{m/e 61/63}}{[CH_2CCl]^{+\cdot}} \longrightarrow \underset{\text{m/e 60/62}}{[CHCCl]^{+\cdot}}$$

Scheme 1

Rather, molecular elimination seems more likely, the resulting diradical rapidly rearranging ($<10^{-10}$s) to the chloroacetylene :

$$CH_2CCl(CN) \xrightarrow{-HCN} [CHCCl]^{\ddagger\cdot\cdot} \longrightarrow [HCCCl]^{+\cdot}$$

Scheme 2

It is not until an electron energy of 20 eV that m/e 61 appears, whilst both m/e 61 and 63 are both clearly visible at 70 eV. This suggests that molecular elimination of HCN occurs at a lower electron energy (14 eV, scheme 2) than the stepwise elimination of $CN^{\cdot}$ and H^{+} (20+ eV, scheme 1). Note also that the presence of peaks at m/e 86 and 85 in the 70eV spectrum are compatible with the elimination of H and H_2 from the molecular ion respectively, whilst the peak at m/e 26 could

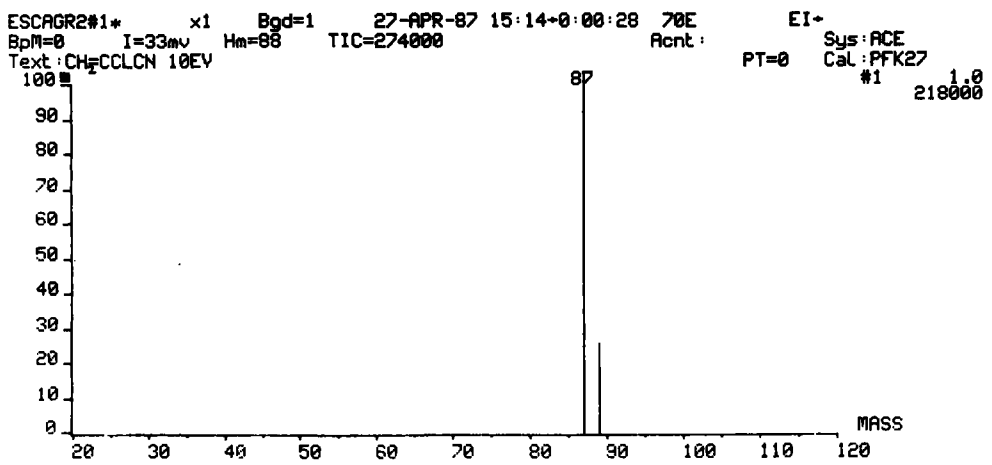

A1

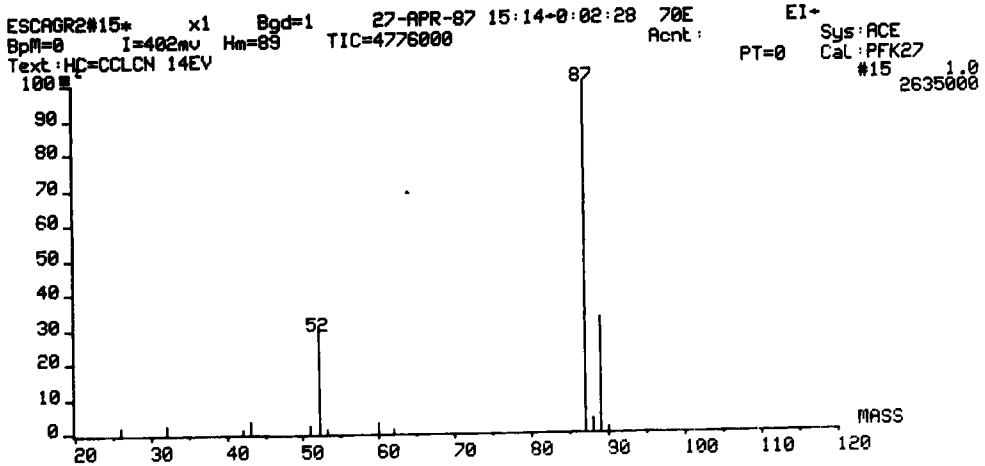

A3

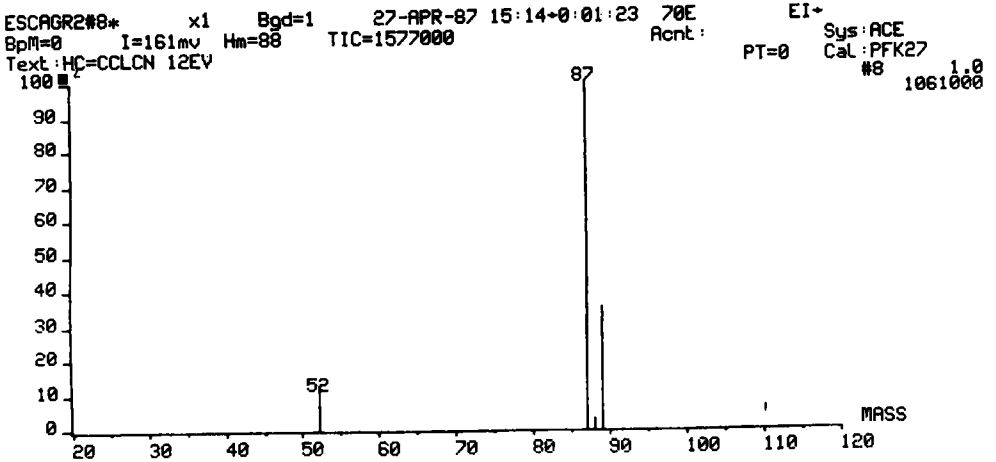

A2

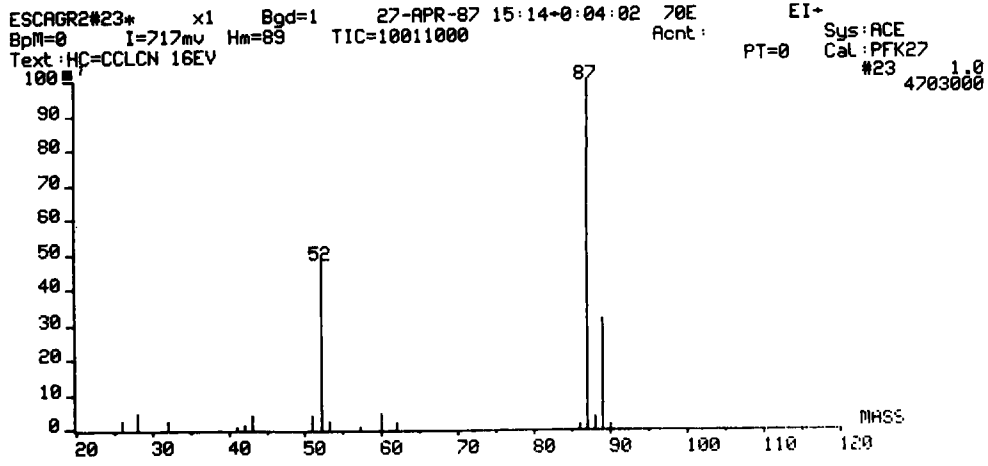

A4

MASS SPECTRA : SEQUENCE A

CHLOROACRYLONITRILE

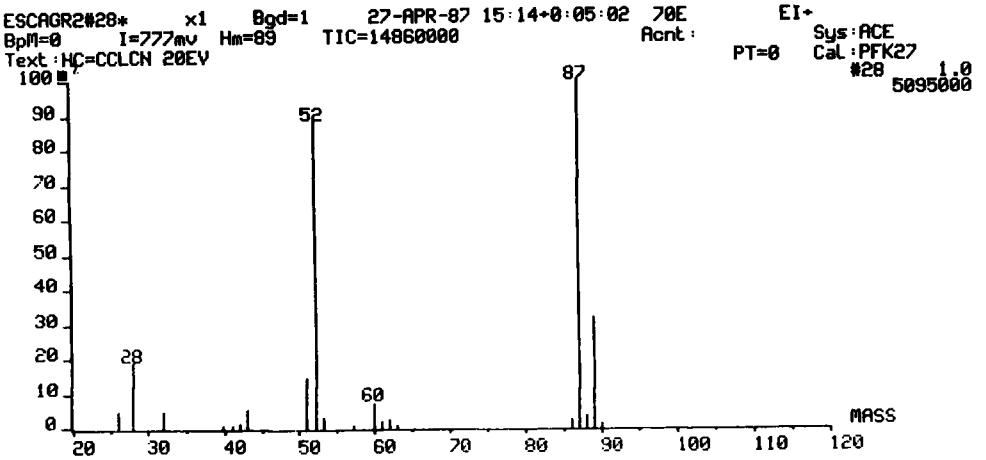

A5

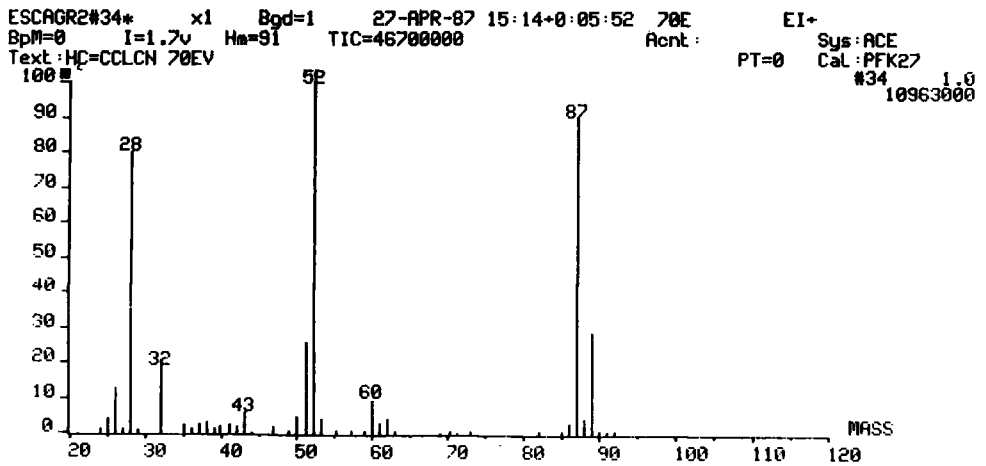

A6

possibly also be due to (molecular) elimination of ClCN to give the diradical $(H_2C{=}C)^{+\cdot\cdot}$. A precedence for this has been seen in the loss of ClCN and FCN in the electrical discharges of compounds containing halogens, carbon and nitrogen.[7]

The fragmentation pattern at 14 eV shows the presence of peaks at both m/e 51 and 52, as well as m/e 53. The first of these (m/e 51) could correspond to cyanoacetylene, HCCCN. The peak at m/e 52 has already been assigned to $(C_3H_2N)^{+\cdot}$, resulting from the loss of $Cl^{\cdot}$ from the parent molecule, and is by far the most abundant ion in the spectrum. Hence, further loss of H to give the acetylene is possible here, whilst addition of H to give acrylonitrile, $(CH_2CHCN)^{+\cdot}$, might be responsible for the peak at m/e 53.

Acrylonitrile and methacrylonitrile were also studied as a function of increasing electron incident energy. For acrylonitrile, Sequence B, the onset of fragmentation occurred at above about 10 eV such that, at 12 eV. the principle fragments are C_2H_2 (m/e 26) and loss of H to give C_3HN (m/e 51) probably as $[CH_2CCN]^{+\cdot}$. 15 eV showed the presence of further peaks at m/e 27 and 28, which become more pronounced at 20 eV. These could be due to loss of CN^{-} to give $C_2H_3^{+}$ (HCN^{+} is thermodynamically less preferable[13]) and formation of CH_2N^{+} respectively. By the time the electron energy is increased to 70 eV, the m/e 26 peak is more abundant than the molecular ion peak with small, but not insignificant, ion peaks occurring at m/e 36, 37, 38 and 39. Note here an immediate difference between acrylonitrile and chloroacrylonitrile - whereas the latter preferentially fragments $Cl^{\cdot}$ to give $[CH_2CCN]^{+\cdot}$, acrylonitrile appears to favour loss of HCN at higher energies to give acetylene. This occurs via molecular elimination and/or loss of H (indicated by the strong peak at m/e 52) followed by loss of CN to give acetylene after rearrangement :

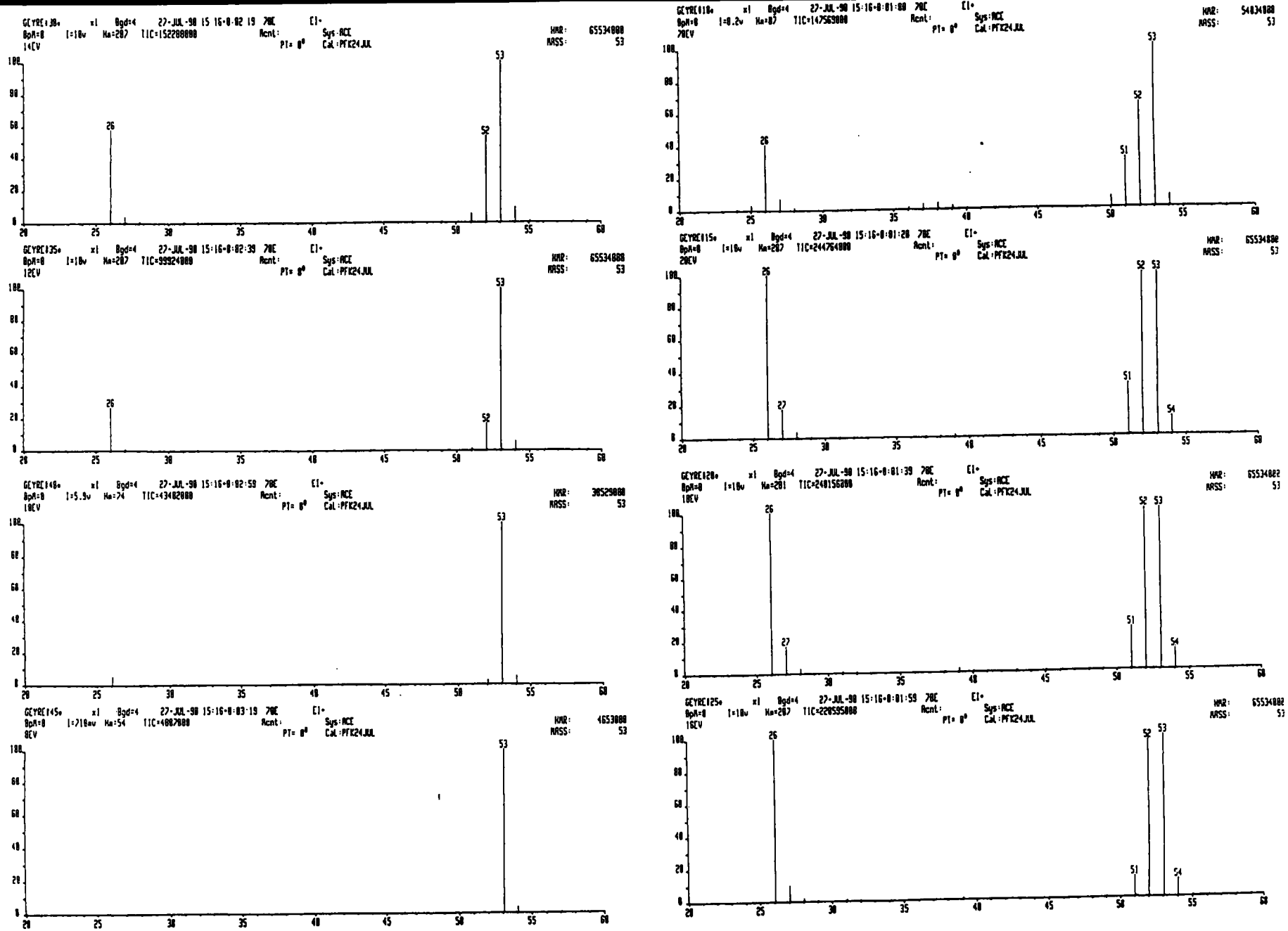

MASS SPECTRA SEQUENCE B : ACRYLONITRILE

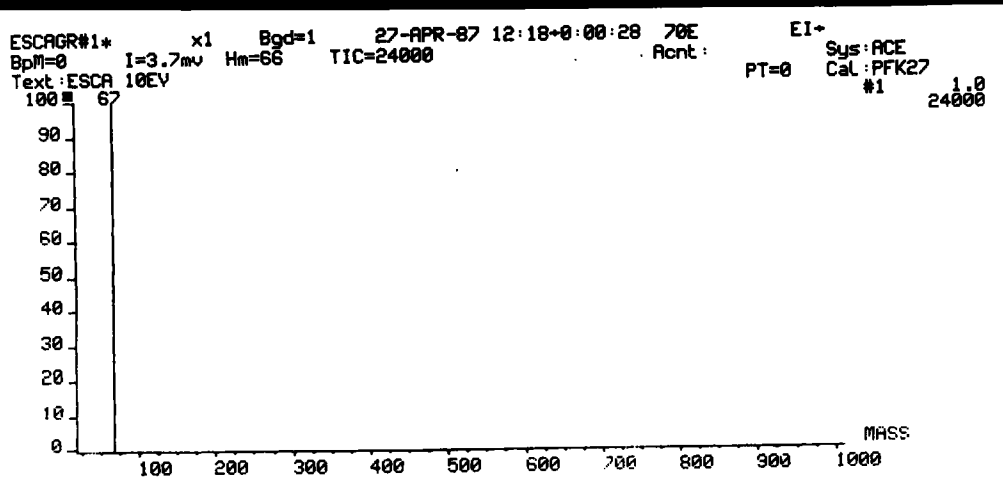

C1

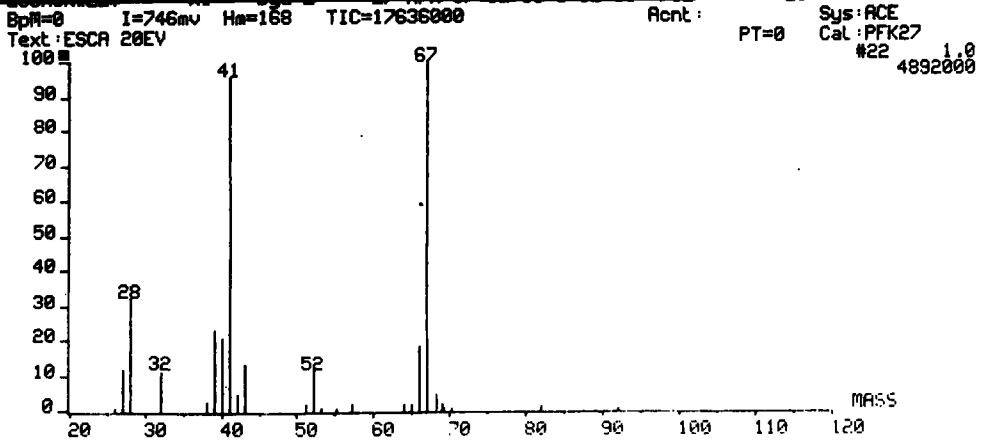

C3

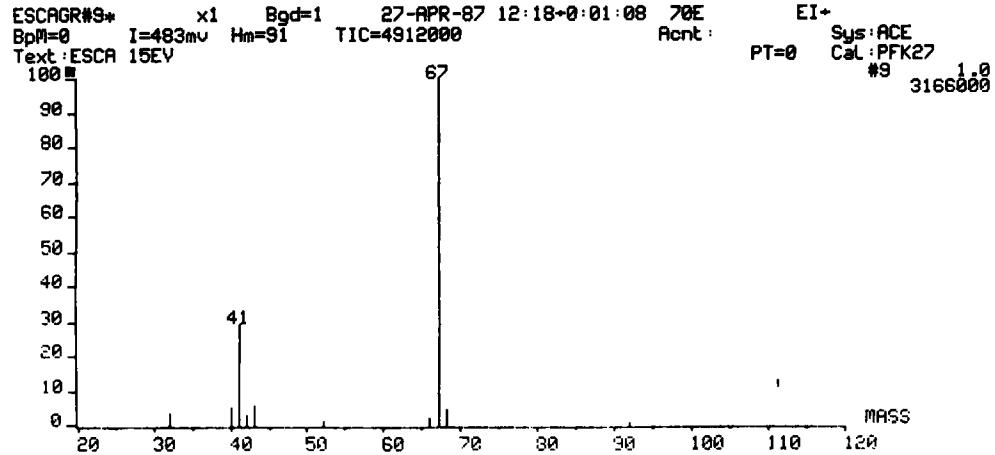

C2

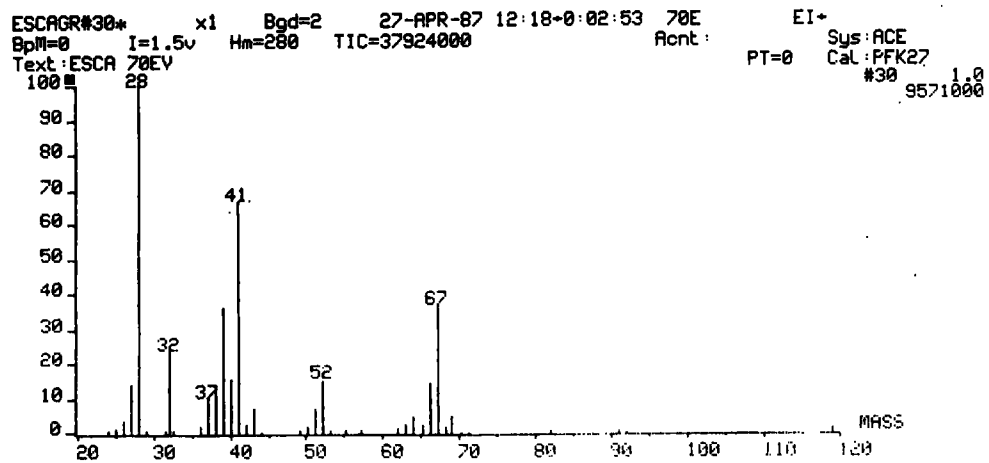

C4

MASS SPECTRA SEQUENCE C

METHACRYLONITRILE

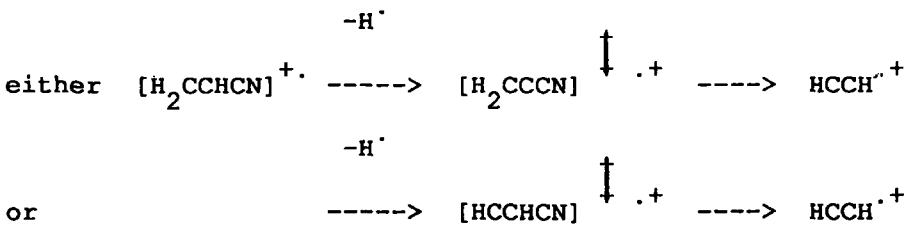

Methacrylonitrile also fragments, Sequence C, to give an ion peak at m/e 26, but not until about 15 eV. If molecular elimination occurs here, the loss of either HCN, CH_4 or MeCN would be seen, corresponding to resultant fragments HCCMe (m/e 40), HCCCN (m/e 51) and HCCH (m/e 26) respectively after subsequent rearrangement. The last of these ion peaks is observed; formation of acetylene via loss of MeCN is therefore possible. However, the appearance of m/e 41, also at 15 eV and corresponding to $[H_2CCMe]^{\cdot+}$, suggests that loss of CN·also occurs. Alternatively, m/e 41 could be attributed to the fragment $C_2H_3N^+$. Molecular Orbital calculations show that this fragment is more stable than $C_3H_5^+$ by over 2 eV, and so is the fragment proposed by Willett and Baer, who similarly proposed that for both methacrylonitrile, and allyl cyanide, m/e 39 corresponds to C_2HN^+.

Overall, Willett and Baer examined the thermochemistry and dissociation dynamics of four nitrogen containing compounds : methacrylonitrile, pyrrole, cyclopropyl cyanide and allyl cyanide, all structural isomers of C_4H_5N.[13] The overall possible fragmentation processes are given in Table 3.4, with a list of appearance potentials for the various ions in Table 3.5. The energy range concentrated on was 8-14 eV, the results of which for methacrylonitrile are presented in Table 3.11. Van Thuijl et al have also examined the collision induced dissociation of butyronitrile and crotonitrile. Both were found to

produce an ion peak at m/e 41, thought, once again, to correspond to ketenimine (1+).

In the case of the C_4H_5N compounds, all four reaction rates for

$$C_4H_5N^+ \longrightarrow C_2H_3N^+ + C_2H_2 \quad (1)$$

were found to be identical. This was interpreted in terms of all four isomers rearranging to the common precursor before fragmentation, though this is thought to occur only in the metastable energy range (12.9 - 13.4 eV) - at higher energies the fragmentation reactions probably directly compete with any initial Isomerization pathways.[13] Statistical theory calculations are consistent with the assumption that this isomerized precursor has a pyrrole structure.[13]

70eV

$$C_4H_5N^+ \longrightarrow C_2H_3N^+ + C_2H_2 \quad (1)$$

$$C_3H_4^+ + HCN \quad (2)$$

$$C_2H_2N^+ + C_2H_3 \quad (3)$$

$$C_3H_3^+ + CH_2N \quad (4)$$

$$C_2H_2N^+ + C_3H_3 \quad (5)$$

8-14eV

$$C_4H_5N^+ \longrightarrow C_4H_4N^+ + H \quad (6)$$

$$C_3H_2N^+ + CH_3 \quad (7)$$

$$C_2H_3^+ + C_2H_2N \quad (8)$$

TABLE 3.4 Possible Fragmentation Processes of Structural Isomers of C_4H_5N.

COMPOUND	ION FRAGMENTS						
	$C_4H_4N^+$	$C_3H_2N^+$	$C_2H_3N^+$	$C_3H_4^+$	$C_3H_3^+$	CH_2N^+	$C_2H_3^+$
PYRROLE	12.85	12.5	11.75	12.00	12.60	12.40	13.60
CH_2CMeCN	12.55	12.20	11.65	11.75	12.30	12.05	13.20
CH_2CHCN	12.30	12.05	11.10	11.50	12.10	11.90	12.90

NOTE : Appearance energies in eV.

TABLE 3.5 Appearance Potentials for Various Ions of C_4H_5N.

$[CH_2=C=NH]^+$. The implications of this for plasma polymerization are various - in particular the above mass spectrometric studies show that (i) some 12+ eV are required to cause formation and fragmentation of ions in the spectrometer - and hence presumably also in the plasma; and (ii) ion fragmentation occurs via dissociation pathways involving much rearrangement. Thus, any involvement of ions in the polymerization process will cause deposition of a film somewhat different from that expected via "conventional" polymerization.

3.4.2 Methacrylonitrile

The substitution of the chlorine moiety found in chloroacrylonitrile by a methyl group to give methacrylonitrile changes the relative molecular mass, M - hence differing behaviour between the two analogues should occur for the same conditions of W/F. In order to test this three series of experiments were performed, examining the effects of power and flow rate on the chemical composition of methacrylonitrile plasma polymers.

I. Variable Power

The influence of power in the range 3-65W was studied at two different flow rates - 0.42 ± 0.06 cc (STP) min^{-1} and 1.3 ± 0.25 cc (STP) min^{-1}. The results are presented in graphical form (Figures 3.10 to 3.15).

Results for F=1.3 cc min^{-1} showed little difference in behaviour of the nitrogen content (as shown by the C:N ratio) for the in-coil and tail regions, both showing a minimum at 17W, whilst the amount of oxygen incorporated was greater in coil, probably reflecting the creation of a higher degree of unquenched free radical sites in this position compared to the film deposited in the tail region. The overall oxygen and nitrogen content of the films deposited at 0.42 cc min^{-1} monomer flow rate is greater than at 1.3 cc min^{-1}. The former was expected, since the observed leak rate was similar in both cases, such that there was a higher concentration of oxygen molecules in the plasma at 0.42 than at 1.3 CC (STP) min^{-1}, leading to a higher level of incorporation of oxygen in the polymer film. The N:C ratio showed little difference between the two regions for either flow rate until high power, when (for 0.42 cc (STP) min^{-1}) a maximum occurred at 52W, followed by a sharp drop at 63W. This contrasts to the behaviour for high flow rate which saw little change over the whole power range.

In the C1s envelopes (Figures 3.11 and 3.14), the absence of a chlorine functionality reduces the contribution from the 287.8 eV peak, previously due to Cl-C-CN and C=O, but now due to carbonyl alone. This peak, together with that at 289.2 eV ($-CO_2-$) appears to account for the majority of the oxygen content. The hydrocarbon and quaternary carbon environments (centred at 285.0 eV) show some difference in behaviour

METHACRYLONITRILE PLASMA POLYMER

Variable W, F=0.4cc(STP)/min

FIGURE 3.10 - Atomic Ratios

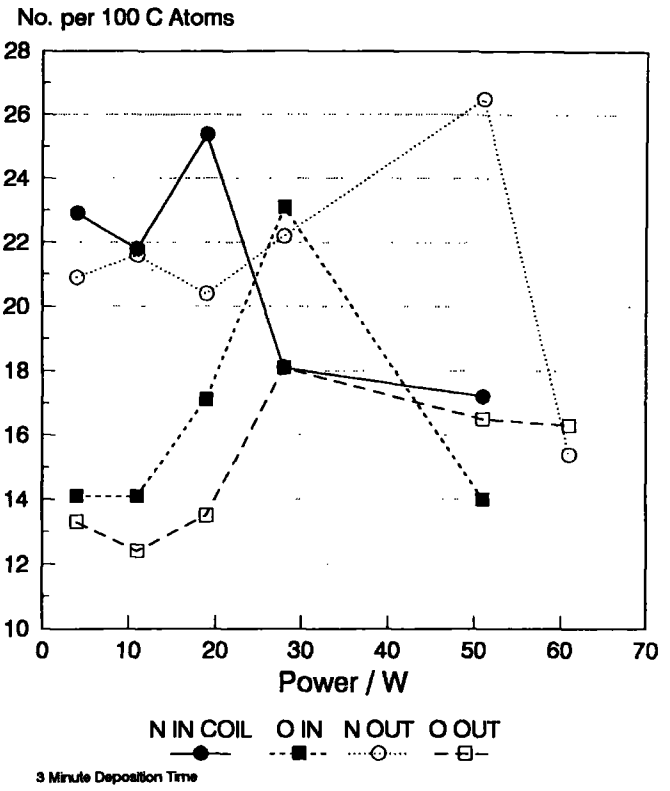

ETHACRYLONITRILE PLASMA POLYMER

Variable W, F=0.4cc(STP)/min

FIGURE 3.11 - C1s Envelope

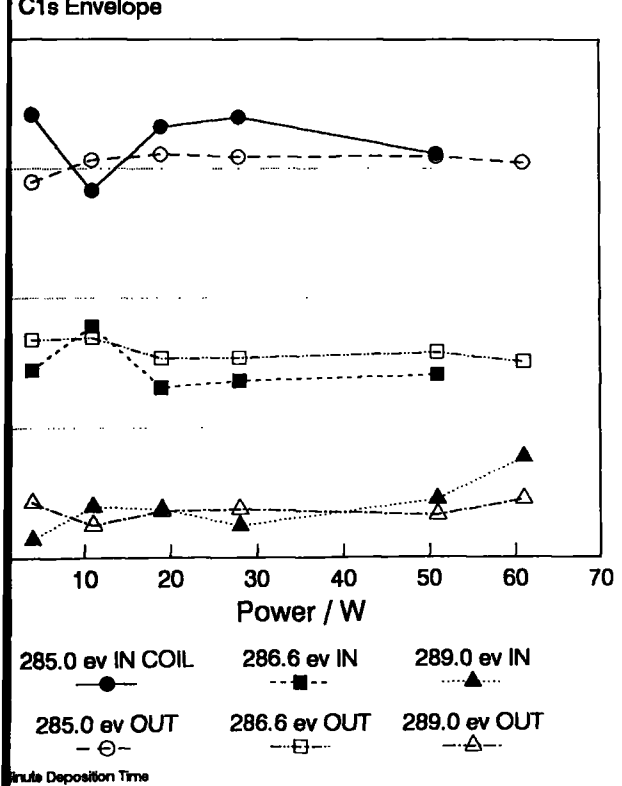

METHACRYLONITRILE PLASMA POLYMER

Variable W, F=0.4cc(STP)/min

FIGURE 3.12 - N1s Envelope

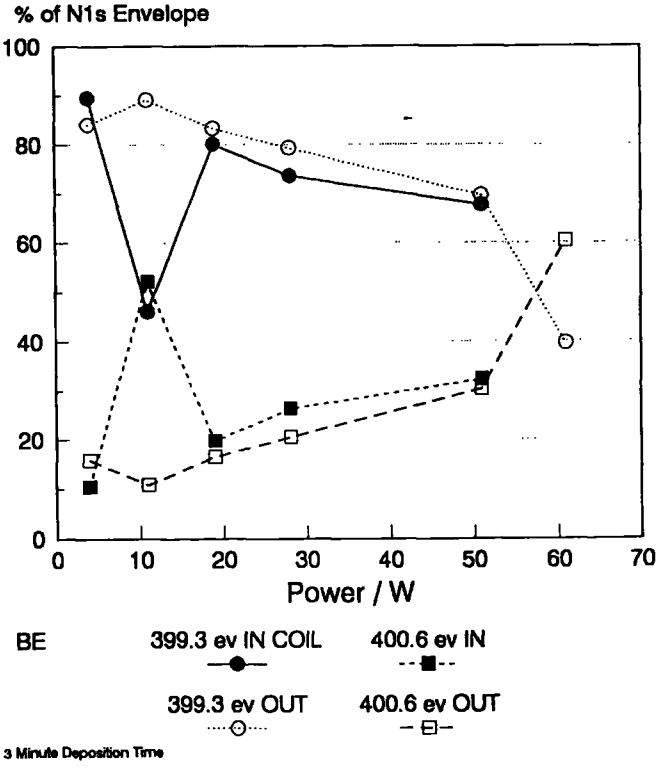

METHACRYLONITRILE PLASMA POLYMER

Variable W, F=1.3cc(STP)/min

FIGURE 3.13 - Atomic Ratios

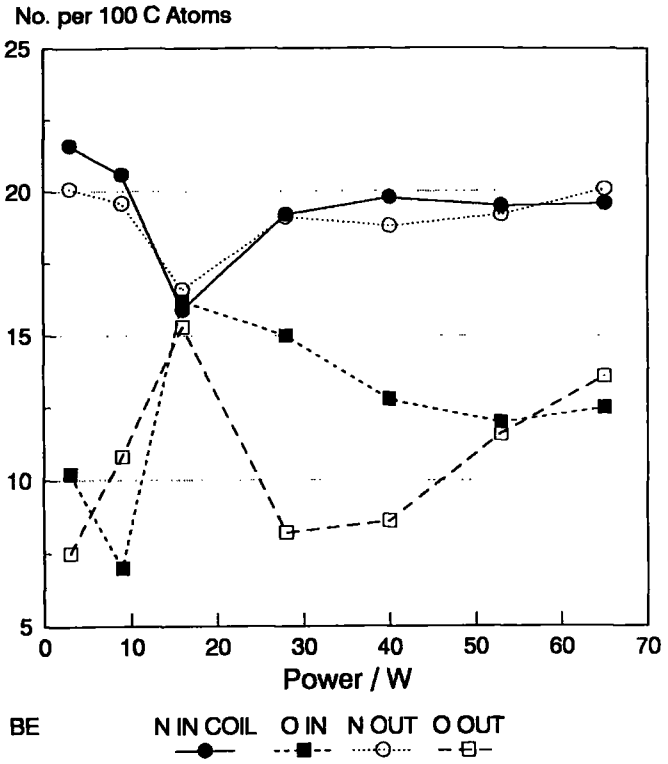

METHACRYLONITRILE PLASMA POLYMER

Variable W, F=1.3cc(STP)/min

FIGURE 3.14 - C1s Envelope

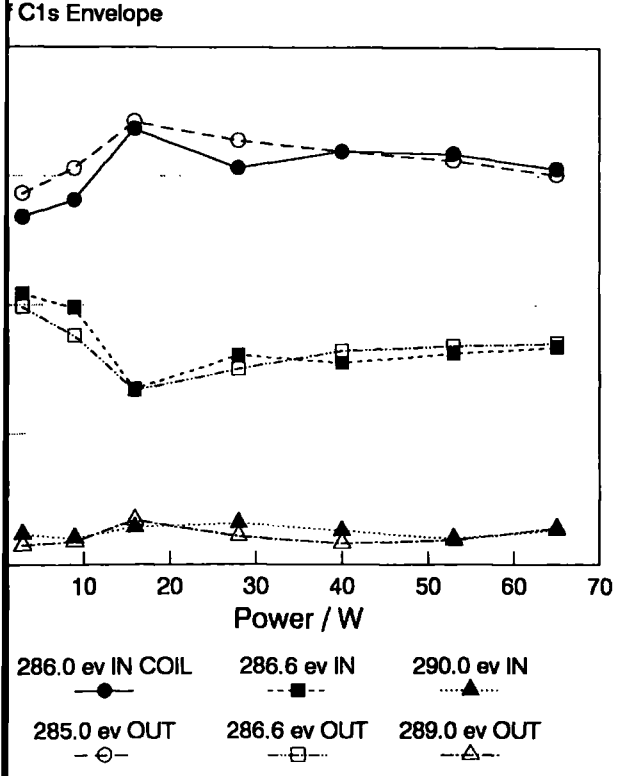

METHACRYLONITRILE PLASMA POLYMER

Variable W, F=1.3cc(STP)/min

FIGURE 3.15 - N1s Envelope

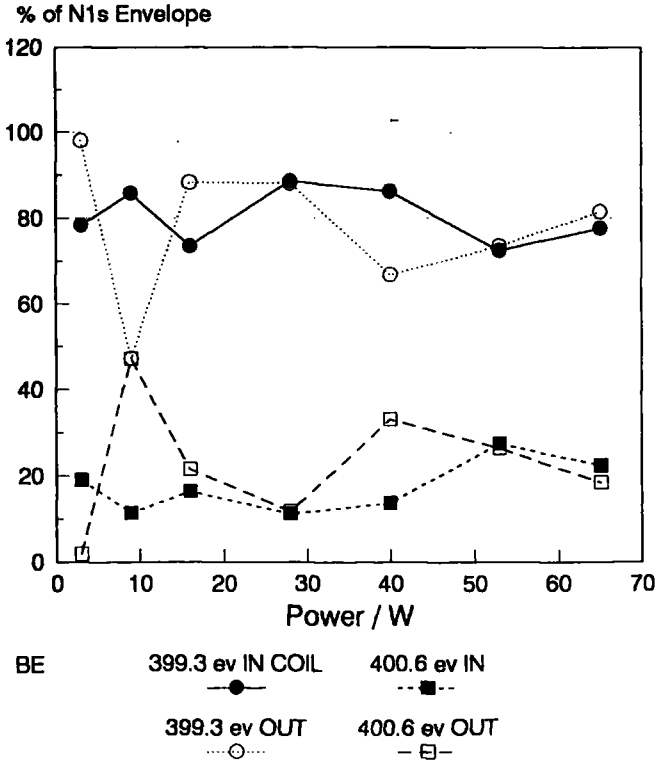

between the two flow rate series, with that at 0.42 cc (STP) min^{-1} being somewhat erratic, that at 1.3 cc (STP) min^{-1} exhibiting a maximum at 17W corresponding to the minimum in the nitrogen content obtained by elemental stoichiometry analysis, and hence probably due to the resultant higher number of carbon atoms in the film not directly bonded to either nitrogen or oxygen. The 286.6 eV peak - corresponding mainly to C-N, C=N, C≡N and C-O environments, also showed a difference between the two flow rate series. In particular, the higher flow rate caused a much higher contribution at 286.6eV for lower powers (3, 10W), dropping to a minimum at 17W (again corresponding to the minimum in overall nitrogen content) before rising again to a plateau of 32-34% of the overall C1s envelope between 27-63W. In contrast, at 0.42 cc (STP) min^{-1}, a maximum occurs at only 10W, the percentage contribution to the total C1s envelope being consistently less throughout.

The N1s envelopes (Figures 3.12 and 3.15) showed overall erratic behaviour with respect to the two peak components. The peak separation, at 1.3 eV, was less than that observed for chloroacrylonitrile (average 1.5eV), possibly due to the influence of methyl groups adjacent to nitrile groups in the system rather than electronegative chlorine substituents. More surprising was the occasionally high contribution from the higher binding energy component - for example, at 10W the contribution from both N1s peaks is approximately equal, showing that there is a very much higher reaction of the carbon - nitrogen triple bond to give -N-C and -N=C- environments. This demonstrates the importance of the N1s envelope as a source of information since the C1s envelope alone is thus demonstrated to be unable to differentiate between C-N and C=N environments in the films.

Overall, a study of methacrylonitrile over the power range 0 to 65W at two different flow rates shows both similarities and differences between the two sets of results. In particular, the effect of higher power input to the system appears more marked than the increase in flow rate - unsurprising, since 65W is almost a 22 fold increase over the lowest power setting used (3W), whereas the increase in flow rate was only threefold. Hence the parameter W/F is power dominated. Differences between the nature of the films produced in the coil and tail regions once again show that the balance of species leading to deposition in each case probably differs - presumably as a result of the change in the electron energy distribution of the system, which in turn controls the nature of the excited state, and hence depositing, species formed in the gas phase. These will include ions and excited states (accessed via electron impact); the fragmentation patterns of these will give rise to, amongst others species, radical species.

Overall, the influence of M in W/FM is felt in a) the differing nature of the thermodynamics of the system, b) the exact nature of the excited state species and dissociation pathways found, c) the kinetics and deposition rate of the system, since these are obviously dependent on the monomer used. The differences between the plasma polymers of chloro- and methacrylonitrile are thus attributable to the substituent effect of changing the chlorine atom in CH_2=CClCN for a methyl group. In particular, whereas the gas phase chemistry of chloroacrylonitrile appears to be dominated by the presence of a chlorine atom directly attached to an unsaturated carbon, in both acrylo- and methacrylonitrile the absence of such a halogen (and its negative inductive effect) means that scission of the C-CN bond, or else else

elimination of HCN, preferentially occurs, depending on the actual energy input to the system.

II. Variable Flow Rate

Two separate experimental series were carried out to examine the reproducibility of results, as well as the possible influence of flow rate on the chemical composition of the films formed.

In addition to examination of the usual "in coil" substrate position on top of the glass slide, an extra strip of aluminium foil was placed on the floor of the reactor directly beneath the first position. The location of the substrate in the tail region was left unaltered. The results for both experimental series are displayed in Figures 3.16 to 3.19.

(i) IN COIL, there was no significant variation in nitrogen content of the deposited film over the flow rate range studied. Results between the two series were within $\pm$ 15%, i.e. within the typical experimental error observed for these ESCA analyses. The sample position underneath the glass slide showed slightly differing behaviour between the two series - although both had a similar nitrogen content over the majority of the flow rate range, an initially lower value was found at 0.3cc(STP) min^{-1} for the repeat series. The oxygen content fluctuated throughout.

Trends in the C1s envelopes were similar for the two experimental series, absolute values differing slightly. The 285.0eV peak showed an overall decrease as the flow rate increased, whilst the contribution at 286.6 eV rose. This suggests that, while the overall nitrogen content of the films does not depend on flow rate, the distribution of the

METHACRYLONITRILE PLASMA POLYMER

Variable F, W=23w

FIGURE 3.16 - Atomic Ratios

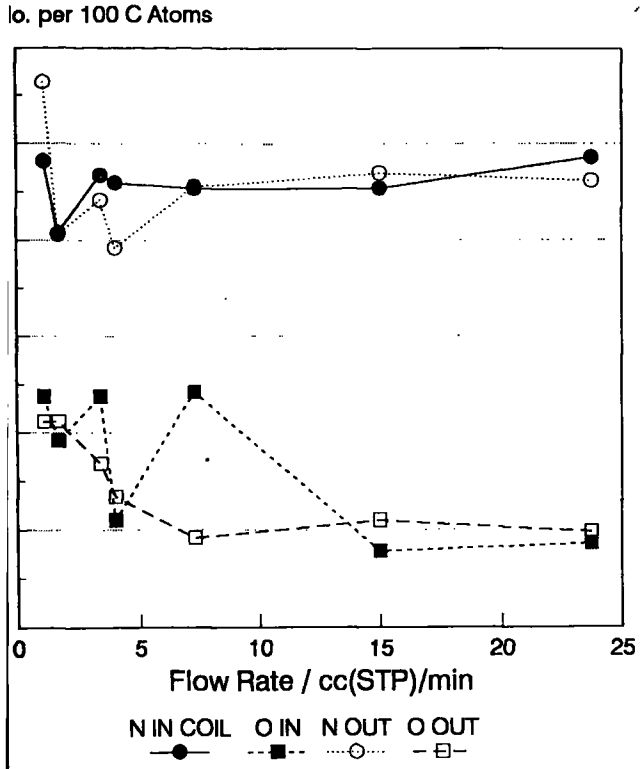

METHACRYLONITRILE PLASMA POLYMER

Variable F, W=23w

FIGURE 3.17 - C1s Envelope

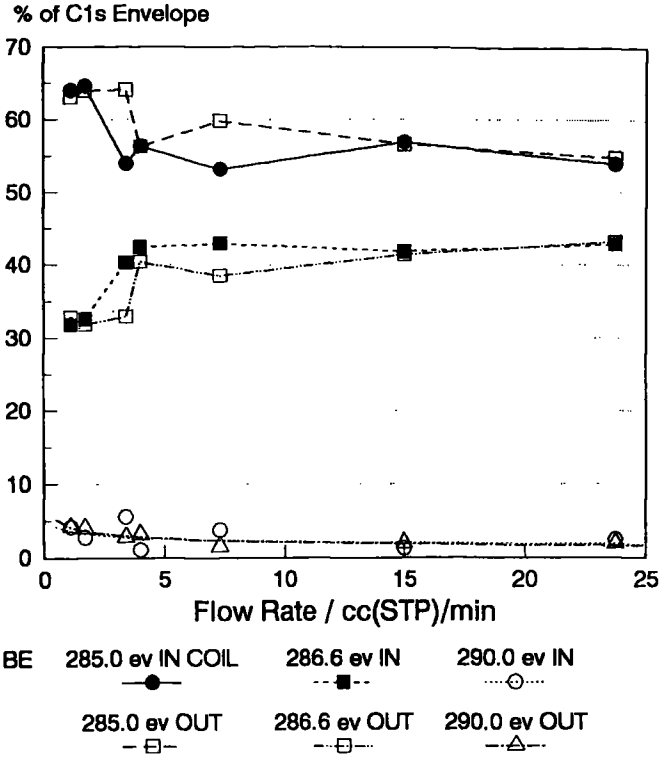

METHACRYLONITRILE PLASMA POLYMER

Variable F, W=23w

FIGURE 3.18 - N1s Envelope

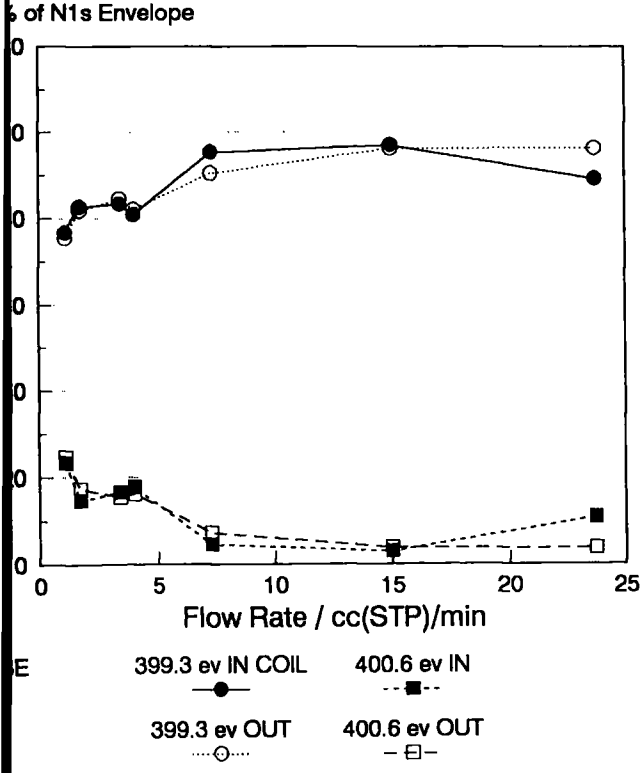

METHACRYLONITRILE PLASMA POLYMER

Variable F, W=23w

FIGURE 3.19 - Atomic Ratios & C1s Envelope

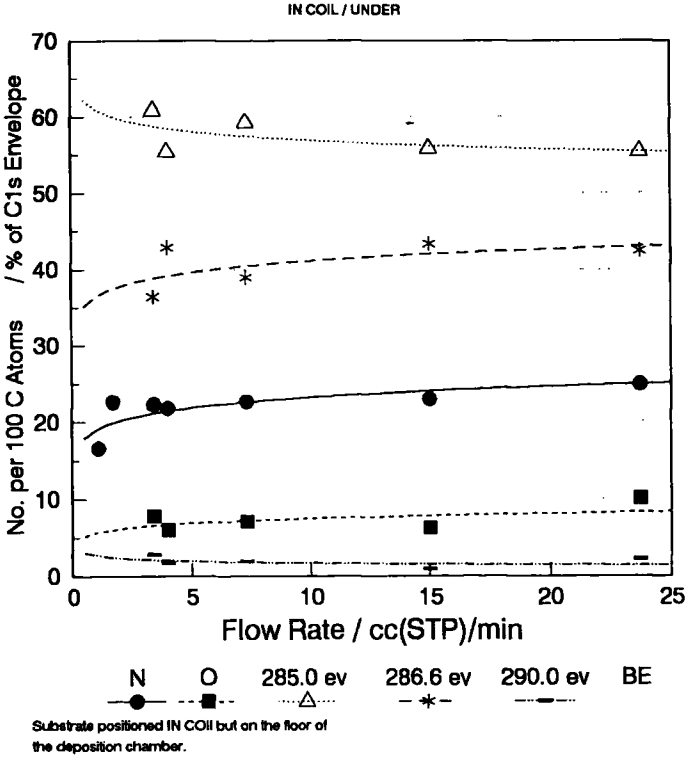

Substrate positioned IN COIl but on the floor of the deposition chamber.

actual nitrogen - containing moieties does. This is confirmed by the N1s envelope, which in general showed a lower retention of nitrile groups in their original state at lower flow rate (as evidenced by the larger contribution of the higher binding energy environment at 400.5eV to the overall N1s peak area). Hence the W/F parameter influences the chemical nature of the films deposited here; in particular, at lower flow rates the increased power availability per monomer molecule present in the system causes the carbon-nitrogen triple bond to react to give C-N and C=N moieties. This probably occurs via ii^{*} <-- n excitation in the unsaturated nitrile group. In addition, since the C≡N triple bond is electron rich, it would be a prime target for possible electrophilic attack, for example by any carbocations in the system:

$$-C{\equiv}N \; + \; -C^{+}- \; \text{-----}> \; -C{=}N{-}C$$

(ii) OUT OF COIL the C:N ratio showed discrepancies between the two experimental series - one yielded little variation over the flow rate range, whilst the second showed a minimum at about F=4.0cc(STP)min^{-1}. Also, the absolute values obtained in the first series for nitrogen content were consistently higher.

Both series gave similar results for the C1s envelope, the overall trend being a decrease in contributions due to hydrocarbon and quaternary carbon atoms (285.0 eV). Those environments centred at 286.6 eV (nitrile C-N, C=N, C-O) showed a general increase with flow rate. The amount of oxygen uptake was variable, whilst the N1s

envelope again showed an increasing proportion of unreacted nitrile groups present in the film surface as the flow rate increases.

In summary, for methacrylonitrile both power and flow rate have an influence in the chemical nature of the plasma polymer film produced. Further, of the two parameters the power input to the system has the more marked effect on the nitrogen content of the deposited films. Increasing the flow rate alters the nature and distribution of the nitrogen-containing moieties found. Finally, since differences have been found in both the nature of the films deposited by metha- and chloroacrylonitrile (and also their excited state species and fragmentation pattern behaviour) due to the replacement of a chlorine substituent by a methyl group, the influence of all three parameters in Yasuda's overall W/FM parameter has been shown. This influence was found to be qualitative rather than quantitative with respect to interpreting the results obtained in this chapter. However, as the next section shows, the deposition rate of allyl cyanide plasma polymers under similar experimental conditions as those for methacrylonitrile described above is much faster, despite the fact that the two are structural isomers and hence have the same molecular weight, contradicting the expected result predicted using Yasuda's W/FM parameter.

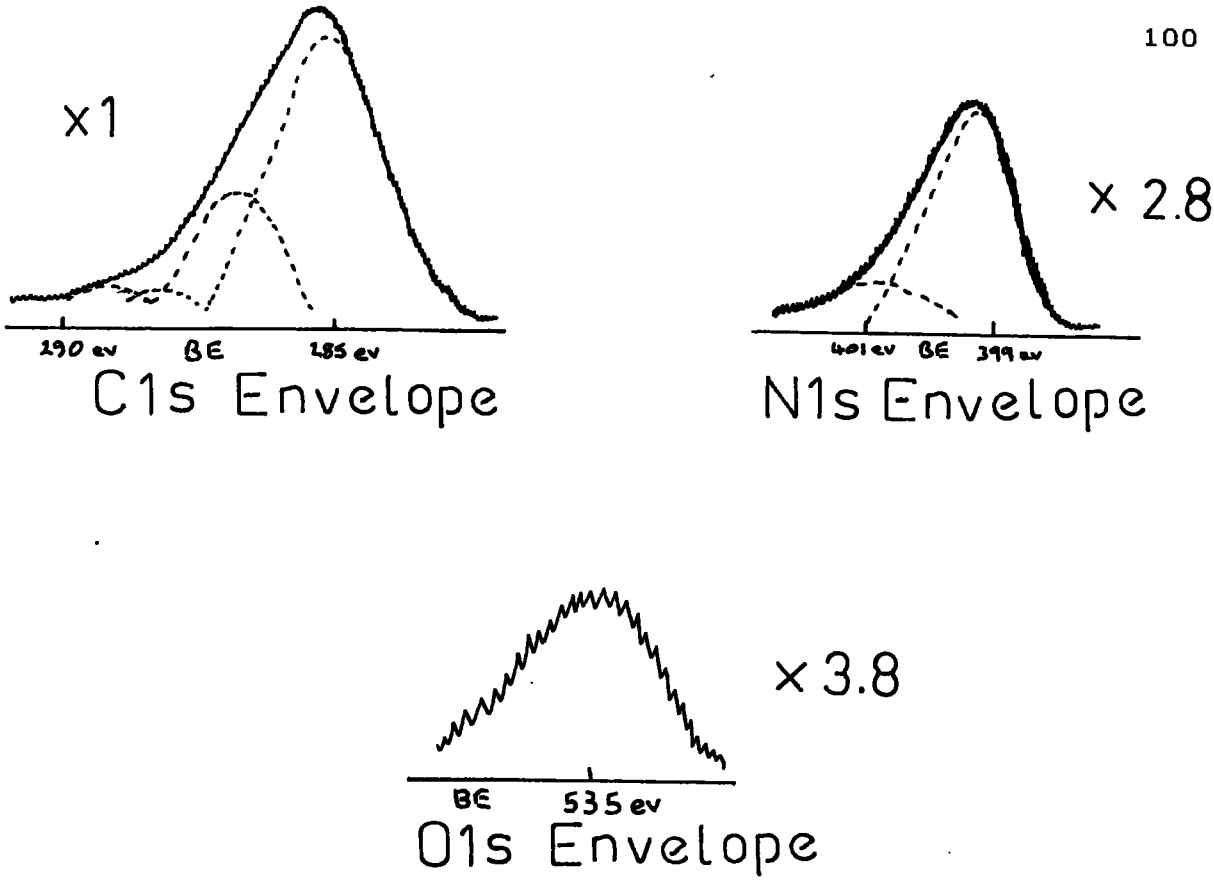

FIGURE 3.20 C1s, N1s and O1s Core Level Spectra for Plasma Polymers of Methacrylonitrile

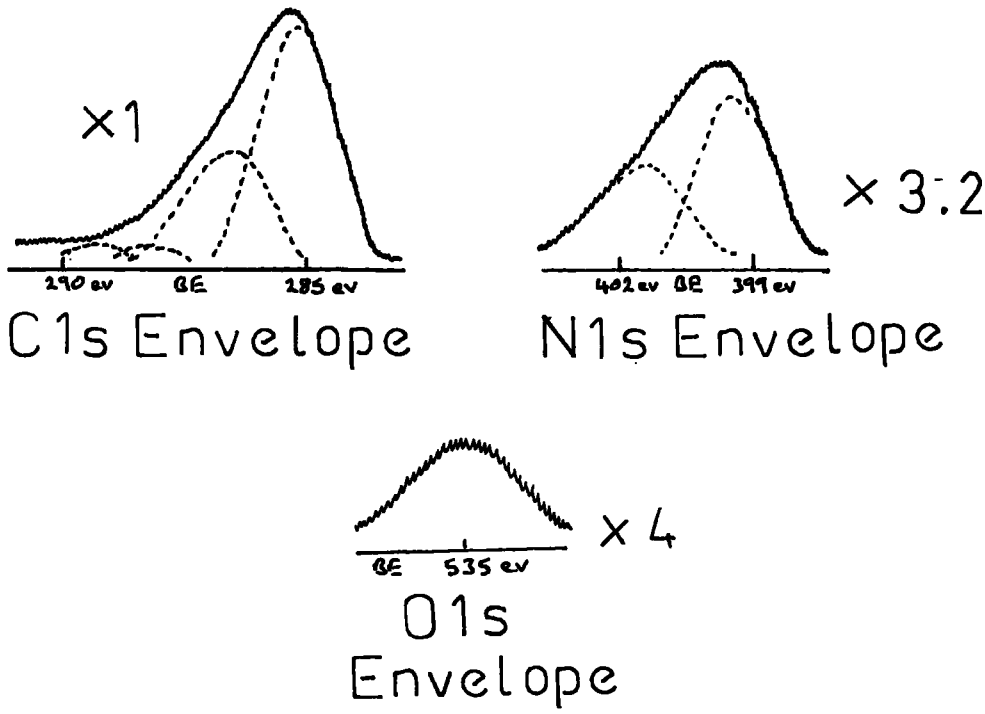

FIGURE 3.21 C1s, N1s and O1s Core Level Spectra for Plasma Polymers of Allyl Cyanide

3.4.3 Allyl Cyanide

Allyl Cyanide, $CH_2=CH-CH_2CN$, was chosen as a monomer for plasma polymerization to provide a comparison with the acrylonitrile family studied earlier. In the latter the nitrile group was directly adjacent to, and hence exerted a primary substituent effect on, an unsaturated carbon atom. In contrast, the cyano group in allyl cyanide is removed by a methylene (CH_2) unit. Hence, any substituent effect on the carbon-carbon double bond observed should now be markedly reduced due to this secondary (beta), rather than alpha, effect. As before, the influence on the system of both power and flow rate were examined, the parameter ranges studied being comparable to methacrylo- and chloroacrylonitrile for power, but differing for flow rate due to the difference in vapour pressure between the monomers.

I Variable Power

Allyl Cyanide was found to deposit very rapidly throughout the power range (3-60W) - more so than for methacrylonitrile. Hence, after only three minutes, a sufficiently thick film was formed to be visible to the naked eye. In order to see if the chemical nature of the film changed with respect to time, selected experiments in the series were repeated for a deposition time of six minutes (a flow rate of 0.5cc(STP)/min was used throughout). The ESCA spectra obtained were very similar in shape to those found for methacrylonitrile (Figures 3.20, 3.21).

(i) IN COIL

The nitrogen content of the films formed after three minutes (Figure 3.23) was initially constant at low power, decreasing overall with increasing power. The level of oxygen incorporation was variable throughout. The number of hydrocarbon and quaternary carbon environments in the C1s envelope (285.0 eV) steadily increased with power, whilst the total number of carbon-nitrogen environments was reduced. The N1s envelope showed that, of the nitrogen containing moieties, an overall increase occurred in the proportion of N-C and N=C environments in relation to unreacted (i.e. intact) nitrile groups, with a maximum at 33W. On raising the deposition time to six minutes this maximum is shifted to higher power (49W). However, a comparison of absolute values between the two sets of results shows a discrepancy of less than 15% - i.e. within experimental error, showing fairly good reproducibility. The greatest discrepancy was shown in the total nitrogen content of the films.

The similarity of the chemical composition of the films deposited after 3 and 6 minutes suggests that, once the aluminium substrate is fully covered, the chemical nature of the film macroscopically speaking changes little with time. This agrees with the results of variable take-off angle experiments performed not only for allyl cyanide (Table 3.7) but also the acrylonitriles, which showed that, in general, the plasma polymer films produced in this work were homogeneous.

Comparing the results obtained for the nitrogen content of allyl cyanide with those for the acrylonitriles (Table 3.6), the former showed an overall decrease for the in coil region. In contrast, chloroacrylonitrile exhibited a minimum at 40W and methacrylonitrile a

LLYL CYANIDE PLASMA POLYMER

Variable W, F=0.5cc(STP)/min

FIGURE 3.23a - Atomic Ratios IN COIL

, per 100 C Atoms

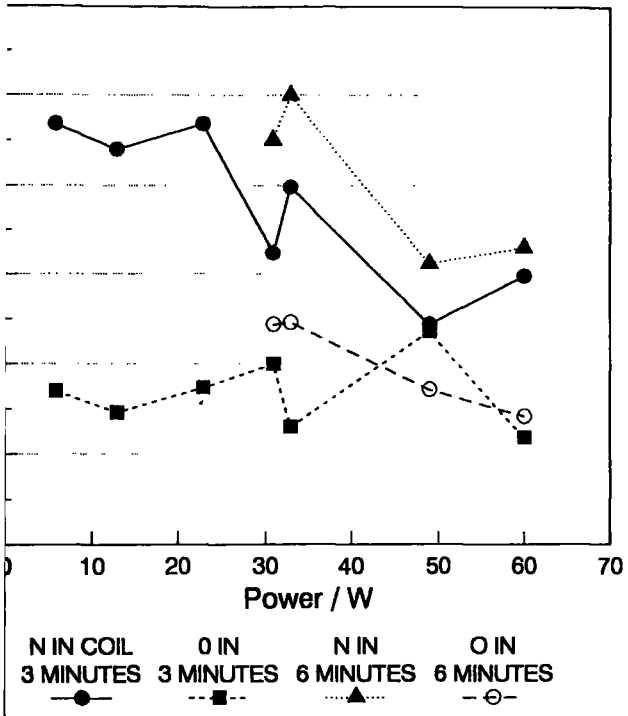

ALLYL CYANIDE PLASMA POLYMER

Variable W, F=0.5cc(STP)/min

FIGURE 3.23b - Atomic Ratios OUT OF COIL

No. per 100 C Atoms

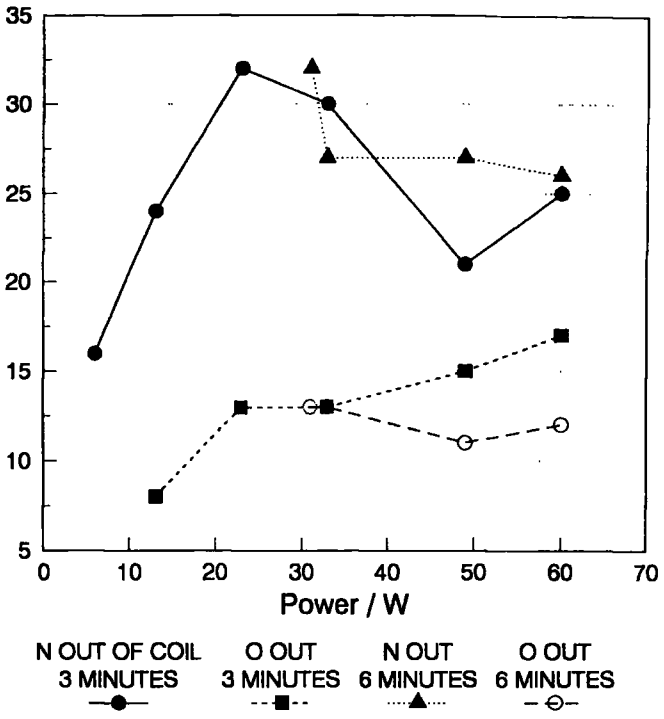

ALLYL CYANIDE PLASMA POLYMER

F=0.5 cc(STP)/min, Variable W

FIGURE 3.24 - C1s Envelope

No. per 100 C Atoms

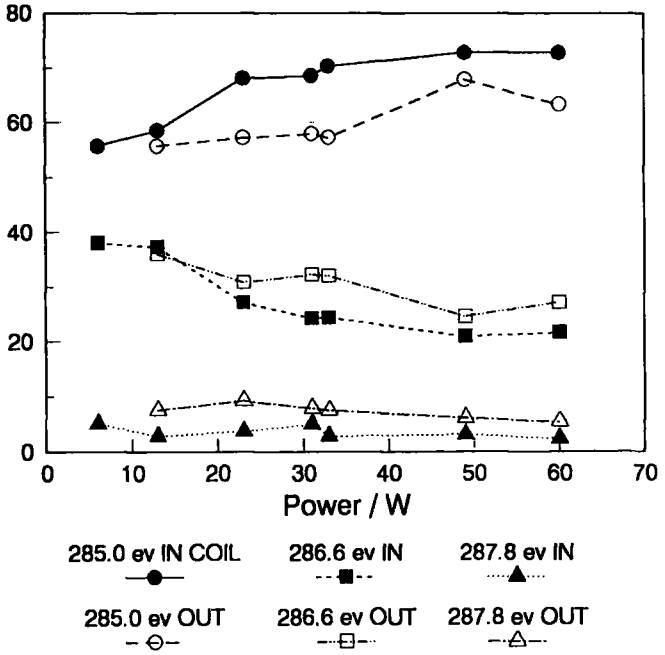

1. 289.0 ev component initially <4 %, increasing throughout. 2. 6 min vs 3 min deposition time for W=21-60w gives the same results.

minimum at 17W. The C1s and N1s envelopes correspondingly differ. Since methacrylonitrile and allyl cyanide are both structural isomers of C_4H_5N, and hence have the same molecular weight, M, in Yasuda's parameter W/FM, the observed differences in trends observed over the power range studied are most likely due to the change in chemical structure between the monomers. Also, the difference in deposition rates between the two isomers suggests that W/FM is not the paramount factor in controlling the deposition rate of a plasma polymer system.

(ii) TAIL REGION

A maximum was found for the nitrogen content of the tail region films at 20-30W for a three minute deposition period, in contrast to the plateau found prior to decrease in coil, whilst the oxygen content showed an overall rise with increasing power. The C1s and N1s envelopes also revealed that power influences the chemical composition of the films since a higher input to the system once again results in an increased oxygen content - once again thought to occur via the production of more free radical reactive sites in the film surface capable of quenching via uptake of oxygen species.

In the C1s envelope, the 285.0 eV peak showed an increase with increasing power, that at 286.6 eV (corresponding to nitrogen moieties in the film) showing an overall downward trend. Hence the maximum at 286.6 eV that might have been expected to correlate with the overall maximum in the total number of nitrogen containing moieties at 20-30W, as evidenced by the N:C ration, was not observed. Possibly the doubling in oxygen content from 8 to 17 oxygen atoms per 100 carbon atoms between 13W and 60W is responsible for a larger than usual

SUBSTRATE	MONOMER		POWER / W					
POSITION			05	12	20	30	50	60
IN COIL	MAN	N:C[1]	23	22	25	18	17	-
	AC	"	23	22	23	16	12	15
TAIL	MAN	"	21	22	20	22	27	15
	AC	"	16	24	32	30	21	25
IN COIL	MAN	399.3[2]	90	46	80	74	68	-
	AC	"	82	91	80	75	75	72
	MAN	400.6[2]	10	54	20	16	32	-
	AC	"	18	09	20	25	25	28
TAIL	MAN	399.3	84	89	83	79	70	40
	AC	"	93	87	75	55	51	57
	MAN	400.6	16	11	17	21	30	60
	AC	"	07	13	15	45	49	43

NOTES : 1. The ratio is given as the number of N atoms per 100 C atoms present in the film. 2. Binding energy in the N1s spectrum, in eV.

TABLE 3.6 Comparison of Nitrogen Content, Allyl Cyanide versus Methacrylonitrile.

TABLE 3.7 Results for Allyl Cyanide Plasma Polymer - 60 vs 30 Degrees Take Off Angle

TOA in Degrees			C1s Envelope				N1s Envelope	
	N	O	285.0	286.6	287.7	289.0	399.3	400.6
30	21	7	67	28	2	3	61	39
60	16	8	67	26	4	3	60	40

NB: 1) Atomic Ratios are /100 C atoms
2) Envelopes are in %; Binding Energies in ev

contribution to the 286.6eV peak from C-O bonds. The impact of this on the overall peak trend is hard to assess; however, a maximum in the carbonyl contribution (287.8 eV) occurs at 33W. This, taken in conjunction with the overall increase in oxygen content with power, suggests that the number of C-O environments at 49W and 60W progressively increases. Hence, unusually, carbon-oxygen environments appear to play a more dominant in the C1s envelope under these conditions than previously seen, whilst analysis of the N1s envelopes showed a dramatic increase in the number of N-C and N=C environments in proportion to nitrile groups in the film across the power series, such that, for the tail region, the ratio of peak areas (399.3 eV versus 400.6 eV) was almost 1:1. Such a high ratio was also observed for some methacrylonitrile films. However, overall a lower number of cyano groups are incorporated into the allyl cyanide film in their original form compared to the acrylonitriles, especially chloroacrylonitrile, which has a much higher ratio of nitrile environments to C-N and C=N. This increased contribution from the latter environments must be a structural facet caused by the insertion of the methylene unit between the cyano group and the carbon-carbon double bond on changing the monomer to allyl cyanide. In particular, this prevents molecular elimination of HCN occurring from an unsaturated environment to give the corresponding diradicals and acetylenic compounds via rearrangement, although ethynes could still occur via elimination of molecular hydrogen. This lack of elimination of HCN may account for the high retention of the original nitrogen content observed for many of the allyl cyanide films. However, it should be pointed out that, since the molecular formula is C_4H_5N, maximum retention of nitrile

groups, intact or not, should give rise to a N:C ratio no larger than 25:100. This is in fact exceeded - hence some carbon-containing fragments other than nitrile groups must be lost from the monomer before deposition, such that this maximum ratio is exceeded. Elimination of HCN from the aliphatic position of the allyl cyanide molecule would not satisfy this criterion - rather, for electron impact excitation above the ionization potential fragmentation and rearrangement of the sort outlined in the mass spectrometric studies performed by Willett and Baer probably occurs, whilst excited state chemistry below the ionization potential most likely involves scission of the carbon-carbon bond beta to the double bond.

II. Variable Flow Rate

Although the pressure range studied was similar to that used in the previous experiments (0.08-0.02 mb), the generally lower vapour pressure of allyl cyanide in comparison to the acrylonitriles resulted in a lower spread of flow rates at 0.18-1.67 $cc(STP)min^{-1}$.

(i) IN COIL

A variable take-off angle experiment was performed at 35 and 60 degrees to enable depth profiling to be carried out. The results (Table 3.7) showed excellent agreement for a flow rate of 0.18 $cc(STP)min^{-1}$ for both the C1s and N1s envelopes as well as the oxygen content; however, the nitrogen content at the surface of the film was found to be slightly lower than expected. The lack of any identifiable repeat unit in the highly cross-linked films formed may possibly give

LLYL CYANIDE PLASMA POLYMER

18W, Variable F

FIGURE 3.25 - Atomic Ratios

. per 100 C Atoms

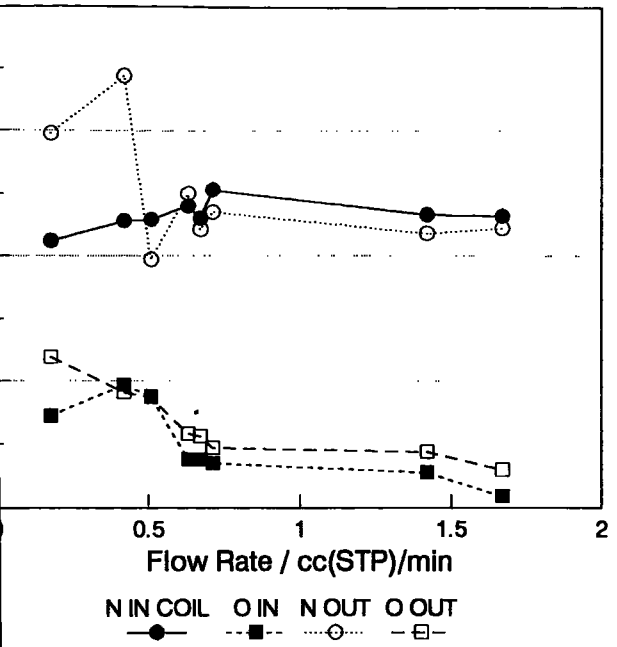

ion times of 6 & 10 minutes yielded the
sults within experimental error for
cc(STP)/min

ALLYL CYANIDE PLASMA POLYMER

18W, Variable Flow Rate

FIGURE 3.26 - C1s Envelope

% of C1s Envelope

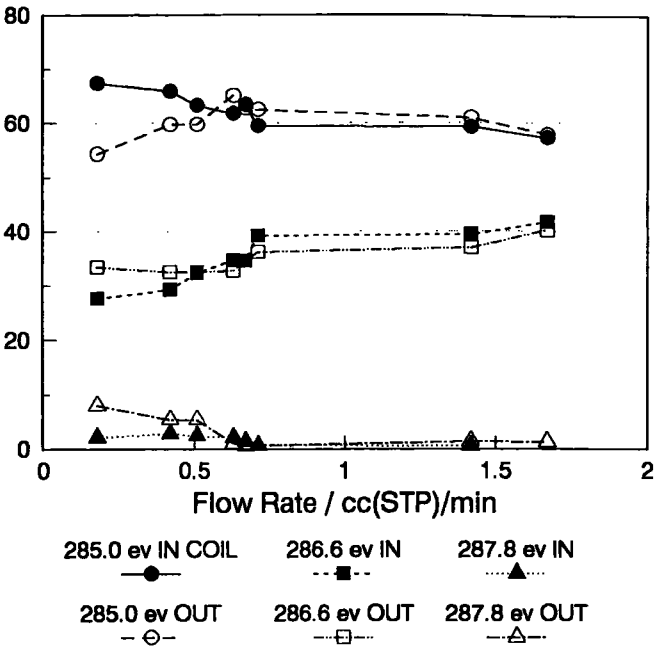

1. 289.0 ev component initially <4 %, decreasing throughput. 2. 10 min vs 3 min deposition time for F=0.5cc/min gives the same results.

LLYL CYANIDE PLASMA POLYMER

F=0.5 cc(STP)/min, Variable W

FIGURE 3.27 - N1s Envelope

of N1s Envelope

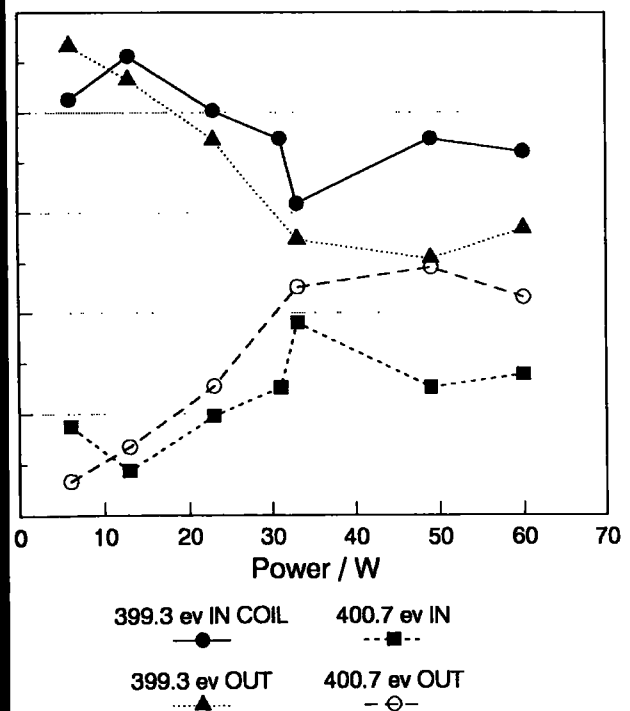

ALLYL CYANIDE PLASMA POLYMER

18 W, Variable Flow Rate

FIGURE 3.28 - N1s Envelope

% of N1s Envelope

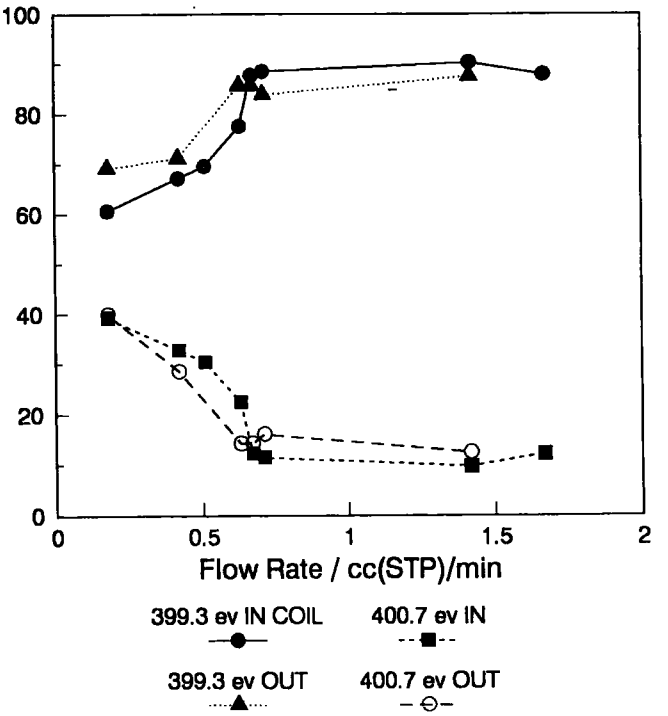

rise to local variations in the chemical composition; however, the larger the sampling depth the more likely any such inhomogeneities will be averaged out.

Overall the nitrogen content of the films was found to be constant throughout within experimental error, whilst the oxygen content dropped with increasing flow rate. The C1s and N1s envelopes showed that, though the overall N:C ratio remained fairly constant with flow rate, the distribution of chemical environments changed. The 285.0 eV peak contribution to the C1s envelope dropped with increasing flow rate; conversely, the 286.6 eV peak contribution rose, suggesting that the number of nitrogen containing moieties increases across the series - i.e. a direct contradiction to the result obtained from the N:C ratio. The N1s spectra showed that the large proportion of N-C and N=C environments at low flow rates gave way to a 60% and 90% majorities of cyano groups at high flow rate. For each such group, there must be a carbon atom directly attached also appearing at 286.6 eV in the C1s spectrum. Now, the total number of nitrogen atoms per 100 carbon atoms is approximately the same for each film analysed in the series, allowing direct comparison of the relative proportions of each N1s envelope. Hence for F=0.18 cc(STP)min^{-1} and assuming the N1s envelope as a whole represents 100 nitrogen atoms, if 60% are cyano groups then 60 C-CN and 40 C-N or C=N bonds must also be present, making a total of 160 carbon atoms contributing to the 286.6 eV peak in the C1s envelope. For F=1.67 cc(STP)min^{-1} 90% of the nitrogen is present as cyano groups, giving 90 C-CN and 10 C-N or C=N bonds as well, a total of 190 carbon environments occurring at 286.6 eV. Hence this component of the C1s spectrum duly increases with increasing flow rate, despite the total

number of nitrogen atoms per 100 carbon atoms in the film remaining more or less constant throughout.

(ii) OUT OF COIL

Once again the tail region exhibited differing behaviour to that in coil. Initially the nitrogen and oxygen contents of the lowest flow rate film was high (Figure 3.25), the latter dropping as the monomer flow rate was increased. The C1s envelope showed a maximum for hydrocarbon and quaternary carbon environments at mid-flow rate, with a small minimum in the 286.6 eV environments. The latter lies within experimental error of the results obtained at lower flow rates, but the subsequent increase was sufficiently marked to echo the overall increase found in coil. The contributions from the 287.8 and 289.2 eV peaks decreased with flow rate, reflecting the lower level of oxygen uptake in the films, whilst the trend in the N1s envelope was the same as that found in coil. Taking the C1s and N1s envelopes together the results suggest that there must be structural differences between the in-coil and tail regions; hence, as found for the acrylonitriles, the nature of the films formed is positionally dependent within the reaction chamber. This must again reflect both the nature of the electron energy distribution, and the nature and relative abundance of the depositing species, throughout the system.

3.5 Summary

This Chapter has examined the effect of power, flow rate, positional dependence within the reactor, length of deposition period and nature of monomer used (both in terms of relative molecular mass and structural Isomerization) on the chemical composition of the plasma polymer thin films formed in a vacuum system using an inductively coupled rf generator. Nearly all these parameters have been found to influence the exact nature - and hence properties - of the films formed, the most marked being (i) the type of monomer used and (ii) the power input to the system. The effect of flow rate was less marked than expected over the ranges studied, whilst the contrasts between films produced in the "in coil" and "tail" regions illustrate localised differences within the deposition chamber. Overall, whilst the three components of Yasuda's W/FM parameter do influence the system, and hence the nature and properties of the films formed, this is qualitative rather than quantitative. Finally, an attempt has been made to interpret, at a basic level, the type of species and nature of the processes involved in the plasma and deposition processes, especially with regard to the structure of the monomer. Reproducibility of results within experimental error show that these processes, and hence plasma polymerization in general, can be controlled by the parameters studied.

CHAPTER 4

PLASMA POLYMERIZATION IN THE PRESENCE OF HALOGEN VAPOURS

4.1 Introduction

The plasma polymerization of organic compounds in the presence of non-polymerizable gases such as argon and hydrogen has been investigated by a number of authors[1]. In many cases the desired effect was to influence the overall pressure and flow rate of the system whilst leaving those of the monomer unchanged. Till[2] examined such effects for the plasma polymerization of perfluorobenzene, extending the investigation to study the effect of iodine on the system. Munro and Grunwald[3] similarly investigated the deposition of acrylonitrile in the presence of iodine vapour, finding that the glow volume of the reaction was dramatically reduced and concentrated mainly in the coil region. On analysis of the latter films by ESCA, iodine was found to have been incorporated, effectively doping the plasma polymer such that a small but positive conductance could be measured - ie the polymer was no longer perfectly insulating, unlike the film deposited using acrylonitrile alone. This result was felt to be of potential application as a (semi) conducting polymer. Other workers have also studied incorporation of iodine into plasma polymer systems. Dully et al[4] reported an iodine containing film derived from iodomethane with an iodine to carbon elemental ratio of 1:11, whilst Ward[5] has examined the role of iodinated polymers as potentially useful resist materials in the electronics industry. In particular, this latter work[5] attempted to discover methods of reducing the loss of iodine during plasma polymerization by looking at plasma copolymers of iodobenzene with benzene, and plasma homopolymers of allyl iodide. Both Till[4] and Ward[5] found evidence in the $I3d_{5/2}$ ESCA spectrum for negative iodine species in the film surface, the latter subsequently finding evidence from

ultraviolet spectra for the initial presence of I_3^- in plasma polymerized allyl iodide, the species disappearing with time on exposure to the atmosphere.

Since iodine is known to be a free radical scavenger[6], it is also possible to use such studies to try and gain some mechanistic insight into the plasma polymerization process, especially if the scope is widened to include surface photopolymerization. Chloroacrylonitrile was thus chosen as a monomer, since its photochemistry is examined in chapter 5, whilst allyl cyanide was chosen as a contrast to the work carried out on allyl iodide by Ward.[5] In particular, since allyl compounds plasma polymerized at low power and high flow rates have been found in general to retain a high proportion of their functional groups[7], as shown in chapter 3 for allyl cyanide, it was expected that the thin films produced for the latter in the presence of iodine would retain carbon-nitrogen functionalities as well as incorporating those of carbon-iodine.

4.2 Experimental

The apparatus used was identical to that in chapters 2 and 3, except that the iodine and monomer tubes were attached to a T-piece upstream of the reaction chamber to ensure mixing of the reactants prior to entering the reaction chamber, Figure 4.1. Iodine was vacuum sublimed into a monomer tube secured by a Young's tap; chloroacrylonitrile and allyl cyanide were degassed prior to use by freeze-thaw cycles in the usual way.

Iodine vapour was bled into the chamber at its vapour pressure (0.95mb as measured by the Pirani head used); whilst the partial

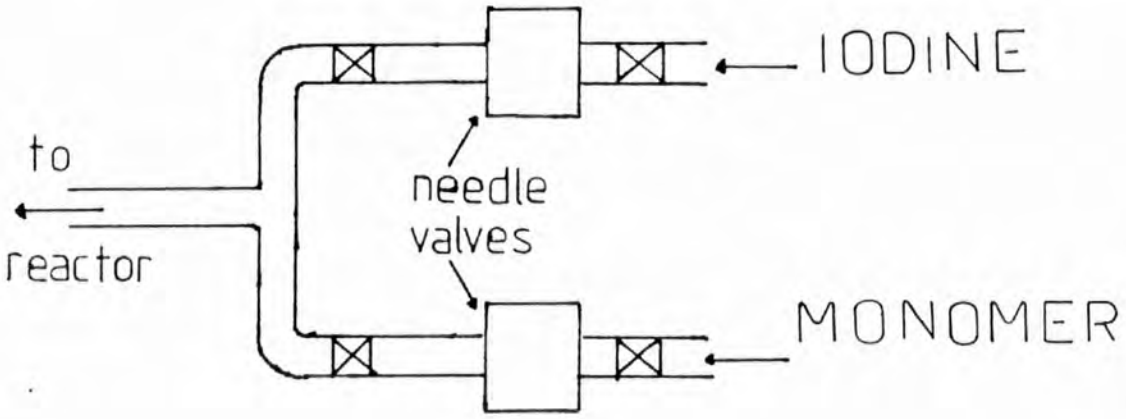

FIGURE 4.1 "T-Piece" Arrangement for Iodine Experiments.

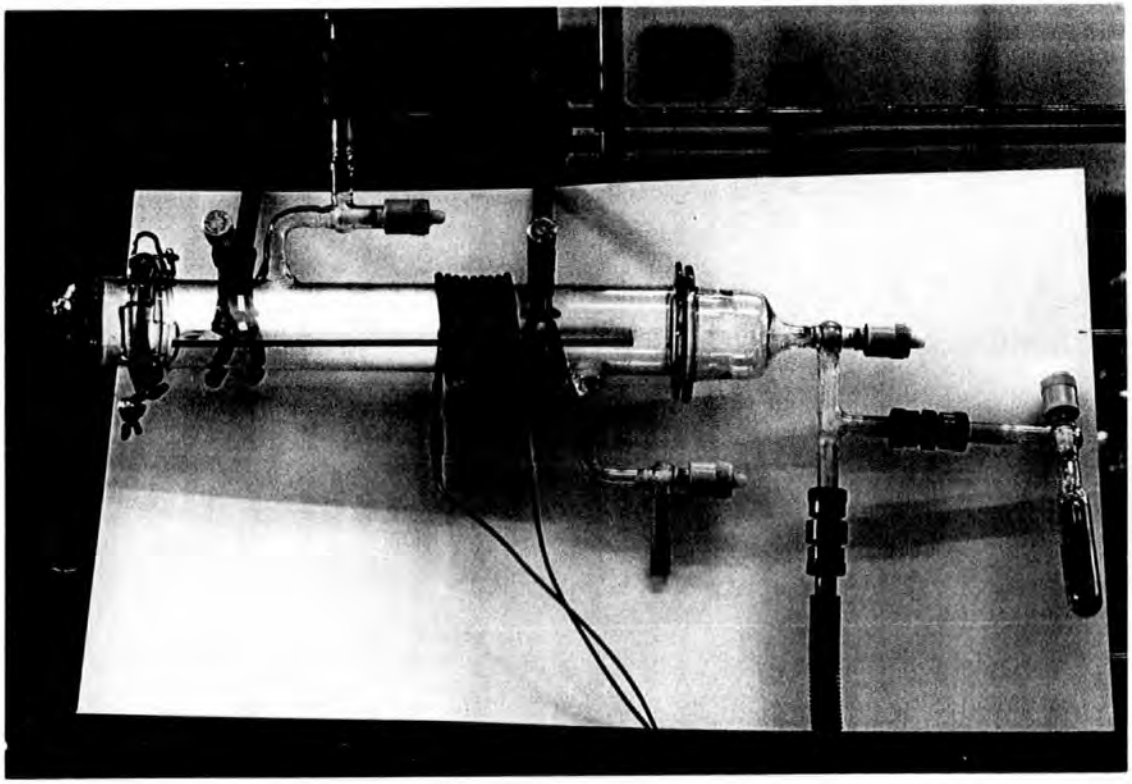

PLATE 4.1 RF Plasma Ignited in Allyl Cyanide.

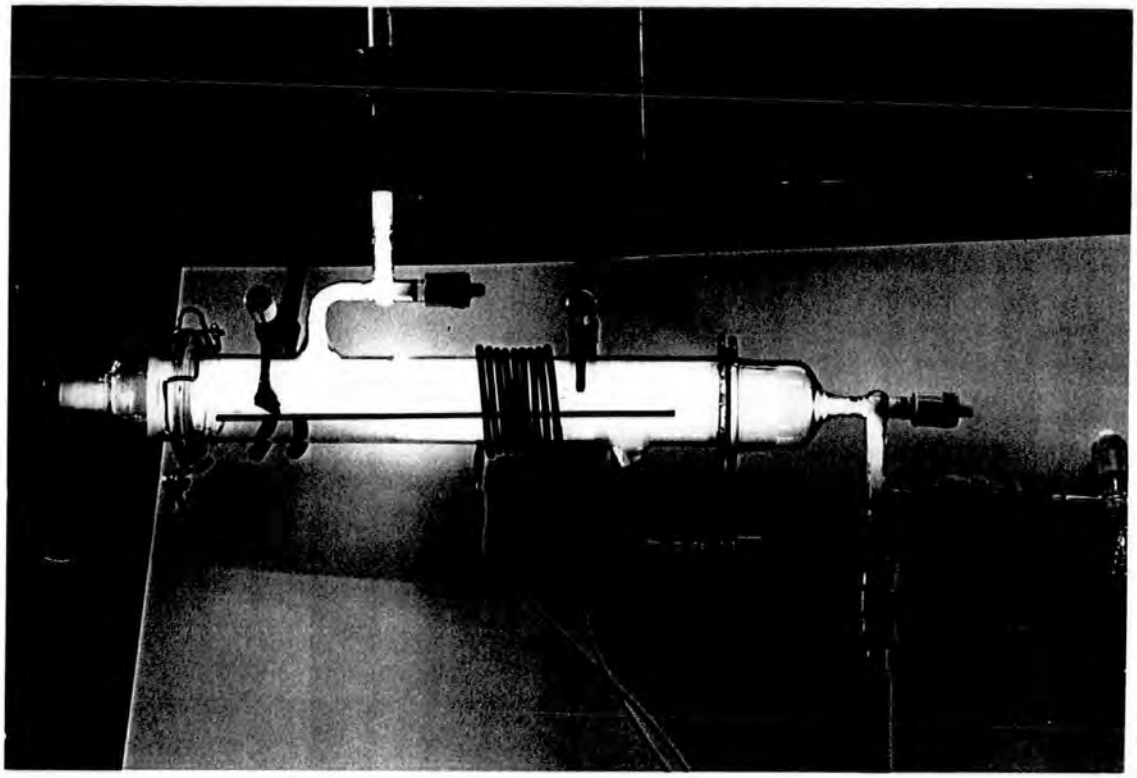

Plate 4.2 RF Plasma Ignited in Allyl Cyanide - Effect of Introducing Iodine Vapour.

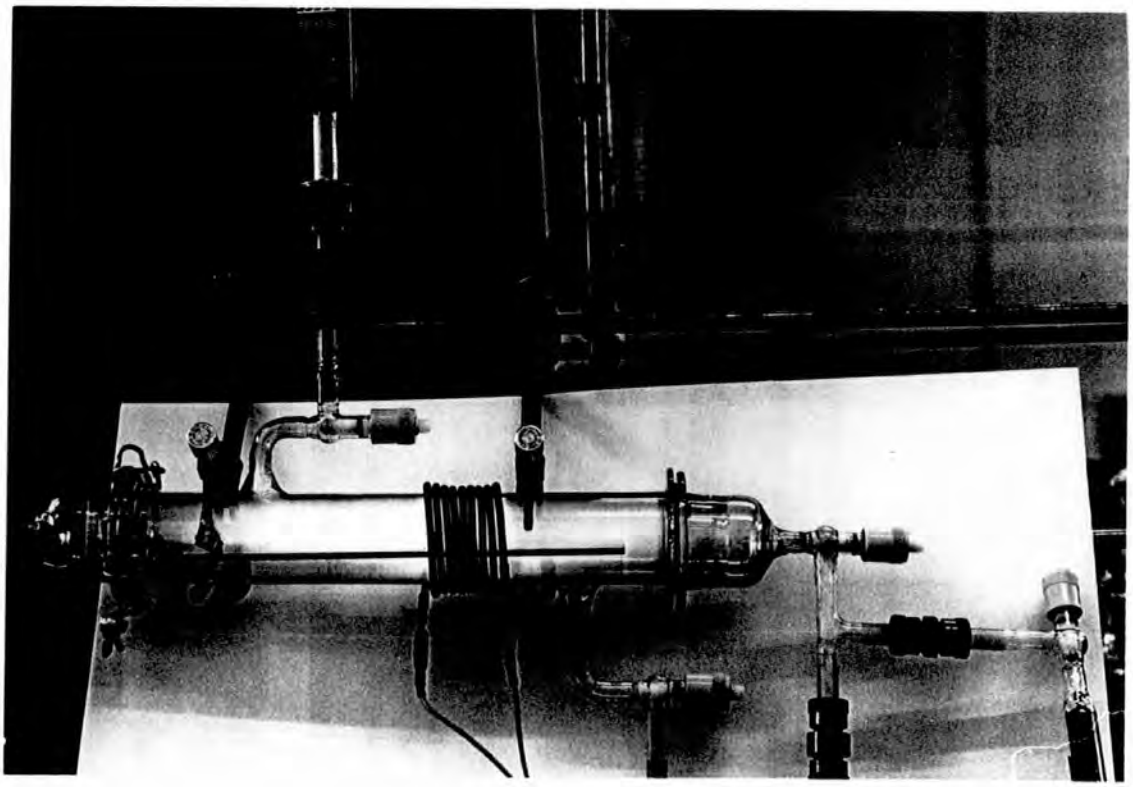

Plate 4.3 RF Plasma Ignited in Allyl Cyanide, 3 Minutes After Introduction of Iodine Vapour.

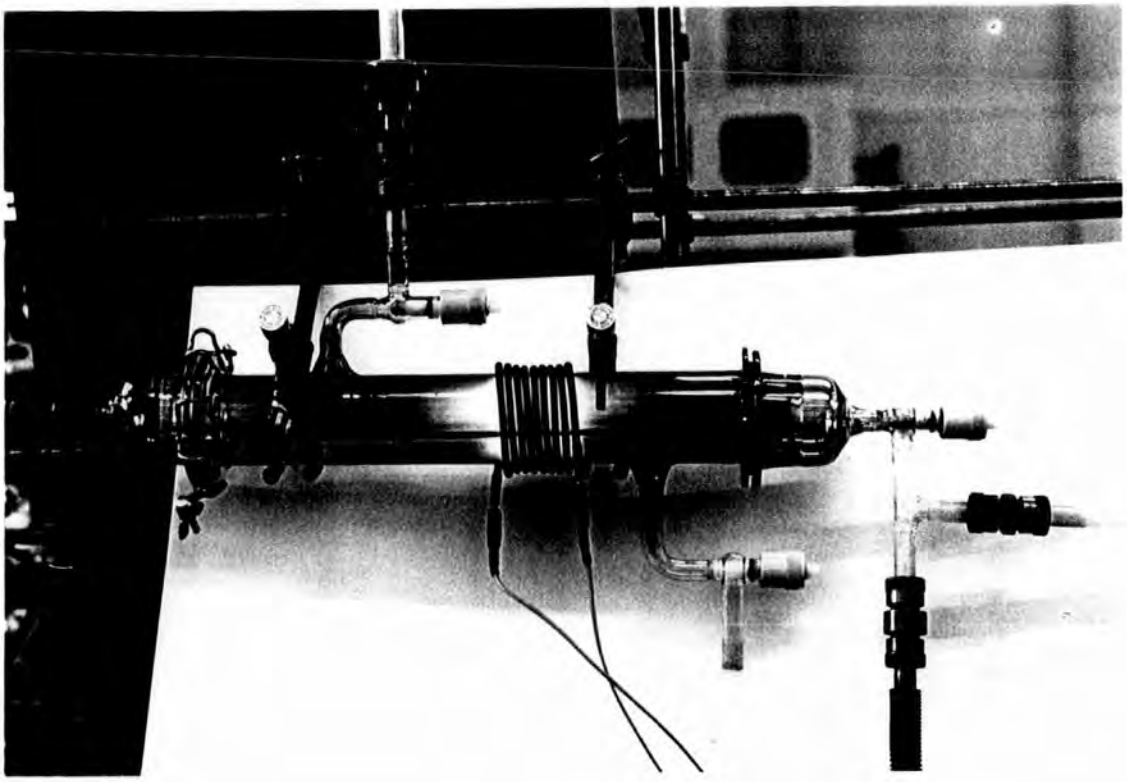

Plate 4.4 Effect of Heating Iodine Monomer Tube - Glow Volume Restricted to the Vicinity of the Coil Region.

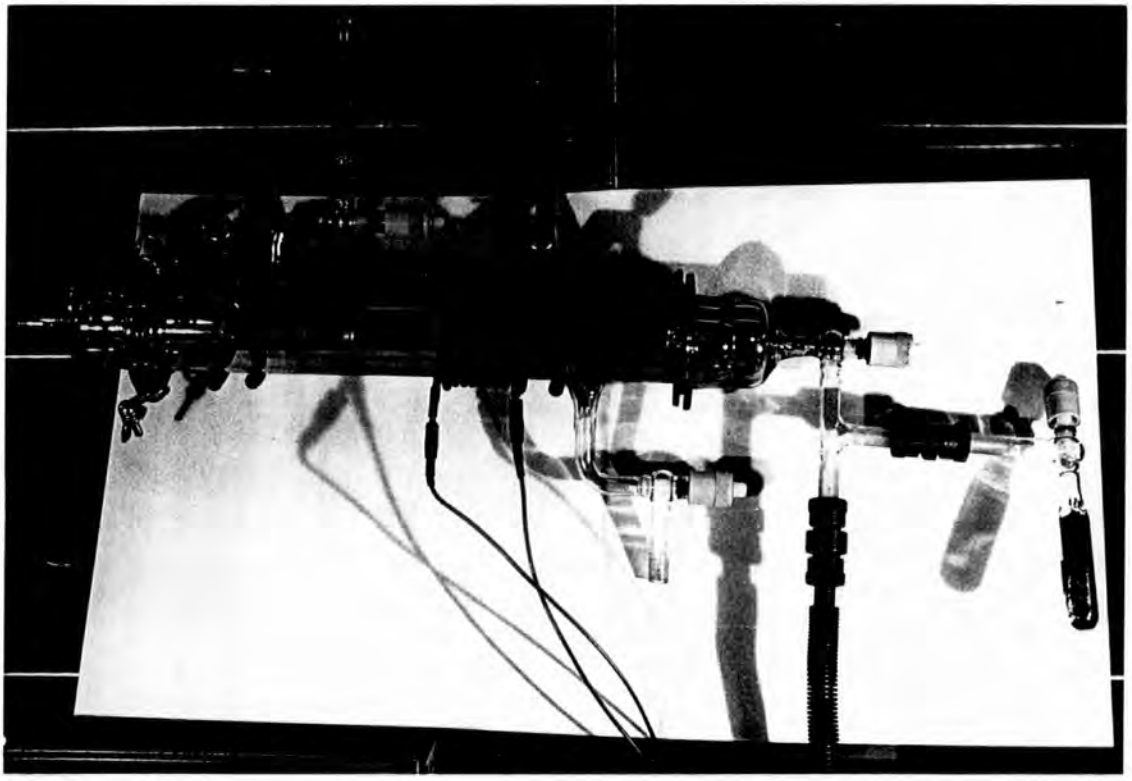

Plate 4.5 Allyl Cyanide Plasma Polymerized in the Presence of Iodine Vapour - Deposition Pattern After Ten Minutes.

pressure of bromine, which was found to have a higher vapour pressure in excess of 0.4mb, was controlled using an Edwards needle valve. In each experiment, the partial pressure and flow rate of the monomer were determined separately before addition of halogen vapour to the system. Only once the total pressure and flow rate of the system had been determined was the rf plasma ignited. The effect of introducing monomer into the system after initiation of a plasma in monomer vapour alone can be seen in Plate 4.2 Time increases on descending the photographic series, such that the initial purple glow of the monomer (Plate 4.1) was immediately turned, on introduction of iodine vapour, a characteristic white, which became on off-white / yellow colour as film built up on the walls of the reactor. The glow volume also began to reduce in size. Next, as the iodine monomer tube was heated with a hairdryer (to increase the concentration of iodine vapour in the system) the glow volume rapidly shrank in size until it occupied only the coil region. Deposition was found not to occur outside this glow, but rather was concentrated inside the coil region itself - Plate 4.5 shows the distribution of the deposited film at the end of the experiment. The visible deposition in the tail region occurred during the early stages of the experiment, immediately prior to and after after the introduction of iodine vapour such that the glow volume still encompassed the entire chamber. In general, deposition occurred only in the glow region for allyl cyanide, although this was not always the case for chloroacrylonitrile, perhaps reflecting a difference in deposition mechanism between the two monomers.

Ratios of elemental stoichiometries with respect to carbon were determined by ESCA in the usual manner using a Kratos ES300

spectrometer, except that C1s envelopes were not fitted since the carbon-iodine environments proved unresolvable from the carbon-nitrogen, carbon-chlorine (for chloroacrylonitrile) and carbon-oxygen environments in the film.

UV absorption spectra were taken by depositing plasma polymer onto quartz windows prior to running on a Phillips PU 8720 UV/Visible Scanning Spectrophotometer.

4.3 Chloroacrylonitrile / Iodine

Initial experiments showed that the plasma glow volumes were significantly reduced in the presence of iodine vapour (this was also true of added bromine), being confined at low power to the immediate area inside and surrounding the coil region (see Plates 4.1 - 4.4). Glow volumes were found to increase for a given flow rate on increasing the power input to the system. This effect, which was also observed for acrylonitrile,[3] is thought to be due to molecular iodine in the plasma chamber scavenging the free electrons responsible for the production of excited states (both neutrals and/or ions) via electron impact excitation. Since the characteristic plasma glow is due to the light emitted when these excited states return to their ground states, removing the incident electrons from the system extinguishes the glow. Increasing the power available to the system increases the numbers of, and kinetic energies available to, the electrons such that sufficient remain unquenched to initiate and maintain the glow. Deposition within the glow volume occurred more readily upstream of the coil region than in the tail region; a third aluminium substrate was therefore positioned 6cm upstream of the in-coil substrate. Absence of the glow

volume was found to roughly correspond with absence of film formation. However, some (incomplete) deposition was observed immediately downstream of the glow region and thought to be caused by species activated in the glow volume flowing and/or diffusing downstream. This suggests that electron impacted excited states (both neutrals and ions) are responsible for film deposition. This would be consistent with the observation by Clark et al[8] who proposed that radical cations are the depositing species in the plasma polymerization of the perfluoroethylenes, rather than the radical rapid step growth mechanism suggested by Yasuda[9] for plasma polymerization in general. However, decomposition of excited states of unsaturated ethylenic compounds below the ionization potential can lead to radical products via both valence shell and Rydberg states[10], which in turn can be quenched in the presence of iodine. That these excited states can lead to thin film formation is shown in chapter 5, which details chloroacrylonitrile surface photopolymers formed in both the conventional and vacuum ultraviolet regions. This in turn indicates that the iodine here is indeed acting as a free radical, as well as a free electron, scavenger (NB that the latter must occur as well is shown by the presence of ionic iodine species in the deposited films as detailed below). In addition to positioning aluminium substrates in the in-coil and tail region positions outlined in chapter 3, a third substrate was placed 6cm upstream of the coil on the basis of preliminary experiments in which deposition occurred more readily upstream of the reactor than downstream in the tail region. Two experimental series were carried out - varying the power input to the system, W, for a fixed flow rate, F; and vice-versa.

I. Variable Power

A power range of 9-55W was used to plasma polymerize 0.1mb of chloroacrylonitrile ($F=0.48cm^3_{STP}min^{-1}$). Introduction of iodine vapour into the system raised the total pressure of the mixture to 0.11mb (measurement of the total flow rate proved unreliable with the equipment available). No deposition occurred in the tail region except at the highest power setting used (55W), whilst deposition upstream of the coil (up-coil) did not occur until moderately high power (45W), taking place more rapidly than in the tail region. Full coverage of the aluminium substrate in coil occurred throughout the series.

Analysis of the resultant films by ESCA revealed that the chlorine content was quite low, with a Cl:C elemental ratio in-coil of 1:10 or less, rising to 1.3:10 in the upstream position. The ratio in the tail region at 55W was found to be only 2:100. Variation of results in-coil showed no discernible pattern, Table 4.1. The nitrogen content in all the films was moderately high throughout, varying between 15 and 20:100 for the N:C elemental ratio, whilst that for I:C varied even more between 18 and 56:100. The high iodine content can possibly be attributed to some physical incorporation of molecular iodine into the film, whilst the behaviour of the nitrogen and chlorine to carbon ratios must be a result of iodine introduction, since the results for monomer alone (chapter 3) showed, respectively, an overall decrease and a minimum. Oxygen uptake was low.

Although the C1s spectrum was not resolvable, so that no functional group analysis was possible, both N1s and $I3d_{5/2}$ envelopes were useful in this respect, Table 4.2. The N1s, Figure 4.2c, was resolved into two main peaks centred at 399.3 eV (corresponding to

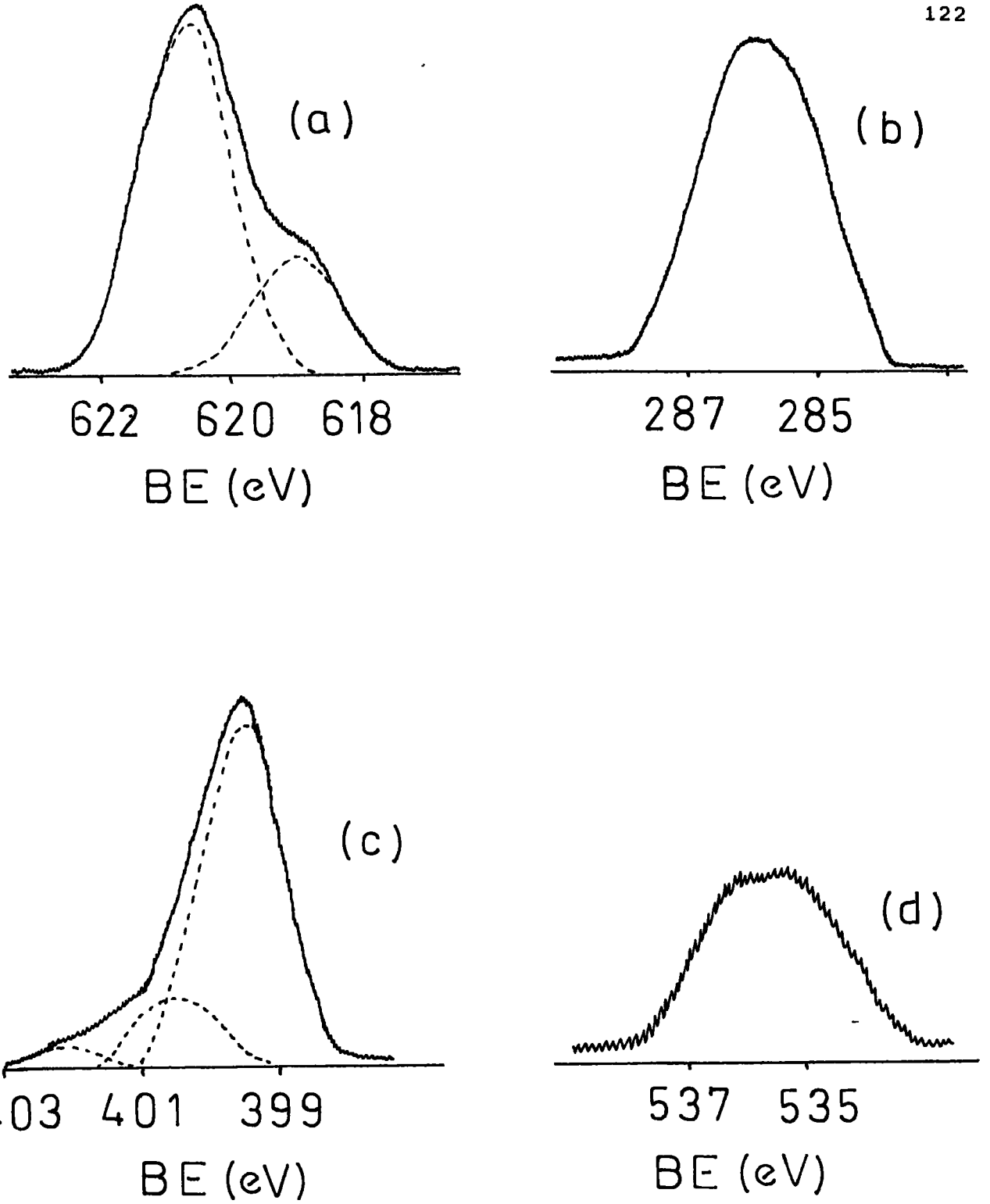

IGURE 4.2 Chloroacrylonitrile / Iodine 25W Plasma Polymer - Core Level Spectra : (a) I3d5/2; (b) C1s; (c) N1s; (d) O1s.

		No per 100 C atoms				N1s / eV			I3d5/2 / eV	
SUBSTRATE	POWER	Cl	I	N	O	399.3	400.8	402.3	618.5	620.5
POSITION	in W									
UPSTREAM	9,25,35	no deposition								
	45	13	32	23	9	71	22	7	7	93
	55	12	20	17	9	72	22	6	10	90
OUT OF	9,25,35,45	no deposition								
COIL	55	2	21.5	33	9	64	30	6	0	100

OTES : Table 4.1 relates to the determined elemental ratios er 100 C atoms, Table 4.2 to the N1s and I3d5/2 core level pectra. The latter are expressed as a % contribution of each inding energy component to the total area of that spectrum.

ABLE 4.1 and 4.2 Chloroacrylonitrile / Iodine Plasma Polymer. In coil results, F = 0.48 $cm^3 STP min^{-1}$.

UBSTRATE OSITION	DAYS IN AIR	No. per 100 C atoms Cl	N	I	O	N1s / eV 399.3	400.8	I3d5/2 / eV 618.5	620.5
PSTREAM	0	12	20	18	4	73	27	6	94
	1	8	12	18	10	72	28	6	94
	2	7	9	16	14	69	31	6	94
N COIL	0	8	30	17	5	76	24	5	95
	1	5	16	16	10	73	27	5	95
	2	5	13	13	11	74	26	5	95
	3	3	10	10	14	75	25	5	95

OTE : 1. Original samples were analysed immediately after ynthesis, then stored at atmosphere in sample bottles prior to eanalysis. 2. N1s & I3d5/2 envelopes are expressed as a % ontribution of each component binding energy to the total area bserved for the relevant core level spectrum.

ABLE 4.3 Chloroacrylonitrile / Iodine Plasma Polymer - Effect of Storage in Air.

nitrile groups) and 400.8 eV (corresponding to N-C and N=C). A shoulder at high binding energy suggests a third component centred at 402.3 eV. Its origin is unclear, but its appearance seems to be linked, at least in part, with that of a shoulder in the $I3d_{5/2}$ spectrum centred at 618.5 ± 0.3 eV, Figure 4.2a. Since the latter would be consistent with ionic iodine species being present in the film[5], the N1s shoulder would not be inconsistent with a nitrogen cation, although this was not proven. No overall pattern emerged for the N1s envelope with respect to power, analysis giving the ratio of nitrile to C-N and C=N groups at 2.5 ± 0.5 : 1 throughout.

The main component of the $I3d_{5/2}$ spectrum is centred at 620.5 ± 0.3 eV, corresponding to iodine covalently bonded to carbon, as well as any molecular iodine incorporated into the polymer film. The second iodine environment (618.5 eV) was only found to be in any real evidence for chloroacrylonitrile for a 25W power input. This latter binding energy could be accounted for by the iodide ion, I^-; however, the UV absorption spectrum, Figure 4.4, showed two distinct peaks centred at 288 nm and 368 nm, which are very similar to those found by Popov and Swenson[11] at 291nm and 360nm and determined to be characteristic of the I_3^- ion. In addition, the gradual increase in absorption of the film with decreasing wavelength is probably due to free radicals trapped in the polymer. Ward found similar evidence for the presence of I_3^- in plasma polymers of allyl iodide[5]. At least part of the negative iodine found by ESCA in the $I3d_{5/2}$ spectrum for chloroacrylonitrile can therefore be attributed to I_3^-. No peak was found in the UV spectrum at 548.3nm or 499.5nm, which would be due to adsorption by molecular iodine[12] suggesting that, for this particular film, the majority, if

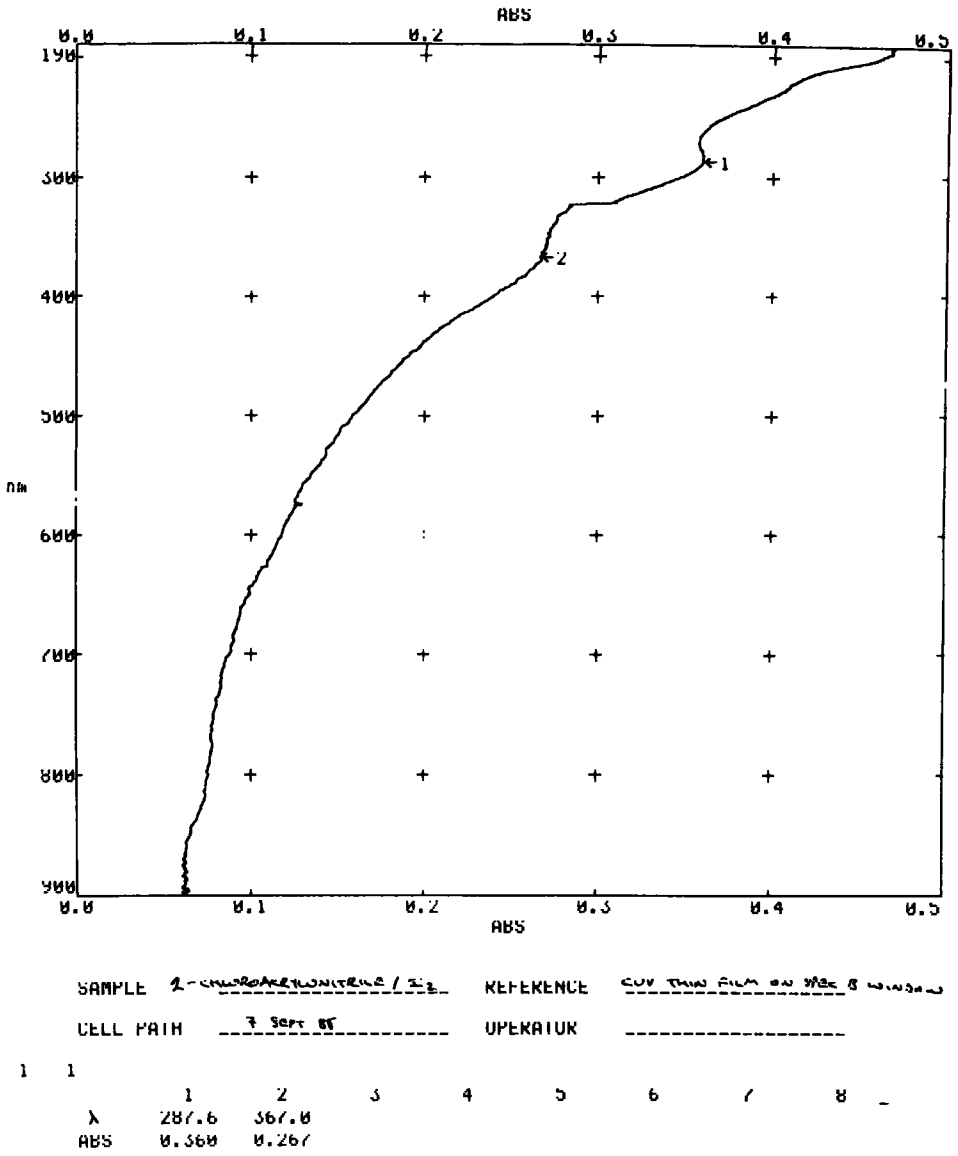

FIGURE 4.4 Chloroacrylonitrile / Iodine 25W Plasma Polymer; UV Absorption Spectrum.

not all, of the iodine present as indicated by the 620.5 eV peak in the $I3d_{5/2}$ spectrum is due to covalently bonded iodine. The ratio for the intensity of the low binding energy shoulder to the main peak at 620.5 eV decreases with the increasing iodine to carbon elemental ratio determined by ESCA, reinforcing the idea that the ionic content of the plasma polymer is low.

The possible nature of a positive counterion still needs to be considered. Carbocations are notoriously unstable except in strongly acidic media; however, Ward suggested that the most likely counterion for allyl iodide plasma polymerized in the presence of iodine is an allylic cation with the positive charge spread over the three carbon atoms (such that it might be expected to be resonance stabilised, and hence survive for a short while in the polymer).[5] The structure of chloroacrylonitrile does not lend itself so readily to such allylic carbocation formation as to cleavage of the carbon-chlorine bond to give $CH_2C{+}CN$. In addition, the possibility exists that a nitrogen cation might be present (the nitrile group may react to give $-C-N^{+}=C\ I^{-}$ and/or $-C-N^{+}\equiv C\ I_3^{-}$), although the true nature of any such counterion is unclear. In contrast, plasma polymerization of allyl cyanide in iodine vapour might be expected to give rise to a higher proportion of ionic iodine environments in the deposited film since the formation of an allylic counterion is likely to be easier. This postulate is examined in section 4.4.

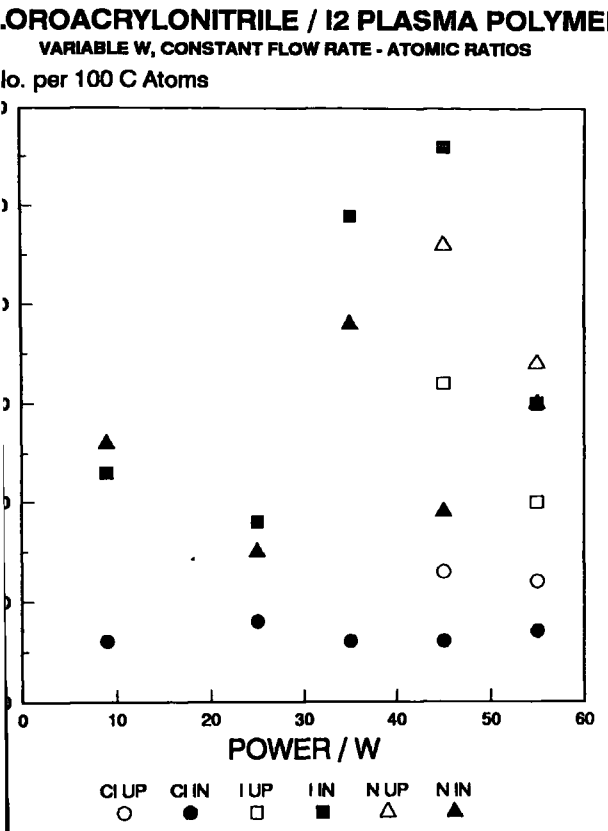

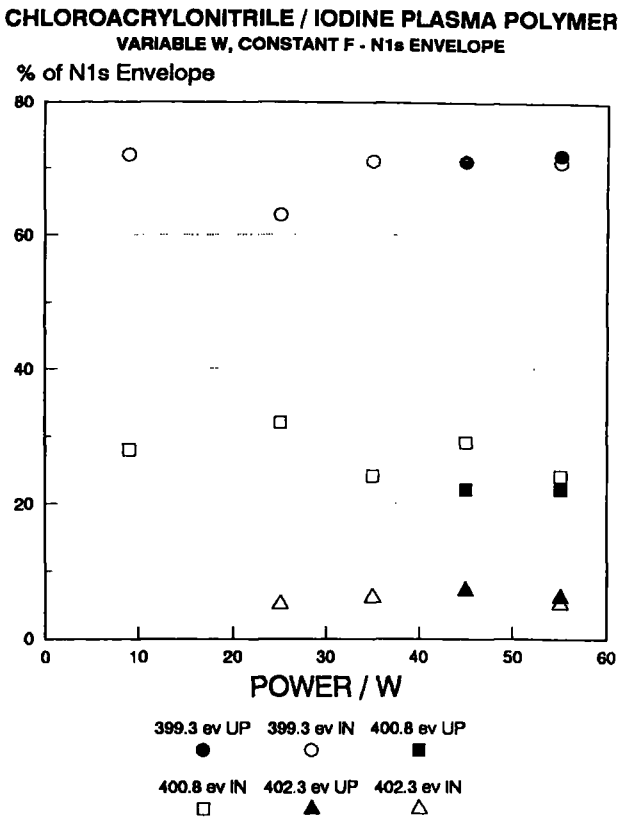

FIGURE 4.3 Chloroacrylonitrile / Iodine Plasma Polymer; Results for Variable Power, Constant Flow Rate.

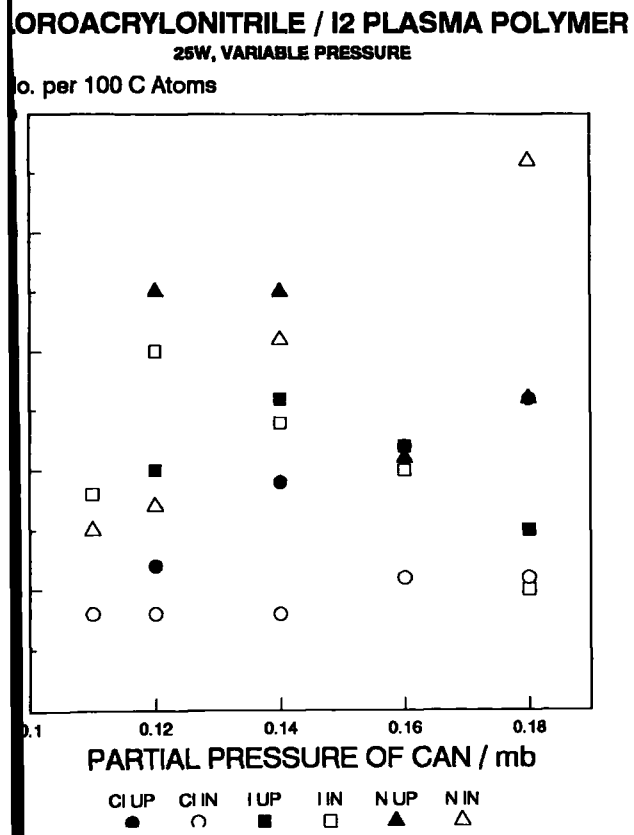

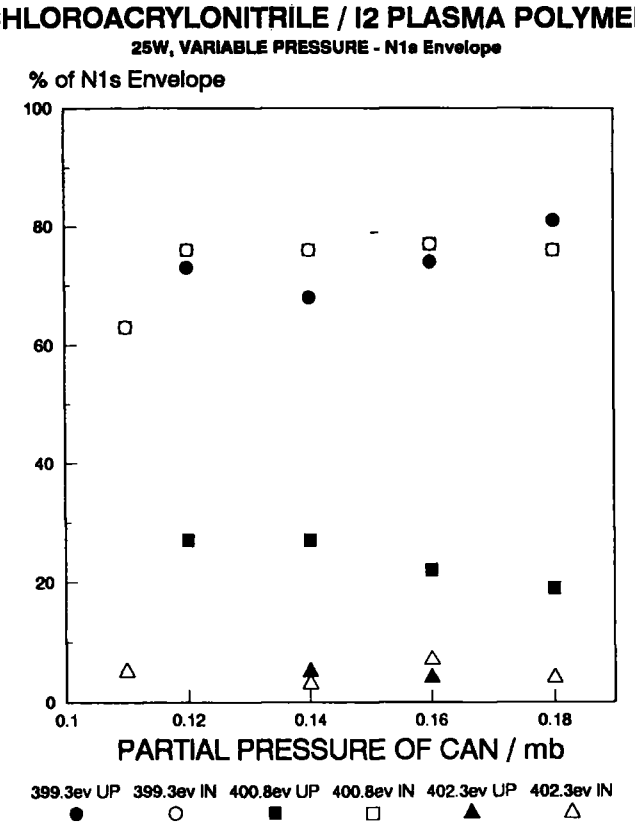

FIGURES 4.5 & 4.6 Chloroacrylonitrile / Iodine Plasma Polymer; Results For Variable Monomer Partial Pressure, Constant Power.

II Variable Flow Rate, 25W

Three substrate positions were studied as above. Partial pressures of 0.1mb to 0.18mb of chloroacrylonitrile were used, corresponding to flow rates of approximately 0.4-0.6 $cm^3_{STP}min^{-1}$. The addition of iodine vapour was found to decrease the measured total flow rate in all cases, the most marked effect occurring at the mid-series flow rates of chloroacrylonitrile. However, repeated coating of the Pirani-head by molecular iodine during subsequent experiments was found to make any total flow rate (ie chloroacrylonitrile + iodine) measurements unreliable. The results, Figures 4.5 and 4.6, are therefore displayed as a function of the partial pressure of chloroacrylonitrile used. Only the N1s spectra were fitted for the reasons outlined in section I.

Deposition occurred readily both in, and upstream, of the coil for all conditions except 0.1mb. Hence increases in power and monomer flow rate each lead to increased deposition rates in the latter substrate position. In contrast, no deposition was observed in the tail region under any conditions, suggesting that this portion of the reactor chamber falls in the power deficient region proposed by Yasuda and Hirotsu[13], since deposition was found to occur in this position for 55W in section I. Chlorine content of the films was markedly higher up-coil than in the coil region itself: the higher power availability in coil here probably reflects a higher scission rate in the latter substrate position for the carbon-chlorine bond. Both regions exhibited an increase in the Cl:C ratio with higher flow rate, whilst the N:C ratio showed differing behaviour for the two films - in coil, the ratio rising with increasing F, whilst upstream the ratio fell. This

compares to the maxima for both chlorine and nitrogen content found in the absence of iodine (chapter 3), whilst oxygen uptake by the films decreased with (higher) flow rate, as expected. The total iodine content of the film (whether in molecular, covalent or ionic form) showed maxima at 0.13mb and 0.15mb of chloroacrylonitrile respectively for the in coil and upstream positions.

The $I3d_{5/2}$ envelope again gave evidence for the formation of negative iodine species in coil, the most obvious example occurring at low flow rate (0.1mb). Evidence for the presence of I_3^- again came from the UV absorption spectrum, which exhibited two peaks near 288nm and 367nm. These were found to disappear with time on exposure to the atmosphere, indicating that the polyiodide ion is unstable under these conditions, probably eliminating molecular iodine. In order to examine this possibility, two films (in-coil and upstream substrates for 25W, 0.13mb)) were re-examined by ESCA after storage in air for 48 hours. The results, Table 4.3, show that the Cl:C, I:C and N:C ratios all decreased, whilst that of O:C increased. The chlorine to carbon elemental ratio showed the largest overall drop on reanalysis after 24 hours (over 30% for each film), presumably due to degradation of the sample by x-rays (the carbon-chlorine bond is labile, see chapter 3) together with an increase in the hydrocarbon content of the film due to extraneous contamination, not least during the ESCA analyses themselves. The percentage drop for iodine content in coil was only about 10%, rising to 40% for the upstream sample. Again this could be caused by x-ray degradation and/or hydrocarbon contamination of the sample in the spectrometer; however, the differing amounts by which this occurs suggests otherwise. After 48 hours the chlorine was found

to be stabilised; the ratio of iodine to carbon had fallen further. The ratio of ionic to covalent iodine peaks remained effectively constant throughout, indicating that the disappearance of the latter species (as monitored by ESCA) and I_3^- (as shown by the UV absorption spectra) are linked. The nitrogen content of the films throughout the two days remained constant within experimental error, whilst - not unexpectedly - uptake of oxygen, presumably by the free radical sites in the film surface suggested to be present by the UV adsorption spectrum, increased with time, this effect being more marked for the upstream sample than for that in coil.

Analysis of the N1s spectrum for the variable flow rate series showed an overall increase in nitrogen content of the films with flow rate, whilst the ratio between nitrile and other nitrogen environments varied between approximately 2:1 at 0.1mb of chloroacrylonitrile (and hence low flow rate) and 4:1 at 0.18mb (high flow rate). A slight shoulder was again observed to the high binding energy side of the envelope, corresponding to a small shoulder on the low binding energy side of the $I3d^{5/2}$ peak. However, both shoulders were markedly less than those observed for 25W in coil film in section I with the exception of the result obtained for 0.1mb of chloroacrylonitrile.

III Summary

The above results reveal marked differences in the plasma polymerization of chloroacrylonitrile in the presence of iodine vapour compared to that in the presence of monomer vapour alone. In particular, iodine drastically affects the glow volume in the deposition chamber and also inhibits polymerization, especially outside

this region. Such inhibition can occur via iodine either quenching free electrons in the system, and hence preventing electron impact excitation of the monomer, or else by free radical scavenging of depositing species resulting in termination of the deposition process. Overall, the plasma system (the tail region in particular, where deposition only occurred at 55W) is found to be power deficient according to the model of Yasuda and Hirotsu[13]. Analysis of the resultant films by ESCA and UV absorption spectrometry reveal the presence of small amounts of ionic iodine species, probably I^- and I_3^-. On standing film samples in air for 48 hours the iodine content decreases with time, presumably due to decomposition of the observed polyiodide (I_3^-). Since oxygen uptake also occurs during this process some free radical sites must be left unquenched in the film surface by the iodine. In addition, although the decrease in the Cl:C elemental ratio after 24 hours can be attributed to lability of the carbon-chlorine bond, the lack of further degradation suggests that about half of the chlorine environments are not labile.

4.4 Allyl Cyanide / Iodine

Allyl cyanide was found to exhibit different behaviour to chloroacrylonitrile in the presence of iodine, but showed remarkable similarities to allyl iodide as studied by Ward[5]. The latter compound was found to have a C:I stoichiometry of 13:1 for a flow rate of $1cm^3_{STP}min^{-1}$ at 4W[5], the ratio increasing with higher power. 25% of the iodine present was found to be in the form of ionic species - ie I^- and/or I_3^-, whilst storage in air was again found to decrease this ionic contribution to the I3d spectrum, such that after 24 hours the

peak observed at 619 eV completely disappeared. The corresponding cation was thought to be allylic in nature, evidence for which came from the solid state NMR spectrum of (allyl iodide) plasma polymer.[5] This result was thought to be the first example of a polymer in which ions can be detected in the bulk, although the observation of negative ions at the interface between a perfluoropropane plasma polymer and its substrate has been claimed by Haque and Ratner[14]. A radical addition mechanism was subsequently suggested not to occur for allyl iodide plasma polymerization on the basis that surface photopolymerization using both conventional and vacuum ultraviolet radiation failed to deposit a film, indicating that UV excited state chemistry is not responsible for film deposition for this monomer.[5] However, iodine is an integral part of the monomer in allyl cyanide; the allyl cyanide / I_2 system therefore provides a comparison.

I Variable Power

As with chloroacrylonitrile / iodine, three substrate positions were used - in coil, upstream of the coil, and in the tail region. Attention was paid to the effect of power on the glow region, and the effect of the glow itself on both the deposition rate and the chemical nature of the film deposited. A flow rate of $0.28 cm^3_{STP} min^{-1}$ was used throughout, the power being increased in stages from 8-60W. The glow volume was found to increase with increasing power, suggesting that addition of iodine to the system causes it to be power deficient. The colour distribution of the glow volume differed from that obtained for chloroacrylonitrile - the mauve-blue of pure monomer gave way, on introduction of iodine vapour, to a pure white glow downstream of the

coil. An off-white colour tinged with the original mauve-blue was observed in-coil, whilst a tinted orange/yellow glow occurred upstream of the coil region near the monomer/iodine inlet. This colour distribution - from pure white to orange-yellow - was found to reflect the observed film deposition rates, since the walls of the reactor were rapidly coated with polymer in the yellow, upstream, glow region - the yellow colour being due to the film depositing so quickly that it filtered the visible emission - and also in the coil region itself. Coating occurred more slowly in the white glow volume, and not at all outside. In a separate experiment a pure iodine plasma was found to be white in colour; hence it is excited iodine species in the plasma which are responsible for the main change in colour throughout the reactor, which obscures that due to excited species of allyl cyanide. The maximum deposition rate only occurred in coil at the lowest power setting used (8W), so polymer ablation and etching must dominate the plasma polymerization process here under high power conditions - ie the coil region is monomer deficient. This contrasts with the upstream and tail regions, and also the chloroacrylonitrile system as a whole, which were all found to be power deficient.

The colours of the glow volume also reflected the differences seen in the colour of the films formed, varying from orange (upstream and 8W in coil samples) through to grey (obtained in the tail region at 60W, the only power setting at which the white glow volume incorporated this substrate position). Overall, the relationship between glow volume and plasma polymer formation can be summed up by :

NO GLOW = NO FILM DEPOSITION

This is different to the acrylonitrile and chloroacrylonitrile / iodine systems, in which some deposition occurred outside the glow volume, even although insufficient to completely cover the substrate.

Quantitative analysis of the films by ESCA (Table 4.4) revealed the following :

a) Iodine content of the film in coil showed an overall decrease with increasing power, whilst for the upstream position at 40W the I:C ratio was more than twice as great (2.3:1) as that in coil. The one tail region substrate showing deposition (60W) also revealed a higher iodine content than the corresponding film in coil by 3.3:1.

b) The N:C ratio was initially low (12:100) at low power (8W), rising to 19 $\pm$ 1 : 100 thereafter. The C1s envelope was not fitted, whilst the N1s envelope gave no discernible pattern over the power range used. However, a preliminary experiment at 8W using a higher flow rate gave a higher nitrogen content (N:C ratio 22:100), together with a much increased ratio of 7:1 for the 399.3 eV peak component versus that at 400.8 eV. This compares with 2.5:1 or less for the remainder of the series, and suggests that elimination of nitrogen containing species - probably as cyanide radical or ion - occurs more readily at lower flow rates. This again classifies the system as monomer deficient, as outlined above.

c) Oxygen content of the films generally decreased as the monomer flow rate increased. On exposing the 60W sample to air for 30 hours, the oxygen uptake almost quadrupled the O:C ratio. This, together with the increasing UV absorbance below 500nm (Figure 4.7), again suggested that some free radicals were present in the film surface. The out of coil sample showed similar behaviour.

ELEMENTAL RATIOS

SUBSTRATE POSITION	POWER	No.per 100 C atoms I	N	O	Al	N1s / eV 399.3	400.8	402.3	$I3D_{5/2}$ / eV 618.5	620.5
IN COIL	8W	22	12	10	-	87	13	-	31	69
	20	17	20	2	-	56	35	9	36	64
	40	8	19	5	-	68	27	5	22	78
	60	7	17	3	-	62	35	3	30	70
	60[1]	4	15	11		66	34	-	18	82
TAIL	8	-	-	-	Y[2]	-	-	-	-	-
	20	-	-	-	Y[2]	-	-	-	-	-
	40	-	-	-	Y[2]	-	-	-	-	-
	60	23	15	-	Y[2]	53	44	3	29	71
	60[1]	5	11	17	Y[2]	64	36	-	11	89
UPSTREAM	40	18	16	4	-	56	44	-	42	58
	40[3]	16	14	4	-	61	39	-	45	55

NOTES : 1. Sample stored in air for 30 hours prior to reanalysis.

2. Y indicates an Al2p signal was visible. An overlayer calculation was therefore used to calculate elemental ratios with respect to carbon.

3. X-ray degradation experiment - sample retained in spectrometer and immediately reanalysed.

TABLE 4.4 - Quantitative ESCA analysis of Allyl Cyanide Plasma Polymerized in the Presence of Iodine Vapour.

ALLYL CYANIDE / IODINE PLASMA POLYMER

FIXED FLOW RATE, VARIABLE POWER

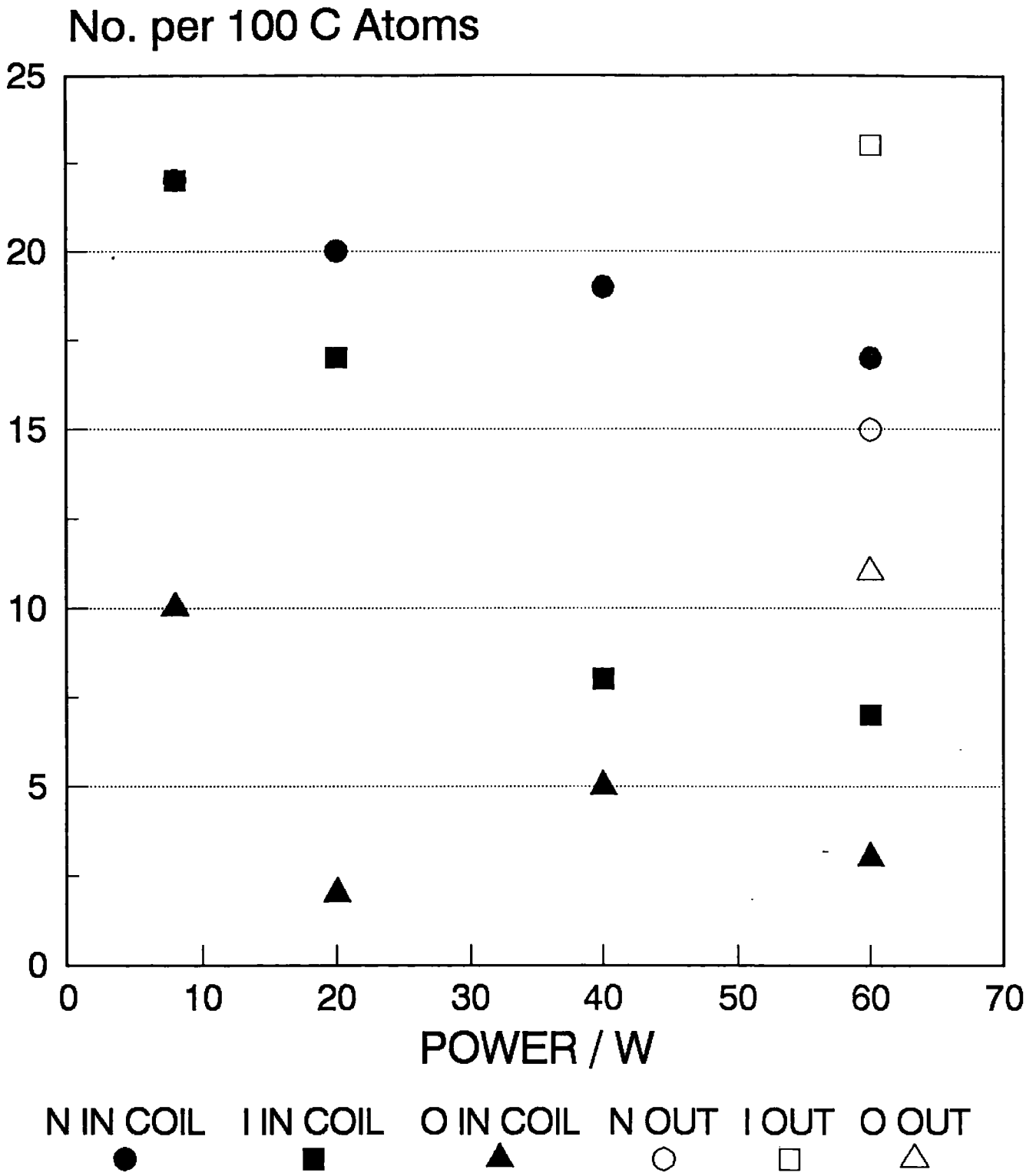

0.08 mb PARTIAL PRESSURE OF ALLYL CYANIDE
USED THROUGHOUT

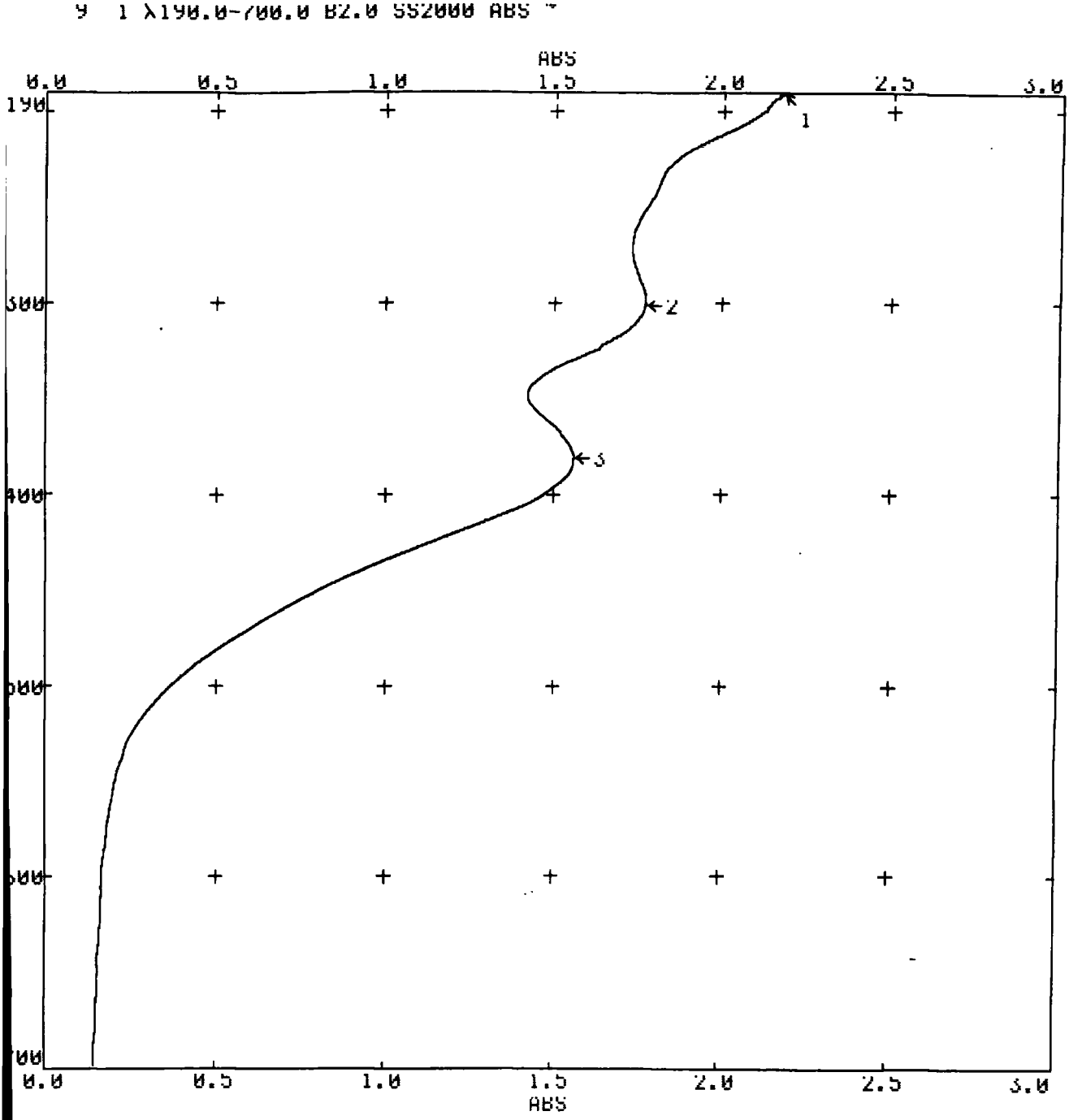

SAMPLE Allyl Cyanide / I_2 REFERENCE P = 0.15 mb, W = 30 W

CELL PATH Plasma Polymer OPERATOR 3 minute deposition

1 λ190.0-700.0 B2.0 SS2000 ABS

	1	2	3	4	5	6	7	8
λ	190.6	301.0	380.5					
ABS	2.176	1.773	1.562					

FIGURE 4.7 Allyl Cyanide / Iodine Plasma Polymer - UV Absorption Spectrum.

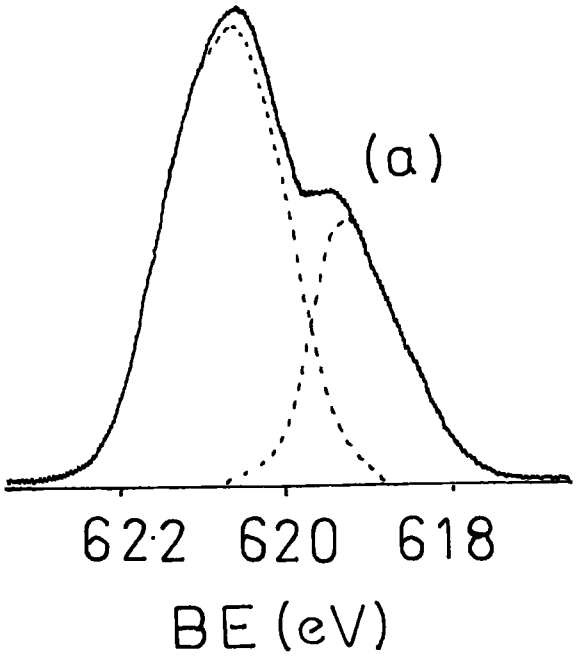

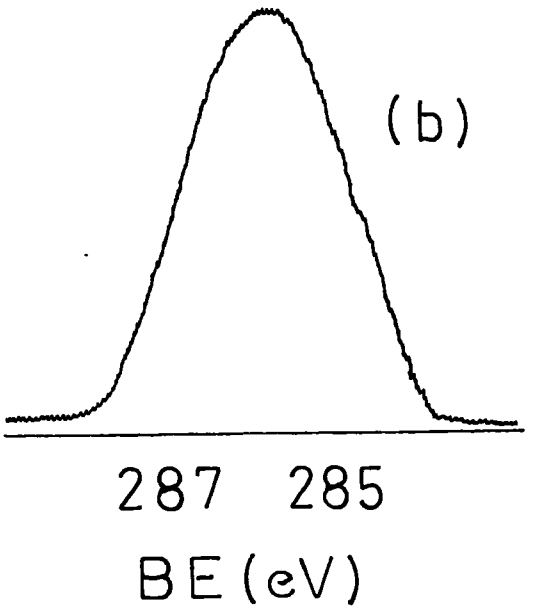

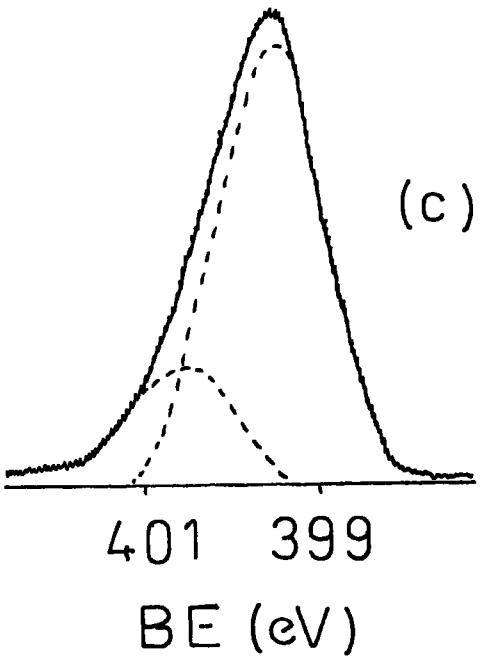

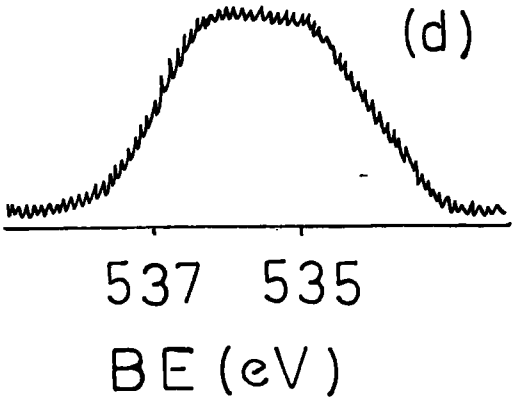

FIGURE 4.8 Allyl Cyanide / Iodine Plasma Polymer - Typical Core Level Spectra : a) I3d5/2; b) C1s; c) N1s; d) O1s.

d) Exposure to the atmosphere also dramatically decreased the iodine content of the film, especially for the out of coil sample. In order to eliminate the possibility that x-ray degradation of the sample during reanalysis is responsible for this result, the 40W sample was retained in the spectrometer and immediately rerun. The results showed only a slight decrease for both I:C and N:C ratios, in line with those expected for build-up of extraneous hydrocarbon on the surface of the film, confirming that the iodine species were not labile, and that the result for storage in air is accurate. Further confirmation of this came from the $I3d_{5/2}$ spectrum itself, resolution of which showed a substantial increase in the ratio of covalent and molecular, to ionic, iodine environments from 2.3:1 to 4.6:1 (in coil) and from 2.4:1 to 8.1:1 (in the tail region). The ratio of the two peaks remained unchanged after attempted x-ray degradation, and had not been found to show any pattern in variation with respect to power.

e) The films left standing in air overnight were also studied by UV absorption spectroscopy. The absolute intensities were found to have decreased as expected; however, the relative intensities of the 301nm peak to that at 380nm were also found to have changed, increasing from 1.1:1 before exposure to 1.5:1 after. No absorptions were found at 548.3nm or 499.5nm corresponding to molecular iodine.

f) Whereas plasma polymers of pure allyl cyanide (and the acrylonitriles) were found to be insoluble in all solvents tried, both organic and inorganic, those of allyl cyanide / iodine were soluble in acetone. This suggests that the latter films are not as highly crosslinked.

The above data thus indicates a greater ionic iodine content of the allyl cyanide / I_2 films compared to either chloroacrylonitrile or (on the basis of ESCA data) allyl iodide plasma polymers, since the $I3d_{5/2}$ envelope for the former often gave 618.5 eV to 620.5 eV peak area ratios between 1:8 and - more importantly - 4:1, as detailed in section I and II below. Thus, unlike allyl iodide or chloroacrylonitrile, the nature of allyl cyanide plasma polymers can be dominated by ionic, rather than by covalent species. Attempts to characterise an allyl cation using solid-state carbon-13 NMR were unsuccessful; however, this remains the likely counterion.

II Variable Flow Rate at 21W and 42W

The flow rate of allyl cyanide monomer proved difficult to control in the presence of iodine vapour, which was used at vapour pressure throughout. Three substrate positions were used as before. Results are presented in Table 4.5. The main trends were :

a) The colour distribution in the glow volume was similar to that for the variable power series. However, on increasing the monomer flow rate, the film deposition rate in the tail region increased, showing this region to be monomer deficient.

b) The nitrogen content of the deposited films showed random variation with flow rate within experimental error. A power dependence was seen as in section I - a higher N:C ratio occurring in coil at the lower power used (21W). This is close to the 1:4 maximum ratio expected for a conventional allyl cyanide polymer, indicating that nitrogen containing groups were increasingly eliminated as the power input to the system increased.

			ELEMENTAL RATIOS								
			No. Per 100 C atoms				N1s / eV			$I3d_{5/2}$ / eV	
SUBSTRATE POSITION	POWER in W	FLOW RATE	I	N	O	Al	399.3	400.8	402.3	618.5	620.5
IN COIL	21	0.28	17	20	2	-	56	35	9	36	64
		0.48	34	27	4	-	36	64	-	62	38
		0.48[1]	21	22	3	-	42	58	-	63	37
		0.48[3]	23	19	3	-	58	42	-	37	63
		0.67	33	26	5	-	17	83	-	79	21
	42	0.28	8	19	5	-	68	27	5	22	78
		0.28	12	15	2	-	not fitted			15	85
UPSTREAM	21	0.28	20	13	6	-	60	40	-	34	66
		0.48	26	17	2	-	60	40	-	32	68
		0.48[3]	26	17	2	-	64	36	-	33	67
		0.67	26	16	2	-	60	40	-	32	68
	42	0.28[a]	18	16	4	-	56	44	-	42	58
		0.28[1]	16	14	4	-	61	39	-	45	55
		0.28[2]	22	21	1	-	53	44	-	35	65
TAIL	21	0.28	no deposition			Y					
		0.48	no deposition			Y					
		0.48[3]	no deposition			Y					
		0.67	no deposition			Y					
	42	0.28	no deposition			Y					
		0.48	no deposition			Y					
		0.67	no deposition			Y					

NOTES :

1. X-ray degradation experiment.
2. Repeat experiment for a.
3. Power measure in W, flow rate in $cm^3_{STP}min^{-1}$.

TABLE 4.5 - Quantitative ESCA Analysis of Allyl Cyanide Plasma Polymerized in the Presence of Iodine Vapour

c) Iodine content of the films increased with monomer flow rate. Since the system is overall monomer deficient and the partial pressure of iodine was kept constant throughout, this suggests that chemical incorporation into the plasma polymer occurs rather than molecular iodine simply being physically adsorped. Oxygen incorporation was small for all the films analysed, and showed no obvious trend.

d) C1s spectra were not fitted. Resolution of N1s envelopes showed the ratio of cyano (399.3 eV) to other nitrogen environments (400.8 eV) decreases at higher flow rate for 21W. No evidence was found for a shoulder centred at 402.3 eV. In contrast, the 618.5 eV shoulder in the $I3d_{5/2}$ spectrum was significantly increased compared to previous samples. Quite distinct, its area ratio versus the 620.5 eV peak was found to be at a maximum ratio of 4:1 for a 21W power input/high flow rate film produced in coil (Figure 4.10). Little variation was found with flow rate at 42W, the area ratio remaining approximately constant at 2:1 in favour of the 620.5 eV peak.

f) No deposition was observed in the tail region under any of the experimental conditions used.

X-ray degradation was found to occur for the two samples chosen at random : a mid-flow rate, in coil sample deposited at 21W and a low flow rate sample deposited upstream at 42W. The overall iodine content decreased for both samples, although the ratio of covalent to ionic environments remained unchanged for the 21W film. Converting the peak percentages for each component to a ratio with respect to carbon gives:

	ELEMENTAL RATIOS			Binding Energy / eV N1s		Binding Energy / eV $I3d_{5/2}$	
SAMPLE	I	N	O	399.3	400.8	618.5	620.5
21W undegraded	34	27	4	10	17	21	13
degraded	21	22	3	9	13	13	8
42W undegraded	22	21	1	11	10	8	14
degraded	16	14	4	8.5	5.5	7	9

TABLE 4.6 X-ray Degradation of Allyl Cyanide / Iodine Plasma Polymers

All figures are given as a ratio per 100 carbon atoms. Hence both ionic and covalent iodine are degraded for the 21W sample, but only covalent iodine is lost to any extent from the 42W film. Similarly, it is the 400.8 eV peak area which is degraded in absolute terms for the N1s envelope, indicating that the nitrile groups are not labile here.

Exposure of the 42W low flow rate sample to the atmosphere over a period of 4 days, Table 4.7, showed that the iodine content dropped by 50% in the first 24 hours. This result is partially due to x-ray degradation of the sample as shown above; however, uptake of oxygen was also observed. Again, the maximum rate of uptake - presumably due to quenching of free radicals in the film surface - occurs over the first day, falling to about 1/6th of its original value overall.

The decrease seen in the nitrogen content of the films was probably caused by x-ray degradation together with build-up of extraneous hydrocarbon contamination on the surface of the film during repeated analysis by ESCA, as suggested by the lower nitrogen to carbon ratios found for a 70 degree take-off angle. The N1s envelopes showed a 9:7 ratio in favour of nitrile groups, increasing to 2:1 after 48

				ELEMENTAL ANALYSIS			Binding Energy / eV			
				No. per 100 C atoms			N1s		$I3d_{5/2}$	
SUBSTRATE POSITION	POWER	FLOW	DAYS in air	I	N	O	399.3	400.8	618.5	620.5
UPSTREAM	42	0.28	0	18	16	4	56/9	44/7	42/8	58/10
			1	9	13	9	64/8	36/5	34/3	66/6
			1[1]	5	11	11	65/7	30/3	32/2	68/3
			2	7	12	10	63/8	37/4	41/3	59/4
			4	4	12	14	63/8	37/4	34/1.5	66/2.5
			4[1]	3	9	12	66/6	34/3	31/1	69/2

NOTE : 1. Those samples annotated by 1 were run at a 70 degree take-off angle; the remainder at 35 degrees.

2. The nitrogen and iodine envelopes are shown as both a percentage of the envelope and a ratio versus carbon. Thus 56/9 in the N1s represents 56% of the N1s peak area and a ratio of 9:100 for N:C.

Table 4.7 - Allyl Cyanide Plasma Polymerized in the Presence of Iodine Vapour and stored in Air

hours, whilst the covalent to ionic iodine ratio - as shown in the $I3d_{5/2}$ envelopes - increases from 1.25:1 to 2:1 over 4 days. How much of these latter observations are due to exposure of the films to the atmosphere, and how much to X-ray degradation, is unclear.

All the plasma polymerizations outlined above were carried out using allyl cyanide / iodine premixed in a T-piece prior to entering the plasma chamber. The system was therefore altered such that iodine vapour did not come into contact with the monomer vapour until the

latter was itself already in the main chamber, Figure 4.11. A 42W plasma was ignited in a medium flow rate of allyl cyanide ($0.48cm^3_{STP}min^{-1}$) in order to see what effect, if any, this alteration of iodine inlet position might have on the system. This proved quite marked for the in coil substrate position, Table 4.8, with both iodine

		ELEMENTAL RATIOS			Binding Energy / eV			
		No. per 100 C atoms			N1s		$I3d_{5/2}$	
SUBSTRATE POSITION	INLET	I	N	O	399.3	400.8	618.5	620.5
IN COIL	O	34	27	4	36/10	64/17	62/21	38/13
	C	23	19	3	58/11	42/8	37/8.5	63/14.5
UPSTREAM	O	26	17	2	60/10	40/7	32/8.5	68/17.5
	C	26	17	2	64/11	36/6	33/8.5	67/17.5

NOTE : 1. The nitrogen and iodine envelopes are shown as both a percentage of the envelope and a ratio versus carbon. Thus 36/10 in the N1s represents 36% of the N1s peak area and a ratio of 10:100 (ie 1:10).

2. O = monomer inlet in original position, C = in main chamber.

TABLE 4.8 Effect of Moving Iodine Vapour Inlet

and nitrogen contents decreased in comparison with the original result obtained. Only the oxygen content remained unchanged, since the N1s and $I3d_{5/2}$ envelopes also showed changes - the N1s indicating that the ratio of nitrile groups to carbon atoms in the film was unchanged at about 1:10, whilst the ratio of other nitrogen environments (N-C and N=C) to carbon dropped by about half. The ratio of the latter to nitrile groups also fell from 1.7:1 to 0.73:1 - ie nitriles now account for more than half of the nitrogen present. The ratios of ionic and covalent iodine to carbon respectively changed from 0.21:1 and 0.13:1 to 0.09:1 and 0.15:1, such that the abundance of ionic species in the film over covalent previously found (1.6:1) was reversed (to 1:1.7). In contrast, the film deposited in the upstream region showed little difference as a result of the inlet change. No deposition occurred in the tail region for either position. Why this positional dependence of the iodine inlet affects only the in coil substrate is not fully understood. However, the result indicates that the decrease in the iodine content in the plasma polymer is linked to the ratio of nitrile to other nitrogen species occurring in the film - the lower the nitrile content of the film, the higher the ratio of ionic to covalent iodine. This can be accounted for by the loss of CN by monomer molecules to give allyl cations as counter ions for I^- and I_3^-.

III Summary

Allyl cyanide plasma polymers deposit quite readily in the presence of iodine vapour, but only in the glow volume. Hence the nature of the films formed is dependent not only on the power and flow rate of the system, but also the position of the substrate and iodine

vapour inlet in the reactor chamber in relation to the extent of the glow region. Analysis of the films formed by ESCA (Figure 4.2b) and UV absorption spectrometry (Figure 4.7) revealed the presence of ionic iodine environments. Although, the peak separation is the same as for chloroacrylonitrile (79 $\pm$ 0.5 nm), such that I_3^- is again thought to be responsible, a greater absolute absorbance occurred for the allyl cyanide films, reflecting a much higher ratio of ionic to covalent environments as found in the $I3d_{5/2}$ spectrum. Some of the films proved to be X-ray degradable, whilst all took up oxygen on standing in air. This also caused loss of iodine species, in particular the polyiodide ion, the absorbance of which in the UV was found to have disappeared after four or five days. The ratio of ionic to covalent iodine was found to be linked to that for nitrile to other (N-C and N=C) nitrogen environments, and was attributed to formation of allylic cations to balance the number of ionic iodine species in the film to effect overall neutrality.

Since the visible plasma glow is due to emissions in the visible region from electron impacted excited states (whether ions or neutral species) returning to their ground states, the absence of these must again be linked to the absence of film deposition outside the glow volume. Using Ward's evidence that surface photopolymers of the analogous compound allyl iodide could not be obtained in the UV,[5] it seems likely that excited state chemistry below the ionisation potential does not play the same important role in plasma polymerization here as for the acrylonitrile family. In particular, the radical addition mechanism suggested for the latter is unlikely to occur for the allyl cyanide system, firstly in view of the probable

existence of allyl cations in the deposited polymer film, together with the strong presence of ionic iodine species, both of which illustrate not only the importance of ion chemistry in this case, but also the differing excited states, and hence chemistry, compared to the acrylonitrile family.

4.5 Allyl Cyanide / Bromine

Bromine was introduced to the system as a direct substitute for iodine in order to compare the effect between the two halogens. Since bromine was found to have a much higher vapour pressure as measured by the Pirani head (0.4mb), an Edwards needle valve was used to control its partial pressure and hence flow rate. Variation of the plasma polymerization process was monitored with respect to power and monomer flow rate.

I Variable Power

$0.18cm^3_{STP}min^{-1}$ of allyl cyanide, corresponding to a partial pressure of 0.08mb, was premixed in a T-piece with bromine vapour prior to entry into the main chamber at 0.1mb total pressure. A plasma was ignited in the usual manner, the glow volume (purple in colour) being initially confined to the coil region. Increasing the power input to the system increased the glow volume. More importantly, deposition was found to occur outside this, immediately providing a contrast with allyl cyanide / iodine. Substantial deposition occurred in both the upstream and tail regions in addition to in-coil; ie similar to the case for a plasma of pure allyl cyanide. Initiation of a plasma in the latter followed by introduction of bromine vapour at a later stage

resulted in a shrinkage of the glow volume. Heating the bromine monomer tube with a hairdryer increased the amount of bromine in the main chamber and restricted the glow volume to that of the coil region.

The chemical composition of the films obtained at 20W and 40W was obtained by ESCA, Table 4.9. Typical core level spectra are shown in Figure 4.9. Depth profiling studies showed that the polymer was effectively homogeneous; however, an x-ray degradation study proved the bromine content to be labile. This last result, together with the relative lack of reproducibility for the 20W sample for the bromine level (those of nitrogen and oxygen remained constant within experimental error) suggested that at least some bromine might be physically, rather than chemically, incorporated into the film. That physical adsorption onto surfaces easily occurs was shown by a control experiment in which bromine was introduced into the reactor in the absence of monomer, coating all surfaces (glass and substrate) quite thickly. Repeated use of the Edwards needle valve was also found to result in bromine deposition inside the valve itself over a period of time, necessitating regular cleaning.

The main points of interest re chemical composition as revealed by ESCA were :

a) Elemental analysis gave an initially very high Br:C ratio (68:100) at 7W for the in-coil region which dropped on increasing the power. However, the lack of reproducibility of this ratio (as commented on above) is difficult to explain but would be consistent with differing amounts of molecular bromine being adsorped into the film. The N:C ratio showed a minimum at 40W, whilst the oxygen level generally increased with power.

b) Upstream of the coil the maximum bromine uptake occurred at 20W, similarly large amounts being found at 7W and 60W. The nitrogen level increased between 7W and 20W, remaining constant within experimental error thereafter. Incomplete coverage of the aluminium substrate was observed at 7W, no deposition occurring outside of the glow volume under this condition . Full deposition occurred as the power was increased, indicating that the allyl cyanide / bromine system is power deficient compared to that of allyl cyanide / iodine, which was found to be monomer deficient. Introduction of a fourth substrate 3cm upstream from the in coil position(1) - ie mid-way between this and the original upstream position(2) - gave a nitrogen content and N1s envelope similar to (2), whereas the bromine content proved more similar to that for the in-coil sample (1).

c) Full deposition occurred in the tail region except at 7W (as for the upstream position). The level of bromine content was erratic with respect to power and showed little evidence of reproducibility even at the same power. A ratio of 2:1 was maintained in the N1s envelope in favour of the 399.3 eV peak (corresponding to intact cyano / nitrile groups in the film) over that at 400.8 eV (N-C and N=C environments). This ratio showed no change within experimental error over the series. The corresponding ratio for the upstream position was 7:3, whilst that in coil dropped from 4:1 at 7W to about 2:1 at 20W. Since no shoulder was visible in the N1s spectrum, the presence of nitrogen cations can be discounted.

d) The Br3d envelope was peak fitted to check for the presence of ionic environments. In addition to the expected (spin coupled) peaks occurring at 69 and 70 $\pm$ 0.5 eV (due to $Br3d_{3/2}$ and $Br3d_{5/2}$, Figure

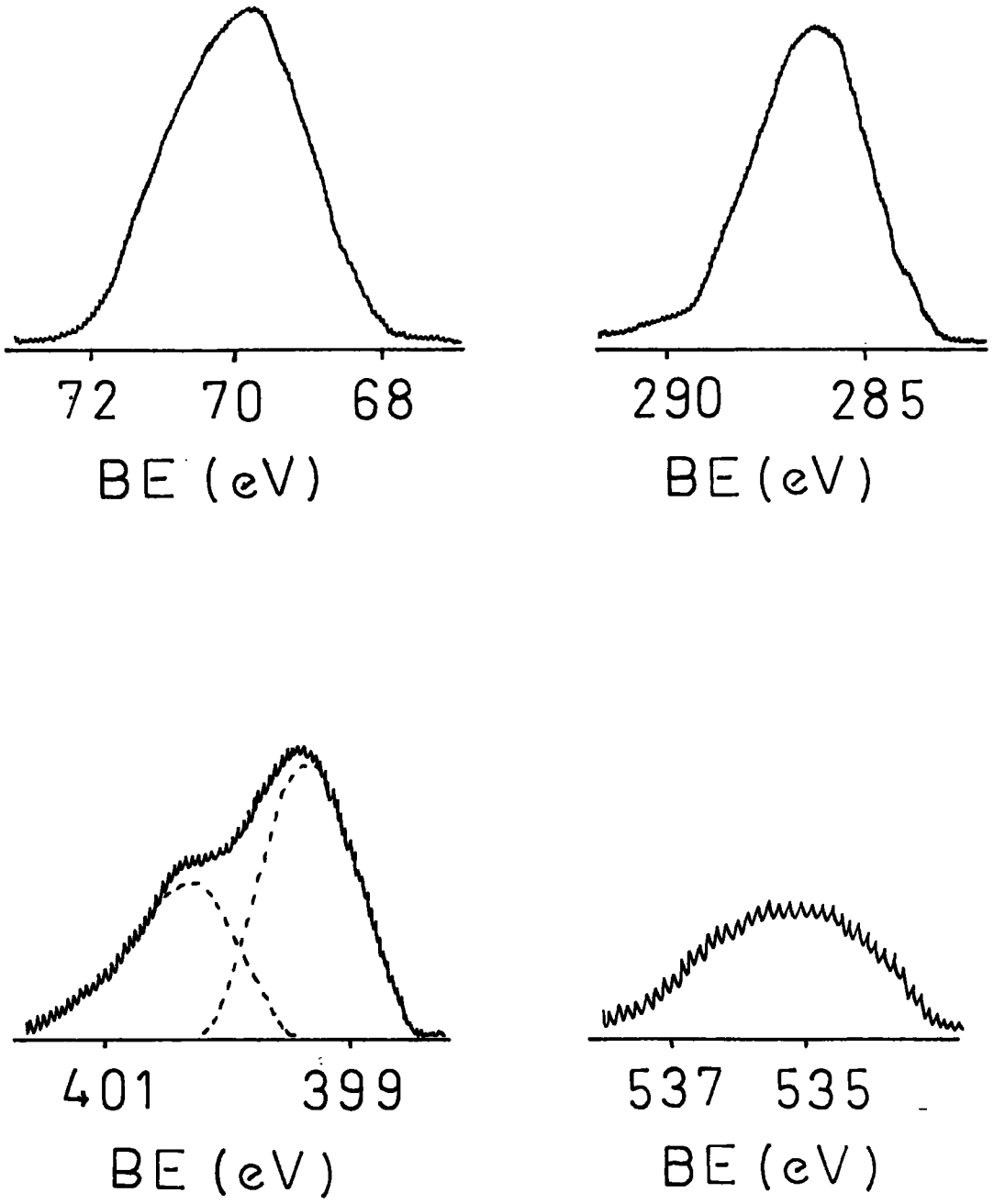

FIGURE 4.9 Allyl Cyanide / Bromine Plasma Polymer - Typical Core Level Spectra : a) Br3d; b) C1s; c) N1s; d) O1s.

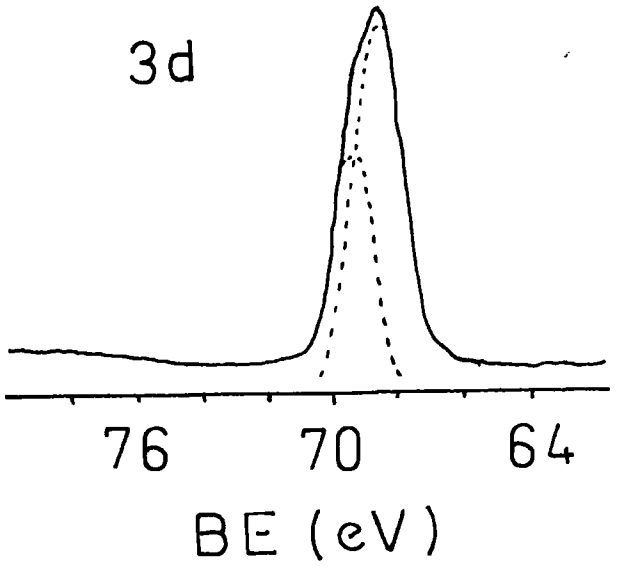

FIGURE 4.10 Br3d Core Level Spectrum (Molecular Bromine).

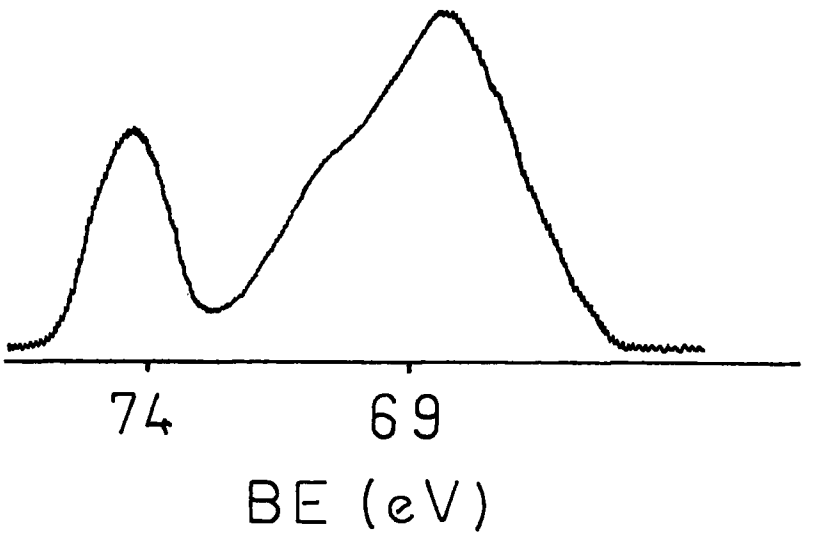

FIGURE 4.11 Br3d Core Level Spectrum - Allyl Cyanide Plasma Polymer; Incomplete Coverage of the Aluminium Substrate.

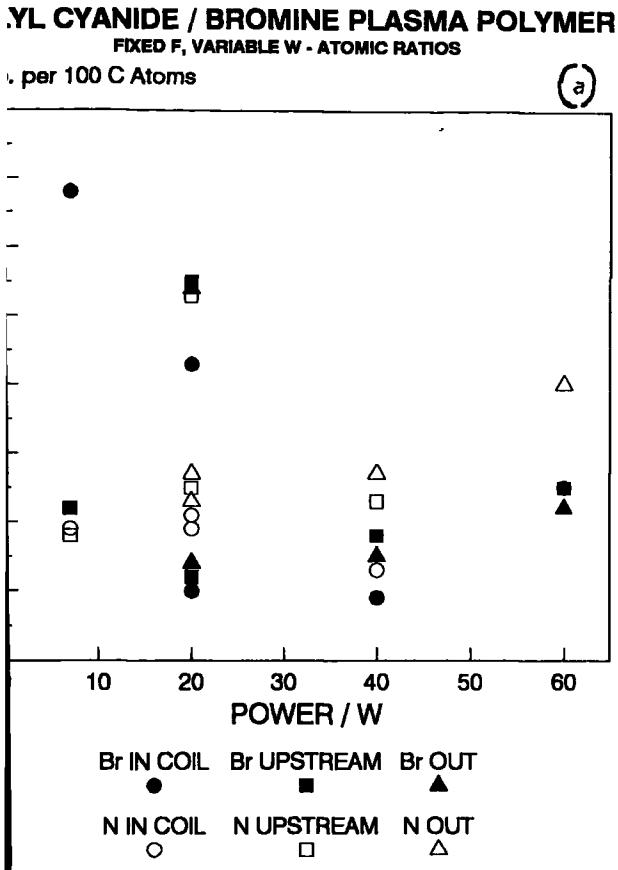

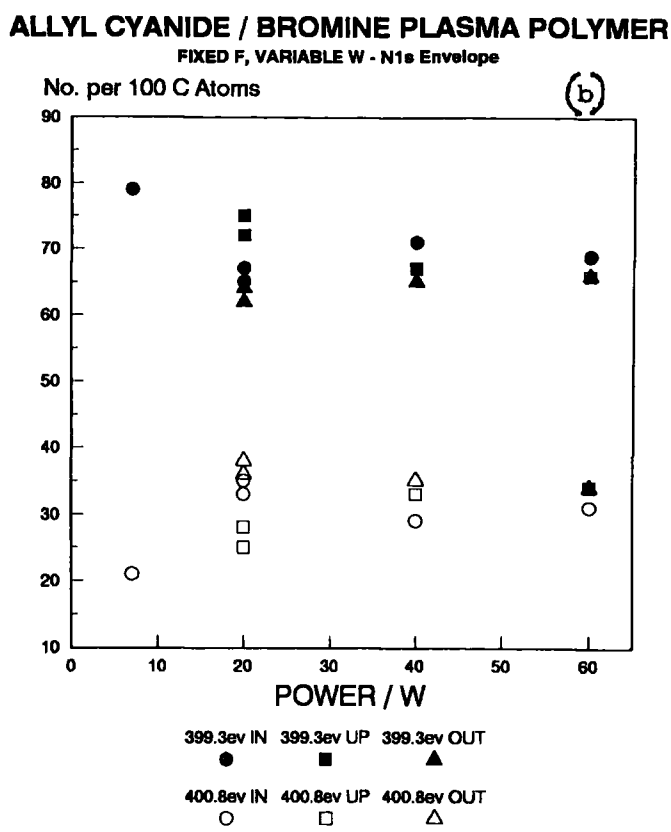

FIGURE 4.12 Results - Allyl Cyanide / Bromine Plasma Polymer

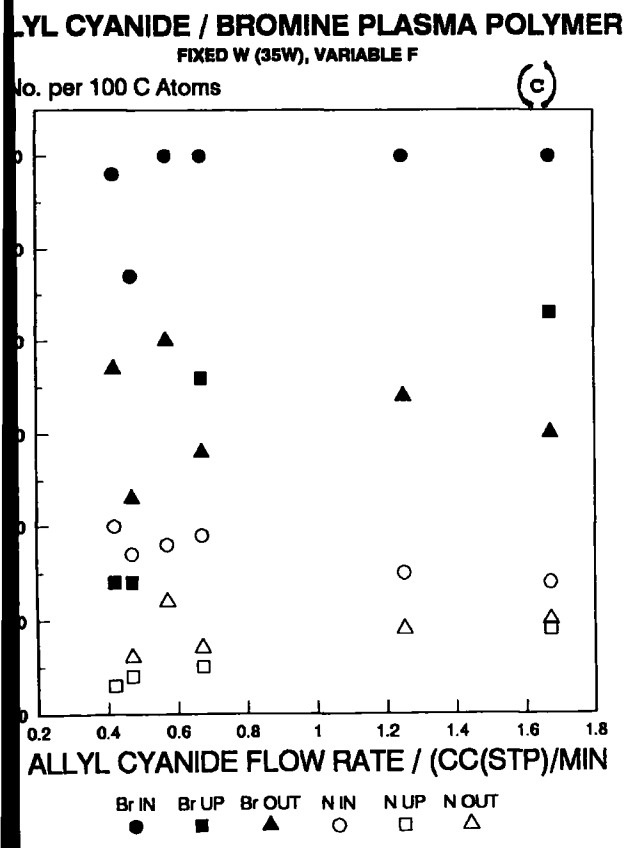

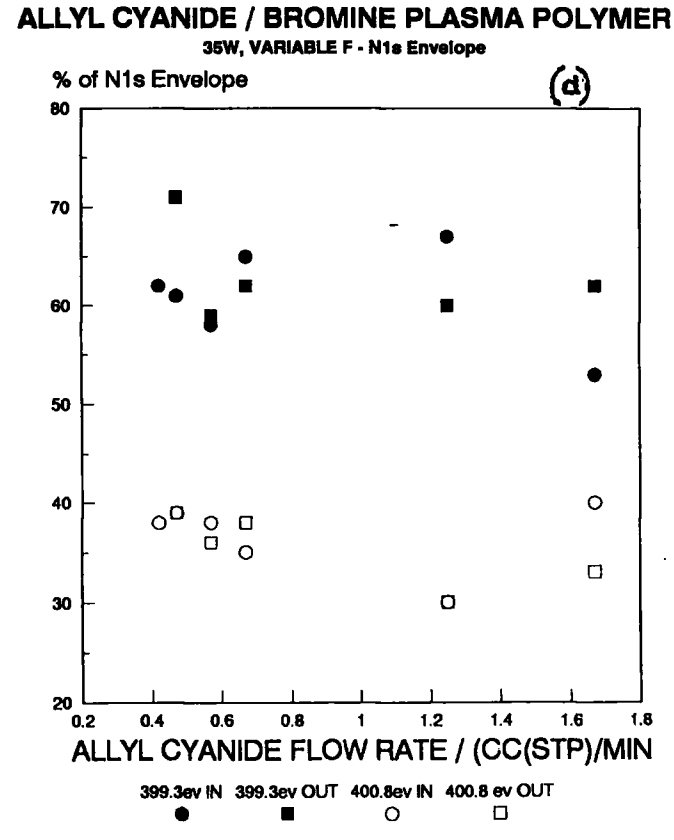

4.10), attributed to bromine covalently bonded to carbon and/or molecular bromine, a shoulder was evident in many films, to the low binding energy (BE) side which could not be accounted for by spin coupling , so that at least two environments were present. The chemical shift was determined to be about 2 eV to lower BE, and so was assigned to ionic bromine. Two further environments were also seen. The first, some 2 eV to higher binding energy than those peaks assigned to bromine covalently bonded to carbon (the latter being found at 69 $\pm$ 0.3 eV and 70 $\pm$ 0.3 eV) only arose for one sample, the repeat experiment at 20W which gave an abnormally high bromine to carbon ratio; the second, Figure 4.11, some 4 eV higher again, was seen whenever an Al2p signal was visible, ie whenever incomplete coverage of the substrate occurred, and so must be due to interaction between bromine and the aluminium substrate surface. Table 4.9 also shows a rough correspondence between the peak area ratios of the Br3d peaks due to ionic species and the overall bromine content of the films - a high number of ionic relative to covalent environments occurred when the bromine to carbon elemental ratio was low, and vice-versa. No obvious link was apparent between the level of ionic bromine in the film and the percentage of nitrile groups or other nitrogen environments as seen in the N1s envelope, in contrast to the situation for ionic iodine species in sections 4.3 and 4.4. However, the ratio of peak areas (399.3 eV : 400.8 eV) remained remarkably constant at about 2:1 for the tail region films, varying slightly for both the in-coil and upstream positions.

		ELEMENTAL RATIOS									
		No./ 100 C atoms				N1s (BE/eV)		Br3d ENVIRONMENTS[1]			
SUBSTRATE POSITION	POWER in W	Br	N	O	Al	399.3	400.8	(A)	(B)	(C)	(D)
								relative %'s			
IN COIL	7	68	19	5	-	79/15	21/4	0	100	-	-
	20	10	19	10	-	67/13	33/6	40	60	-	-
	20[2]	43	21	10	-	65/14	35/7	5	95	-	-
	40	9	13	8	-	71/9	29/4	24	76	-	-
	40[3]	8	13	9	-	72/9	28/4	18	82	-	-
	60	25	25	13	-	69/17	31/8	8	92	-	-
UPSTREAM	7	22	18	-	Y	not fitted		5	64	-	31
	20[4]	12	26	11	-	72/19	28/7	60	40	-	-
	20	55	25	-	-	75/19	25/6	6	94	-	-
	40	18	23	12	-	67/15	33/8	38	62	-	-
	60	25	25	10	-	66/16	34/9	66	34	-	-
TAIL	7	no deposition			Y	not fitted		not fitted			Y
	20	14	27	14	-	63/18	34/9	65	35	-	-
	20	54	23	13	-	62/14	38/9	7	42	52	-
	20[5]	38	27	14	-	62/17	28/10	11	89	-	-
	40	15	27	15	-	65/18	35/9	46	54	-	-
	60	22	20	20	-	66/13	34/7	21	78	-	-

NOTES: 1. (A) corresponds to the low BE (ionic) peaks; (B) to covalent (69&70V $\pm$ 0.3 eV); (C) to a +2 eV shift, (D) to +6 eV shift, both compared to (B). 2. Repeat experiment. 3. Run at 70° take-off angle. 4. Substrate here 3cm upstream only. 5. X-ray degradation experiment. 6. 66/26 in N1s data= 66% of total peak area and an N:C ratio of 26:100

TABLE 4.9 Allyl Cyanide / Br_2 Plasma Polymers - ESCA Data

Finally, on igniting a plasma at 60W with the bromine tap fully open (ie at vapour pressure) and heated with a hairdryer to increase the ratio of bromine to allyl cyanide molecules in the main chamber to a maximum, the glow volume was confined to the coil region. Unlike the case for allyl cyanide / iodine, deposition was still found to occur in the upstream and tail regions, although an Al2p signal was seen on ESCA analysis, indicating that the substrate was not completely covered by the deposited film.. The results, Table 4.10, showed a high nitrogen content in the plasma polymer. The nitrogen to carbon ratio in the tail region, at 1:4, was the same as that expected from a conventional allyl cyanide homopolymer.

		ELEMENTAL RATIOS									
		No./ 100 C atoms				N1s (BE/eV)		Br3d ENVIRONMENTS[1]			
SUBSTRATE POSITION	POWER in W	Br	N	O	Al	399.3	400.8	(A)	(B)	(C)	(D)
								relative %'s			
IN COIL	60	33	17	-	Y	66/11	34/6	41	38	-	21
UPSTREAM	60	32	18	-	Y	66/12	34/6	8	82	-	10
TAIL	60	20	26	-	Y	66/17	34/9	31	48	-	21

NOTES: 1. (A) corresponds to the low BE (ionic) peaks; (B) to covalent (69&70V $\pm$ 0.3 eV); (C) to a +2 eV shift, (D) to +6 eV shift, both compared to (B). 2. N1s peaks are expressed both as a % of the total envelope area and as a ratio with respect to carbon, ie 66/11 = 66% and a ratio of 11:100.

TABLE 4.10 Effect of Heated Bromine Vapour

The ratio of the peak area for 399.3 eV to that for 400.8 eV was 2:1 for all substrate positions whilst a high level of ionic bromine was found for the upstream and tail regions. The high binding energy Br3d environment, due to interaction with the aluminium substrate, was seen throughout.

II Variable Flow Rate

On increasing the partial pressure of bromine in the system it was found that the inside of the Pirani head quickly became totally coated, such that determination of the true system total pressure and flow rate was unreliable. The series was therefore carried out by measuring the partial pressure and flow rate of allyl cyanide in the absence of bromine and then isolating the Pirani head prior to introducing bromine into the T-piece at its vapour pressure. The total pressure was then quickly measured before coating of the Pirani head could occur, and was found to be a constant 0.19mb throughout. The results are presented as a function of the partial pressure of allyl cyanide, Table 4.11.

a) Bromine to carbon elemental ratios as determined by ESCA showed little variation in the in-coil region, all films giving results in the region of 0.5/0.6 : 1 with respect to carbon. Equivalent figures for the tail region were 0.3 $\pm$ 0.1 : 1., with no discernible pattern. Oxygen content remained low throughout.

b) Nitrogen content in coil was similar to that in section I. The tail region showed a decrease to single figures, all films showing incomplete substrate coverage such that an Al2p signal was visible.

c) The upstream position also gave incomplete coverage, with little evidence for any deposition at all at two pressures. The

presence of a high binding energy environment has already been attributed to interaction of bromine with the aluminium substrate; the extremely high intensity seen on the two occasions when film was not observed to deposit suggests that physical adsorption of molecular bromine onto the surface of the aluminium has in fact occurred. It is worth noting here that both the upstream and tail region substrates fell outside the glow volume, which in turn was found to shrink with increasing allyl cyanide flow rate. The consequent decrease in deposition rate observed for the system as a whole thus again classifies it as power, rather than monomer, deficient (see section I).

d) The two films in the tail region for which complete deposition was observed revealed two Br3d environments at about 2 eV higher binding energy than for the remainder, the core level spectra being similar to those reported in for the 20W tail region sample reported above (section I).

		ELEMENTAL RATIOS									
	PARTIAL	No./ 100 C atoms				N1s (BE/eV)		Br3d ENVIRONMENTS[1]			
SUBSTRATE	PRESSURE	Br	N	O	Al	399.3	400.8	(A)	(B)	(C)	(D)
POSITION	in mb							relative %'s			
IN COIL	0.1	58	20	3	-	62/12	38/8	-	100	-	-
	0.1[2]	38	14	4	-	64/9	36/5	not fitted			
	0.11	47	17	3	-	61/10	39/7	"	"	-	-
	0.11[2]	54	16	5	-	63/10	37/6	"	"	-	-
	0.13	60	18	4	-	58/10	38/8	-	100	-	-
	0.15	60	19	3	-	65/12	35/7	not fitted			
	0.17	60	15	3	-	67/10	33/5	"	"	-	-
	0.2	60	14	3	-	53/7	47/7	-	100	-	-
UPSTREAM	0.1	14	3	-	Y	not fitted		51	24	-	25
	0.11	14	4	-	Y	"	"	30	26	-	44
	0.13	no deposition			Y	"	"				>>50
	0.15	36	5	-	Y	"	"	40	40	-	20
	0.17	no deposition			Y	"	"				>>50
	0.2	43	9	-	Y	"	"	3	82	-	15
TAIL	0.1	37	?	-	Y	"	"	-	86	-	16
	0.11	23	6	-	Y	64/4	33/3	5	83	-	12
	0.13	40	12	-	Y	59/7	41/5	-	89	-	11
	0.15	28	7	-		62/4	38/3	-	36	64	-
	0.17	34	9	-	Y	60/5	40/4	29	56	-	15
	0.2	30	10	-		62/6	38/4	-	5	95	

TABLE 4.11 Effect of Increasing the Allyl Cyanide Flow Rate

4.6 Summary

Plasma polymerization of allyl cyanide and chloroacrylonitrile was carried out in the presence of iodine (both monomers) and bromine (allyl cyanide only). Inhibition of the glow volume and film formation were found to occur when halogen vapour was introduced into the plasma, iodine in particular preventing film deposition outside the glow region. Variation of deposition rate with power input and flow rate showed that chloroacrylonitrile was power deficient according to Yasuda's classification[13], as was allyl cyanide in the presence of bromine. In contrast, the allyl cyanide / iodine system was monomer deficient. All three systems gave rise to ionic halogen species, the I_3^- ion being determined by UV absorption spectrometry and degrading on standing in air. An allylic cation seems the most likely counterion in the case of allyl cyanide, as proposed by Ward for the plasma polymerization of allyl iodide.[5]

A consideration of results in terms of the likely inhibition mechanism of film deposition suggests that a free radical mechanism is dominant in the case of chloroacrylonitrile plasma polymerization, but not for allyl cyanide, which gives rise to a higher proportion of ions in the resultant film deposited in the presence of iodine. However, the presence of free radical sites in the deposited films - as evidenced by the UV absorption spectra and also the uptake of oxygen on prolonged exposure to air - show that radicals must play at least some role in the deposition process. This contrasts with the case for chloroacrylonitrile as monomer, which is thought to deposit mainly via a free radical mechanism.

Chapter 5

DEPOSITION OF ORGANIC THIN FILMS BY PHOTOCHEMICAL TECHNIQUES

5.1 Introduction

Absorption of radiation may have varying effects on a chemical reaction, from subtle changes in reaction rate to drastic alteration of reaction pathway.[1] Hence photochemistry is a commonly used technique in both synthetic organic, and inorganic, chemistry. Energies available in ultraviolet (UV) and vacuum ultraviolet (VUV) photochemistries in particular, although less than those available in a plasma (see chapter one), are greater than for thermal reactions such that new reaction pathways are available. Use of photochemical techniques to initiate polymerization reactions in the liquid or solid states involves creation of free radicals which promote chain growth. Gas phase photopolymerization at low pressure have been carried out by Melville on methyl methacrylate,[2] and by Gee[3] and Srinivasan[4a,b] on butadiene. The last of these, carried out in the early 1960s, preceded a number of studies during that decade which showed thin films could be photochemically deposited from the vapour phase using UV irradiation, with "monomers" styrene,[5] divinyl benzene,[6] acrolein,[6] tetrafluoroethylene[7] and acrylonitrile,[5] amongst others. These monomers all contain C=C unsaturation which would be expected to undergo polymerization via thermal techniques; however, other compounds not normally thought of as "conventional" monomers in this sense can also give rise to thin film deposition on gas-phase UV irradiation, including benzene[8a,b] and the perfluoroaromatics,[9,10] cyclohexanol, phenol and other aromatic compounds.[11] This means of thin film polymeric deposition has been termed Surface Photopolymerization.[12] The deposition of benzene was only observed for the VUV region (ie <200nm, as opposed to conventional, or CUV,

irradiation, which occurs at >200nm), Ward and Wishnok[8b] proposed that initial excitation to high electronically excited states (eg S_3) was followed by intersystem crossing to a vibrationally excited ground state (S_o^v), from which the photoproducts are thought to occur. A similar scheme was proposed by Till for the surface photopolymerization of perfluorobenzene.[9]

Organometallic and inorganic compounds can also give ultraviolet enhanced deposition; for example trimethyl aluminium deposits aluminium in the VUV at room temperature;[13] iron carbonyl ($Fe(CO)_5$) similarly gives rise to films of both iron and carbon on irradiation using a laser,[14] whilst tungsten hexafluoride[15] and diethyl zinc[16] also give rise to metallic films. All these systems deposit in a manner similar to plasma induced chemical vapour deposition.

Although "non-conventional" monomers in the thermal polymerization sense can give rise to surface photopolymers (eg benzene above), this occurs because the "monomer" concerned has both suitable chromophore able to absorb UV/VUV radiation, and also a reaction pathway via excited state gas phase chemistry that leads to photodepositing / polymerizing species. This assumes that the incident radiation is below the ionisation energy threshold of the compound being irradiated. The latter is important, since many compounds possessing chromophores do not give rise to film deposition; rather they undergo isomerization and/or decomposition or even cycloaddition reactions. Deposition usually occurs from the gas-phase onto a suitable substrate, such as aluminium foil, that is in contact with the monomer vapour. Kunz et al[17] deposited a patterned film on the substrate by placing a mask between the UV source and the

deposition system. However this work shows that such patterning does not always occur; nor do surface photopolymers have to be essentially the same in character as those produced by conventional means. Indeed, although that for methyl methacrylate is similar,[10] those obtained for the unconventional "monomers" benzene and perfluorobenzene (which do not have ordinary homopolymers) more closely resemble their respective plasma polymers,[9] such that the latter were proposed to occur via excited state chemistry rather than the radical cation mechanism as proposed by Clark and Shuttleworth for the plasma polymerization of the difluoroethylenes[18]. Munro and Till also proposed that surface photopolymerization could be used as a simplified model for plasma polymerization.[19]

An intermediate case was found for N-vinyl pyrrolidone (NVP), for which the surface photopolymer, when produced at a low power to flow rate ratio (W/F) was similar to the conventional polymer, that produced at high W/F being considerably different.[10] The polymerization process was also suggested to be flow rate dependent, being two-photon and one-photon respectively for low and high F. The related compounds N-methyl and N-ethyl pyrrolidone were found not to give rise to surface photopolymers,[10] suggesting that it is the vinyl functionality that is important in this case rather than that of the C=O chromophore. On the basis of this information and that of Till,[9] the plasma polymerization of NVP was proposed to occur via an excited state mechanism, with the role of the vinyl group in particular being important at low W/F.

Finally, the similarity between the thin films deposited for some monomers by both plasma and photochemical techniques suggests that the

applications should be much the same in many cases. Accordingly, surface photopolymers have been considered for use in capacitors,[12] positive and negative resists[17] and (using organometallics) photoinitiated deposition and etching of materials relevant to semiconductor devices.[20] Potential uses outside the electronics world include as a method for deposition of a film exhibiting anti-blood clotting behaviour.[21]

5.2 Experimental Techniques

5.2.1 Light Sources

Many light sources are used in photochemistry; the most commonly found for UV work is the resonance arc lamp, in which a low pressure gas or vapour is excited in an electric discharge producing visible and ultraviolet light, which is emitted as a series of resonance lines of particular wavelengths. For the medium pressure mercury arc lamp - the most common source for CUV (ie >200nm) radiation - the most intense emission line occurs at 254nm and dominates the spectrum, the remaining emissions arising at 297nm and 365nm, as well as in the visible and infra-red regions. A full account of light sources, and experimental methods in photochemistry in general, can be found in reference 22, chapter 7. The region below 200nm is known as the vacuum ultraviolet (VUV); the 185nm mercury emission occurs in this region, and so (low pressure) mercury arc lamps are useful here as well. However, VUV irradiation in this work was carried out using the relevant emissions from plasmas excited in nitrogen. That such plasmas are a source of VUV was noted by Clark and Dilks.[23]

Gas	Principal Emission	Energy	Gas	Principal Emission	Energy
	nm	eV		nm	eV
Mercury	185	6.7	Krypton	124	10.0
Nitrogen	174	7.1		116	10.7
	149	8.3	Hydrogen	121	10.3
Xenon	147	8.4	Argon	105	11.7
Chlorine	139	8.9	Neon	74	16.8
Oxygen	130	9.6	Helium	58	21.4

NB: 1 eV = 1.6×10^{-19} J

TABLE 5.1 Resonance Line Sources for Photochemical Work in the Vacuum Ultraviolet (VUV) Region

NOTE: Lamps using the gases in Table 5.1 as VUV sources generally use pressures of about 1 torr, since at higher pressures (eg 200 torr) the resonance lines broaden into a continuum. Although useful as light sources over larger wavelength ranges (a few tens of nm) the intensity at any particular wavelength is much reduced compared to that obtained at low pressure.

Gas	Useful Range (A°)	Optimum Pressure (torr)
Helium	580-1100	40-55
Neon	740-1000	>60
Argon	1050-1550	150-250
Krypton	1250-1800	>200
Xenon	1480-2000	>200

TABLE 5.2 Rare Gas Continua[24]

5.2.2 Lasers

Lasers have also found increasing use in photochemistry over the past twenty years or so. Initially, these were restricted to the far-visible and near-infrared - as recently as 1966 no lasers were available commercially for most of the visible and ultraviolet ranges; indeed, the latter were still an area of research rather than production.[22] Since then a variety of lasers have been produced and used in both the CUV (eg Argon ion laser at 257.2 nm,[26] Krypton fluoride at 248 nm[27]) and VUV (eg ArF excimer laser at 193 nm), as well as multi-photon absorption infra-red lasers[28], the latter causing molecules to absorb many photons of (infra-red) light which gives them energies comparable to those obtainable using UV irradiation. The majority of work using lasers to probe gas phase photochemistry has not been aimed at the deposition of organic thin films, although the photodeposition of metals is fairly common.[29] However, an argon ion laser of 257.2 nm was used by Tsao and Erlich[26] to form a surface photopolymer of methyl methacrylate, and reviews of recent advances in UV laser photochemical vapour deposition have been presented,[30a,b] whilst Solanki has looked at possible applications in microelectronics. Tsao and Ehrlich in particular contrasted techniques relying on gas-phase and surface-phase photochemistry, suggesting that surface photochemistry promoted nucleation prior to subsequent growth by pyrolitic chemical vapour deposition[26]. Other workers have seen polymer as a by-product. For example, Irion and Kompa[32] observed a polymer during their study of acetylene using an argon fluoride laser at 193 nm, in addition to the reaction products ethylene and hydrogen atoms. Their evidence pointed to a pure

excited-molecule mechanism based on $C_2H_2^*$ (^1Au). Becker and Hong also saw a polymer for the VUV irradiation of acetylene,[33] together with diacetylene, ethylene, benzene, vinylacetylene and phenylacetylene. Interestingly, they also observed a brown polymeric deposit for VUV irradiation of hydrogen cyanide gas, together with $(CN)_2$, methane, ammonia and CH_3NH_2. Other photochemical studies in this area have shown that, at high laser intensity, photolysis of cyano- and dicyanoacetylene themselves give rise to excited state fragments, together with $CN^\cdot$ in the ground state, a two photon process occurring with C_3N occurring as an intermediate that undergoes secondary photolysis.[34]

It has already been noted that infra-red multi-photon lasers exist (IRMPD), leading to dissociation (IRMPD) of compounds with similar energies to those directly irradiated by (non-laser) sources in the UV region. Multi-photon absorption can also occur for UV/VUV lasers; for example, molecular chlorine and hydrogen chloride are eliminated from chlorinated methanes on irradiation at 193 nm with an ArF laser via a two photon process - absorption of the first photon giving intermediates prior to Cl_2 / HCl generation on absorption of the second;[35] irradiation with a KrF laser (248 nm) can also give rise to excited state molecular chlorine together with -HCl in a vibrationally hot ground state.[35] Similarly, acrylonitrile irradiated at 193 nm can give rise to the following primary dissociations[36] :

$$C_2H_3CN + h\nu \longrightarrow C_2H_3^\cdot + CN^\cdot \quad (3)$$

$$C_2H_3CN + h\nu \longrightarrow C_2H_2 + HCN \quad (4)$$

together with the secondary products of these primary fragments.

Laser flash photolysis (in which the system under study is subjected to a high intensity flash of short duration, typically of the order 10^{-9} to 10^{-10}s) has been extensively used to determine the lifetimes of those compounds which do not emit fluorescence or phosphorescence, and so cannot be determined by methods dependent on the measurement of emitted radiation[37]. The technique has also been used to investigate the nature of photolysis; hence Mori and coworkers have used ArF laser flash photolysis to observe the formation and collisional relaxation of hot molecules in hexafluorobenzene,[38] whilst Shimo et al investigated the flash photolysis of 1-alkenes in the gas phase to monitor the effect of size on the formation yield of (vibrationally hot) allyl radical.[39]

5.2.2 Window Material

Suitable window materials for work in the conventional and vacuum ultraviolet are given in Table 5.3[25]. Spectrosil B windows were used in the CUV, and calcium fluoride in the VUV regions. Magnesium fluoride (cut-off ca. 120 nm) was also considered, but CaF_2 preferred to ensure that all irradiation was carried out below the ionisation threshold (most organic molecules have ionisation energies in the region of about 10 eV, ie 120nm)[10]. Since transmission characteristics are generally poor for about 10-20 nm above the cut-off point, 100% transmission probably only occurred above 140 nm.

Material	Cut Off Wavelength nm
Pyrex	290
Quartz	180
Fused Silica*	160
Calcium Fluoride	122
Magnesium Fluoride	115
Lithium Fluoride	105

*Known commercially as Suprasil or Spectrosil B

TABLE 5.3 Window Materials for Photochemical Work[10]

5.3 Potential Monomers

Chapters 2 and 3 outlined the plasma polymerization of fluorine and nitrile containing compounds whilst reference has been made above to similarities observed for films deposited by plasma and surface photochemical techniques for perfluobenzene[9] and NVP[10]. Chloroacrylonitrile has been shown to give a surface photopolymer by Hiraoka and Lee[69a]. It was therefore chosen here together with trifluoroethylene as potential compounds for surface photopolymerization in the CUV and VUV regions due to the presence of ethylenic unsaturation and carbon - halogen chromophore. Methacrylonitrile was chosen as a contrast since the C-Cl chromophore in this monomer is replaced by a methyl group. The effect of power (in the form of photon flux), flow rate and wavelength on the chemical composition of the resultant films was investigated as revealed by ESCA to see if there was any similarity to

the results for plasma polymerization. If so, it was felt that a knowledge of the excited state photochemistry involved might give an insight into the excited state chemistry occurring in the plasma.

5.4 Experimental

Initial polymerization experiments were carried out in the same reactor chamber as that described in chapter 2, except that a calcium fluoride window was inserted into the system to separate it into a two halves, Figure 5.1. Each side was pumped by an Edwards ED2M2 $21s^{-1}$ pump, a typical base pressure of 0.02mb being achieved. VUV irradiation was carried out by initiating an Argon (later Nitrogen) plasma at 0.4mb on the right hand side of the window, the monomer vapour of interest entering the left where deposition was to occur on aluminium foil as substrate. The 50W plasma was sustained for a controlled time period (1-12 hours) using a Tegal Corporation 13.56 Mz RF generator with matching LC network. Analysis was carried out on the Kratos ES300 spectrometer in the usual manner (see chapter 3). Irradiation in the CUV was achieved by replacing the plasma chamber with an Oriel Scientific 200W medium pressure Hg/Xe arc lamp. This set-up was prone to high leak rates compared to the monomer flow rate, leading to high oxygen uptake, and so was refined to a one inch diameter system as shown in Figure 5.3, which also enabled the CaF_2 window to be scaled down in size (to 30mm x 5mm instead of 50mm x 5mm). The window was cleaned after each experiment using a 100W oxygen plasma and its UV spectrum taken to check that all polymer had been removed.

EXPERIMENTAL CONFIGERATION

FOR VACUUM UV SURFACE PHOTOPOLYMERIZATION

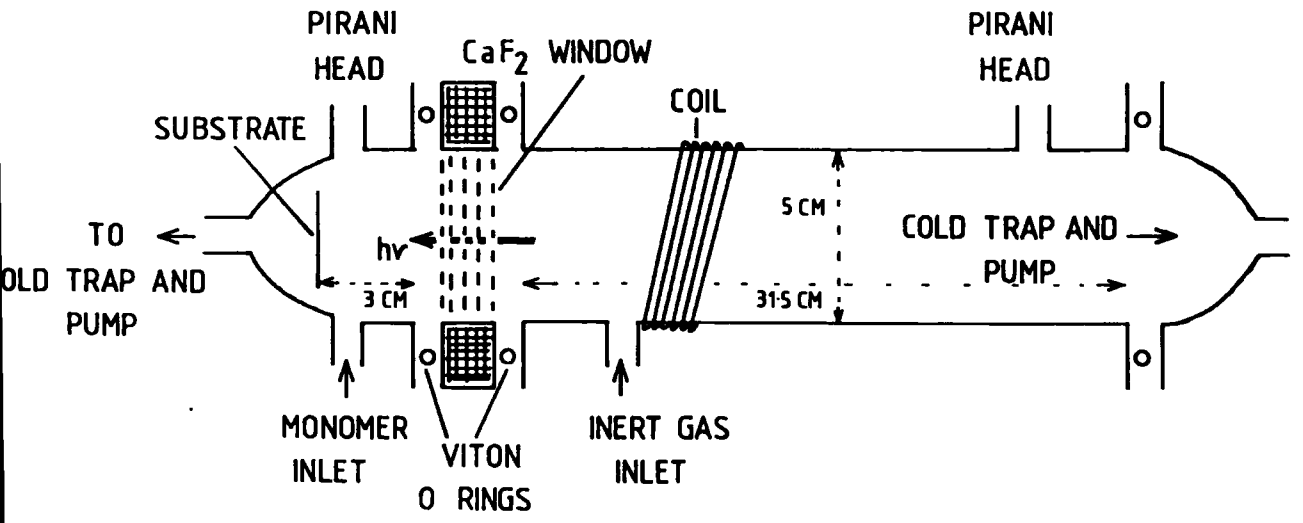

FIGURE 5.1 Initial Surface Photopolymerization Apparatus

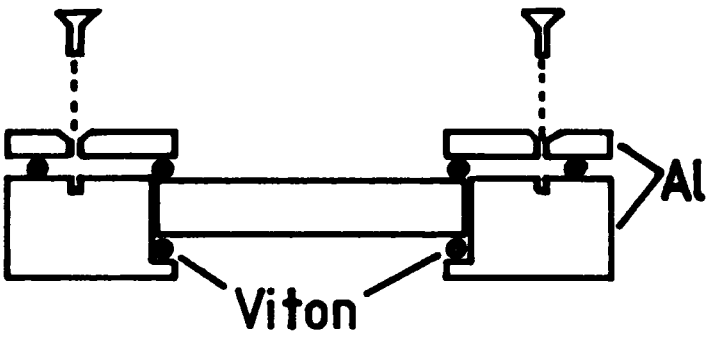

FIGURE 5.2 Calcium Fluoride Window Assembly

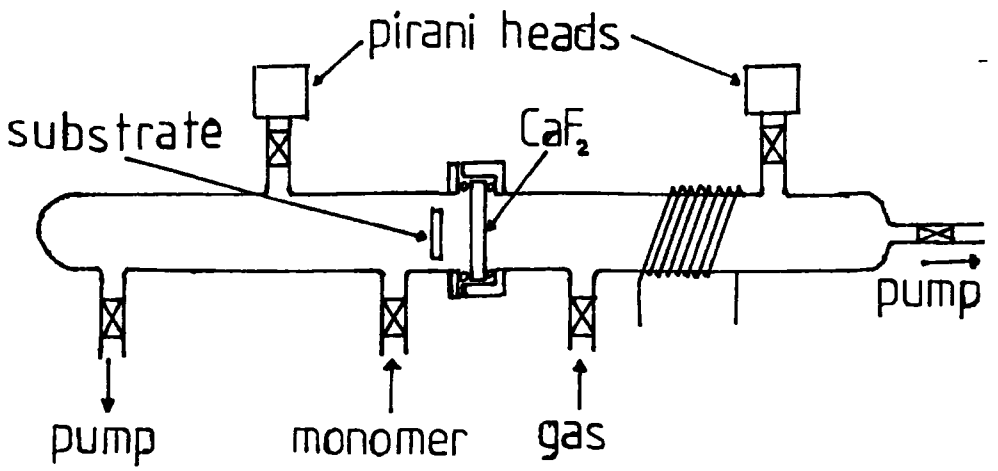

FIGURE 5.3 One Inch Diameter Photopolymerization Apparatus

5.5 Trifluoroethylene and Related Compounds

5.5.1 Results

The first monomer studied was trifluoroethylene, irradiated in the VUV using an argon plasma. An initial deposition period of four hours on a gold substrate gave only a C1s spectrum typical of hydrocarbon contamination, Figure 5.4a. Raising the deposition time to 12 hours showed possible evidence for peaks at higher binding energies than the 285.0 eV hydrocarbon peak. Using the Kratos Data Analysis Package, the typical C1s envelope was subtracted from the actual spectrum obtained to give that shown in Figure 5.4b. Although qualitative rather than quantitative, the shifts of the peaks detected correspond to the following carbon-fluorine environments - $\underline{C}H$ (and carbon not directly bonded to fluorine), $\underline{C}$-CF, $\underline{C}$-CF_n, $\underline{C}$-F, $\underline{C}F_2$ and $\underline{C}F_3$, and so the presence of a surface photopolymer was inferred. Since $\underline{C}F_3$ groups and carbon atoms not directly bonded to a fluorine atom were present in the surface photopolymer but not the monomer, polymerization cannot have taken place via either a free radical chain or step growth mechanism. Comparison with the C1s envelopes obtained in chapter 2 indicates that the chemical composition of the surface photopolymer is akin to the plasma polymer. Substrate overlayer calculations indicated the film thickness at about 10A°. Replacing the gold substrate with aluminium foil was found to increase this thickness to about 25A° over a similar time period. Thus the deposition time for surface photopolymerization in this instance is negligible compared to that for plasma polymerization.

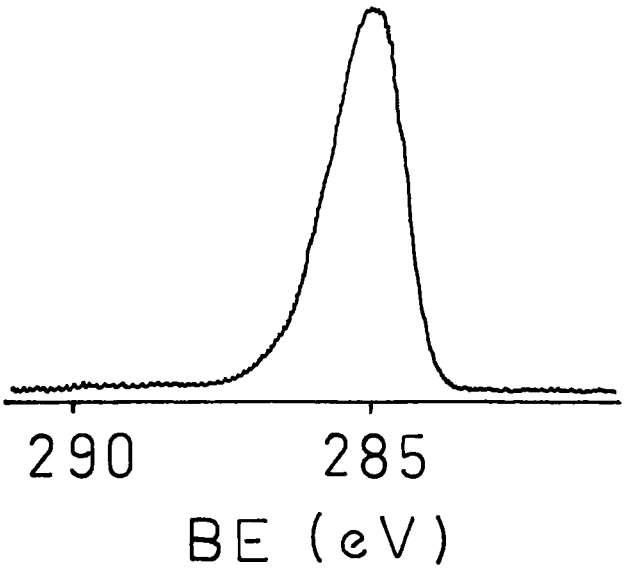

FIGURE 5.4a Trifluoroethylene "Failed" Photopolymer - C1s

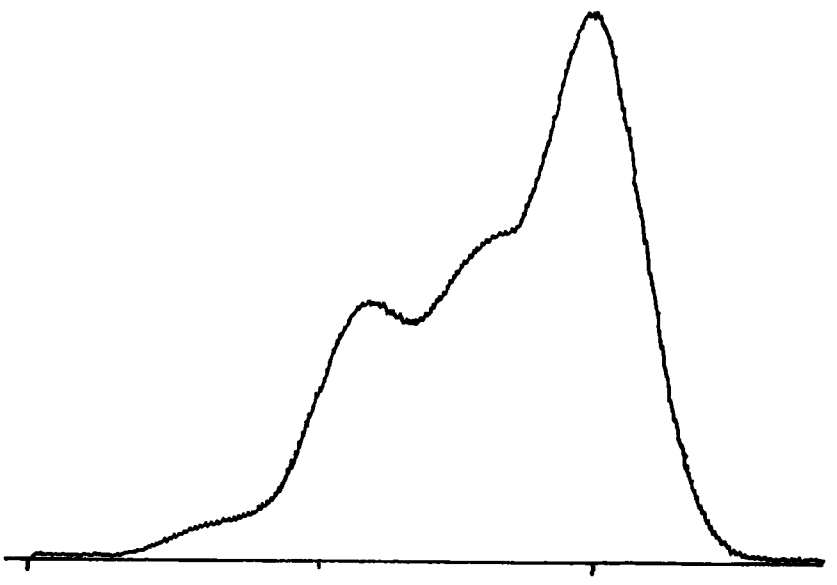

FIGURE 5.4b Trifluoroethylene Photopolymer - C1s Envelope

5.5.2 Discussion

The main gas phase primary processes for ethylene itself are[44] :

$$CH_2{=}CH_2 + h\nu \longrightarrow CH_2C + H_2 \quad (A)$$

$$\longrightarrow HC{\equiv}CH$$

$$\longrightarrow CH_2C + H + H \quad (B)$$

$$\longrightarrow HC{\equiv}CH + H_2 \quad (C)$$

$$\longrightarrow HC{\equiv}CH + H + H \quad (D)$$

$$\longrightarrow CH_2CH + H \quad (E)$$

The main singlet-singlet transition in the ethylene absorption spectrum was found by Merer and Mulliken to occur at 162 nm[43] with molar extinction coefficient ca. 10,000[45] and corresponds to the π^* <-- π transition. It is proceeded by a very long progression whose origin is probably as low as 265 nm, this emission constituting a strong indication of the perpendicular structure of the π^* state. Partly superimposed on this band is the first member of a Rydberg series (nR<--N) which converges to the first ionisation potential at 10.51 eV.[43] The UV absorption spectrum of trifluoroethylene[46] shows a maximum π^* <-- π band at 160 nm. A broad Rydberg band was observed at about 190 nm assigned to 3R (molar extinction coefficient ca. 2000) which was not found to be present on examining the spectrum of its thin solid film. Since the π^* <--- π band was essentially unaffected, the excited state was concluded to be Rydberg in character.[47]

At first sight, the similarity in the C1s envelopes between that found for the small amount of surface photopolymer obtained and those for the corresponding plasma polymers suggests that the chemical composition of the two types of films are the same, such that the film

deposition processes occurring in the two systems might also be similar. However, although sufficient VUV radiation is absorbed[47] to give rise to photolysis, little surface photopolymerization occurs. It therefore might also be reasonable to assume that the primary photochemical processes occurring for trifluoroethylene are not those primarily responsible for deposition in the analogous plasma polymerization process, otherwise a much faster deposition rate would have been observed.

The actual mechanism of trifluoroethylene photodecay may shed light on this problem. It is likely to be similar to that of fluoroethylene (FE) and 1,1-difluoroethylene (1,1DFE - see Figure 5.5) and so involve direct 1,2 HF elimination,[48-50] together with α-elimination from the =CHF functionality.[51,52] Simultaneous H + F ejection can also occur from FE via 147 nm steady-state photolysis, products including HCCF, CH_2CH_2, CH_3CH_3, and methane, CH_4.[48] 1,1DFE was concluded to eject H atoms via the parent triplet states when exposed to short-wavelength VUV radiation.[49] Similarly, Sirkin and Pimentel[53] used flash photolysis to confirm that, above 155 nm, direct molecular elimination of HF occurs from both compounds. Primary branching ratios for the decay of photoexcited FE were measured: molecular elimination of HF, 0.82; F atom ejection, 0.13; HH molecular or diatom elimination, 0.05 (single H atom ejection was not measured). Pressure dependent studies also indicated that the difluoroethyl radical (formed by F atom ejection) reacted with another molecule of FE to give DFE via a $C_2H_2F_3$ intermediate.

No report was made of photopolymer or thin film deposition in any of the above. However, this does not mean that it does not occur, as

By analogy with the known photochemistry of vinylidene fluoride, the decay of 1,1-difluoroethylene can be expected to follow the sequence :

$$CH_2CF_2^* \rightarrow HF^{\dagger} + HCCF$$

$$CH_2CF_2^* \rightarrow F + CH_2CF^{\dagger}$$

$$F + CH_2CF_2 \rightarrow [C_2H_2F_3]^{\dagger}$$

$$[C_2H_2F_3]^{\dagger} \rightarrow CHFCF_2 + H$$

$$[C_2H_2F_3]^{\dagger} + He \rightarrow [C_2H_2F_3] + He$$

$$[C_2H_2F_3] + CH_2CF_2 \rightarrow CH_2FCF_2CH_2CF_2, \text{ etc.}$$

$$CH_2CF^{\dagger} + CH_2CF_2 \rightarrow CH_2CHF + CF_2CH$$

$$[C_2H_2F_3]^{\dagger} \rightarrow \textit{trans}\text{-CHFCHF } (\textit{cis}\text{-CHFCHF}) + F$$

$$CH_2CF_2^* \rightarrow \textit{trans}\text{-CHFCHF } (\textit{cis}\text{-CHFCHF}).$$

FIGURE 5.5 The Vacuum UV Photochemistry of 1,1-Difluoroethylene.

reported here, but rather that the deposition rates might once again be extremely low. Assuming a free radical chain or step growth mechanism, this could be explained by the abundance of potential terminating steps compared to those for initiation and propagation, so that the chance of propagation - and hence overall polymerization - are small. This may possibly increase with time such that a conventional free radical mechanism could occur; however, this would still not account for the formation of CF_3 groups as seen in the ESCA spectrum. A second possibility is that production of polymerizing (ie depositing) species occurs via secondary photolysis of the primary products. This was suggested by Haller and Srinivasan[60] to occur for the surface photopolymerization of 1,3-butadiene, on the basis that an induction period was seen - the polymer deposition rate observed was five times greater when the photolytic products were allowed to build up in the reaction cell for 20 minutes as opposed to 5. Formation of polymer was also found to depend on the square of the number of absorbed photons. In the case of trifluoroethylene a dynamic system was used, such that any primary products not depositing on the substrate or the walls of the reactor would have been pumped out of the photolytic chamber and into the cold trap before secondary photolysis products were able to build up in any quantity. The possibility that surface photopolymerization in this case occurs via deposition of secondary photolysis products therefore cannot be discounted, such that the species responsible for deposition occurring in surface photopolymerization and plasma polymerization may still be the same. Further evidence for the possible role of secondary photolysis is that acetylene, found to be a major primary product for

FE and 1,1-DFE photolysis, has been shown to give a photopolymer both in the VUV (193 nm)[32,33] and CUV (235 nm), the latter using mercury sensitisation,[61] whilst phenyl acetylene has also been shown to give rise to a surface photopolymer resembling the homopolymer produced by more conventional methods.[62]

In contrast to trifluoroethylene, vapour phase polymerization of tetrafluoroethylene (TFE) has been observed by a number of workers. Atkinson (1949)[54] noted that, on illuminating TFE vapour at 253.6 nm in the presence of mercury as sensitiser, hexafluorocyclopropane (main product) and a polymer identified as $(CF_2)n$ were formed, the latter proposed to occur via a radical mechanism. Polymerization has also been photochemically initiated in the gas phase under a variety of other conditions,[55] including the presence of second a element or compound (eg mercury,[54] mercury bromide,[56] N_2O[57] and oxygen[58]). Many of these polymers appeared as white powders or flocs,[55,57] such that the first example of photopolymerization of TFE occurring on an irradiated substrate recorded by Wright in 1967[7], direct photolysis being carried out at a pressure of 3 torr. However, Wright also noted the presence of CF_3 groups in the infra-red spectrum of the photopolymer. The importance of this is two fold. Firstly it supports the appearance noted above using ESCA for the surface photopolymer of trifluoroethylene; secondly it suggests that the surface photopolymerization mechanism for TFE is also analogous to that for its plasma polymerization, since the latter is also known to give rise to CF_3 groups. More recently Koda[59] used irradiation by Xe (147 nm) and Kr (116,124 nm) resonance lamps to produce difluoromethylene radicals, $CF_2^{\cdot}$, in the $^1A_1$ and $^1B_1$ states:

$$C_2F_4 + h\nu \longrightarrow CF_2(^1A_1) + CF_2(^1B_1)$$

Although the photodepositions noted by Wright[7,55] occurred above 200 nm, it may be that difluorocarbenes are also of importance in TFE surface photopolymerization in the VUV, enabling crosslinking of the film to occur, as suggested by Yasuda for plasma polymerization.[62] It is also worth noting that an increase in the pressure of the monomer under irradiation can also affect the deposition process, since, in a subsequent experiment at 10-760 torr Wright deposited a white powder, or floc[55], which coated all internal surfaces of the reactor as well as the substrate and was found to have a slightly different chemical composition to that of the "true" surface photopolymer previously reported.[7]

5.5.3 Summary

Trifluoro- and tetrafluoroethylene both give rise to surface photopolymers under UV irradiation, albeit with differing film deposition rates. Both photopolymers contain CF_3 groups which are not present in the monomer, indicating that a simple chain or step growth radical mechanism cannot be invoked, whilst the C1s XPS spectrum for trifluoroethylene is remarkably similar to those obtained for the corresponding plasma polymer, showing that the depositing species are likely to be similar in both cases. The main difference between the two polymerization techniques for trifluoroethylene is also the observed film deposition rate, which is negligible for surface photopolymerization in comparison to that in the plasma. However, a possible explanation for this is a surface photopolymerization mechanism involving secondary photolysis of the primary products, the

latter being pumped out of the photolysis chamber under the dynamic flow conditions used before sufficient depositing species can be formed to give an observable film deposition rate. The possibility also exists that polymerization is mainly initiated and propagated on the surface of the substrate (and walls of the reactor), rather than in the gas phase. However, this would involve adsorped species such that photopolymerization due to secondary photolysis on the substrate surface would be largely independent of the flow dynamics of the system, the opposite of the effect found for 1,3-butadiene[60]. The nature of the substrate in the surface photopolymerization of trifluoroethylene is borne out by the higher deposition rate observed when using aluminium foil as opposed to gold, the difference being attributed to varying sticking coefficients for the depositing species on the two surfaces involved.

5.6 Chloroacrylonitrile

5.6.1 Results

Chloroacrylonitrile surface photopolymerization was investigated as a function of Yasuda's parameters[62] W - in the form of photon flux - and F, the monomer flow rate in the photolysis cell, and incident wavelength. The experimental apparatus initially used was that shown in Figure 5.1. VUV irradiation was carried out using an argon plasma together with a calcium fluoride window. The Oriel Scientific medium pressure arc lamp together with quartz window was used as a source of CUV radiation. Photopolymer was found to deposit much more readily in the VUV than for trifluoroethylene, full coverage of the aluminium substrate being observed after about four hours (compared to a 25A^{o}

film after 12 hours for trifluoroethylene). Analysis by ESCA gave the typical core levels shown in Figure 5.6, which show remarkable similarity to those obtained for the corresponding plasma polymer in chapter 3. This was found to be quantitative as well as qualitative, Table 5.5. The results are for different flow rates in two different systems, but show that the chemical composition of the films obtained by both plasma and photochemical techniques are essentially the same for both the in coil and tail regions, Table 5.6.

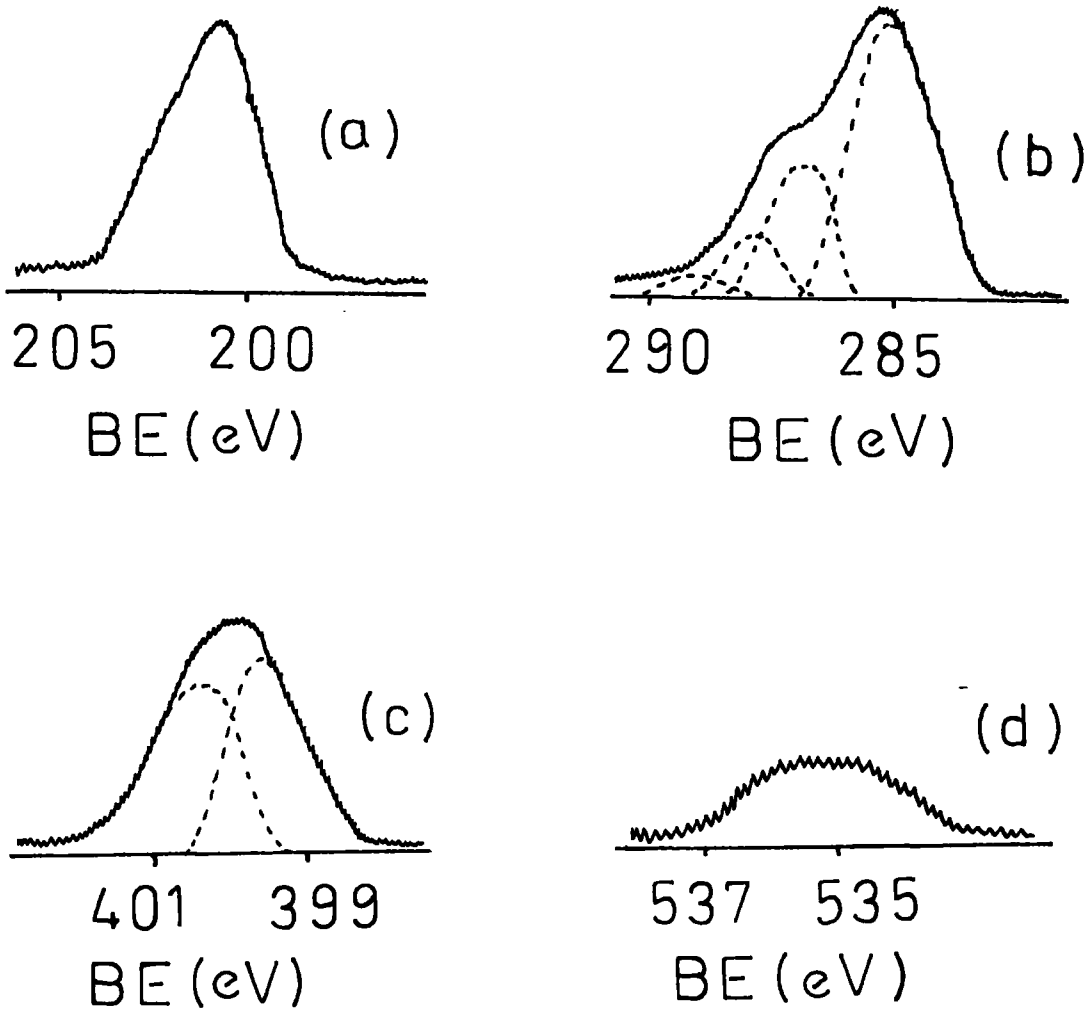

FIGURE 5.6 Typical C1s, C12p, N1s and O1s Core Level Spectra for a Chloroacrylonitrile Vacuum UV Photopolymer.

VUV Surface Photopolymers of Chloroacrylonitrile

Elemental Ratio[1]			C1s (% of total envelope area)			
VUV Photopolymer - $F=0.54cm^3_{STP}min^{-1}$						
Cl	N	O	285.0	286.6	287.7	289.2[2]
11	19	7	49	32	15	4
Plasma Polymer (tail region) - $F=10.3cm^3_{STP}min^{-1}$						
10	22	8	49	34	15	2

NOTES : 1. No. per 100 C atoms. 2. Binding Energies in eV.

TABLE 5.5 VUV Photopolymer versus Plasma Polymer

Type	Power /W	$F/cm^3_{STP}min^{-1}$	Substrate Position	Elemental Ratio (No/100 C atoms) Cl	N	O
VUV	-	0.13	Next to Window	27	26	7
PP	7	10.3	In coil	31	26	8
PP	8	5.2	" "	31	25	8
VUV	-	0.22	Next to Window	19	21	5
PP	62	10.3	In coil	19	24	11
PP	8	2.9	" "	18	21	11
VUV	-	0.03	Next to Window	32	23	5
PP	7	10.33	In coil	31	26	5
VUV	-	0.54	Next to Window	11	19	7
PP	7	10.3	Out of Coil	9	22	8
VUV	8	0.18	Next to Window	18	21	-
PP	8	2.9	In coil	18	21	11

TABLE 5.6 Comparison of Elemental Ratios vs Substrate Position

If the analogy between photopolymerization and plasma polymerization is to hold, the former should also depend on the monomer flow rate and power. However, the apparatus previously used did not always give complete coverage of the substrate within a reasonable time scale (two hours); therefore the refined apparatus in Figure 5.3 was developed. When used with a nitrogen plasma as the VUV irradiation source, incomplete deposition was only seen for the lowest flow rate used (0.01 $cm^3_{STP}min^{-1}$). The aluminium foil substrates in this second reactor were laid at 90^o to the calcium fluoride window, such that direct irradiation of the substrate did not occur. This was different from the previous apparatus, in which the full surface area of the substrate faced the window and irradiation of the surface such that irradiation of the surface occurred. A second substrate was therefore inserted into the photolysis cell in the analogous position, parallel to the window but 90^o to the first substrate. The results,

SUBSTRATE POSITION	FLOW RATE cm^3min^{-1}	ELEMENTAL RATIO Cl	N	O	C1s Envelope 285.0	286.6	287.7	289.0	N1s 399.3	400.8
Horizontal	0.25	13	16	7	60	27	11	2	not fitted	
Vertical	0.25	8	15	6	65	26	7	2	94	6
Horizontal	0.1	16	15	7	52	27	16	5	86	14
Vertical	0.1	13	17	7	54	32	12	2	89	11
Horizontal	V.P	34	26	3	29	47	21	3	90	10
Vertical	V.P	32	24	1	31	43	23	1	95	5

NOTE: V.P - monomer used at vapour pressure, flow rate not determined.

TABLE 5.7 Chloroacrylonitrile VUV Photopolymer - Substrate Orientation

Table 5.7, show that the film deposited in the two positions is essentially the same. This also indicated that film deposition does not rely on the surface of the sample being irradiated in order for film deposition to occur, ie that in situ photopolymerization of adsorped monomer on the surface (whether the initial substrate or growing polymer film) does not play an important part in the overall surface photopolymerization process. In order to test this a third substrate was placed in the photolysis chamber immediately behind the second so that it, too, was parallel to the window, but completely shielded from irradiation. Photodeposition was carried out for the usual irradiation time and all three substrates analysed by ESCA. The reverse side of the horizontal substrate was also analysed, since it, too, was completely masked from the window. Complete substrate coverage, as expected, was found for the original two substrate positions. However, deposition was also found to have occurred in the two masked positions, Table 5.8, with varying thickness. The reverse side of the horizontal substrate was found by an overlayer calculation to be about 23A^{o} thick, whilst that for the masked vertical position was only about 10A^{o} thick.

SUBSTRATE POSITION	FLOW RATE cm^3min^{-1}	ELEMENTAL RATIO Cl	N	O	C1s Envelope 285.0	286.6	287.7	289.0	N1s 399.3	400.8
Horizontal	0.43	9	15	5	57	34	9	2	44	56
Horizontal*	0.43	7	12	-	not fitted				not fitted	
Vertical*	0.43	7	17	-	not fitted				not fitted	

* - masked substrate position

TABLE 5.8 Effect of Masking

Thus surface photopolymerization does occur when the substrate surface is not directly illuminated, but the deposition rate is markedly reduced in comparison to those substrates which are not masked. This means that formation of polymer in the gas phase does occur, but photon activated reactions are also occurring on the surface of the substrate. Further evidence that this must be the case is that, even in those instances when incomplete film deposition occurred on the substrate, film was observed to occur on the calcium fluoride window itself. An alternative explanation - that all depositing species are produced in the gas phase but are not long-lived enough to diffuse from the irradiated volume of the reactor to the masked substrate surface - can be discounted, since chapter 6 shows that the lifetime of the depositing species involved is of the order of 0.1s.

Once the orientation (horizontal or vertical) of the substrate was shown to have no observable effect on the chemical composition of the film formed, the latter was then studied as a function of flow rate. Figure 5.7 shows the elemental composition of films deposited in the VUV as determined by ESCA; Figure 5.8 shows the corresponding C1s envelopes. The chlorine and nitrogen contents of the film both rise with increasing flow rate. That for chlorine in particular rises from almost zero at $0.03cm^3_{STP}min^{-1}$ to a Cl:C ratio of about 1:5 at $0.52cm^3_{STP}min^{-1}$, rising to 1:3 at monomer vapour pressure, whilst the N:C ratio, again initially very small at 1:26, also rises in a similar manner, the ratio at vapour pressure being about 1:4. Thus, at vapour pressure, the C:Cl:N elemental composition is about 12:4:3, or almost the 4:1:1 ratio expected for a conventional radical chain or step

Chloroacrylonitrile VUV Photopolymer

FIGURE 5.7 Elemental Ratios

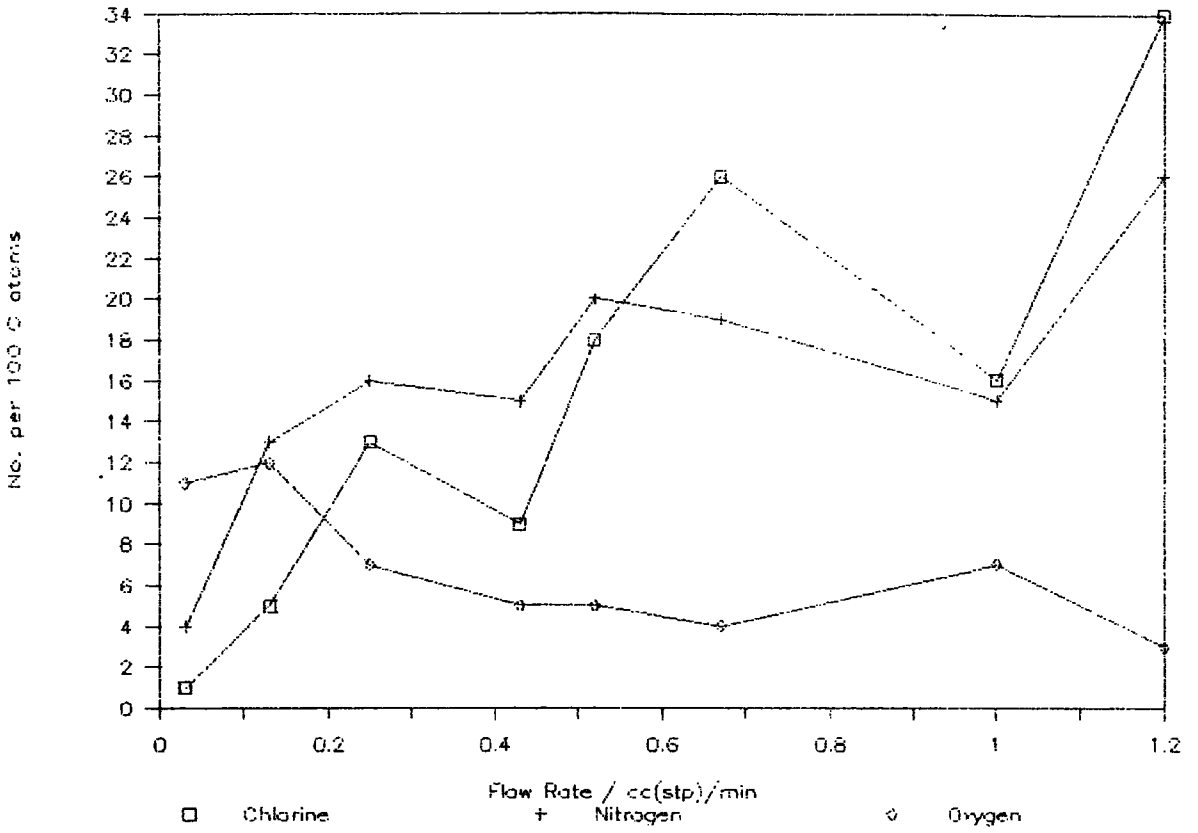

Chloroacrylonitrile VUV Photopolymer

FIGURE 5.8 C1s Envelope

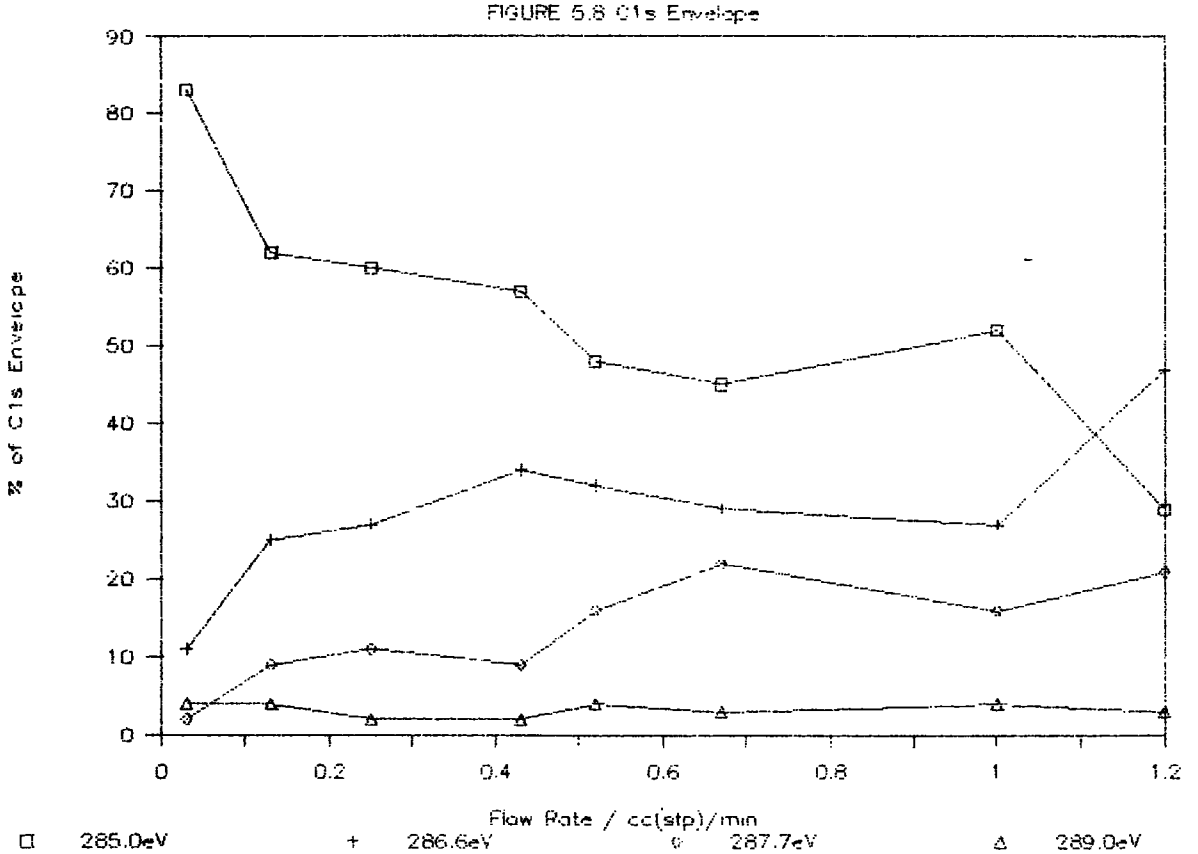

Chloroacrylonitrile CUV Photopolymer

FIGURE 5.9 Elemental Ratios

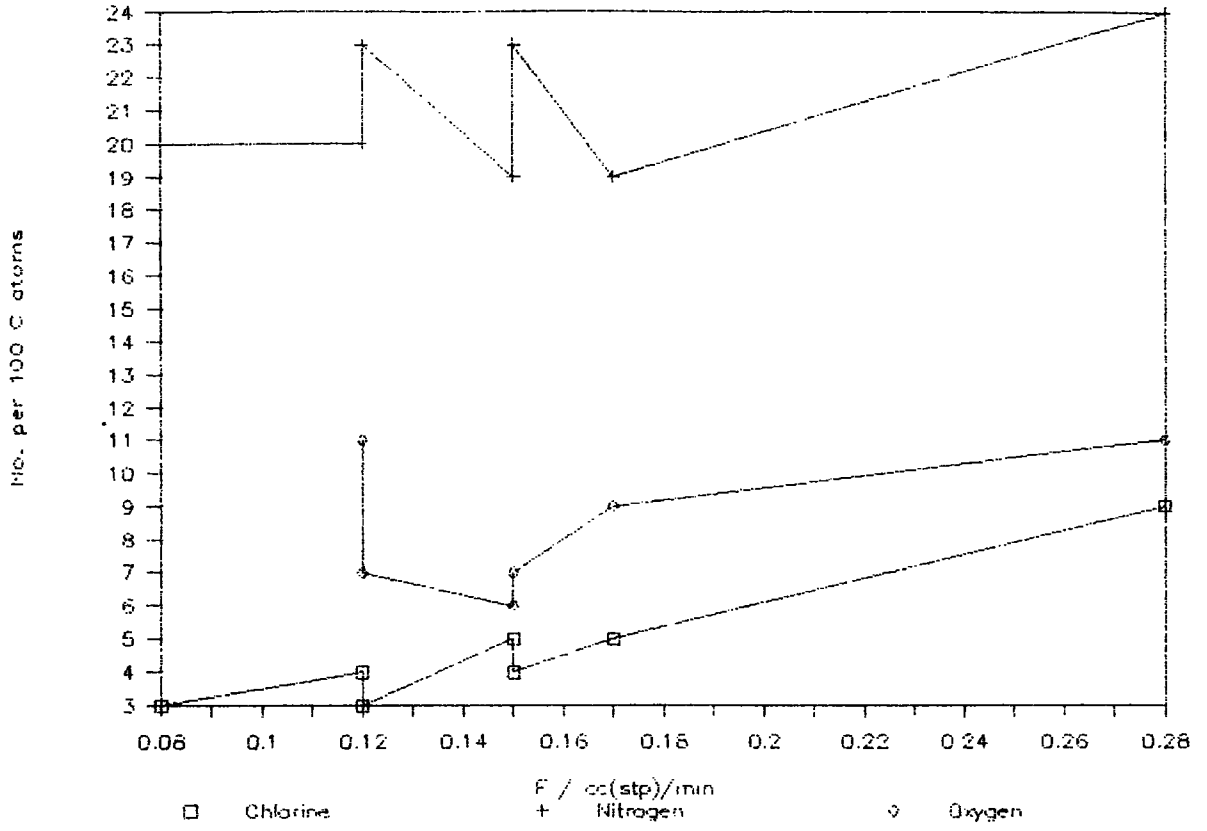

Chloroacrylonitrile CUV Photopolymer

FIGURE 5.10 C1s Envelope

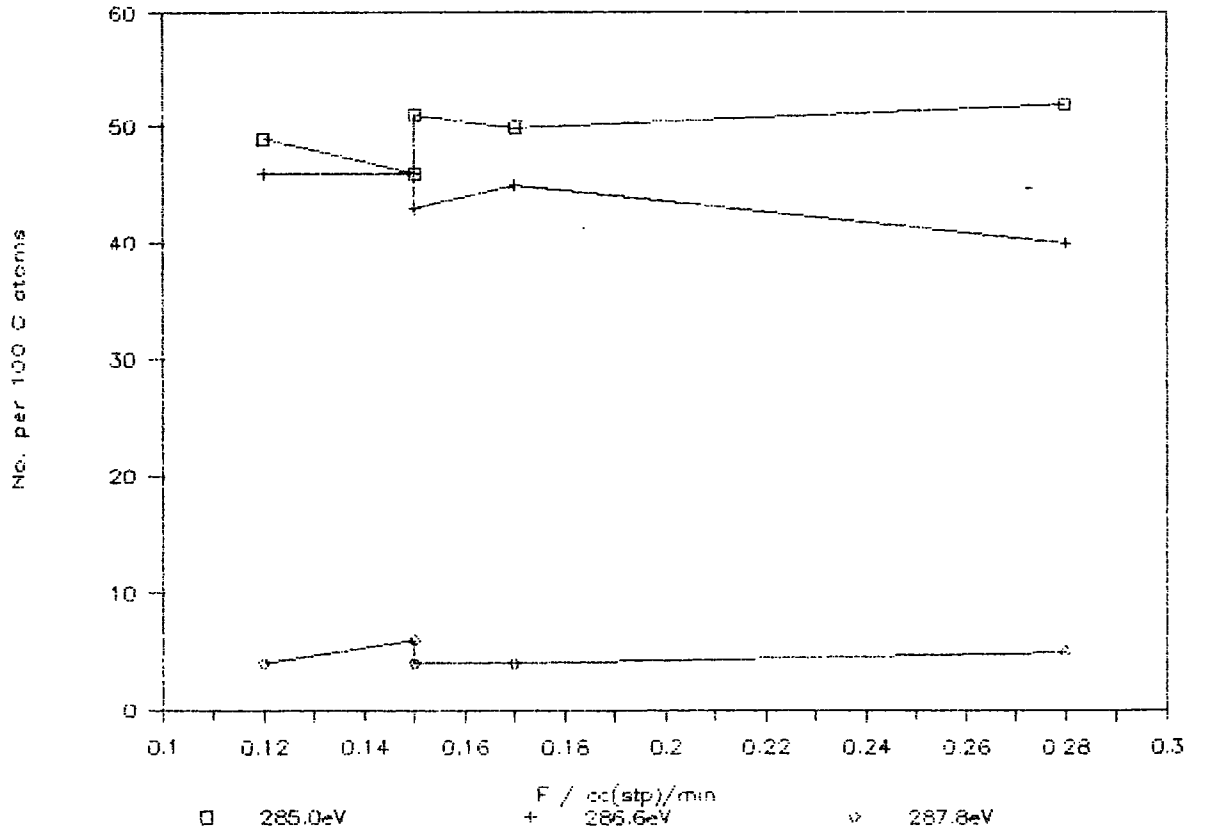

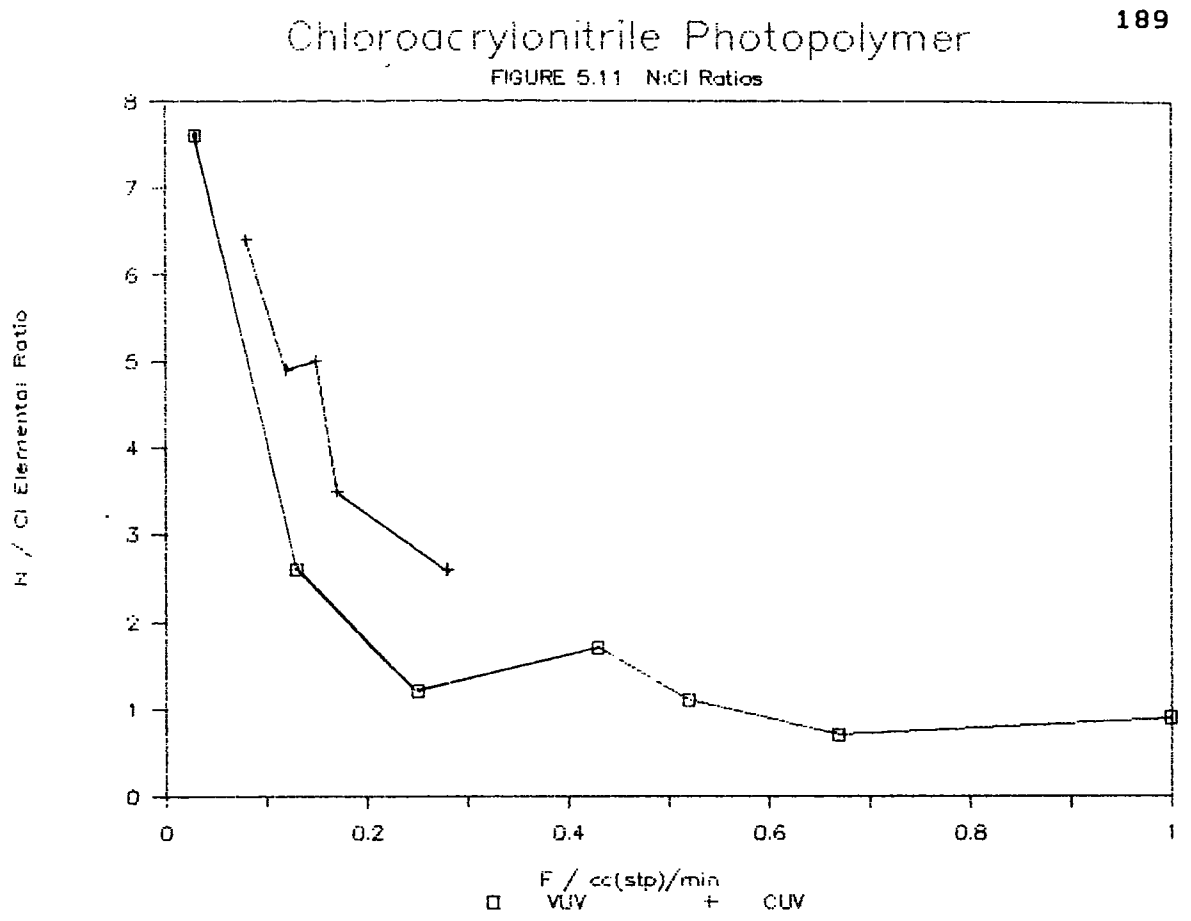

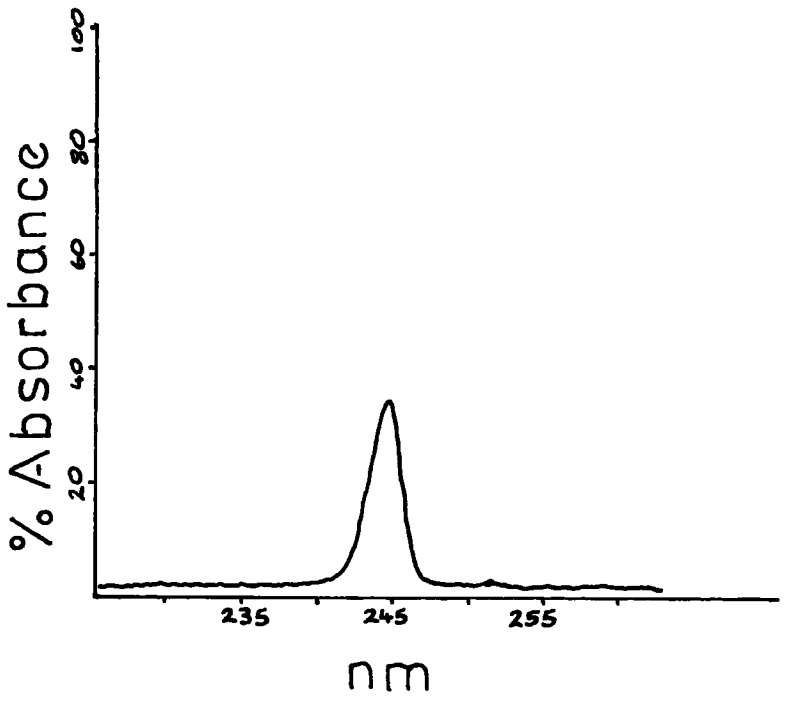

FIGURE 5.12 UV Absorption Spectrum of Chloroacrylonitrile in Acetonitrile.

growth mechanism. However, this mechanism cannot account for the much lower ratios of both heteroatoms seen at the remaining flow rates, which, at best, gives a C:Cl:N ratio of 5.3:1.4:1 at $0.67 cm^3_{STP} min^{-1}$. The nitrogen : chlorine ratio is also initially greater than unity at low flow rate, changing over above $0.5 cm^3_{STP} min^{-1}$, after which the situation is reversed. The oxygen content of the film is low throughout, although higher at low flow rate, in line with the results obtained for plasma polymerization (chapter 3).

The C1s envelope also reveals trends. The 285.0 eV peak initially accounts for over 80% of all carbon environments at low flow rate, reflecting the low chlorine and nitrogen to carbon stoichiometries obtained, before rapidly dropping to about 60% on initial flow rate increase. A plateau then occurs before a further steady decrease with rising flow rate. The peak is still visible in the film formed at monomer vapour pressure, so that there are carbon atoms in the photopolymer not directly bonded to a heteroatom or adjacent to a carbon atom which is. This again rules out a simple radical photopolymerization method, since the the peaks obtained for the model compound, polychloroacrylonitrile, were centred at 286.6 eV (due to $\underline{C}NCl$ and to $\underline{C}H_2$-CClCN) and 288.0 eV (due to $\underline{C}$-CClCN), all $\pm$ 0.3 eV - see chapter 3. Conversely, the % contribution to the C1s envelope from the 286.6 eV and 287.7 eV peaks found in the photopolymer rises with increasing flow rate, that at 286.6 occurring more rapidly than at 287.7 eV. This again reflects the increasing ratio of heteroatoms to carbon in the films. An increase in the number of intact nitrile groups is supported by the change seen between 0.03 and 0.13 $cm^3_{STP} min^{-1}$ for the N1s envelope, in which a

ratio of 3:1 in favour of C-N and C=N environments as opposed to nitrile groups (occurring at 399.3 eV and 400.8 eV respectively) at the lower flow rate is reversed to 5:1 in favour of nitrile groups at the higher. This ratio continues to increase with flow rate until it reaches about 9:1 at high flow rate. The 400.8 eV peak is still visible even at monomer vapour pressure, showing that the nitrile group plays an active role in the photopolymerization process - further proof that a simple radical mechanism cannot occur. Finally, the 289.0 eV peak is low throughout, again reflecting the low O:C ratio in the polymer.

The next step was to establish whether or not a wavelength dependence existed. This was achieved by replacing the nitrogen plasma as irradiation source with a mercury/xenon medium pressure arc lamp (254 nm), and substituting a quartz window (cut off 180 nm) for calcium fluoride. ESCA analysis revealed that a thin film was again formed over a two-four hour deposition period which gave complete coverage of the aluminium substrate. A flow rate dependence was again seen, Figures 5.9 and 5.10, in that the chlorine content did increase with flow rate, but only from 3 to 9 per 100 carbon atoms in the polymer. The nitrogen content stayed fairly steady throughout, showing no overall trend, as did the oxygen content. The C1s envelope showed little variance with flow rate either, the 285.0 eV peak contribution remaining at about 47 $\pm$ 5 %, whilst that at 286.6 eV likewise remains steady at 45 $\pm$ 5 %. Decreasing the photon flux by pulling the UV lamp back from the window by some 8cm also gave complete substrate coverage with no change in chemical composition or C1s envelope, suggesting that photon flux has no effect on the nature

of the film formed. In the N1s envelope the ratio of peaks was about 88:12 in favour of that at 399.3 eV throughout, showing that some nitrile groups had undergone photolysis.

The most noticeable feature of the results is the very low chlorine content of the CUV photopolymers compared to those obtained in the VUV, together with a much lower flow rate effect. At first sight this can be accounted for by the difference in flow rate ranges studied - 0.03-vapour pressure in the VUV, but only 0.01-0.28 $cm^3_{STP}min^{-1}$ in the CUV. However, the chemical composition of the films produced is different on closer examination, since the nitrogen to chlorine ratio in the VUV is consistently lower than that obtained in the CUV region, Figure 5.11. This is reflected in the C1s envelope, for which the 285.0 eV peak in the VUV falls from 80% to 60% of the total in the VUV, compared to a fairly constant 47% contribution in the CUV for the same flow rate range. Similarly, the 286.6 eV peak in the VUV rapidly rises from 11% to 27%, whereas that in the CUV again remains fairly static at about 45%. Thus the chemical composition of the surface photopolymers formed in the two regions <u>does</u> differ as a result of changing the incident wavelength. This in turn suggests that the photochemistry involved in the two regions is different, and this is discussed below.

5.6.2 Discussion

The differences between VUV and CUV surface photopolymers is likely to be caused by the difference in photochemistries occurring at the two wavelengths involved. This is therefore examined.

No photochemistry should result from the carbon-chlorine chromophore in the VUV, since this absorbs at about 244 nm (this was found by running the UV absorption spectrum using acetonitrile as solvent), Figure 5.12. The absorption spectrum of acrylonitrile was found by Mullen and Orloff[66] to have three peaks occurring at 210.7 nm, 203 nm and 172.5 nm, corresponding to the transitions π^*<-- n, π^*<--π and σ^*<--σ respectively. The first of these has a molar extinction coefficient of about 150 and is therefore weak; however, the remaining two peaks are of medium intensity (2000). The photochemistry of acrylonitrile vapour at 213.9 nm has been observed by Gandini and Hackett[63] :

$$CH_2{=}CHCN + h\nu \rightarrow C_2H_2 + HCN \quad (1)$$

$$CH_2{=}CHCN + h\nu \rightarrow HCCCN + H_2 \quad (2)$$

The evidence here was for 1,2 molecular elimination (route (1) having the higher quantum yield) together with polymer formation from excited acrylonitrile or acetylene.[63] The production of cyanogen radical has similarly been observed in IRMPD.[64]

The above does not take account of the effect of the chlorine substituent on the C=C ii bond in the VUV. However, photodissociation of chloroethylenes in general is known to yield radicals,[63] whilst the 1,2 elimination of HCl from the $^3B_2$ state of vinyl chloride has been observed to give acetylene.[67] Irradiation of chloroacrylonitrile at 174 nm is therefore likely to give rise to the following photoproducts

- mainly via the π^* <-- π transition of the C=C bond to give the $^3B_{1u}$ excited state (see below) which dissociates via molecular elimination to give HCl, HCN, H_2 and ClCN, together with the corresponding acetylenes (cyanoacetylene, chloroacetylene and HCCH), atomic hydrogen and atomic chlorine, whilst absorption at 213.9 nm will give rise to HCN, H_2, HCCH and cyanoacetylene. Irradiation at 254 nm will give rise to scission of the carbon-chlorine bond as the major photoprocess, since the C-CN bond (bond dissociation energy 133.7 kcal) will not be cleaved at this wavelength.[68] Thus it is possible to account for the very low chlorine and high N:C ratios seen in the CUV photopolymer, since the main photoproducts formed at 254 nm will be $CH_2C^{\cdot}CN$ radicals, which presumable can undergo chain and/or step-growth polymerization. However, the mechanism must again be more complicated than this due to the presence chlorine in the photopolymer, together with a 1:1 ratio in the C1s ESCA spectrum for the 285.0 eV peak against that at 286.6 eV (that for polyacrylonitrile is 2:1)[69a,b] and the presence of the 400.8 eV peak in the N1s spectrum, indicative of N-C and N=C such that at least some nitrile groups must react. However, many of the VUV photoproducts are not easily recognisable polymerizing species likely to cause film deposition. In section 5.3, it was noted that photopolymers were obtained from the 193 nm irradiation of acetylene.[32,33] Thus Irion and Kompa[32] observed a polymer during their study of acetylene using an argon fluoride laser at 193 nm, in addition to the reaction products ethylene and hydrogen atoms. Their evidence pointed to a pure excited-molecule mechanism based on $C_2H_2^*$ (^1Au). Becker and Hong also saw a polymer for the VUV irradiation of acetylene,[33] together

with diacetylene, ethylene, benzene, vinylacetylene and phenylacetylene. Interestingly, they also observed a brown polymeric deposit for VUV irradiation of hydrogen cyanide gas, together with $(CN)_2$, methane, ammonia, CH_3NH_2 and $(NH)_2$. Irradiation of a 5:1 mixture of HCN / acetylene showed that 90% of the light was absorbed by the latter, giving rise only to the products expected for C_2H_2 alone, together with acrylonitrile. On raising the relative amount of HCN in the system, the proportion of resultant ethylene was seen to decrease in favour of cyanoacetylene (C_2HCN). The proposed principal path for formation of diacetylene was via

$$C_2H^{\cdot} + C_2H_2 \text{ ---> } C_4H_2$$

whilst the formation acrylonitrile and cyanoacetylene were proposed to be, respectively, via (1) and (2)

$$C_2H_3^{\cdot} + HCN \text{ ---> } CH_2CHCN \quad (1)$$

$$CN^{\cdot} + C_2H_2 \text{ ---> } C_2HCN \quad (2)$$

Hence it is extremely likely that at least some of the chloroacrylonitrile photopolymer observed in the VUV originates from secondary photolysis of the acetylenes formed. Photopolymerization of the HCN eliminated from the monomer could also occur, but this contribution to film formation seems less likely due to the majority of other, more conventional, polymerizing species in the system, including acetylene, fresh monomer, and other radical species.

There is another consideration here. The chemical composition of the VUV photopolymer changes with an increase in flow rate, which in turn was achieved by increasing the monomer pressure in the system. Since the chlorine and nitrogen contents of the VUV photopolymer also increase with flow rate, this suggests a pressure dependence for the

depositing species responsible for film formation, since their nature must change over the flow rate range in order to produce differing elemental compositions. Thus, since the species are produced by photolysis (either primary and/or secondary), this indicates a pressure dependence of this as well. All the above hypotheses can be accounted for by a deposition mechanism which involves a vibrationally excited ground state (a singlet excited state would not be affected by an increase in pressure since its lifetime before decomposing, typically measured in nanoseconds,[37] is too short for pressure quenching effects to occur). This experimental observation fits with the known literature, since excitation at 174 nm using a nitrogen plasma emission will excite electrons in the ethylenic C-C bonding orbital into the antibonding ii^* orbital. This in turn relieves interelectronic repulsion by twisting into a 90^o conformation about the C-C axis. Since the pair of $2p_{ii}$ orbitals become degenerate in the 90^o conformation, the "90^o ground state" is a triplet, and the energy of the $^3B_{1u}$ level falls below that of the "ground" singlet state ($^1A_{1g}$).[65] Because of the large change in equilibrium geometry, highly energised molecules are produced, ie vibrationally excited ground states, the majority of which dissociate via molecular elimination (both 1,1 and 1,2) and atomic molecule production, although some cis-trans isomerization probably occurs as for ethylene.[65] Irradiation at 254 nm does not access this vibrationally excited ground state, but instead gives rise mainly to scission of the C-Cl bond via dissociation of an electronically excited state (corresponding to o^* <-- o), which would explain the lack of flow rate - and hence pressure - dependence seen in the CUV.

5.6.3 Summary

Chloroacrylonitrile gives rise to surface photopolymers on irradiation in both the VUV (174 nm) and CUV (254) regions. Orientation of the substrate either parallel or perpendicular to the incident radiation was found not to affect the nature of the polymer formed. Masking lead to incomplete film coverage such that, although polymerization must also take place from the gas phase, surface activated processes are important. The nature of the film appeared to be independent of photon flux; however, a dependence on radiation wavelength was found - the chemical composition of the films produced in the the CUV being essentially different from those deposited in the VUV. This can be explained in terms of the different photochemistries involved at the two wavelengths used. The overall photopolymerization mechanism was determined to involve a vibrationally excited ground state for the VUV since a dependence of elemental composition of the film formed on the flow rate - and hence on the pressure - of the system was found; this observation fits the the model for photolysis predicted by examination of the photochemical literature, such that dissociation of the ethylenic $^{3}B_{1u}$ state is an important step in the deposition process. The actual depositing species are likely to include secondary photolysis products, particularly of acetylene, and possibly also of HCN. Finally, the apparent lack of any flow rate dependence for CUV irradiation can be explained in terms of a simple scission of the C-Cl bond as a result of a $o^{*} \leftarrow o$ transition at 244 nm. This involves a singlet excited state which is therefore independent of the pressure of the system.

5.7 Methacrylonitrile

5.7.1 Results

Methacrylonitrile was found to give surface photopolymers in both the VUV and CUV regions, typical C1s, N1s and O1s core level spectra being shown in Figure 5.13. On irradiation for 70 minutes using an argon plasma as radiation source, the results shown in Table 5.9 were obtained.

				ELEMENTAL RATIOS			C1s Envelope			N1s	
SUBSTRATE POSITION	TIME /min	P /mb	FLOW RT $cm^3 min^{-1}$	N	O	Al	285.0	286.6	288.0	399.3	400.8
Horizontal	60	0.15	0.3	14	-	Y	d=20A°			93	7
Vertical	60	0.15	0.3	15	-	Y	d=46A°			92	8
Horizontal	60	0.2	1.3	17	-	Y	d=32A°			92	8
Vertical	60	0.2	1.3	17	-	Y	d=51A°			94	6
Horizontal	70	0.2	1.3	15	4	-	64	35	1	77[4]	
Horizontal[2]	70	0.2	1.3	17	5	-	62	37	1		
Vertical	70	0.2	1.3	20	6	-	61	37	2		
Horizontal	60	0.4	VP[3]	19	4	-	57	41	2		
Vertical	60	0.4	VP[3]	18	5	-	63	35	2		

NOTES: 1. Substrate overlayer calculation used to calculate nitrogen to carbon ratio if Al2p was signal visible.

2. Run at 70° Take Off Angle (remainder run at 35°)
3. The flow rate at monomer vapour pressure could not be accurately determined.
4. Elemental Ratios are per 100 C atoms.
5. Binding Energies are in eV.

TABLE 5.9 Methacrylonitrile VUV Photopolymer

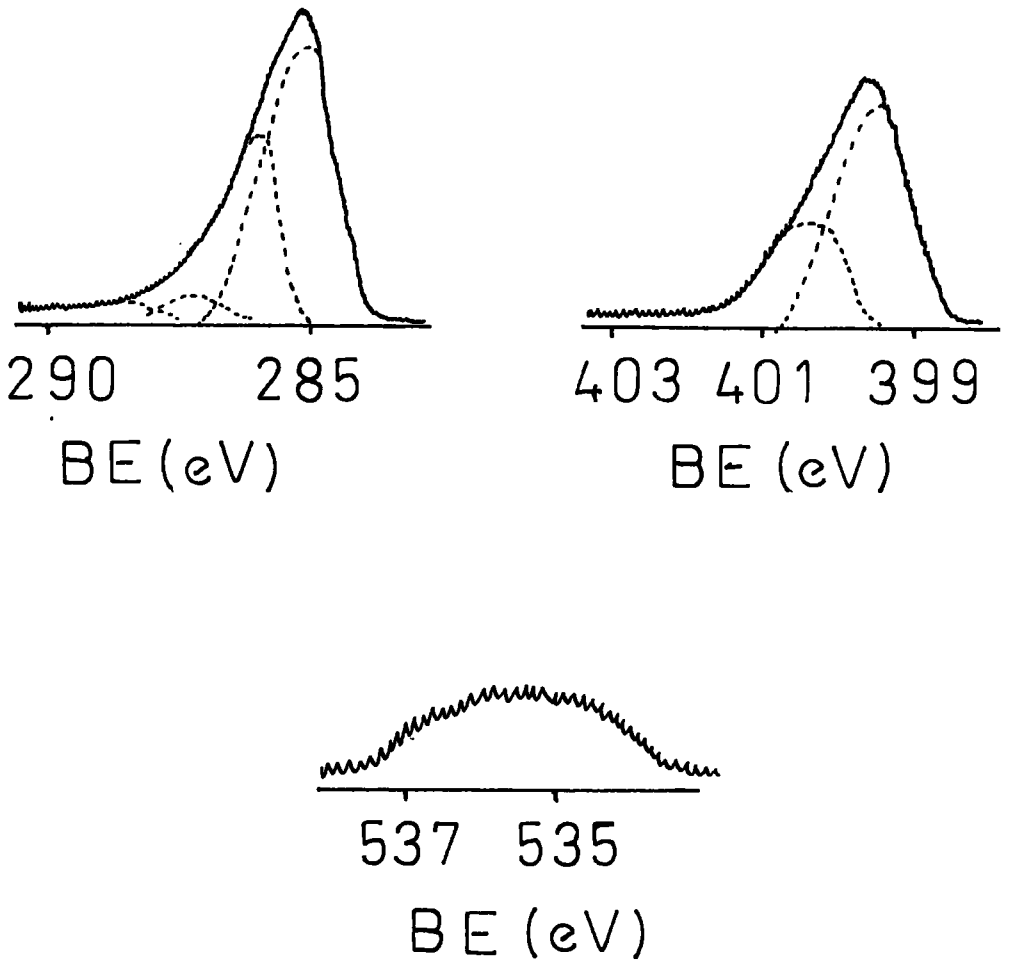

NOTE : Core level spectra for the corresponding conventional UV photopolymer are very similar to those shown above.

FIGURE 5.13 Typical XPS Core Level Spectra of Methacrylonitrile Vacuum UV Photopolymer - a) C1s; b) N1s; c) O1s.

The C1s spectra are again similar to those found in chapter 3 for plasma polymerization, together with its relative peak area ratios, as are the elemental ratios of nitrogen with respect to carbon.

SUBSTRATE POSITION	POWER in W	FLOW RT $cm^3 min^{-1}$	RATIOS N	RATIOS O	C1s Envelope 285.0	286.6	288.0	399.3	400.8
In coil	51	0.4	17	14	62	28	9	68	32
Tail	4	0.4	21	13	58	32	9	84	16

TABLE 5.10 Typical Plasma Polymer Film Analysis - CH_2CMeCN

This suggests that the species responsible for film deposition in methacrylonitrile surface photopolymerization must be similar to those for its plasma polymerization. However, differences exist between the films, most notably that virtually all the nitrogen content of the photopolymers exists in the form of nitrile groups, whilst this is not true for the plasma polymers. The lowest degree of nitrile reaction in the latter appears to occur in the tail region, such that the surface photopolymers are more akin to the plasma polymers produced in this region rather than those produced in the coil region. One anomalous result was obtained during a preliminary photopolymerization experiment, for which a peak at lower binding energy (398.0 eV) was found, indicative of a negatively charged species and corresponding to the result found for an 11W plasma polymer film deposited in coil. However, this result was not corroborated by the vertical substrate film obtained during the same experiment, and so cannot be accounted for. All the remaining experiments showed that, once again, the

chemical composition of the films produced were independent of substrate orientation (perpendicular or parallel) to the window. This was in contrast to the rate of film deposition as shown by the film thickness found using substrate overlayer calculations (Table 5.9), which showed both that polymer is deposited more quickly in the vertical than the horizontal position, and also with an increase in flow rate, for the same irradiation time. This again shows that, although deposition must occur from the gas phase (otherwise polymer would not be seen in the horizontal position), direct irradiation of the substrate is again important, and hence the film is truly a surface photopolymer.

The film deposited in the CUV at monomer vapour pressure by irradiation at 254 nm for 7 hours was different to that formed in the VUV, Table 5.11, since both the nitrogen and oxygen content of the

SUBSTRATE POSITION (cm from window)	RATIOS[1] N	O	C1s Envelope 285.0	286.6	288.0	N1s 399.3	400.8
1	23	14	44	44	8	92	8
1[2]	19	12	49	46	5	94	6
6	23	-	48	48	7	100	0
12	23	-	44	48	9	96	4
18	22	-	45	48	7	94	6

NOTES: 1. No. per 100 C Atoms.

2. Run at 70° TOA (remainder at 35°)

3. $1.3 cm^3 min^{-1}$ used throughout.

TABLE 5.11 Methacrylonitrile CUV Photopolymer

film were higher than those obtained in the VUV, whilst the 285.0 eV to 286.6 eV peak ratios were nearer to 1:1 than the 2:1 ratio previously found in the VUV. The main similarity was the lack of N=C and N-C bonds as shown by the N1s envelope, such that effectively all the nitrile groups in the monomer were left unreacted in the polymer. There was also a lack of change of chemical composition with distance of the substrate from the window, indicating the absence of any photon flux effect in this respect, although the deposition rate was found to be lower.

5.7.2 Discussion

A comparison of the above results with chloroacrylonitrile quickly shows that there are differences between the two photochemical systems. For example, although a flow rate effect was apparent for methacrylonitrile in the VUV, this was more apparent in the deposition rate rather than the chemical composition of the deposited polymer.

A noticeable difference is also seen in the C1s spectra, for which there is a marked absence of a peak at 287.8 eV, corresponding to carbon-chlorine environments (in particular C-ClCN), in the methacrylonitrile spectrum. Insufficient data was obtained to see if a flow rate dependence existed for the two main peaks that were seen (285.0 eV and 286.6 eV), whilst the N1s envelope revealed that little or no nitrile groups reacted in the VUV for methacrylonitrile, whereas a peak was quite marked at 400.8 eV for the corresponding chloroacrylonitrile films, indicative of N-C and N=C environments for the latter. Now, the substitution of a methyl group for chlorine will give rise to differing photoproducts in the two systems. In

particular, methacrylonitrile lacks the absorbance at 244 nm observed in the CUV for chloroacrylonitrile, and hence the exact nature of the films formed should be expected to be different. Thus, in the CUV, photochemistry for the methacrylonitrile must rely on scission of the C-Me and C-H bonds, since the energy input to the monomer at 254 nm is insufficient to break either the C=C or CN bonds. In contrast, methacrylonitrile photochemistry can still occur in the VUV due to the π^* <-- π ethylenic transition. The π^* <-- σ nitrilic transition cannot be of any importance here, since no nitrile groups were found to have reacted. The gas phase dissociation products in the VUV will therefore be analogous to those obtained for chloroacrylonitrile, ie H_2, HCN, HCCCN and HCCH via 1,1 and 1,2 molecular elimination respectively, together with atomic hydrogen and CN. The secondary photolysis of the acetylenes, and possibly HCN, should again contribute to film deposition, an overall free radical mechanism being invoked.

The most stable radical formed in the CUV will be $H_2CC^{\cdot}CN$. Loss of a vinylic hydrogen atom is unlikely, since an unstable radical, $^{\cdot}$HCCMeCN, results. Using this as the (free radical) initiating step, a simple radical addition mechanism might seem likely here; however, although the C:N ratio obtained, at 4:1, corresponds with that expected for polymethacrylonitrile homopolymer, the C1s envelope reveals a 1:1 ratio for the 285.0 eV to 286.6 eV peak areas, rather than the 3:1 expected, ie the experimental data suggests that there are as many C-CN environments in the film as there are carbon atoms not directly bonded to nitrogen. This also rules out a polyacrylonitrile structure, $(-CH_2-CHCN-)$, for which a 2:1 ratio

should be seen in the C1s, together with a 3:1 ratio for C:N.[69] The structure and mechanism are thus more complicated than that occurring in the homopolymer obtained by a conventional free radical addition mechanism.

5.7.3 Summary

Methacrylonitrile forms surface photopolymers at both VUV and CUV wavelengths. Similarities and differences are found when the photopolymer and photochemistry is compared to that of chloroacrylonitrile, but the importance of the substrate surface is once again shown, whilst a consideration of the ESCA results obtained also give an insight not only into the chemical composition of the thin films formed, but the likely photopolymerization as well.

5.8 Chloroacrylonitrile / Iodine

Chloroacrylonitrile was irradiated in the presence of iodine as a free radical scavenger in order to confirm that the surface photopolymerization mechanism is indeed free radical in nature. Monomer flow rates in the range 0.1-0.2 $CM^3_{STP}min^{-1}$ were photolysed at 254 nm and at 185 nm using, respectively, Oriel Scientific medium pressure, and Hanovia Low Pressure, arc lamps. Film deposition at low flow rate was completely inhibited at 254 nm for both substrate orientations in the reactor. However, complete coverage of the aluminium substrate was observed at high flow rate for the vertical substrate position, the horizontal position giving rise to incomplete deposition. The N1s envelope again showed a small peak at 400.8 eV, indicative of N-C and N=C environments. Polymer formation at 185 nm

was completely inhibited at low flow rate, whilst complete suppression of the Al2p signal was seen at high flow rate. The C1s spectra were not fitted due to the presence of a (small) amount of iodine in the films, Table 5.12.

REGION	FLOW RT	ELEMENTAL RATIOS					
	$cm^3 min^{-1}$	C	I	Cl	N	O	Al
UV(254 nm)	0.06	no deposition					Y
	0.14	incomplete deposition					Y
	0.2	100	2	19	24	2	-
VUV(185 nm)	low[1]	no deposition					Y
	high[1]	100	2	26	28	3	-

NOTE : 1. Flow rate could not be accurately determined.

TABLE 5.12 Chloroacrylonitrile / I_2 Photopolymers

Note that, for VUV irradiation, the C:Cl:N ratio is high (3.8:1:1) and very similar to that obtained for a high flow rate in the absence of iodine vapour. However, the chlorine content of the film deposited in the CUV is twice as great as any previously observed. Thus, whereas the addition if I_2 during irradiation below 200 nm appears simply to inhibit the deposition rate, addition above at 254 nm probably alters the exact film deposition mechanism as well, since scission of the carbon-chlorine bond cannot occur to nearly the same extent as in previous experiments. The low incorporation of iodine in the film shows that, although inhibition occurs, the polymerization termination step in the deposited film is unlikely to be of the form:

$$R^{\cdot} + I_2 \rightarrow RI + I^{\cdot}$$

otherwise the C:I ratio would have been lower. This may be because the polymer actually grows on the film surface by combination of existing radicals with those in the gas phase, propagation occurring whenever a diradical or a vinylic/acetylenic species is involved:

$$R^{\cdot} + R'{:} \rightarrow R\text{-}R'^{\cdot} \quad (1)$$

$$R^{\cdot} + CH_2{=}CHX \rightarrow R\text{-}CH_2\text{-}C^{\cdot}HX \quad (2)$$

$$R^{\cdot} + HCCX \rightarrow R\text{-}CHC^{\cdot}X \quad (3)$$

where X = H, Cl, CN

such that the iodine atom is sterically hindered from reacting with the film surface. This in turn suggests that inhibition of the surface polymerization process is in fact by reaction of iodine with the gas-phase radical species, quenching them before they have a chance to diffuse to the substrate position and react with radicals on the growing film surface. This would explain why complete inhibition is only seen at low flow rate, when the ratio of iodine to monomer molecules was greatest - since the iodine partial pressure in the system was limited by its vapour pressure/sublimation rate, the ratio of iodine to monomer molecules decreases with increasing flow rate, such that a point is eventually reached at which there there is physically not enough iodine in the system to quench every free radical photoproduct, and hence polymerization by migration of these species to the surface is now able to occur. If the inhibition took place on the surface itself, then, since the substrate surface area is constant whatever the flow rate, either more iodine should be incorporated into the film and/or there should not be such a marked dependence of the polymerization process on the monomer flow rate.

5.9 Surface Photopolymerization - a Deposition Model

The preceding sections have discussed the nature of the thin films formed when various monomers are irradiated with ultraviolet or vacuum ultraviolet light, and have speculated on the nature of the photochemistry, excited states and depositing species responsible for polymer formation. The importance of surface activation by photons has also been noted, whilst the absence of direct irradiation of the surface was not seen to completely prevent deposition. Drawing together all the evidence found both by experimental observation and also in the literature, the initiation, propagation and termination steps can be summarised as follows:

INITIATION

1. Main route - monomer molecules adsorped onto activated substrate surface undergo primary and secondary photolysis to give HX (via molecular elimination), HCCX, H, X etc, mainly via a vibrationally excited $^3B_{1u}$ ethylenic ground state in the VUV; to give CH_2-C$^{\cdot}$CCN + X in the CUV. Acetylenes undergo secondary photolysis to give $C_2X^{\cdot}$

   Minor route - active radical photolysis products diffuse to the substrate where they are adsorped.

X,Y = H, Cl, CN, Me. Both routes lead to active radical sites on the substrate and photocell surfaces, together with a "soup" of monomer molecules and assorted photolysis products in the gas phase.

PROPAGATION

2. Radical polymerization of monomer molecules (CH_2CXY) and secondary photolysis products (HCCX, HCN) occurs using existing radicals on the film surface as initiators. Chain growth will occur both on the film surface and also with eg dimers, trimers etc and other diradicals in the gas phase, the latter also giving rise to crosslinking.

TERMINATION

3. Radical recombination between R$^{\cdot}$ on the film surface and R$'^{\cdot}$ in the gas phase, or else by cross-linking of two polymer chains in the film surface.

INHIBITION BY HALOGEN VAPOUR

4. Major route - quenching of propagating species in the gas phase before they can migrate to the substrate.
   Minor route - quenching of active radical sites on the growing film surface (this is sterically hindered).

The above mechanism is relatively simple, and does not pretend to be complete. However, further evidence that it is correct in outline can be found in the work of Koizumi et al, who found that vinyl chloride irradiated at 253.7 nm in the presence of mercury deposited a white photopolymer on the irradiated surfaces of the photolytic cell. The rate of reaction was found to depend on the nature of the substrate used, as well as the pressure of monomer and mercury in the photolytic cell :

$$v = k[CH_2=CHCl][Hg]I \quad (1)$$

where I is the intensity of the absorbed incident light, whilst no polymer formation was visible in the absence of mercury. The mechanism for deposition was suggested to be as follows :

1) Initiation of the chain takes place in the gaseous phase.

2) Propagation proceeds in the gaseous phase or on the wall of the photolytic cell.

3) Termination occurs only on the wall of the vessel.

The authors also found that changing the nature of the substrate in the vessel could alter the speed of reaction, and correctly concluded that part of the reaction must therefore take place on the substrate surface. However, it must be the initiation step that is important here, as shown in this work, since only the speed of nucleation of the first few monolayers of the film will depend on the substrate-film interaction; thereafter, collision at the surface will occur between propagating species and the growing organic film only. Thus it is incorrect to say that initiation occurs (only) in the gaseous phase. In addition, the existence of a pressure dependence for vinyl chloride photopolymerization suggests the existence of a vibrationally excited ground state in the deposition process, contrary to the singlet excited state suggested to be involved in scission of the carbon-chlorine bond in chloroacrylonitrile. However, the latter occurred in the absence of mercury vapour, and therefore was not a sensitised reaction. The data of Koizumi et al, which was not fully understood at the time (1953), can be rationalised using the results of Callear and Cvetavonic obtained in 1956. These assumed that two electronically and vibrationally excited states were involved in the

overall sensitisation reaction; both were subject to collisional deactivation, but that only one decomposed via molecular elimination to give the corresponding acetylenes. Using the method of Calvert and Pitts then the primary quenching step (1) is triplet energy transfer from an $Hg(^3P_1)$ state to produce a vibrationally excited triplet state $C_2H_3Cl^*$ which is deactivated to the ground state or isomerized to $C_2H_3Cl^{**}$, probably as vibrationally excited triplet ethylidene (2). This in turn undergoes molecular elimination of HCl or H_2 to give the corresponding acetylenes (4,5), or rearrange followed by deactivation (6) :

$$C_2H_3Cl + Hg(^3P_1) \rightarrow C_2H_3Cl^* + Hg(^1S_0) \quad (1)$$

$$C_2H_3Cl^* \rightarrow C_2H_3Cl^{**} \quad (2)$$

$$C_2H_3Cl^* + C_2H_3Cl \rightarrow 2C_2H_3Cl \quad (3)$$

$$C_2H_3Cl^{**} \rightarrow C_2H_2 + HCl \quad (4)$$

$$C_2H_3Cl^{**} \rightarrow C_2HCl + H_2 \quad (5)$$

$$C_2H_3Cl^{**} + C_2H_3Cl \rightarrow 2C_2H_3Cl \quad (6)$$

The above photochemistry is similar to that obtained for continuous irradiation at ca. 180 nm resulting in ii^* <-- ii excitation of C=C, with the exclusion of atomic hydrogen and chlorine production. The overall photopolymerization mechanism for vinyl chloride is therefore mainly analogous to that obtained in this work for chloroacrylonitrile. The lack of film deposition reported for vinyl chloride irradiated at 253.7 nm in the absence of mercury can be attributed to the lack of availability of a suitable surface sensitive technique, such as ESCA, at the time. In contrast, the latter enabled investigation into the importance of substrate activation in surface photopolymerization by incident photons which, although not strictly

necessary for film growth to occur, promotes nucleation of the first monolayer of polymer, and hence leads to a faster film deposition rate. The idea of "polymerization" here actually being a series of radical copolymerizations is also thought to be new at the time of writing, whilst no mention was found in the literature of inhibition of surface photopolymerization by iodine.

Finally, the surface polymerization model is also applicable to plasma polymerization. By analogy, the latter involves activation of the substrate via impact of ions, promoting interaction of the surface with the first monomer monolayer. Initiation of polymerizing species is via electron impact excitation to give excited state neutrals, metastables and ions. These can decay to give primary products, which can in turn undergo electron impact excitation to give secondary products. Propagation of the polymer is via (multiple) chain growth of the film surface by the species produced in the plasma. The exact nature of these - radicals or ions - will depend on the monomer used and the power input into the system (the latter since it affects the kinetic energy available to the free electrons formed in the plasma, and hence to the amount of energy that can be transferred during electron impact excitation). That the latter can also give rise to photopolymerization has been noted by Sieck at al, who observed ionic polymerization of vinyl halides in the vapour phase initiated by photoionisation using photons with energies over the ionisation threshold. Hence surface photopolymerization is truly a model for plasma polymerization.

CHAPTER 6

POSITIONAL DEPENDENCE WITHIN A PHOTOCHEMICAL REACTOR

6.1 Introduction

Chapter 5 showed that, as for plasma polymerization, the chemical composition of photochemically deposited organic thin films is influenced by the parameters W, F and M in the form of photon flux, flow rate and the monomer used, together with the wavelength of incident radiation. Overall, it was shown that a knowledge of the photochemistry involved in surface photopolymerization can give an insight into the possible mechanism of plasma polymerization. However, since chapters 3 and 4 showed that substrate position within a plasma reactor influences the film deposited, if plasma and surface photo-polymerization are truly analogous, then positional dependence should be observable in the latter as well. In order to test this, the variation of chemical composition of thin films deposited from metha- and chloro- acrylonitrile were investigated as a function of distance from the window of the photolytic cell. The initial results suggested that such a dependence indeed existed for the system; they further indicated that the flow of activated species downstream might also influence the deposition process along the length of the reactor. The investigation was thus widened to examine this second possibility.

6.2 Experimental

The experimental apparatus used for both VUV and CUV studies was the same as that described in Chapter Five, except that in later experiments the monomer inlet position was moved further upstream so that it was now only about 1cm away from the window (cf some 6cm previously).

Chloro- and methacrylonitrile were degassed by freeze-thaw cycles prior to use. VUV radiation was supplied using a 50W inductively coupled plasma excited in 0.4mb of nitrogen; CUV experiments were carried out with the Oriel Scientific medium pressure Hg/Xe arc lamp. Monomer pressures used were in the region of 0.1-0.2mb, corresponding to flow rates of 0.4-0.6 cc(STP)min^{-1} whilst ESCA analysis was carried out using either the Kratos ES300 or ES200 spectrometer, together with their associated data analysis facilities.

6.3 Results and Discussion

I. Positional Dependence

Substrates were placed immediately next to the window, as well as 6, 12, 18 and 24cm downstream. Photon flux decreased down the length of the reactor due to (a) decrease of light intensity with distance following the $1/r^2$ law (where r = the distance of the substrate from the light source); (b) absorption of photons by other monomer molecules nearer to the window. Accordingly, the film deposition rate decreased the further away the substrate was from the window. Initial results for a chloroacrylonitrile 2 hour VUV static photopolymer (Table 6.1) showed a difference in chemical composition between the window and 6cm positions, whilst the remaining substrates showed little other than physical adsorption of monomer. Since substrate overlayer calculations were necessary in the above example,[1] the differences cannot necessarily be attributed to diffusion effects of activated species from one substrate position to the next.

Position	Atomic Ratios			Film Thickness/A
	Carbon	Chlorine	Nitrogen	
1cm	100	15	19	44
6	100	6	24	21
12/18/24	Evidence for physical adsorption only			

TABLE 6.1 Chloroacrylonitrile - 2 Hour VUV (Static) Photopolymer

Further experiments in the VUV showed that complete film coverage of the aluminium substrates was not achievable within reasonable timescales unless these were positioned next to the window. Attention was therefore turned to the higher deposition rates achievable in the near UV region (i.e. > 200 nm) using the Hg/Xe arc lamp in a static monomer system. Raising the deposition time to 18 hours suppressed the Al2p signal for the two nearest substrate positions (i.e. next to, and 6cm away from, the window). Incomplete film depositions were observed for the remaining substrates except for that at the 24cm position, enabling substrate overlayer calculations to be performed to find the chlorine and nitrogen elemental ratios with respect to carbon. Table 6.2 shows the results for the nearest substrate positions for the static systems at different lamp discharge powers (and hence photon fluxes). In two cases the Cl:N ratio is approximately unity for the substrate position nearest to the window (Table 6.2(ii)), with higher retention of chlorine and nitrogen by the depositing film occurring further away.

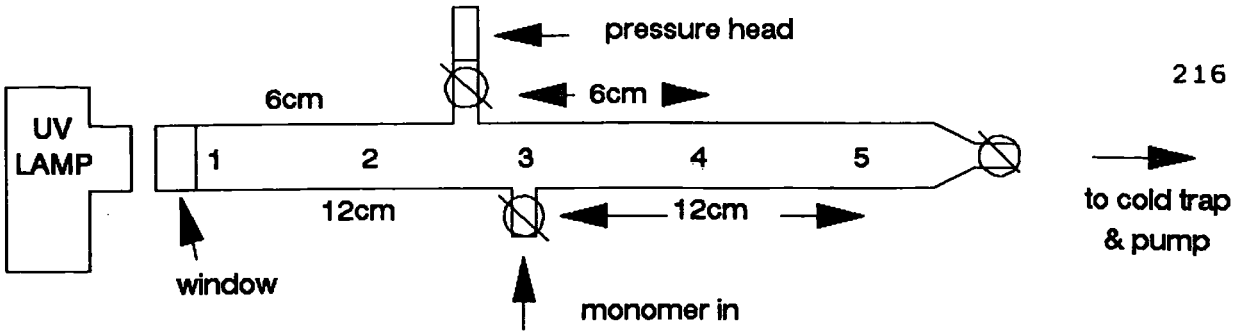

FIGURE 6.1 Experimental Apparatus - Deposition Chamber

(NOTE : UV lamp is replaced by a nitrogen plasma chamber for VUV irradiation)

TABLE 6.2 CHLOROACRYLONITRILE
STATIC UV PHOTOPOLYMER

	ATOMIC RATIOS PER 100 C ATOMS			C1s ENVELOPE				
DISTANCE FROM WINDOW	CHLORINE	NITROGEN	OXYGEN	285.0	286.6	287.7	289.0	THICKNESS/A
160 W								
1 cm	23	23	16	26	41	22	10	>1000
6	27	26	19	20	46	27	7	63
12	14	22						36
18	18	16						25
24								0
195 W								
1 cm	24	23	11	40	27	9		>1000
6	29	24	10	45	25	10		>1000
12	24	21						67
18	19	17						17
24	25	19						15
225 W								
1 cm	15	23	10	34	36	23	7	>1000
6	21	27	15	36	38	20	7	>1000
12	17	22						23
18	14	6						23
24	8	9						29

NB SPECTROSIL B WINDOW USED THROUGHOUT

DISTANCE/cm	1	6	12	18	24
POWER/W	160	0.98	0.95	1.61	0.91	0.87
	195	0.98	0.81	0.88	0.89	0.78
	225	1.5	1.31	1.29	0.44	1.09

TABLE 6.2(ii) Nitrogen : Chlorine Ratio, Static System

The latter observation could be accounted for by activated species next to the window diffusing to the 6cm position and influencing the film deposition. Alternatively, the higher heteroatom retention further from the window could be a photon flux effect, the attenuation of intensity over the 6cm substrate separation being greater than that caused by decreasing the discharge power of the lamp from 190 to 160W.

These static system experiments were consolidated using a flowing system, the results of which for a typical mid range flow rate are listed in Table 6.3 and show that the chemical composition of the films does change with substrate position, complete deposition occurring throughout. The maximum nitrogen and chlorine content occurred at the 12cm position and corresponded to a minimum and maximum in the C1s component peaks centred at 285.0 and 286.6 eV respectively, together with a maximum for that at 287.8 eV (indicative of Cl-C-CN). These maxima and minimum in fact correspond to the substrate position immediately above the monomer inlet, and suggest either (i) that the longer the residence time of the monomer molecules in the photolysis cell, or (ii) the lower the concentration of monomer in the system (such that the power to monomer flow rate (W/F) is high), then the more likely the loss of chlorine and/or nitrogen content is during film deposition.

CHLOROACRYLONITRILE SURFACE PHOTOPOLYMER

Flowing System

FIGURE 6.2a - Atomic Ratios

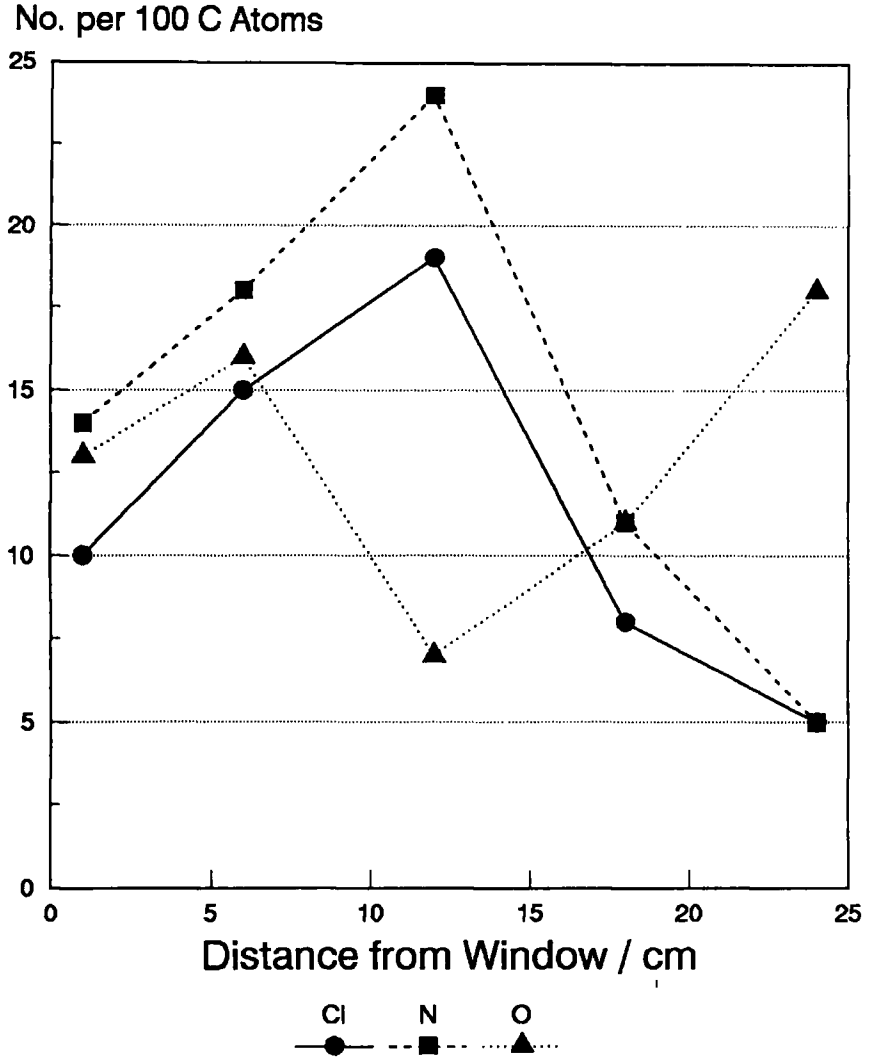

CHLOROACRYLONITRILE SURFACE PHOTOPOLYMER

Flowing System

FIGURE 6.2b - C1s Envelope

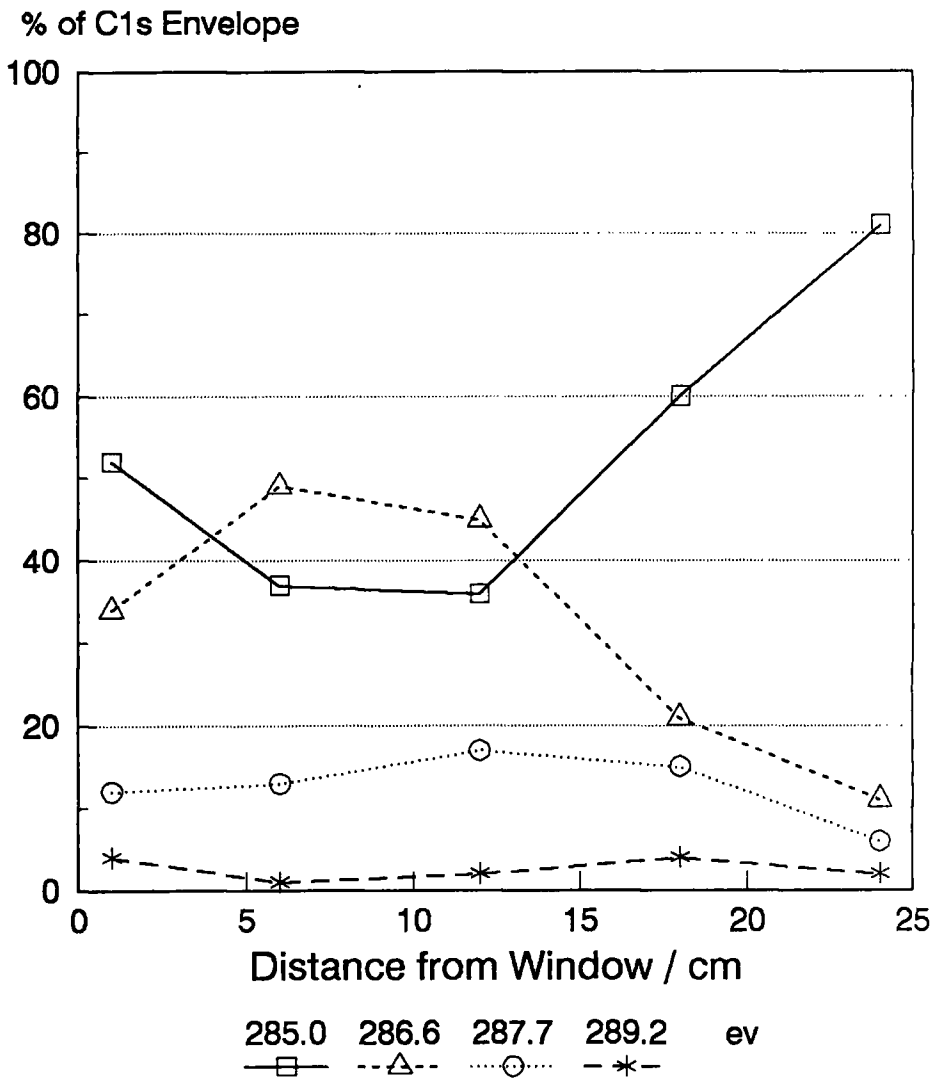

C1s Binding Energies are shown in ev.

DISTANCE from Window / cm	Atomic Ratios C	Cl	N	O
1	100	10	14	13
6	100	15	18	16
12	100	19	24	7
18	100	8	11	11
24	100	5	5	18

TABLE 6.3 Positional Dependence - Flowing System

The monomer inlet position was moved immediately next to the window from its position 12cm downstream (Figure 6.3), in order to see how this influenced the system. 0.13mb of flowing chloroacrylonitrile was irradiated in the CUV for 4 1/2 hours. The results (Figures 6.4, 6.5) again show a maximum for both chlorine and nitrogen content at the 12cm position. Complete coverage of the substrate occurred only within 6cm of the window, a result comparable to that obtained in the VUV by a nitrogen plasma initiated for 10 hours. A comparison of the chemical composition of the two films formed revealed that the Cl:N ratio in the VUV case is close to unity, whereas - as before - in the CUV chlorine is preferentially lost, giving rise to a lower (nearly constant) ratio. Overall, the position of the monomer inlet appears primarily to affect the deposition rate more than the chemical composition of the deposited films; however, it is noticeable that there is greater retention of Cl and N at the window and 6cm positions when the monomer inlet is next to the window, again reflecting the shorter monomer residence time in the photolysis cell before surface photopolymerization occurs at these positions.

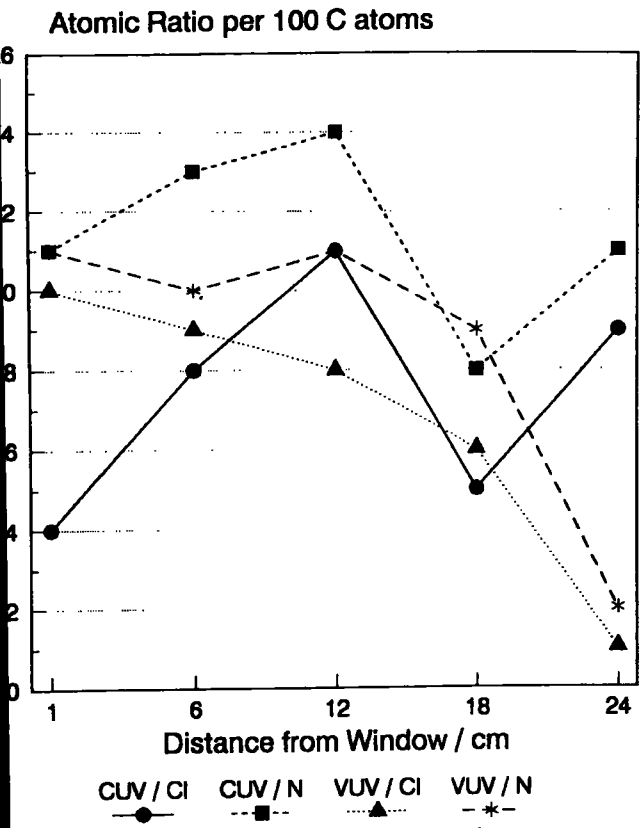

GURE 6.4 Comparison of Positional Dependence
Flowing System, VUV vs CUV Light

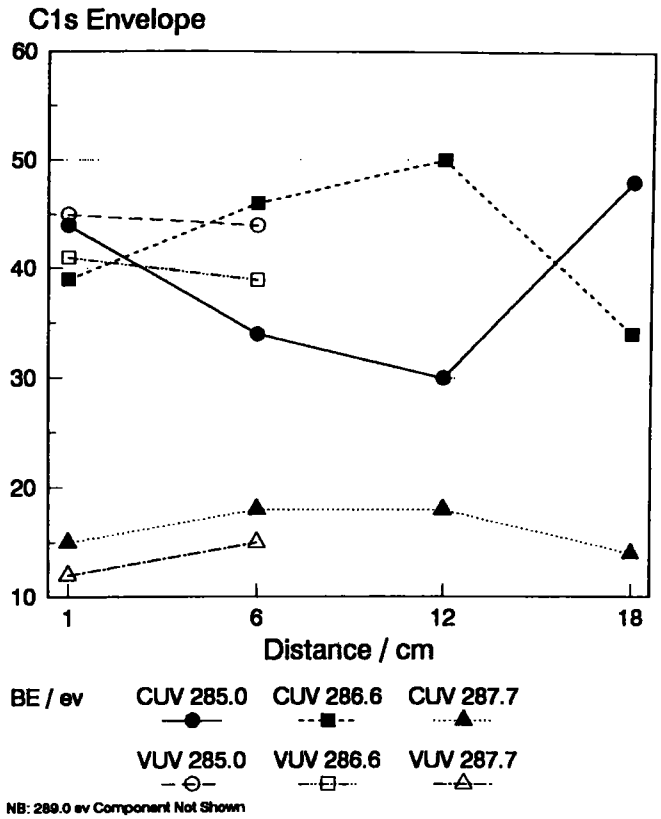

FIGURE 6.5 Comparison of VUV and CUV Results
Flowing System

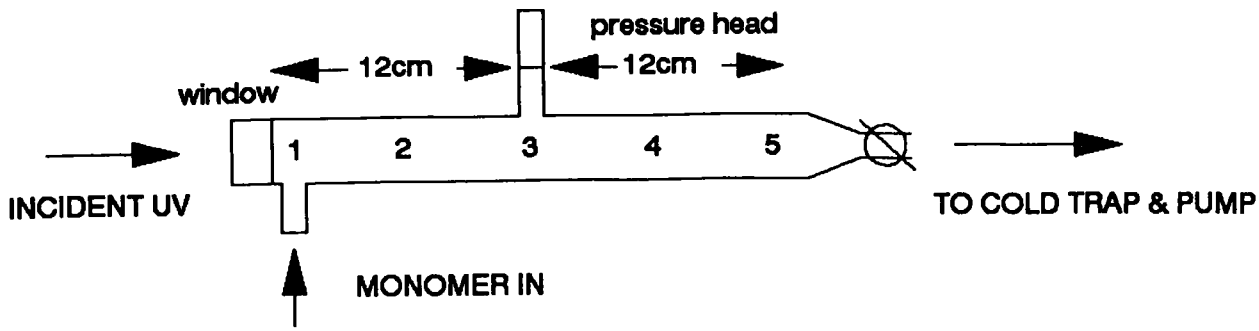

FIGURE 6.3 Experimental Apparatus - new monomer inlet

II. Dependence on Direction of Flow

All the experiments noted above utilised fresh monomer entering the photolytic cell at or near the window, prior to being swept downstream whilst still being illuminated.

In order to find the downstream limit of influence and deposition for molecules activated at a particular position in the cell in the absence of further irradiation, the monomer flow in the experiment was reversed such that fresh monomer entered at the far end of the reactor and was swept towards the window before exiting through 1/2 inch diameter glass tubing. Since the Hg/Xe lamp proved unreliable when used over long deposition periods, it was replaced by an alternative VUV irradiation source, namely a 60W plasma initiated in 0.2mb of nitrogen irradiating 0.13mb of chloroacrylonitrile (equivalent to 0.42 $cm^3(STP)min^{-1}$)) for a 36 hour period. The result was a visible brown polymeric deposit, not only on the CaF_2 window, but also some 6-10cm down the monomer exit tubing. Since this latter was completely shielded from direct illumination by the chamber above, any deposition was concluded to be entirely due to species activated by irradiation in the main chamber which were subsequently pumped straight out of the reactor before depositing. Since the deposited film in the exit (glass) tubing was easily visible to the naked eye, it must have been at least several thousands of Angstroms thick. Taken over a 36 hour deposition time, this gives a deposition rate in the order of hundreds of Angstroms per hour, i.e. a faster rate than that seen in any previous experiments. One possible explanation for such an increased rate could be that polymer film was formed due to the existence of a

very weak plasma in the deposition chamber during the experiment, induced by the presence of the nitrogen plasma in the adjoining chamber. However, this can be discounted for a number of reasons - firstly, both the window and the system as a whole were earthed in order to prevent the rf field extending into the deposition chamber; and secondly, previous experience of just such a phenomenon occurring showed that a film thick enough to be seen with the naked eye was deposited in minutes rather than hours. Regular inspection over the period of the experiment showed that the film appeared to build up gradually; the film was therefore concluded to be formed entirely as a result of the surface photopolymerization process.

Interestingly, deposition only occurred on, and immediately next to, the window - the 6 to 24cm positions downstream showed little evidence of film formation, suggesting that any back-diffusion of depositing species that might occur is swamped by the flow rate effect. This in turn would suggest that deposition observed in these positions in previous experiments (in which the monomer flow was not reversed) is likely to be due, at least in part, to such species being swept downstream from the window region, although the position of the inlet - as a source of fresh monomer - has been shown to be an important consideration here.

The fact that film deposition in the reversed flow case occurred so far down the exit tube suggests that (i) polymer formation here does not occur as a result of monomer being adsorped onto the wall/substrate prior to being irradiated, with polymerization subsequently taking place between molecules already lying on the surface; (ii) the species actually involved in the surface photopolymerization of

chloroacrylonitrile are relatively long lived. This would be in agreement with the observations in chapter 5 on the surface photopolymerization carried out in the presence of iodine vapour, which suggested that free radicals are likely to be responsible - either wholly or in part - for polymer formation.

Knowing the approximate limit of deposition in the exit tube, we can make a simplistic estimate of the lifetime of the depositing species involved :

diameter, d, of exit tubing = 1/2 inch= 1.27 cm

cross-sectional area = $(d/2)^2 \sim 1.27 cm^2$

volumetric flow rate employed = 0.42 $cm^3(_{STP})min^{-1}$ The volumetric flow rate at the pressure used (0.13mb=0.1 torr) is equivalent to :

$$0.42 \times (760/0.1) = 3192\ cm^3\ (0.1\ torr)min^{-1}$$

Dividing by the cross-sectional area gives us an approximate average linear flow rate of 2513 cm min^{-1} at 0.1 torr, equivalent to 42 cm s^{-1}. Since film was observed some 6-10 cm along the exit tubing, this suggests either that some depositing species initially formed live for at least 0.1 s, or else that, if shorter-lived, they may decompose into other long lived species which in turn contribute to film formation.

However, the above view of the problem is too simplistic since

a) although the experimental evidence indicates that the flow of both monomer and depositing species is dominated by the flow rate of the system, diffusion <u>will</u> also play a part.

b) gas kinetics, including diffusion processes, is quite a mathematical topic in its own right, requiring a more sophisticated approach than that above.

The latter can be found for diffusion in the Einstein-Schmoluski Law, which governs the time taken, , for a particle to diffuse a given distance, x, such that :

$$= x^2 / 2D$$

where D is the Diffusion Coefficient of the gas involved (ie here chloroacrylonitrile vapour and the gas phase depositing and non-depositing species formed from it). Actual values of D are proportional to the inverse of the pressure of the system, 1/P, with typical values at 10 torr being in the range 10-100 $cm^2\ s^{-1}$, as suggested by Mulcahy.[2] Using these upper and lower limits an estimate of the time taken for particles to diffuse 10 cm from the main chamber to the limit of visible film deposition in the exit tubing is given by:

UPPER LIMIT - $D = 100\ cm^2 s^{-1}$

Now $D = k / P$ where k is a constant in mb $cm^2\ s^{-1}$

$\Rightarrow k = DP$

$= 100 \times 13.3$ (10 torr = 13.3 mb)

$= 1330$ mb $cm^2\ s^{-1}$

therefore, if $P = 0.13$mb $\Rightarrow D = 10230\ cm^2\ s^{-1}$

such that $= (10)^2 / (2 \times 10230) \sim 5 \times 10^{-3}$ s

LOWER LIMIT - $D = 10\ cm^2 s^{-1}$

Similarly $= 5 \times 10^{-2}$ s

This gives an equivalent linear diffusion velocity of $\sim$ 2 - 20 m s^{-1}, showing that diffusion effects cannot be ignored. In addition, the average time taken for a particle to diffuse to the walls of the exit tube is given by R^2/D, where R is the radius of the cylinder (i.e. tube) involved.[2] This gives a lifetime of

$$(1.27/2)^2 \;/\; 10230 = 4 \times 10^{-5}\ \text{s} \quad \text{(lower limit)}$$

$$\text{"} \quad / \quad 1023 = 4 \times 10^{-4}\ \text{s} \quad \text{(upper limit)}$$

compared to respective limits of about 2×10^{-4} to 2×10^{-3} s for the (1 inch diameter) main chamber.

At first sight, the longer diffusion time calculated for the main chamber - which has the lower film deposition rate compared to the smaller exit tube - might suggest that the depositing species in fact have maximum lifetimes in the order of 10^{-3}s, rather than the 0.1s suggested by the linear flow rate calculation, since the nature of the species involved should be the same in both cases. If true, this would not allow deposition to be seen as far down the exit tube as it was in fact observed. Even if moving at the maximum theoretical diffusion speed (20 m s^{-1}), any molecules activated in the main chamber directly contributing to deposition 5 cm down the exit tube would have to live for <u>at least</u> 10^{-3} s in order to do so - longer than the maximum lifetime calculated above. This rules out excited and vibrationally excited ground states formed during UV irradiation as depositing species themselves (since their lifetimes are too short to travel the required distance), but would support the idea already advanced that it is species subsequently formed from these (eg free radicals and other photolysis products) which are responsible for polymer formation.

An alternative approach to the problem is to calculate the average residence time, t_c, in the first 10 cm of exit tube of any particle, p, which is swept through it by the flow action. This is given by the equation :

$t_c = V / v$ where V = volume of the tube concerned

v = volumetric flow rate

Now, $V = R^2 d = 3.14 \times (1.27/2)^2 \times 10$

$= 12.7\ cm^3$

$v = 0.42\ cm^3(STP)min^{-1} = 3192\ cm^3(0.13mb)min^{-1}$

$\Rightarrow t_c = 12.7/(3192/60) = 0.24\ s$

This is a long time period compared to photochemical excitation and decomposition processes, again suggesting that, for polymer formation to have occurred so far down the exit tube, the depositing species involved must be long-lived.

However, the above still does not explain the increased deposition rate seen due to using reverse monomer flow compared to the previous experiments in which monomer entered next to, and flowed away from, the window; and those subsequently carried out in section III. This could possibly be explained in terms of the reduced diffusion times (from gas phase to wall surface) for the narrower tube involved, and also by a consideration of the number of molecule-wall conditions predicted by kinetic theory. In particular, if the diameter of a tube is halved - as happens here - then, for a given number of gas molecules, n, the volume occupied stays the same whilst the surface area of wall involved increases by a factor of 2. Since the pressure in the exit tube is effectively the same as that in the main chamber, we can conclude that there are twice as many molecule-wall collisions per second in the narrower tube as there are in the larger since we now have twice the original surface area for n unchanged. Assuming that the chance of any

molecule coming into contact with a wall and "sticking" (and hence leading to surface photopolymerization) is constant, then such an increase in the frequency of collisions seems likely to increase the rate of film deposition as well.

Returning to the calculated linear flow velocity, at $\sim$ 0.42 m s^{-1} this velocity is smaller than the calculated rate of diffusion. However, this contradicts the observed evidence, since the reverse-flow experiment showed that little deposition occurs upstream from the point of UV irradiation. This could be explained when one realises that the true nature of the flow dynamics involved is much more complicated than either of the two models above allows. For example, the actual linear velocity of flow in the (cylindrical) apparatus will depend on the radial distance from the longitudinal axis and the axial distance from the entrance. Under likely conditions the gas(es) will move, as a whole, by viscous flow, as given by the Poiseuille Formula :[2]

$$u(r) = 2\,\underline{u}\,(1-r^2 / R^2)$$

where u(r) is the linear velocity at a radial distance, r, from the axis of the tube; R is the radius of the cylinder itself and $\underline{u}$ is the (average) linear flow velocity. This means that the gas near the axis of the tube flows faster than the gas near the wall, causing a radial concentration gradient which makes the reactant molecules present diffuse towards the wall. If diffusion were completely absent, then the molecules present would move with the bulk of the gas in purely viscous flow. This radial concentration gradient exists in addition to the axial concentration gradient which causes the reacting molecules /

depositing species to diffuse down the exit tube towards the cold trap. In addition, a mixture of flow dynamics through the tube, and film deposition removing molecules from the gas phase, will cause a pressure drop along both the reactor chamber and the exit tube.

The above information can be applied to a flowing surface photopolymerization system as follows :

a) a static system relies on diffusion alone to carry gas molecules from the bulk to the wall of the chamber / exit tube.

b) a flowing system helps depositing species formed to diffuse towards a substrate placed on the bottom of the reactor chamber more quickly than in a static one, since the radial effect caused in the former is absent when no flow is present.

c) decreasing the diameter of the tubing used increases the number of molecule-wall collisions for a given volume of monomer vapour used, and hence is likely to increase the number of depositing species reaching the wall and/or substrate.

d) a crude estimate can be made of the lifetimes - and hence nature - of the species involved in film deposition can be made using a rudimentary knowledge of the gas kinetics / flow dynamics involved.

These points possibly help to explain why the deposition rates observed throughout this work for surface photopolymerization were consistently higher for flowing than for static conditions; in addition, they could also explain why the deposition rate in the 1/2 inch tube was much greater, for an equivalent time period, than in the 1 inch diameter main chamber. The linear flow rate calculation in d) leads to an upper lifetime limit of about 0.1 s, whilst that determined by a consideration of diffusion alone is in the order of 0.01 s. These

limits are in agreement, within an order of magnitude, with those estimated by Ward for the surface photopolymerization of n-vinyl pyrrolidone (NVP),using a pulsed irradiation method.[3] Even if the actual lifetimes involved are two or three of orders of magnitude different from these figures, such a long lifetime compared to those of photochemically activated species such as electronically or vibrationally excited states suggests that it is not these latter, but rather their dissociation products, which are in fact responsible for film deposition, and hence polymer formation. These could include, in particular, free radicals, in agreement with the iodine inhibition experiments carried out earlier in this work.

This particular aspect of the photopolymerization process was not pursued further due to a lack of available time; however, the effect of various external parameters on deposition rate are examined in Chapter Seven.

III. Two Window Experiments

Surface Photopolymerization for the non-static system has been shown to be influenced by flow rate, with deposition in the reactor able to occur some way downstream from the point of illumination. To probe this idea further, the experimental apparatus shown in Figure 6.6 was developed. This allowed illumination to take place at either or both of two substrate positions 3cm apart. More importantly, since the irradiation is carried out at ninety degrees to the direction of flow, any deposition resulting further downstream cannot be influenced by continuing irradiation.

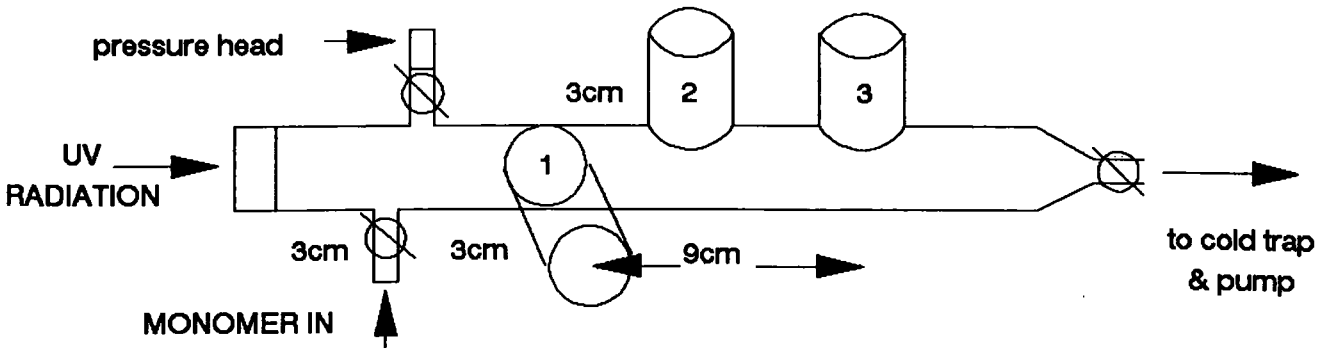

EXPERIMENTS ARE : 1) CUV ONLY AT POSITION 1

2) CUV AT 1 plus VUV AT 2

3) VUV ONLY AT POSITION 3

FIGURE 6.6 Experimental Apparatus - Two Window Experiment

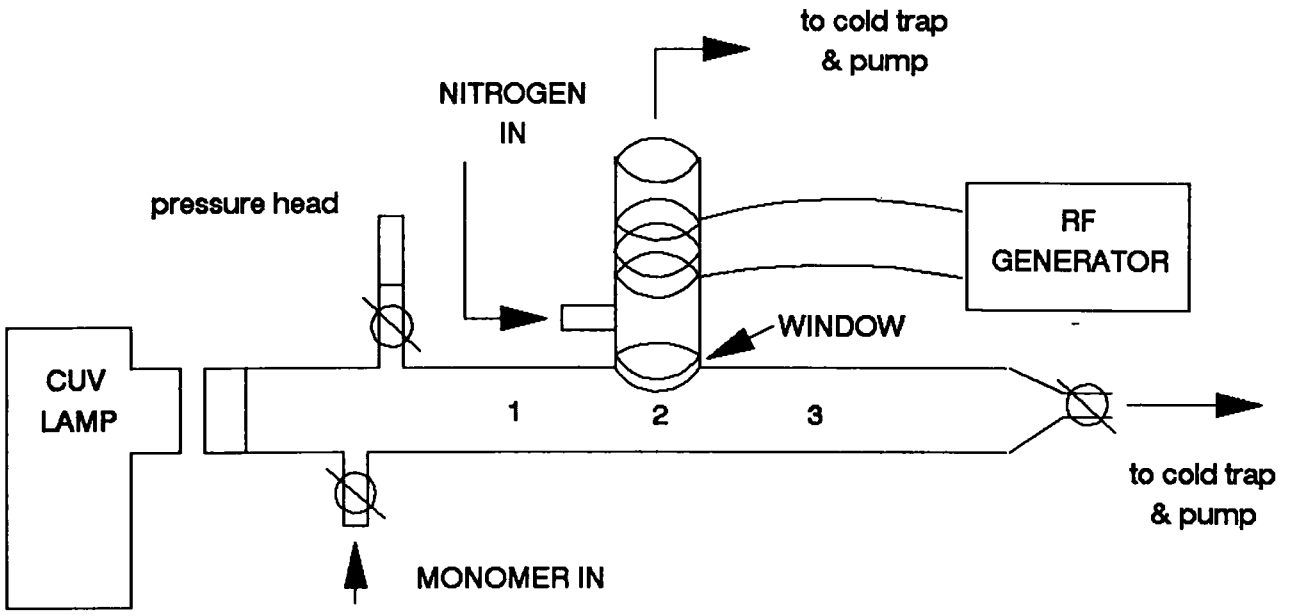

FIGURE 6.7 Experimental Apparatus - Two Window Experiment

Initial experiments employed CUV radiation at position 1, with VUV from an argon plasma at position 2. The films formed by separate irradiations at each position, together with the substrate placed at position 3 were analysed by ESCA and then compared to the results for simultaneous irradiation.

The results are shown in Tables 6.4 and 6.5 as a function of incident radiation (VUV versus CUV), position of substrate within the photolysis chamber, and type of window used for VUV irradiation. Results for the CUV light source showed that deposition only occurred immediately next to the window, the remaining positions only showing evidence for physical adsorption of monomer onto the aluminium foil substrates used (Figure 6.8). Similarly, VUV irradiation resulted in complete deposition only at position 2, although the C1s envelopes obtained at position 3 were possibly indicative of an incomplete overlayer of film rather than simply adsorption of monomer. Simultaneous irradiation with both CUV and VUV sources gave little change in the atomic ratios of chlorine and nitrogen to carbon in position 1, whereas the C1s envelope revealed an increase in the component centred at 286.6 eV, that at 287.7 eV dropping in intensity. Thus there is a change in the distribution of the different moieties types here without an overall change in the stoichiometry of the film surface. In addition the N1s envelope at position 2, which showed a marked increase in the 399.3 eV component compared to irradiation by VUV alone. Replacing the MgF_2 window, which has a wavelength cut-off circa 110 nm, for one made out of Spetrosil B with a higher cut-off at about 150-160 nm, led to incomplete film deposition in position 2 for VUV illumination, both when carried out alone and also on the presence

TABLE 6.4 Two Window Experiments

Results for Apparatus in Figure 6.6

	Cl	N	285.0 ev	286.6 ev	287.7 ev	289.0 ev	399.3 ev	400.8 ev
Position 1								
CUV only	14	20	43	36	17	4	92	8
VUV only	monomer adsorption only							
Both	17	29	43	45	10	2	94	6
Position 2								
CUV only	monomer adsorption only							
VUV only	5	21	58	30	9	3	64	36
Both	11	18	54	31	12	3	89	11
Position 3								
CUV only	monomer adsorption only							
VUV on;y	evidence for incomplete deposition							
Both	evidence for incomplete deposition							

(i) all results obtained using MgF2 Window
(ii) level of deposition at position 3 increased when both light sources used, cf VUV alone

TABLE 6.5 Two Window Experiment

Effect of Replacing MgF2 Window by Spectrosil B

	Cl	N	285.0 ev	286.6 ev	287.7 ev	289.0 ev		
Position 2								
VUV / Mgf2	5	21	58	30	9	3	64	36
VUV / Spec B	8	15	incomplete deposition				93	7
Both / MgF2	11	18	54	31	12	3	89	11
Both / Spec B	incomplete deposition						91	9
Position 1								
Both / MgF2	12	23	43	45	10	2	94	6
Both / Spec B	11	18	50	28	17	5	91	9
(repeat expt)	16	20	37	42	17	4	91	9

of a CUV light source (Table 6.6). Repeating the experiment suggested that the differences observed in chemical composition at position 1 were probably caused by experimental error. In contrast, it appears that the incomplete coverage of substrate observed for position 2 can be attributed to the higher wavelength cut-off of the new window material used. This in turn suggests that the VUV emissions from a nitrogen plasma occurring between 110-160 nm, ie at 149 nm, must be at least partly responsible for polymer formation in this instance.

The above results again suggest that it is photolysis processes in the gas phase which affect the chemical composition of the surface photopolymer formed and which hence account for the differences observed between the films deposited respectively in the vacuum and conventional ultraviolet regions.

The next step in the investigation was to test whether or not two photon processes were occurring in the system. If so, then the film deposited during simultaneous CUV and VUV irradiation should have differing chemical composition compared to those using a single light source. A nitrogen plasma was therefore ignited perpendicular to the flow direction, the Hg/Xe lamp irradiating down the length of the reactor (Figure 6.7).

Three initial experiments employed a 200W Hg discharge in position 1, followed by a 65W plasma initiated in 0.4mb of nitrogen as the VUV source at position 2), prior to simultaneous irradiation. Two substrate positions were used - immediately next to the cell window (the CUV position), and immediately opposite the VUV source (the VUV position) (Figure 6.7). The results are shown in Table 6.6 for a flow

TABLE 6.6 Two Window Experiment

CUV Lamp in Horizontal Position

	Cl	N	O	285.0	286.6	287.7	399.3	400.8
Experiment 1								
Position 1 (CUV)	17	20	4	39	38	20	90	10
Position 2 (VUV)	21	23	5	34	42	20	90	10
Experiment 2								
Position 1 (CUV)	24	26	7	31	43	21	92	8
Position 2 (VUV)	22	25	6	35	43	20	92	8
Experiment 3								
Position 1 (CUV)								
Position 2 (VUV)	10	13	7	56	32	9	95	5
Experiment 4								
Position 1 (CUV)	22	23	4	36	41	20	95	5
Position 2 (VUV)	24	24	4	33	46	21	95	5

3 Experiments in total :
1) CUV plus VUV 2) CUV only
3) VUV only 4) repeat experiment (see text)

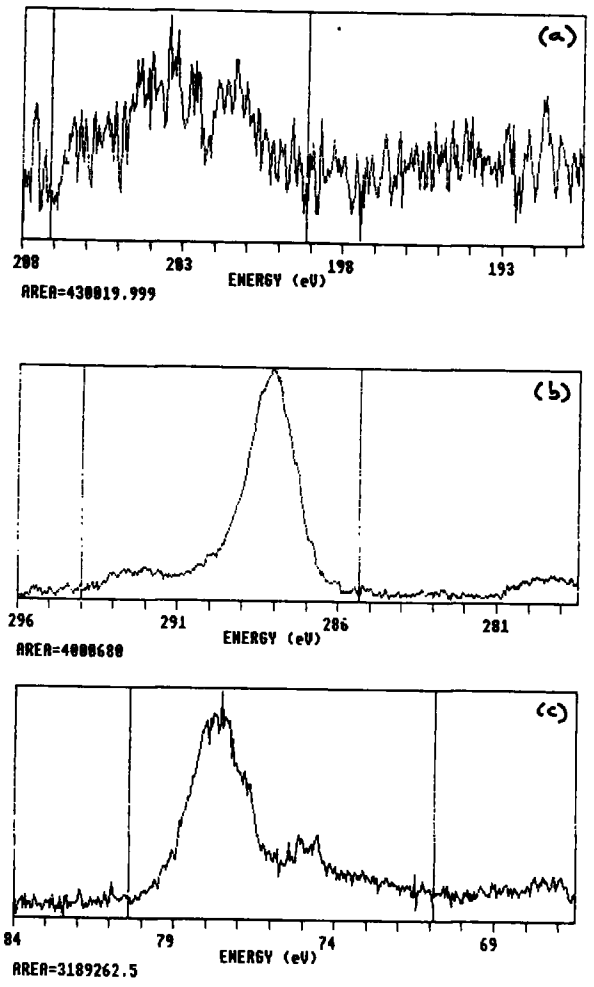

FIGURE 6.8 : CHLOROACRYLONITRILE
Surface Photopolymer - Incomplete Deposition
(a)Cl2p, (b)C1s, (c)Al2p Core Level Spectra

rate of 0.55 cc(STP)min^{-1} of chloroacrylonitrile irradiated for 5 hours. They suggest that, for simultaneous CUV and VUV irradiation, the film formed in the VUV position is dominated by the >200 nm photochemistry of the Hg arc lamp but that the CUV position in fact gives rise to a different film composition compared to near UV irradiation alone.

However, even allowing for some of the fresh monomer entering the photolysis chamber initially flowing towards the window, and hence being illuminated by the VUV source prior to deposition at the CUV position, it was expected that a difference in chemical composition would be seen either at the VUV position alone, or else in both positions. Repetition of the experiment suggested that experimental error probably accounted for the discrepancy between substrate positions, such that the results of the investigation were thus ambiguous - whilst prolonged irradiation appeared to give rise to a downstream influence of depositing species, whether these continue to stay in the light beam or not, the effect on chemical composition was not proven. However, the fact that substrate coverage in position 3 in the initial two window experiments only occurs to any extent under simultaneous illumination at positions 1 and 2 suggests that the VUV source is likely to be contributing to deposition in the system. In later experiments involving higher CUV photon fluxes, and hence higher deposition rates, analysis of the films formed at position 3 again showed them to be similar to those deposited from CUV irradiation only (the effect here is possibly enhanced by the "swamping" of the comparatively lower intensity of the VUV photon flux by that of the CUV). Originally, a difference in chemical composition of the

resultant films was envisaged, due to the photochemistry of chloroacrylonitrile in the vacuum UV (<200nm) compared to the conventional UV wavelengths (>200nm) - the absorption of light in the former case can involve the ii^* <-- ii absorption of the C=C double bond, whereas the latter is dominated by the o^* <-- o photochemistry of the C-Cl moiety, the (free radical) photolysis products differing accordingly, this difference being seen in the comparison of the CUV and VUV surface photopolymers investigated in Chapter 5.

The possibility of two-photon processes occurring during the surface photopolymerization of chloroacrylonitrile therefore remains neither proven nor disproved. However, Ward has used photochemical kinetics to show that the order of reaction for surface photopolymerization of NVP is greater than unity under certain experimental conditions, which suggests that the mechanism in this case involves the absorption of more than one photon.[3]

A more detailed investigation is perhaps possible using lasers, which have been extensively used in recent years to probe the mechanisms of multi-photon dissociation processes in various molecules, not only in the VUV (ArF 193 nm excimer laser) and CUV (KrF 248 nm laser) regions, but also the infra-red. Whilst the application of such a tool to the study of surface photopolymerization is a possibility for the future in order to gain a deeper mechanistic insight into the processes involved, few of the references found at the time of writing acknowledged the presence of organic thin film deposition in a laser system.[4-6] This may be due to the very short irradiation times (eg << 1s) used, for example in flash photolysis, is insufficient for surface photopolymerization to be observed; however, especially in those

studies where longer irradiation periods are involved, it seems likely that thin film deposition does occur, and will be increasingly reported in the future.

CHAPTER 7

PHOTODEPOSITION RATES OF ORGANIC THIN FILMS OF CHLOROACRYLONITRILE

7.1 Introduction

Plasma polymerization deposition rates fall into two main regions. The first is deficient in the amount of monomer present compared to the level of power input to the system, whilst in the second region this situation is reversed. A graph of deposition rate versus the W/FM parameter (Figure 7.1) shows an increase with monomer availability up until the point at which the power input to the system becomes the limiting factor; any further increase in the amount of monomer present in the system results in a decreasing deposition rate.[1] An analogous situation was suggested by Till[2] for photopolymerization of n-vinyl pyrrolidone (NVP), the power input to the system being the photon flux output of the light source used. This chapter investigates possible effects of power (W), flow rate (F), and of various added (non-polymerizable) gases, on the photopolymerization of chloroacrylonitrile at near ultra-violet (>200nm) wavelengths.

7.2 Experimental

The experimental apparatus used, Figure 7.2., consisted of a metal photolysis chamber, the sections of which were bolted together using copper O rings sandwiched between metal flanges. Connection between the chamber and the glass portions of the vacuum system was effected using Cajon ultratorr couplings. Pumping was provided by an Edwards $21s^{-1}$ pump connected to the chamber via a cold trap; the pressure of the system was monitored by a Pirani head whilst deposition rates were recorded using a quartz crystal deposition monitor connected to an amplifier to give a digital readout. The crystal was placed next to the calcium fluoride window of the cell, the latter being mounted in

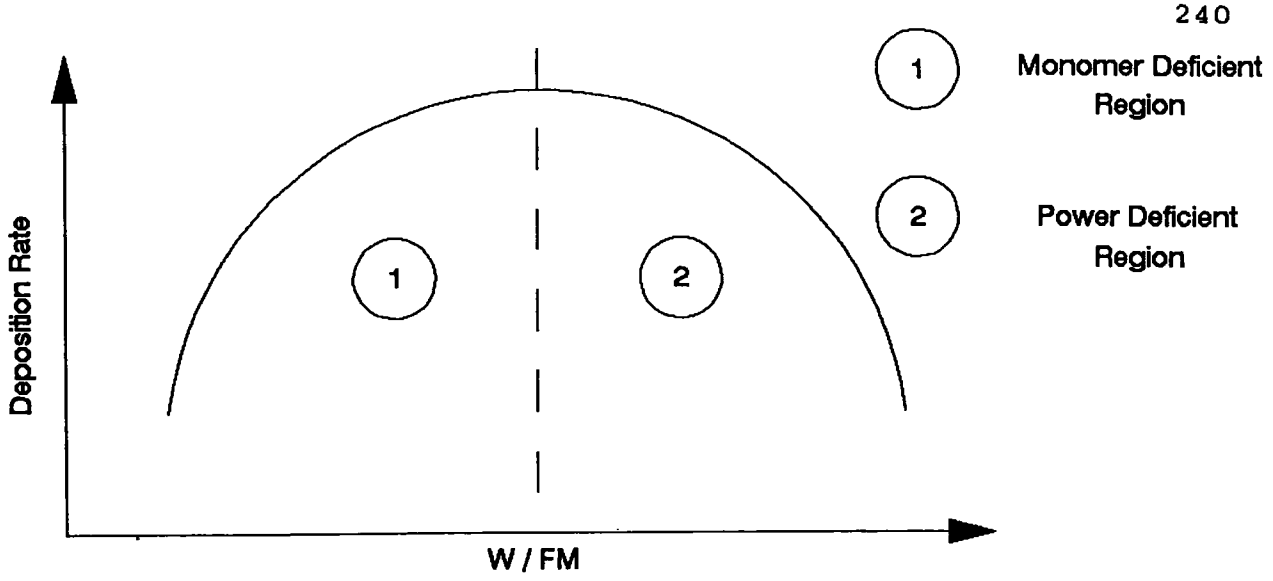

FIGURE 7.1 Effect of Yasuda's Parameter on Deposition Rate

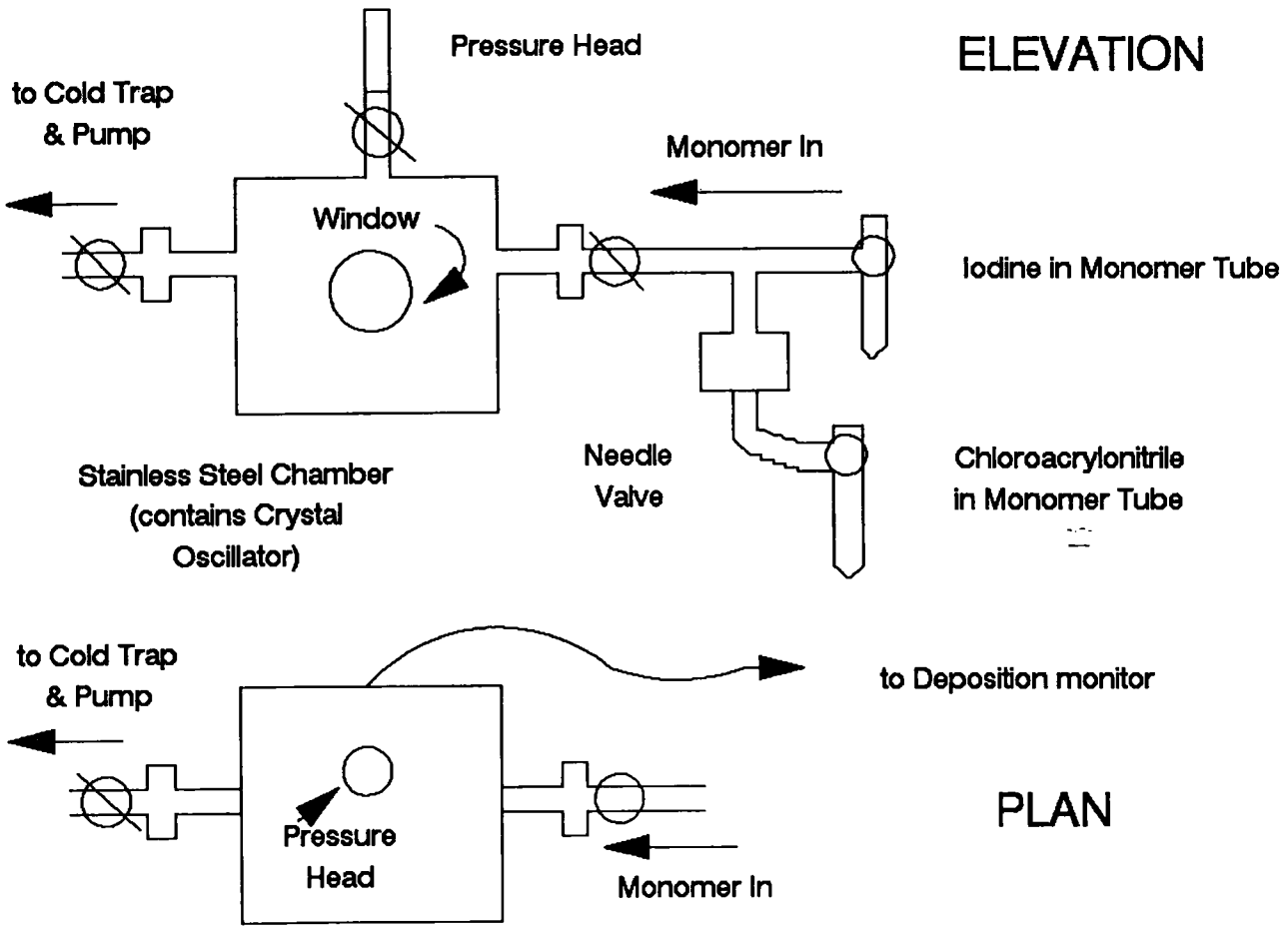

FIGURE 7.2 Experimental Apparatus - Deposition Rate Experiments

the usual window holder and cleaned between experiments using an oxygen plasma to remove the deposited film. The lead for the oscillator passed down the length of the chamber and exited through the rear wall, vacuum tightness being effected by sealing the exit hole with araldite.

Chloroacrylonitrile in a monomer tube was attached to the system via cajon couplings. Measurement of flow rate using an X-Y recorder wired up to a pirani head gave a large experimental error in determining the tangent at the operating pressures used. The results are thus presented as a function of monomer pressure in the system. On adding a non-polymerizable gas to study its effect on the deposition rate of the system, full mixing with the monomer was ensured in a T piece prior to entry into the main chamber. Flow of all vapours was controlled using Edwards needle valves, whilst irradiation was carried out at 185 nm using a Hanovia 1000W, 240V, 50Hz medium pressure Hg arc lamp, used on a 100W setting and placed 1cm from the window (itself 1cm thick) throughout. Experiments fell into two categories:

1) deposition rate experiments, in which the thickness of the depositing film was observed with respect to time for various experimental conditions (an arbitrary, constant setting for the density of the deposition monitor film, which ensured good sensitivity for the 10-15 minute duration of the experiments, allowed a direct comparison of film thickness, and hence rates of deposition, between systems, without the absolute values having to be known).

2) repeat experiments for the same experimental conditions as above, with the addition of an aluminium foil placed immediately on top of the quartz crystal in order to allow analysis by ESCA of the thin film formed.

7.3 Results and Discussion

I. Variable Flow Rate

0.2mb of chloroacrylonitrile was irradiated for ten minutes, the reading on the deposition monitor being noted every thirty seconds. The results, Figure 7.3, show an initial, short, time period prior to a rapid, but steady rise in thickness of the film in the first few minutes. This growth rate tailed off as the light intensity transmitted through the window was increasingly attenuated by build up of polymer film on its surface. It was also discovered that even a 10 minute illumination time markedly heated the metal reactor, causing the reading of the deposition monitor to increase even in the absence of organic vapour. This heating effect, shown in Figure 7.4, was therefore taken into account by adjusting the readings (Figure 7.3) accordingly. The corrected graph is to be found in Figure 7.5, together with the results for 0.1mb and 0.15mb. The overall trends for all three experiments were found to be unchanged whether or not heating effects were taken into account. Film thickness, and hence deposition rate, was found to increase with flow rate as expected (the photon flux was effectively constant throughout). Further experiments on the heating effect of the lamp with various pressures of non-polymerizable gases present revealed little difference with pressure within expected experimental error; further results are thus presented uncorrected for heating since a) the investigation was intended to be qualitative, rather than quantitative; b) correction of the data was previously shown not to alter the overall trend of deposition.

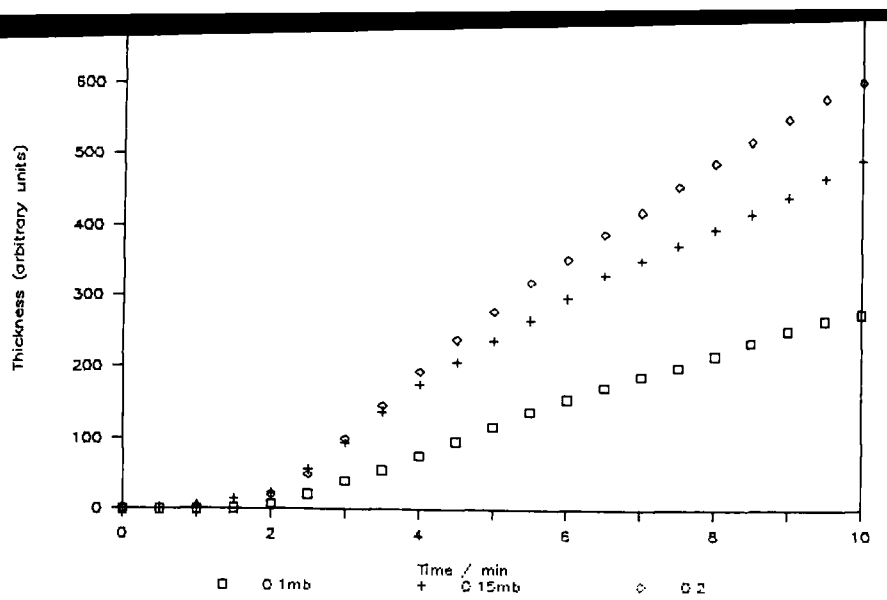

FIGURE 7.3 : 0.2 mb Chloroacrylonitrile Irradiated for Ten Minutes

CHLOROACRYLONITRILE

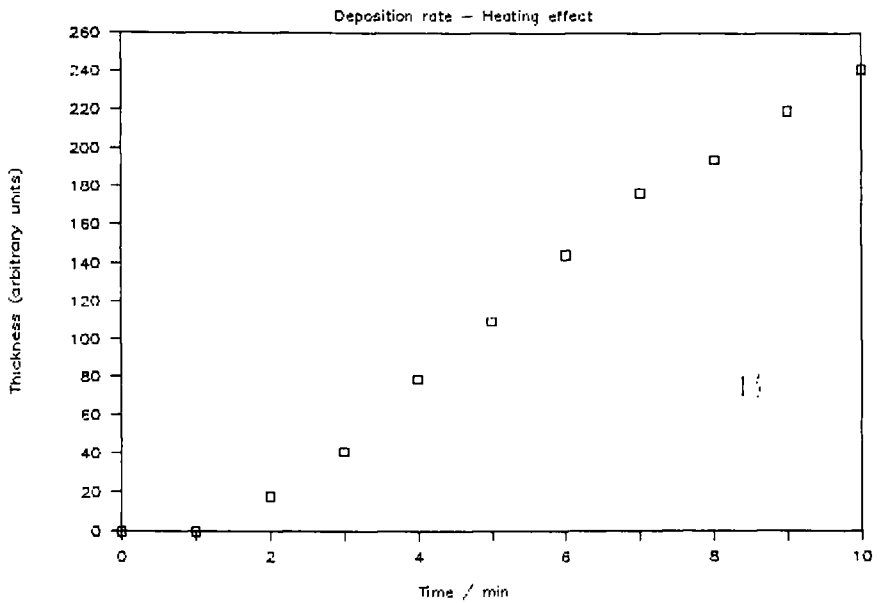

FIGURE 7.4 : Heating Effect

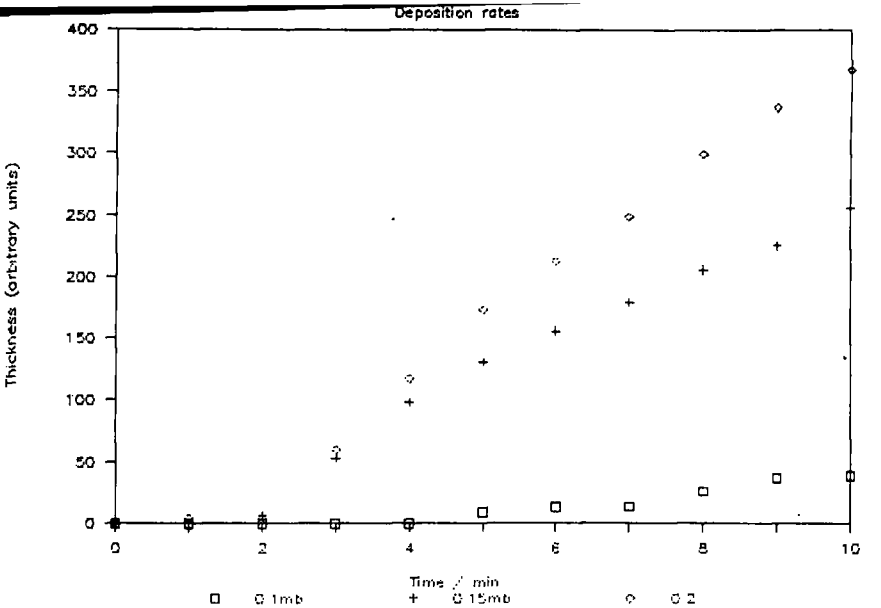

FIGURE 7.5 : Deposition Corrected for Heating Effects

CHLOROACRYLONITRILE

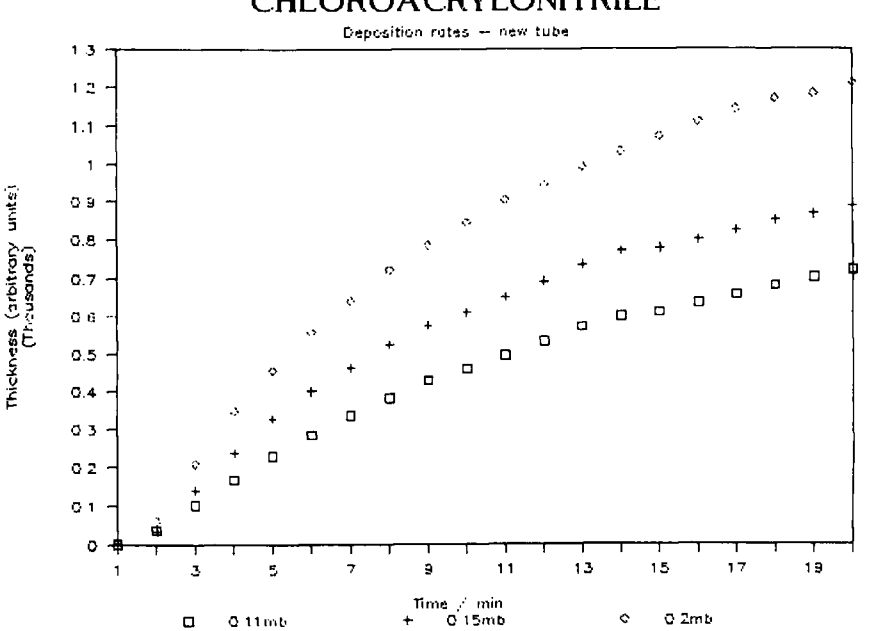

FIGURE 7.6 : Deposition Using new Tube

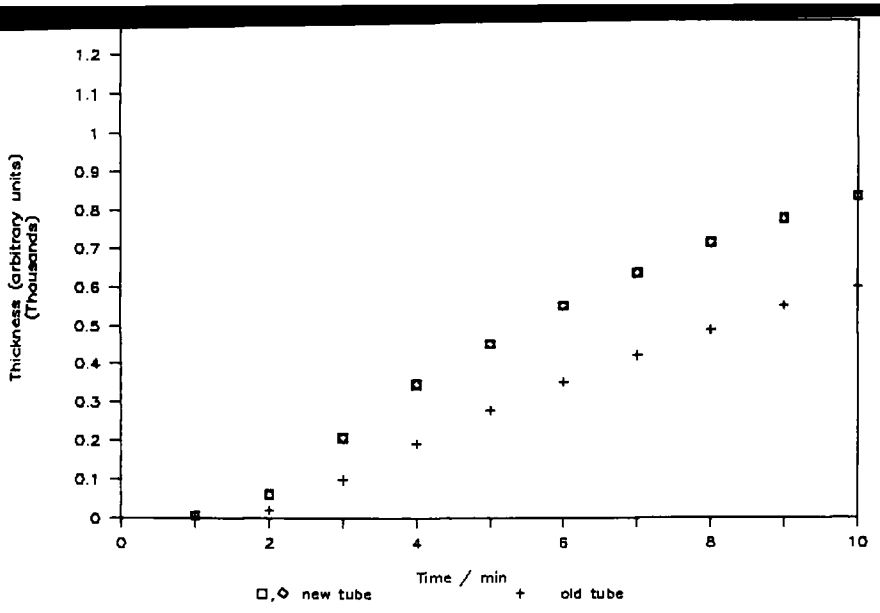

FIGURE 7.7 : New vs Old Discharge Tubes

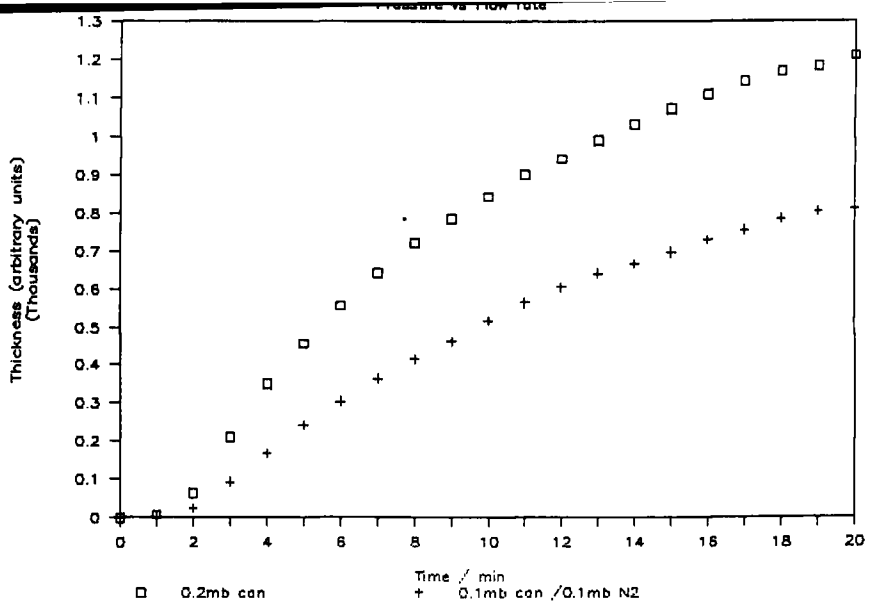

FIGURE 7.9 : Effect of Buffer Gas on Deposition Rate vs Increased Monomer Flow Rate

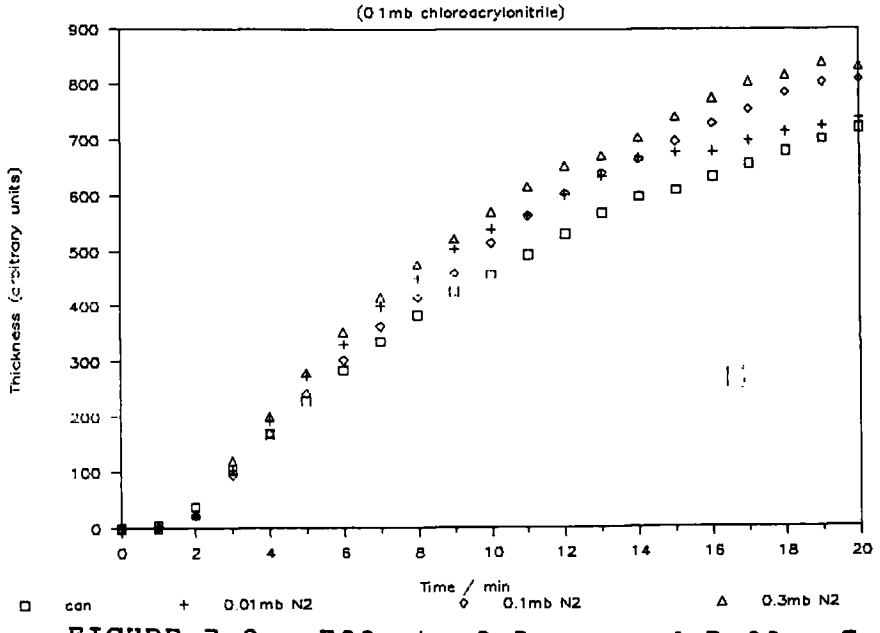

FIGURE 7.8 : Effect of Increased Buffer Gas

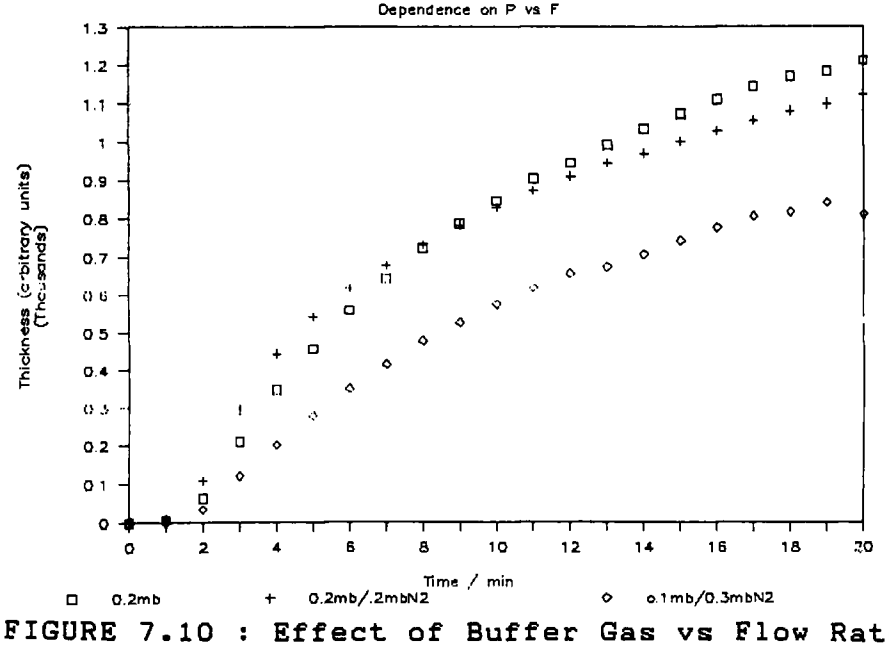

FIGURE 7.10 : Effect of Buffer Gas vs Flow Rate

After completion of these initial experiments, the ultraviolet light source broke down, requiring a new discharge tube for the completion of the work. This in turn resulted in increased deposition rates on repeating the original experimental conditions due to the new tube having a higher photon flux than the old one for the same 100W power setting, the observation showing another similarity between plasma and surface photopolymerization since, if the two processes are truly analogous, then the qualitative effect of W/F should apply to both systems. This appears to be the case since an increase in the photon flux for the given flow rate increases the power available in the parameter W/F, and hence the increased flow rate seen agrees with the model prediction, assuming a power deficient region (the system is unlikely to be monomer deficient, since the pressure of monomer in the reactor chamber was quite high). Similarly, removing the light source from the window by some 8cm - ie decreasing the photon flux by about 95% - was found to result in a lower deposition rate, and also to change the chemical composition of the film formed as studied by ESCA (see section III, Table 7.2). Qualitative reproducibility of results for the variable flow rate series with the new light source was proved for repeated experiments, the trends proving to be the same for the two light sources (Figures 7.6, 7.7).

II Effect of Added Gas

The next stage of the investigation examined the effects of added, non-polymerizable gases on the film thickness formed and hence (qualitative) deposition rate of the system. Using nitrogen as an inert buffer gas, two sets of experiments were performed. The first,

Figure 7.8, maintained a constant partial pressure (0.1mb) of chloroacrylonitrile whilst varying the total pressure of the system using nitrogen. Once again correction of the results to allow for the heating effect of the lamp was found not to alter the overall trends. The results are thus shown in their uncorrected form, and suggest that adding a 0.01mb partial pressure of buffer gas to the system appeared to increase slightly the rate of film deposition in the first 15 minutes of the experiment, although the total film thickness after 20 minutes, as recorded by the crystal deposition monitor, is the same as that for chloroacrylonitrile irradiated alone. Both higher partial pressures of added nitrogen (0.1 mb and 0.3 mb) led to similar results as for 0.01mb over the first portion of the experiment, the final film being noticeably thicker. Thus the results do appear to show a pressure effect on the system with respect to photodeposition rate. A comparison of results for a mixture of 0.1mb of monomer together with 0.1mb of added nitrogen with those for 0.2mb of monomer alone, Figure 7.9, which shows that the latter condition leads to the greater deposition rate - ie it is the monomer pressure and flow rate that is important such rather than that of carrier gas. Coupling this with the dependence of reaction rate on photon flux suggested in chapter 5 and the use of a new discharge tube (above), the rate equation is probably of the form :

$$v = k[\text{monomer}]I$$

where I is the intensity of the incident radiation, and the equation is of the form found by Koizumi and coworkers for the gas-phase photopolymerization of vinyl chloride[4,5]. The dependence of reaction velocity, v, on monomer pressure is further shown in Figures 7.5 and

7.10. In the latter the deposition of 0.2mb of monomer irradiated alone is compared to that on addition of 0.1mb N_2 and 0.2mb N_2, together with the result for 0.1mb monomer in the presence of 0.3mb N_2. Note, that the initial deposition rate for the 0.2 mb CAN / 0.2 mb N_2 mixture is slightly higher than that for the monomer alone, although the thickness of film deposited after 10 minutes is about the same. The existence of a pressure dependence of the overall photopolymer deposition rate would be indicative of a mechanism involving vibrationally excited ground states, since the (quantum) yield of products utilising these are known to decrease as the pressure of the system increases.[3] This result is due to the increased frequency of molecule-molecule collisions per second leading to a greater level of collisional stabilisation and quenching. This would agree with the results of Koizumi et al for gaseous vinyl chloride irradiated at 253.7 nm in the presence of mercury as sensitiser,[4,5] which was observed to give a white surface photopolymer. The photochemistry can be interpreted using the data of Callear and Cvetanovic,[6] which would suggest that collision of $Hg(^3P_1)$ with ground state vinyl chloride molecules leads to a vibrationally excited triplet state which undergoes unimolecular decomposition to give acetylenes. Using the data of Simons[7], this triplet is in fact the ^3B_u ground state. The overall sensitisation photochemistry is effectively the same as that obtained if steady-state photolysis occurs at 185 nm.[3,5]

Oxygen was next added to the system in order to study any uptake occurring during the photodeposition process, rather than incorporated on subsequent exposure of the film surface to air. Figure 7.11 shows the results for various mixtures of CAN + O_2 (0.1mb + 0.1mb and 0.2mb +

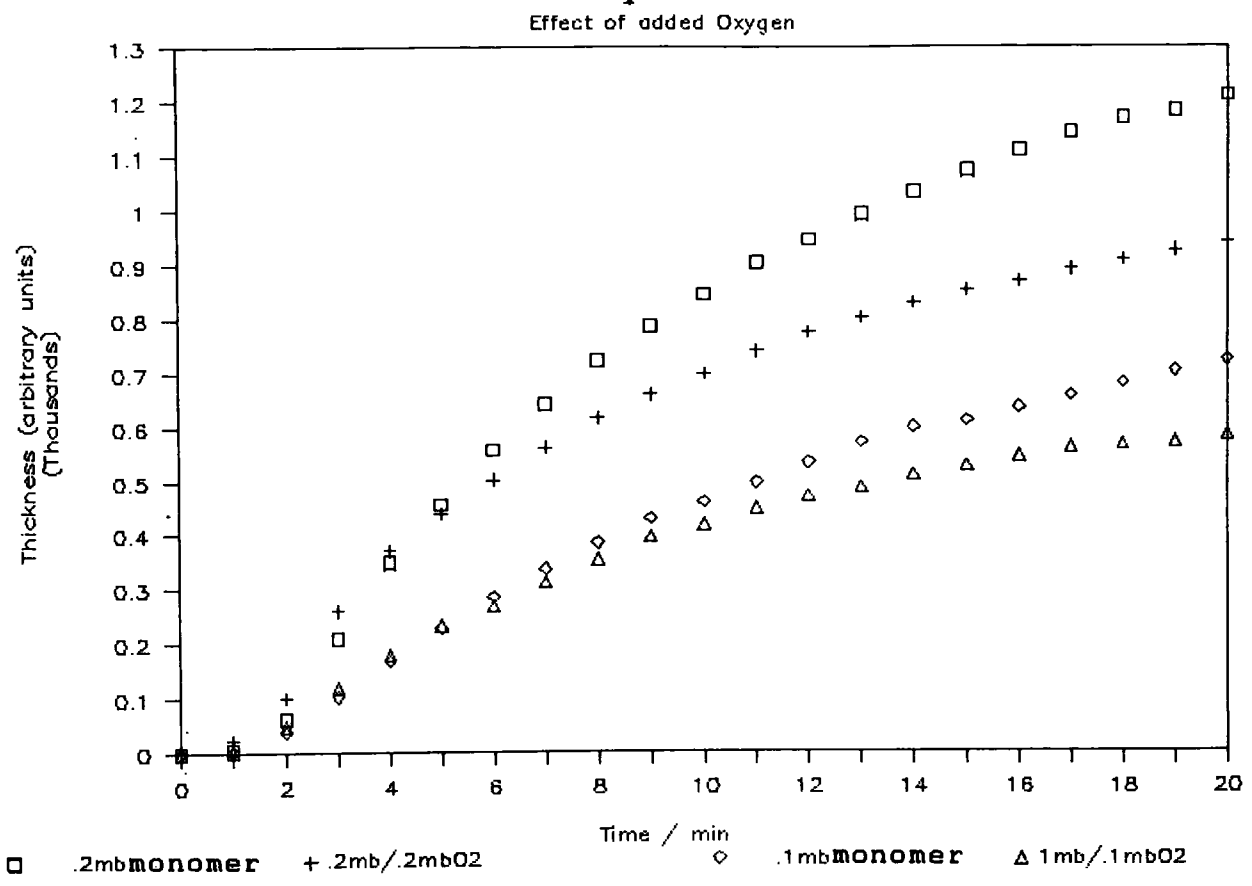

FIGURE 7.11 : Effect of Added Oxygen on the Deposition Rate

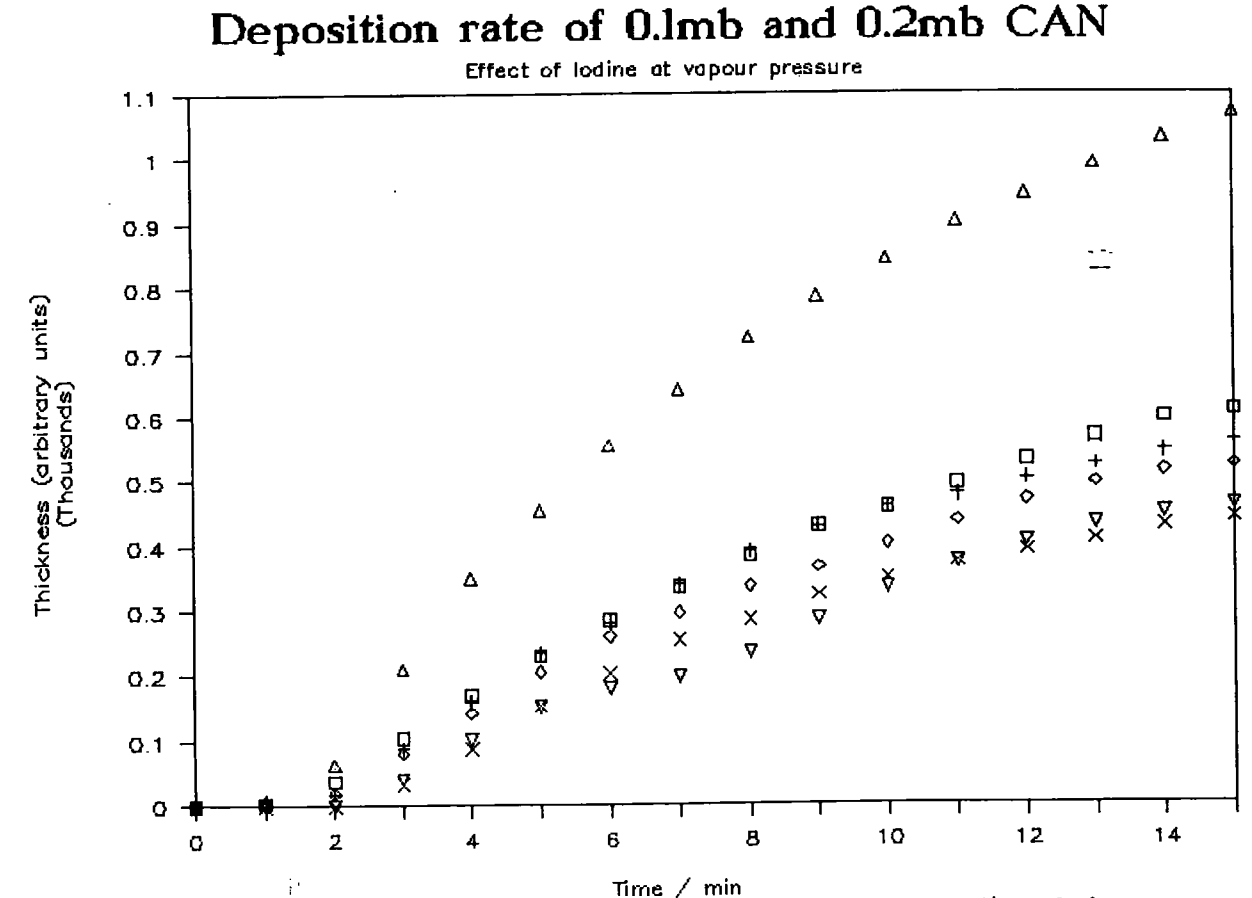

FIGURE 7.12 : Effect of Iodine on the Film Deposition Rate

0.2mb respectively) as well as both 0.1mb and 0.2mb of CAN vapour irradiated alone. These clearly show that the overall amount of film deposited over longer irradiation times (10-20 minutes) is less. Repeating the experiment consistently gave similar results. Since irradiation occurred above the vacuum ultraviolet threshold for oxygen photochemistry , it is possible to discount oxygen acting as a quencher of electronically excited states. This suggests that reaction probably occurs with free radicals formed in the film surface as it deposits, an idea subsequently reinforced by ESCA analysis of photopolymer deposited onto aluminium substrates irradiated under the same experimental conditions (see below), which confirmed that oxygen uptake by the photopolymer films had indeed taken place.

The above evidence reinforces the possible importance of free radicals in the photochemistry of chloroacrylonitrile surface photopolymerization as suggested by the iodine inhibition experiments reported in Chapter 5. Similar experiments using the crystal deposition monitor also exhibited inhibition - the results shown in Figure 7.12 indicating that the deposition rate for 0.2mb of CAN in the presence of iodine at vapour pressure is somewhat less than that of even 0.1mb of CAN vapour alone. Surprisingly, the plot also suggests a lower deposition rate for the 0.2mb CAN/I_2 system than for 0.1mb CAN/I_2, even though ESCA analysis showed complete coverage of the aluminium substrate in the former case whilst a large Al2p signal was observable for the latter. This was accounted for in a control experiment in the absence of monomer, which iodine molecules were found to be physically adsorped onto the surface of the exposed foil substrate, a process that must therefore occur during the inhibition

experiment as well as iodine species being chemically incorporated into the polymer. Deposition of large amounts of iodine in the short time period of the experiment would therefore cause the deposition monitor - which assumes a constant film density due to chloroacrylonitrile polymer alone - to give a higher reading than anticipated, since I_2 is a heavier molecule than the monomer. ESCA analyses of the two films formed supports this idea, since incomplete deposition for the 0.1mb CAN/I_2 system exhibited both an Al2p and a large I3d signal - ie an incomplete photopolymer overlayer together with a high presence of molecular iodine - whilst the 0.2mb CAN/I_2 experiment gave complete coverage of the substrate, with only a very low level of iodine incorporation, Table 7.1.

ELEMENT	Carbon	Chlorine	Nitrogen	Oxygen	Iodine
ATOMIC RATIOS	100	26	28	3	2

TABLE 7.1 Atomic Ratios - 0.2 mb CAN + Vapour Pressure of Iodine

Note that this latter result agrees with that found for a high flow rate of chloroacrylonitrile in the presence of I_2 found in Chapter 5 and previously thought to be possibly spurious. Thus, although inhibition of the photodeposition process does occur, it does not constitute complete suppression due to the large ratio of monomer to iodine molecules achieved in the gas phase. This contrasts sharply with the lower flow rate situations in which the the concentration of iodine molecules - and radicals - becomes sufficiently high to prevent photopolymerization taking place to any great extent, presumably by free radical recombination, either with potential depositing species in

the gas phase and/or with active radical sites on the surface of the growing film. Given a sufficient concentration of iodine radicals, and other (excited state) species, complete inhibition of film formation may be possible.

Transferring this knowledge to the plasma polymerization system, (Chapter 4) it can be seen that film deposition from chloroacrylonitrile outside the glow region - and hence in the absence of ions and free electrons - could therefore occur via free radical mechanisms when the concentration of iodine is sufficiently low. This contrasts with the case for allyl cyanide. Here, not only does the presence of I^- and/or I^{3-} ions in the plasma polymer films suggest the importance of ion chemistry in the deposition process, but also the absence of deposition outside the glow region for similar concentrations of monomer and iodine in the gas phase as for the CAN/I_2 system suggests either a) that the number of free radicals produced in the plasma is much lower for the former than the latter, resulting in complete quenching of any free radicals present by the iodine, or b) free radicals in the system do not deposit. Case (a) is felt to be more likely, although any such proof is outside the scope of this work. Whichever, the overall results for allyl cyanide plasma polymer suggest a minor role for free radical chemistry in the plasma polymerization process compared to ion chemistry, as opposed to the opposite suggested for chloroacrylonitrile.

Future work in this area should include a study of the surface photopolymerization of allyl cyanide in the gas phase, since the absence of any film deposition would reinforce the idea of the dominance of ion chemistry for this monomer.

III ESCA Analyses

Each experiment in the above series of experiments was repeated using an aluminium foil substrate placed immediately on top of the quartz crystal monitor to enable subsequent ESCA analyses of the deposited film to be carried out. The results for elemental stoichiometries compared to carbon are shown in Table 7.2 - 7.4. Looking at the results for CAN vapour irradiated alone, Table 7.2, it can be seen that an increase in pressure (and hence flow rate) results in an increase in chlorine content of the film, in accordance with the results in Chapter 5. The N:C ratio hardly changes throughout whilst - again as expected - the oxygen content drops with increasing flow rate, the minimal amount reflecting both the level of vacuum tightness achieved in the system and the lower ratio of oxygen to monomer at the higher operating pressures used. Moving the lamp to a position 8cm from the window on repeating the experiment - ie again decreasing the incident intensity by about 95% - increased both chlorine and nitrogen retention quite markedly, such that they were both very close to the 1:3 ratio with carbon expected from a conventional chain growth polymerization mechanism, though it was felt that this observation was a photon flux effect rather than a change of polymerization mechanism from the expected step growth anticipated at the lower pressures (< 0.3mb) used. However, such a phenomenon has been found to occur for higher pressures (>> 1 torr) of methyl methacrylate.[8] The C1s envelopes (not shown) reflect these stoichiometries, whilst the N1s spectra showed a higher proportion of nitrile to other environments at both higher power and lower photon flux.

Table 7.3 tabulates the results for the addition of nitrogen to the system, which appears to have no apparent effect on the nitrogen and oxygen content of the film formed. The Cl:C ratio increased above the 15-20% experimental error limit usually found; however, a lower chlorine content for 0.3mb than for only 0.1mb of added nitrogen, together with the similarity of the C1s and N1s envelopes, suggests that such error is in fact likely to be the cause, such that any effect of nitrogen on both chemical composition and/or deposition rate (as measured by film thickness) is believed to be unobservable with this apparatus.

Table 7.4 shows that, as expected, more oxygen incorporation into the polymer film occurs during the photodeposition process in the presence of O_2 in the photolysis chamber than can be accounted for by uptake from the atmosphere on transferring the film sample from apparatus to the ESCA spectrometer. Rather, incorporation occurs throughout the thickness of the film, probably as each "surface" of the depositing film - complete with active radical sites - reacts with oxygen species in the gas phase before itself being coated by further polymeric deposit. In contrast, on exposure of pure chloroacrylonitrile photo- and plasma polymer films (ie those deposited in the absence of any other gas, including oxygen) to the atmosphere only those free radicals which lie in the actual surface layers will be able to take up oxygen, hence limiting the amount of oxidation that might occur. This suggestion is borne out by a depth profiling study, which revealed an identical chemical composition - including oxygen content - throughout the film, which therefore appeared to be homogenous. One other interesting feature noted was that the

proportion of nitrile to other nitrogen environments, typically accounting for some 80-85% of the N1s envelope, was consistently somewhat less than the 90% plus observed for the organic vapour irradiated alone. Why the presence of oxygen might promote opening of the carbon-nitrogen triple bond is unknown.

					C1s Envelope				N1s Envelope	
PRESSURE of CAN	C	Cl	N	O	285.0	286.6	287.8	289.0	399.3	401.8
lamp next to window										
0.1 mb	100	18	26	3	31	58	11		88	12
0.2 mb	100	26	28	1	28	59	13		92	8
lamp moved 8cm from window										
0.1 mb	100	24	26	1	33	47	17	3	95	5
0.2 mb	100	34	31	2	27	58	14	1	94	6

TABLE 7.2 Elemental Stoichiometries Obtained from ESCA

P(CAN) in mb	$P(N_2)$ in mb	C	Cl	N	O	C1s Envelope 285.0	286.6	287.8	289.0	N1s Envelope 399.3	401.8
0.1	0.1	100	24	27	3	29	58	13		92	8
0.1	0.3	100	21	26	3	35	53	12		91	9
0.2	0.2	100	26	28	3	31	60	9		91	9

TABLE 7.3 Effect of Added Nitrogen

P(CAN)	$P(O_2)$					C1s Envelope				N1s Envelope	
in mb		C	Cl	N	O	285.0	286.6	287.8	289.0	399.3	401.8
0.1	0.1	100	30	33	12	24	43	18	15	82	18
0.1	0.1	100	29	25	17	20	46	19	15	85	15
0.1	0.3	100	25	36	18						
0.2	0.2	100	25	27	15	24	43	18	15	85	15
0.2	0.2	100	24	21	13						

TABLE 7.4 Effect of Added Oxygen

Conclusion

This work illustrates both the variety and apparent complexity of organic thin films deposited by plasma and photochemical techniques. The nature of the monomers - together with the power / photon flux, flow rate and, where appropriate, incident wavelength used are all shown to influence the respective film deposition rates and processes, together with the chemical composition (as determined by ESCA) of the polymers formed. For the monomers studied, the Yasuda parameter W/FM appears to influence the polymerization process qualitatively rather than quantitatively. This is especially true for the two structural isomers of C_4H_5N, allyl cyanide (CH_2=CH_2CHCN) and methacrylonitrile (CH_2=CMeCN), which - if Yasuda's parameter holds true - should exhibit identical behaviour with regard to deposition rates for the same experimental conditions, rather than the marked differences actually found for both these and the chemical composition of the plasma polymer films formed.

The effect of substrate position within the reactor chamber - whether plasma or photochemical - was also found to be of importance, whilst the addition of iodine or bromine to the system generally altered and/or inhibited the expected polymerization process, the resultant films exhibiting both physical and chemical halogen incorporation. Evidence was found in both the ultraviolet and ESCA spectra for the existence of I^- and/or I^{3-} ions in the plasma polymers of allyl cyanide and chloroacrylonitriele deposited in the presence of iodine vapour. Such a change in the chemical composition of the film can, in turn, alter its physical characteristics - for example plasma polymers of acrylonitrile are non-conducting insulators, whereas incorporation of iodine moieties into the deposited film is known to give rise to a small but detectable conductance (see chapter 4).

A comparison of the two deposition techniques shows that both similarities and some differences exist between them. Reference to the literature - already well documented for the area of gas phase photochemistry with respect to mechanistic data, much less so for plasmas - shows that such similarities are to be found at the molecular as well as the macroscopic level. In summary, the processes involved in plasma polymerization be therefore be explained in terms of the current knowledge of the photochemical processes involved in surface photopolymerization. Future photochemical literature should therefore increase our overall understanding of both polymerization systems. In addition, despite being a phenomenon that has been known to occur for over fifty years, and freely acknowledged as existing by more recent authors, a survey of the wealth of photochemical literature available at the time of writing showed few references to surface

photopolymerization, despite many of the steady-state gas-phase photolysis experiments reported utilising similar experimental conditions to those employed throughout this work. In particular, some workers observed that their results in the area of quantum yields, used in the determination of mechanistic pathways, were directly affected by the build-up of thin films on the windows of their apparati, which increasingly attenuated the intensity of the irradiation source as the experiments progressed with respect to time, and affecting the accuracy of the results obtained. It seems likely that such deposits might have actually occurred in the majority of such experiments carried out, rather than only in those reported. If true, the validity of a large amount of quantum yield and other data reported - especially in that literature where relatively long irradiation times are used - should accordingly be questioned. The thin films deposited are, of course, surface photopolymers. In view of this and the potential impact on the area of gas phase photochemistry as a whole, it seems surprising that the field has received little attention in the photochemical literature to date.

REFERENCES -- CHAPTER ONE

1. L. Tonks and I. Langmuir, Phys. Rev., 33, 195 (1929)

2. A.T. Bell, in "Techniques and Applications of Plasma Chemistry", J.R. Hollahan, A.T. Bell (Eds.), Wiley, N.Y. (1974), Chapter 1.

3. R. Carpenter and C. Till, Analyst (London), 109, 881 (1984)

4. F. Kaufman, in "Chemical Reactions in Electrical Discharges" R.F. Gould (Ed.), American Chem. Soc., Advances in Chemistry Series 80, Washington, D.C. (1969), Chapter 3.

5. W.L. Fite, in ref. 15, Chapter One.

6. J.M. Meek and J.D. Craggs (Eds.), "Electrical Breakdown of Gases", Wiley, Chichester (1978), Chapter One.

7. R.F. Gould, in ref. 15.

8. P. Brassem and F.J.M.J. Massen, Spectrochimica Acta, 29B, 203 (1974).

9. D.T. Clark and A.Dilks, "Characterization of Metal and Polymer Surfaces", Vol. 2, L.H. Lee (Ed.), Academic Press, N.Y. (1977).

10. D.T. Clark and A. Dilks, J.Polym.Sci, Polym.Chem.Ed, 18 1233 (1980).

11. C. Till, Ph.D. Thesis, Durham University, UK (1986).

12. e.g. a) B. Lipschultz, I. Hutchinson, B. La Bombord and A. Wan, J.Vac.Sci.Technol.B., 4, 1810 (1986); b) J. Felts and E. Lopata, ibid, 5, 347 (1987).

13. L. Martinu and H. Biederman, Plasma Chem. Plasma Processing, 5, 81 (1985).

14. a) S. Pang and S.R.J. Brueck, in "Laser Diagnostics and Photochemical Processing for Semiconductor Devices", R.M. Osgood, S.R.J. Bruesk and H.R. Schlossberg (Eds.), North-Holland, N.Y. (1983); b) P.J. Hargis, Jr. and M.J. Kushner, Appl.Phys.Lett., 40, 779 (1982).

15. a) H. Sakai, P.Hansen, M.Esplin, R. Johanseon, M. Peltola and J. Strong, Appl.Opt., 21, 228 (1982); b) H.U. Poll, D. Hinze and H. Schlemm, Appl.Spec., 36, 445 (1982).

16. D.E. Tevault and J.A. Rehrmann in Symp.Proc.Int. Symp.Plasma Chem 7th, C.J. Timmermans (Ed.), 2, 546 (1985).

17. R.R. Smardzewski and D.E. Tevault, ibid, 2, 651 (1985).

18. A. Dilks and E. Kay, Macromolecules, 14, 855 (1981).

19. a) S.K. Ritenkov, V.N. Srekov and C.A. Fedotov, Symp.Proc. Int.Symp.Plasma Chem 7th C.J. Tmmermans (Ed.), 2, 622 (1989) b) Z. Ondracek, Scr.Fac.Sci.Nat.Univ.Purkynianace Brun, 15, 173 (1985).

20. e.g. a) J. Loureiro and C.M. Ferreira, J.Phys.D.,Appl.Phys., 19, 17 (1986); b) J. Vlcek and V. Pelikan, ibid, 19, 1879 (1986).

21. F.K. McTaggart, "Plasma Chemistry in Electrical Discharges", Elsevier, Amsterdam (1967), Chapter One.

22. H. Suhr, "Applications of Non-equilibrium Plasma to Organic Chemistry", in ref. 3 and references therein.

23. a) N. Morosoff and H. Yasuda in "Plasma Polymerization", M. Shen and A.T. Bell (Eds.), ACS Symposium Series, 108, Washington D.C. (1979), Chapter Ten; b) N. Morosoff and H. Yasuda, ibid, Chapter 17.

24. Ref. 11, p15.

25. Ibid, p11.

26. D.T. Clark and D. Shuttleworth, J.Polym.Sci., Polym.Chem.Ed. 18, 27 (1980).

27. H. Suhr, Plasma Chem. Plasma Processing, 3, 1 (1983).

28. Ref. 11, p13.

29. a) C.I. Simonescu, F. Denes, Cellulose Chem. Technol., 14, 285 (1980); b) A.E. Pavloth and K.S. Lee, J.Macromol.Sci. Chem.A., 10, 579 (1976).

30. M.M. Millard and A.E. Pavlath, Text.Res.J., 42, 460 (1972).

31. M. Hudis in ref. 3, Chapter 3.

32. E. Kay in Conf.Proc.Int.Symp.Plasma Chem. 4th, S. Veprek and J.Hertz (Eds.), 1, 30 (1979).

33. E. Kay, J. Coburn and A. Dilks, Top.Curr.Chem. 1, 94 (1980).

34. J. Hertz, in ref. 32.

35. G. Turban and Y. Catherine, Actual.Chim. 59 (1981).

36. R. D'Agostino, F. Cramarossa, V. Colaprico and R.D'Ettole, J.Appl.Phys., 54, 1284 (1983).

37. D. D'Agostino, P. Capezzuto, G. Bruno, F. Cramarossa, Pure Appl.Chem., 57, 1287 (1985).

38. R.D'Agostino, Acta.Cient.Venez., 36, 19 (1985).

39. D.I. McBriar, Ph.D. Thesis, Durham University, UK, in press.

40. G. Legeay, F. Eppaillard and J.C. Brosse, Proc.Annu.Int.Conf Plasma Chem.Technol., 2nd, H.V. Boenig (Ed.), 29 (1984).

41. F. Arefi, J. Amoureux, F. Rouzbeki and M. Goldman, ibid, p1.

42. J.C. Boeda, M. De Mendez, G. Legeay and J.C. Brosse, Rev. Gen.Electr., 15, (1987).

43. Nitto Electric Industrial Co. Ltd, Japanese Patent 59 53,542 dated 28 Mar 1984.

44. H. Kasai, M. Kogoma, T. Moriwaka and S. Ozaki, J.Phys.D., Appl.Phys.Ed., 19, 1225 (1986).

45. H. Suhr, H. Schid, J. Uslar, D. Iacocca and H. Aguilar, Symp Proc.Int.Symp.Plasma Chem. 6th, M.I. Boulos and R.J. Munz (Eds.), 3, 657 (1983).

46. G. Dagli and N.H. Sung, Report 1983, AMMRC-TR-83-46, 66pp.

47. a) H.H. Madden and R.E. Alred, J.Vac.Sci.Technol.A., 4, 1705 (1986); b) J.B. Donnet, T.L. Dhami, S. Dang and M. Brendle, J.Appl.Phys.D., Appl.Phys.Ed., 20, 269 (1987). c) G. Dagli, Ph.D. Thesis, Tufts University, Medford, MA, USA, 1986.

48. G. Dagli and N.H. Sung, Polym. Mater.Sci., 56, 410 (1987).

49. H.K. Yasuda, Polym.Mater.Sci.Eng., 50, 135 (1984).

50. N. Morosoff, Sagamore Army Mater.Res.Conf.Proc. 30th, 471 (1983).

51. a) H.H. Beale, Ind.Res.Dev., 23, 135 (1981); b) H.S. Munro and C. Till, Thin Solid Films, 131, 255 (1985).

52. a) R.K. Sadhir, W.J. James, R.A. Auerbach, Thin Solid Films, 97, 17 (1982); b) R.K. Sadhir and W.J. James, Thin Solid Films, 242, 533 (1984).

53. E. Kay, M. Hecq, J.Appl.Phys., 55, 370 (1984).

54. E. Kay and M. Hecq, Adv.Low Temp.Plasma Chem. Technol.Appl. 1, 263 (1984).

55. L. Mertinu and L. Biederman, Symp.Proc.Int.Symp.Plasma Chem. 7th, C.J. Timmermans (Ed.), 4, 1313 (1985).

56. L. Martinu, H. Biederman, J. Zemek, Vacuum, 35, 171 (1985).

57. Ref. 55 p1318.

58. T. Yoneda, M. hori, H. Yamada, S. Morita, ibid, p1272.

59. L. Martinu, Thin Solid Films, 140, 307 (1986).

60. H. Biederman and L. Martinu, Acta.Phys.Slovaca, 35, 207 (1985).

61. L. Martinu and H. Biederman, Plasma Chem. Plasma Process. 5, 81 (1985).

62. E. Kay, A. Dilks, U. Hetzler, J.Macromol.Chem., A12, 1393 (1978).

63. R.K. Sadhir and H.E. Saunders, J.Vac.Sci.Technol.A., 3, 2093 (1985).

64. R.K. Sadhir, H.E. Saunders, W.J. James, ACS Symp.Ser., 242 555 (1984).

65. H. Suhr, A. Etspueler, E. Feurer, C. Oehr, Plasma.Chem. Plasma Process., 8, 9 (1988).

66. H.S. Munro and C. Till, J.Polym.Sci., Polym.Chem.Ed., 22, 3933 (1984).

67. H.S. Munro and J.G. Eaves, J.Polym.Sci., Polym.Chem.Ed, 23, 507, (1985).

68. N. Morosoff, R. Haque, S.D. Clymer and S. Crumbiis, J.Vac. Sci.Technol.A., 3, 2098 (1985).

69. H. Gruenwald, H. Suhr, H.S. Munro and C. Till, German Patent 3,522,817, dated 2 Jan 1987.

70. a) H. Biederman, L. Martinu, D. Slavinska, Pure.Appl.Chem., 60, 607 (1988); b) L. Martinu, Sol.Energy.Mater., 15, 21 (1987); c) Y. Osada, K. Yamada, I. Yoshiza, Thin Solid Films, 151, 71 (1987).

71. Ref. 11 p154.

72. H. Yasuda, Thin Film Processes, 361 (1978).

73. H. Yasuda, Contemp.Top.Polym.Sci., 3, 103 (1979).

74. H. Yasuda, Polym.Mater.Sci.Eng., 50, 135 (1984).

75. H. Yasuda, ACS Symp.Ser., 287, 89, (1985).

76. M. Shen and A.T. Bell, ACS Symp.Ser., 108, 1 (1978).

77. A.T. Bell, M. Shen, Org.Coat.Plast.Chem., 38, 550 (1978).

78. D. Shuttleworth, Macromol.Chem., 2, 7783 (1982).

79. E. Drauglis, R.F. Wielonski, F.A. Sliemers, Org.Coat.Appl. Polym.Sci.Proc., 447, 554 (1982).

80. N. Morosoff, Sagamore Army Meter.Res.Conf.Proc. 30th, 471 (1983).

81. R. D'Agostino, P. Cappezzuto, G. Bruno, F. Cramarossa, Pure.Appl.Chem., 57, 1287 (1985).

82. D.T. Clark, Org.Coat., 7, 113 (1984).

83. Y.S. Yeh, I.N. Shyy, H. Yasuda, Polym.Mater.Sci., 56, 141 (1987).

84. H. Biedernan, Vacuum, 37, 367 (1987).

85. H.V. Boenig, Encycl.Polym.Sci.Eng., 11, 248 (1987).

86. H. Yasuda, M. Gazicki, Biomaterials, 3, 68 (1982).

87. H.V. Boenig, Pure.Appl.Chem., 57, 1277 (1985).

88. H.V. Boenig, in Proc.Annu.Int.Conf.Plasma.Chem. Technol. 1st, H.V. Boenig (Ed.), 55, (1982).

89. A. Dilks and E. Kay, Macromolecules, 14, 855 (1981).

90. A. Dilks, S. Kaplan, A. Van Laekan, J.Polym.Sci.Polym., Chem.Ed., 19, 2987 (1981).

91. S. Kaplan and A. Dilks, Thin Solid Films, 84, 419 (1981).

92. E. Kay, Polm.Prep.Am.Chem.Soc., Div.Polym.Chem., 21, 64 (1980).

93. U. Carmi, I. Inspektor, R. Auni, Plasma.Chem.Plasma.Process. 1, 233 (1981).

94. N. Hozumi, T. takao, Y. Kasama, Y. Ohki, Jpn.J.Appl.Phys., Part 1, 22, 636 (1983).

95. D.R. McKenzie, R.C. Mcpherson, N. Savvides, D.J.H. Cockayne, Thin Solid Films, 108, 247 (1983).

96. J. Kammermaier, G. Rittmayer, R. Schulte, Thin Solid Films, 2, 547 (1983).

97. K. Kobayashi, N. Matsukara, Y. Machi, Thin Solid Films, 158, 233 (1988).

98. L.L. Miller, A. Szabo, S. Bezuki, M. Tokuda, Conf.Proc.Int. Symp.Plasma.Chem. 4th, 2, 396 (1979).

99. M.Y. Boluk, G. Akovali, Polym.Eng.Sci., 21, 664 (1981).

100. K. Ohno, N. Ishii, J. Sohma, Jpn.J.Appl.Phys. Part 1, 22, 996, (1983).

101. S. Kaplan, A. Dilks, J.Polym.Sci., Polym.Chem.Ed., 21, 1819 (1983).

102. Y. Takai, T. Mitzutami, M. Ieda, Jpn.J.Appl.Phys., Part 1, 26, 812 (1987).

103. Z. Sanche, M. Urrutia, H.P Schrieber, M.R. Wertheimer, J.Appl.Polym.Sci., Appl.Polym.Symp., 42, 305 (1987).

104. N. Inagaki, J. Ohkubo, J.Membr.Sci., 27, 63 (1986).

105. Y.S. Yeh, I.N. Shyy, H. Yasuda, J.Appl.Polym.Sci., Appl. Polym.Symp., 1, 42 (1987).

106. R. Claude, M. Moisan, M.R. Wertheimer, Z. Zakrzewski, Polym. Mater.Sci.Eng., 56, 134 (1987).

107. For effect of frequency on discharges see : a) S. Morita, S. Ishibashi, M. Shen, A.T. Bell, ACS Symp.Ser., 121, 321 (1980); b) R. Claude, M.Moisan, M.R. Wertheimer, Z. Zakrewski, ApplPhys.Lett, 50, 1797, 1987.

108. H. Yasuda, T. Hirotsu, J.Polym.Sci., Polym.Chem.Ed., 16, 229, (1978).

109. Ref. 11, Chapter 3, and references therein.

110. N. Morosoff, W. Newton, H. Yasuda, J.Vac.Sci.Technol., 15, 1815 (1978).

111. R.J. Buss, Mater.Res.Soc.Symp.Proc., 68, 453 (1986).

112. M.Ohno, K.Ohno, J.Sohma, J.Polym.Sci., Polym.Chem.Ed., 25 1773 (1987).

113. W.R. Gomboltz, A.S. Hoffman, J.Appl.polym.Sci., Appl.Polym. Symp., 42, 285 (1987).

114. S.H. Kim, H.K. Xie, K.C. Kao, J.Appl.Polym.Sci., 32, 5543 (1986).

115. P.V. Hinman, A.T. Bell, M. Shen, J.Appl.Polym.Sci., 23, 3651 (1979).

116. R. Hernandez, A.F. Diaz, R. Waltman, J. Bargon, J.Phys.Chem. 88, 3353 (1984).

117. H. Yasuda, T. Hirotsu, J. Appl.Polym.Sci., 21, 3139 (1977).

118. H. Yasuda, T. Hirotsu, ibid, 22w, 1195 (1978).

119. A. Morinaka, Y. Asano, ibid, 27, 2139 (1982).

120. S. Ivanov, Eur.Polym.J., 20, 415 (1984).

121. H.S. Munro, H. Gruenwald, J.Polym.Sci., Polm.Chem.Ed., 23, 479)1985).

122. T. Hirotsu, J.Macromol.Sci., A15, 633 (1981).

123. J.H. Dully, F.J. Wodarczyk, J.J. Ratto, J.Polym.Sci., Polym.Chem.Ed., 25, 1187 (1987).

124. R.J. Ward, Ph.D. Thesis, Durham University, UK, 1989.

125. T. Masuoka, H. Yasuda, N. Morosoff, Polym.Prepr., Am.Chem. Soc., Div.Polym.Chem., 19, 498, (1978).

126. H. Yasuda, T. Masuoka, J.Polym.Sci., Polym.Chem.Ed., 20, 2633 (1982).

127. N. Inagaki, K. Kimura, T. Minamidani, K. Katsuura, J.Polym. Sci., Polym.Chem.Ed., 20, 2303, 2982.

128. N. inagaki, K. Katsuura, J.Macromol.Sci.Chem. A18, 661 (1982).

129. R. D'Agostino, F.Cramarossa, V.Colaprico, R. D'Ettole, Eur. J.Polym.Sci., 15, 265 (1979).

130. J. Kammermaier, G. Rittmayer, R. Schulte, Symp.Proc.Int. Symp.Plasma.Chem. 6th, 2, 547, 1983.

131. N. Inagaki, H. Kawai, J.Polym.Sci., Polym.Chem.Ed., 24, 3381 (1986).

132. R. D'Agostino, Polym.Mater.Sci.Eng., 56, 221 (1987).

133. a) D.T. Clark, D. Shuttleworth, Eur.Polym.J., 15, 265 (1979)
b) A. Dilks, E. Kay, Macromolecules, 14, 855 (1981)
c) N Inagaki, D Tsutsumi, Polym.Bull(Berlin) 16, 131 (1986).

134. a) K. Nakajima, A.T. Bell, M. Shen, M. Millard, J.Appl.Polym Sci., 23, 2627 (1979); b) K. Hozumi, K. Kitamura, T. Kitade, Bull.Chem.Soc.Jpn., 54, 1392 (1981); c) T. Masuaoka H. Yasuda, J.Poloym.Sci., Polym.Chem.Ed., 19, 2937 (1981); d) K. Yanagihara, H. Yasuda, J.Polym.Sci., Polym.Chem.Ed., 20, 1833 (1982); e) B.D. Washo, Proc.Annu.Int.Conf.Plasma. Chem.Technol. 1st, 131 (1982); f) Y. Ohki, T. Nakano, K. Yahagi, Symp.Proc.Int.Symp.Plasma.Chem. 7th, 4, 1313 (1985).

135. See ref. 11 p i.

136. a) E. Kay, J. Coburn, A. Dilks, Top.Curr.Chem. 94, 1 (1980) b) E. Kay, Conf.Proc.Int.Symp.Plasma.Chem. 4th, 2, 396 (1979); c) M.R. Pender, M. Shen, A.T. Bell, M. Millard, ACS Symp.Ser., 108, 147 (1978); d) N. Inagaki, Proc.Annu.Conf. Plasma.Chem.Technol. 2nd, 51 (1984).

137. J. Goodman, J.Polym.Sci., Lett.Ed., 44, 551 (1960).

138. H. Yasuda and T. Tsu, Surf.Sci., 26, 232 (1976).

139. H. Yasuda 'Plasma Polymerization' Academic Press N.Y. (1985)

140. E. Kay, Invited Paper, Int.Round.Table.Plasma.Polym.Treat., IUPAC.Symp.Plasma.Chem. (1977).

141. D. Shuttleworth, Ph.D. Thesis, University of Durham, UK (1978) and references therein.

142. Ref. 11 p10.

143. R. Dressler, M. Allan, E. Haselbach, Chimia, 39, 385 (1985).

144. M. Heni, I. Illenberger, J.Electron.Spectrosc.Relat.Phenom., 41, 453 (1986).

145. M. Heni, I. Illenberger, Int.J.Mass.Spectrom.Ion.Processes, 73, 127 (1986).

146. H.S. Munro, Polym.Mater.Sci.Eng., 56, 318 (1987).

147. C. Sandorfy, Top.Curr.Chem., 8, 86 (1987).

148. H. Yasuda, C.R. Wang, J.Polym.Sci., Polym.Chem.Ed., 23, 87 (1987).

149. H. Yasuda, T. Hsu, Surf.Sci., 76, 232 (1978).

150. H. Kobayashi, M. Shen and A.T. Bell, J.Macromol.Sci., Chem, 8, 373 (1974).

151. Ref. 11 Chapter 7.

152. eg a) S. Kadifachi, Chem.Phys.Lett., 108, 233 (1984); b) D.A. Dixon, T. Fukunaga, B.E. Smart, J.Am.Chem.Soc., 108 1585 (1986).

REFERENCES - CHAPTER TWO

1. K. Yanagihara, M. Kimura, K. Numata and M. Niinomi, Polym. Mater.Sci.Eng., 56, 415 (1987).

2. H. Yasuda, Org.Coat.Appl.Poly,.Sci.Proc., 47, 434 (1982).

3. D.T. Clark and M. Abushak, J.Polym.Sci., Polym.Chem.Ed., 21, 907 (1983).

4. A. Bradley, J.P. Hanimes, J.Electrochem.Soc., 110, 15 (1963)

5. a) D. Shuttleworth, Ph.D. Thesis, University of Durham, UK (1978); b) C. Till Ph.D. Thesis, University of Durham, UK (1986).

6. H. Yasuda, "Plasma Polymerization", Academic Press, London (1985).

7. a) Agency of Industrial Sciences and Technology, Japanese Patent, 99,325 (1983); b) J. Sakata, M. Hirai, M. Yamamoto, J.Appl.Polym.Sci., 34, 2701 (1987).

8. H. Yotsui and T. Nishimoto, Japanese Patent, 287,421 (1986).

9. Y.S. Yeh, Y. Iriyama, Y. Matsuzawa and H. Yasuda, Polym. Mater.Sci.Eng., 56, 715 (1987).

10. R.K. Sadhir, H.E. Saunders, Proc.Electr.Electron Insul.Conf. 17th, 282 (1985).

11. H.S. Munro and H. Gruenwald, J.Polym.Sci., Polym.Chem.Ed., 23, 479 (1985) and references therein.

12. M. Hudlicky, "Chemistry of Organic Fluorine Compounds - A Laboratory Manual", John Wiley and Sons, New York, 2nd edition (1976) and references therein.

13. a) N. Kogoma, T. Moriwaki and S. Ozaki, Proc.Int.Ion.Eng. Cong., 3, 1499 (1983); b) G. legeay, J.J. Rousseau and J.C. Brosse, Eur.Polym.J., 21, 1 (1985); c) J.A. Thornton, Thin Solid Films, 107, 3 (1983); d) H. Yasuda, J.Membr.Sci. 18, 273 (1984); e) M. Gazicki and H. Yasuda, Plasma Chem. plasma Process., 3, 279 (1983).

14. a) D.T. Clark and D. Shuttleworth, J.Polym.Sci., Polym.Chem. Ed., 18, 27 (1980); b) D.T. Clark and M.Z. AbRahman, ibid, 19, 2129 (1981); c) D.T. Clark and M.Z. AbRahman, ibid, 20, 1717, 1729 (1982); d) D.T. Clark and M.Z. AbRahman, ibid, 21, 2907 (1983).

15. D. Shuttleworth, Ph.D. Thesis, University of Durham, Uk (1978) and references therein.

16. a)D.T. Clark and D. Shuttleworth, J.Polym.Sci., Polym.Chem. Ed., 16, 1093 (1978); b) D.T. Clark and D. Shuttleworth, ibid, 17, 1317 (1979).

17. D.T. Clark in "Polymer Surfaces", D.T. Clark and W.J. Feast (Eds.), Wiley, London (1978).

18. M.Z. AbRahman, Ph.D. Thesis, University of Durham, UK (1981)

19. D.T. Clark, H.R. Thomas, D. Shuttleworth and A. Dilks, J.Electron.Spectrosc.Relat,Phenom., 10, 455 (1977).

20. A. Dilks in "Photon, Electron and Ion Probes", Dwight, Fabish and Thomas (Eds.), ACS, New York (1981).

21. D.A. Dixon, T. Fukunaga and B.E. Smart, J.Am.Chem.Soc., 108, 1585 (1986).

22. See Chapter 4.

23. A.N. Wright, Nature, 215, 935 (1967) and references therein.

24. R. Dressler, M. Allan E. Hasselbach, Chimia, 39, 385 (1985).

25. a) C. Sandorfy, topp.Curr.Chem., 8, 86 (1987); b) M. Heni and I. Illenberger, Int.J.Mass.Spectrom.Ion.Processes, 73, 127 (1986).

REFERENCES - CHAPTER THREE

1. H. Yasuda, "Plasma Polymerization", Academic Press, London (1985).

2. T. Hirai and O. Nakada, Jap.J.Appl.Phys, 7, 112 (1968).

3. H. Yasuda and T. Hirotsu, J.Appl.Polym.Sci., 21, 3167 (1977)

4. K. Doblhofer and W. Durr, J.Electrochem.Soc., 125, 1041 (1980).

5. A. Bradley, J.Electrochem.Soc., 119, 1153 (1972).

6. H.S. Munro and H. Grunwald, J.Polym.Sci., Polym.Chem.Ed., 23, 479 (1985).

7. A.E. Laird and J.K. Taylor, J.Chem.Soc., Chem.Comm., 335 (1978).

8. C.D. Wagner, W.M. Riggs, L.E. Davis, J.F. Moulder and G.E. Muilenberg, Perkin Elmer, Minnesota (1979).

9. R. Dressler, M. Allan, E. Haselbach, Chimia, 39, 385 (1985).

10. C. Sandorfy, Top.Curr.Chem., 8, 86 (1987).

11. H. Okabe, J.CHem.Phys., 75, 2772 (1981).

13. G.D. Willett and T. baer, J.Am.Chem.Soc., 102, 6774 (1980).

REFERENCES -- CHAPTER FOUR

1. a) U. Carmi, A. Inspektor and R. Avni, Plasma Chem. Plasma Process, 1, 233 (1981); b) Japan Synthetic Rubber Co. Ltd, Japanese Patent 81 47,403 (1981); c) M. Miinomi and K. Yanagihara, UK Patent 2,023,152 (1979); d) R.F. Wielonski and H.E. Beale, Eur.Pat. 25,772 (1981).

2. C. Till, Ph.D. Thesis, University of Durham, UK (1986).

3. H.S. Munro and H. Gruenwald, Unpublished Data.

4. J.H. Dully, F.J. Wodarczyk and J.J. Ralto, J.Polym.Sci., Polym.Chem.Ed., 25, 1187 (1987).

5. R.J. Ward, Ph.D. Thesis, University of Durham, UK (1989).

6. B. Ranby and J.F. Rabek, "Photodegradation, Photooxidation and photostabilization of Polymers", Wiley-Interscience, London (975).

7. W.R. Gomboltz and A.S. Hoffman, ACS Polym.Mater.Sci.Eng., 56 720 (1987).

8. a) D. Shuttleworth, Ph.D. Thesis, University of Durham, UK (1978); b) D.T. Clark, D. Shuttleworth, J.Polym.Sci.Polym. Chem.Ed., 16, 1093 (1978); c) op.cit., 17, 1317 (1979).

9. H. Yasuda, "Plasma Polymerization", Academic Press, London (1985).

10. C. Sandorfy, Top.Curr.Chem., 8, 86 (1987).

11. A.I. Popov and R.F. Swenson, J.Am.Chem.Soc., 77, 3724 (1955).

12. G. Herzberg, "Spectra of Diatomic Molecules", 2nd edition, D. Van Nostrand Co., Princeton, N.J. (1950).

13. H. Yasuda and T. Hirotsu, J.Polym.Sci., Polym.Chem.Ed., 16, 743 (1976).

14. Y. Haque and B.D. Ratner, J.Polym.Sci., Polym.Phys.Ed., 26, 1237 (1988).

15. D.T. Clark and A. Dilks, J.Polym.Sci., Polym.Chem.Ed., 18, 1233 (1980).

REFERENCES - CHAPTER FIVE

1. D.O. Cowan and R.L. Drisko, "Elements of Organic Photo-Chemistry", Plenum Press, N.Y. (1976).

2. H.W. Melville, Proc.Roy.Soc.A., 163, 511 (1937).

3. G. Gee, Trans.Faraday.Soc., 43, 712 (1938).

4. a) R. Srinivasan, J.Am.Chem.Soc., 82, 5063 (1960).
   b) I. Haller and R. Srinivasan, J.Chem.Phys.Soc., 40, 1992 (1964).

5. A.N. Wright, Postprints of Soc.Plast.Eng.Regional.Tech.Conf. Ellensville, New York (1967), p110.

6. L.V. Gregor and H.L. McGee, Proc.Fifth.Annu.Electr.Beam Symp., (Alloyd Corp.), Cambridge Press, Mass. (1963), p211.

7. A.N. Wright, Nature, 215, 935 (1967).

8. a) J.E. Wilson, and W.A. Noyes Jr., J.Am.Chem.Soc., 63, 3025 (1941); b) H.R. Ward and U. Wishnok, J.Am.Chem.Soc., 90, 5333 (1968).

9. C. Till, Ph.D. Thesis, University of Durham, UK (1986).

10. R.J. Ward, Ph.D. Thesis, University of Durham, UK (1989).

11. A. Christopher and A.N. Wright, J.Appl.Polym.Sci., 16, 1057 (1972).

12. A.N. Wright in "Polymer Surfaces", D.T. Clark and W.J. Feast (Eds.), Wiley Interscience, London (1978).

13. T.A. Galantowicz and W.R. Fenner, J.Vac.Sci.Technol.A., 1, 534 (1983).

14. J.R. Swanson, C.M. Friend and Y.J. Chabal, J.Chem.Phys., 87, 5028 (1987).

15. M. Toyama, H. Itch and T. Moriya, Jap.J.Appl.Phys., 25, 688 (1986).

16. R.R. Krachnavek, H.H. Gilgen, J.C. Chen, P.S. Shaw, T.J. Licata and R.M. Osgood, J.Vac.Sci.Technol.B., 5, 20 (1987).

17. C.O. Kunz, P.C. Long and A.N. Wright, Polym.Eng.Sci., 12, 209 (1972).

18. a) D.T. Clark and D. Shuttleworth, J.Polym.Sci., Polym.Chem. Ed., 16, 1093 (1978);
    b) D.T. Clark and D. Shuttleworth, ibid, 17, 1317 (1979).

19. H.S. Munro and C. Till, J.Polym.Sci., Polym.Chem.Ed., 26, 2873 (1988).

20. J. Haigh, M.R. Aylett, Prog.Quantum.Electron, 12, 1 (1988).

21. A.N. Wright, U.S. patent, 3,677,800 (1972).

22. J.G. Calvert and J.N. Pitts Jr., "Photochemistry", John Wiley and Sons, N.Y., (1966).

23. D.T. Clark and A. Dilks, J.Polym.Sci., Polym.Chem.Ed., 18, 1233 (198).

24. J.A.R. Samson in "Techniques of Vaccum Ultraviolet Spectroscopy", Wiley, N.Y. (1967), Chapter 5.

25. J.A.R. Samson, ibid, Chapter 6.

26. J.Y. Tsao and D.J. Ehrlich, Appl.Phys.lett., 42, 997 (1983).

27. W. Hack and W. Langel, J.Phys.Chem., 87, 3462 (1983).

28. J. Pola, V. Chvalovsky, E.A. Volnina and L.E. Guselnikov, J.Organomet.Chem., C13, 341 (1988).

29. D.J. Ehrlich, R.M. Osgood and T.F. Deutsch, J.Vac.Sci. Techno., 21, 23 (1982).

30. a) J.Y. Tsao and D.J. Ehrlich, in Mater.Res.Soc.Symp.Proc., 29(Laser.Controlled.Chem.Process.Surf.), 115 (1984).
b) D.G. Eden, K.K. King, E.A.P. Cheng, S.A. Piette, and D.B. Geohegan, Proc.SPIE.Int.Soc.Opt.Eng., 710 (Excimer Lasers Opt.), 43 (1987).

31. R. Solanki, in AIP Conf.Proc., 160 (Adv.Laser.Sci.2), 594 (1987).

32. M.P. Irion and K.L. Kompa, Appl.Phys.Part.B, B27, 183 (1982)

33. R.S. Becker and J.H. Hong, J.Phys.Chem, 87, 163 (1983).

34. J.B. Halpern, L. Petway, R. Lu, W.M. Jackson, V.R. McCrary, Report TR-27 (1987), Order No. AD-A183597, Avail. NTIS.

35. R.D. Kenner, H.K. Haak and F. Stuhl, J.Chem.Phys., 85, 1915 (1986).

37. C.H.J. Wells, "Introduction to Molecualr Photochemistry", Chapman and Hall, London (1972).

38. Y. Mori, N. Nakashima and K. Yoshihari, J.Chem.Phys. 83, 117 (1985).

39. N. Shimo, N. Nakashima, N. Ikeda and K. Yoshihara, J.Photochem., 33, 279 (1986).

40. M.C. Sauer Jr., L.M. Dortman, J.Chem.Phys., 35, 497 (1961).

41. H. Okabe and J.R. McNesby, J.Chem.Phys., 36, 601 (1962).

42. L.C. Jones Jr. and L.W. Taylor, Anal.Chem., 27, 228 (1955).

43. A.J. Merer and R.S. Mulliken, Chem.Rev., 69, 369 (1969).

44. Ref. 22 p504.

45. Ibid., p494.

46. G. Belanger and C. Sandorfy, J.Chem.Phys., 55, 2055 (1971).

47. M.B. Robin, R.R. Hart and N.A. Kuebler, J.CHem.Phys., 44, 1803 (1966).

48. A.W. Kirk and E. Tschuikow-Roux, J.Chem.Phys., 53, 1924 (1970).

49. W.A. Guillory and G.H. Andrews, J.Chem.Phys., 62, 3208, 4667 (1975).

50. C.R. Quick Jr. and C. Wittig, Chem.Phys., 32, 75 (1978).

51. M.J. Berry and G.C. Pimentel, J.Chem.Phys., 53, 3453 (1970).

52. a) O.P. Strausz, R.J. Norstrum, D. Salahub, R.K. Gosaki, H.E. Gunning and I.G. Csizmadio, J.Am.Chem.Soc., 92, 6392 (1970); b) R.J. Nostrum, H.E. Gunning and O.P Strausz, ibid 98, 1690 (1976).

53. E.R. Sirkin G.C. Pimentel, J.Phys.Chem., 88, 1833 (1984).

54. B. Atkinson, Nature, 163, 291 (1949).

55. See E.V. Wilkins and A.N. Wright, J.Polym.Sci., Polym.Chem. Ed., 9, 2071 (1971) and references therein.

56. B. Atkinson, Experimentia, 14, 272 (1958).

57. J.W. Vogh, US Patent 3,228,865, Jan11 (1966).

58. F. Gozzo and G. Cammaggi, Tetrahedron, 22, 2181 (1966).

59. a) S. Koda, Chem.Lett., 1, 57 (1980).
b) S. Koda, Chem.Phys.Lett., 69, 574 (1980).

60. I. Haller, and R. Srinivasan, J.Chem.Phys., 40, 1922 (1964).

61. W. Kemula E.M. Rauchfleisch, Rocniki.Chem., 26, 221 (1952).

62. H. Yasuda, "Plasma Polymerization", Academic Press, London (1985).

63. A. Gandini and P.A. Hackett, Can.J.Chem., 56, 2096 (1978) and referneces therein.

64. S. Kubota and Y. Udagawa, Chem.Lett., 7, 901 (1980).

65. J.P. Simons, "Photochemistry and Spectroscopy", Wiley Interscience, London (1971).

66. P.A. Mullen and M.K. Orloff, Thoer.Chim.Acta, 23, 278 (1971)

67. A. Fahr and A.H. Laufer, J.Phys.Chem., 89, 2906 (1985).

68. H. Okabe and V.H. Dibbeler, J.Phys.Chem., 59, 2430 (1973).

69. a) H. Hiraoka and W. Lee, Macromolecules, 11, 622 (1978)
b) H.S. Munro, unpublished data.

70. a) K. Nakatsuka and M. Koizumi, J.Institute.Poly.Osaka.City Univ., 4C, 211 (1953).
b) M. Koizumi, N. Makatsuka and S. Kato, Bull.Chem.Soc.Jpn., 27, 185 (1954).

71. A.B. Callear, R.J. Cvetanovic, J.Chem.Phys. 24, 873 (1956).

72. Ref. 22 p99.

REFERENCES - CHAPTER SIX

1. See Appendix 1.

2. M.F.R. Mulcahy, "Gas Kinetics", Thomas Nelson & Sons, London (1973).

3. R.J. Ward, Ph.D. Thesis, University of Durham, UK (1989).

4. J.Y. Tsao and D.J. Ehrlich, Appl.Phys.lett., 42, 997 (1983).

5. M.P. Irion and K.L. Kompa, Appl.Phys.Part.B, B27, 183 (1982)

6. R.S. Becker and J.H. Hong, J.Phys.Chem, 87, 163 (1983).

REFERENCES - CHAPTER SEVEN

1. H. Yasuda, "Plasma Polymerization", Academic Press, London (1985).

2. C. Till, Ph.D. Thesis, University of Durham, UK (1986).

3. J.G. Calvert and J.N. Pitts Jr., John Wiley & Sons, New York (1966).

4. K. Nakatsuka and M. Koizumi, J.Institut.Poly.Osaka City Univ., 4C, 211 (1953).

5. M. Koizumi, K. Nakatsuka and S. Kato, Bull.Chem.Soc.Jpn., 27, 185 (1954).

6. A.B. Callear, R.J. Cvetanovic, J.Chem.Phys., 24, 873 (1956).

7. J.P. Simons, Photochemistry and Spectroscopy", Willey-Interscience, London (1971).

8. R.J. Ward, Ph.D. Thesis, University of Durham, UK (1989).

APPENDIX ONE

Calculation of Atomic Ratios From XPS Data

If the sampling depth seen by the spectrometer is infinitely thick, atomic ratios can be calculated according to rhe formula :

No. of atoms of element X per 100 C atoms

$$= A(X)/A(C1s) \times sf(X)/sf(C1s)$$

where A(X) = area under the core level spectrum of element X

A(C1s) = " " " " " " " Carbon 1s

sf(X) = sensitivity factor for element X

sf(C1s) = " " " Carbon 1s

Sensitivity factors used throughout this work are : C1s = 1.0; C12p = 0.41; N1s = 0.78; O1s = 0.56; I3d$_{5/2}$ = 0.112; Br3d = 0.28.

In those cases where the sampling depth of the X-rays exceeds that of the sample under study (such that a signal due to the aluminium substrate can be seen) some of the C1s signal detected is due to hydrocarbon contamination on the substrate surface. Similarly the O1s core level spectrum will partly reflect the oxygen present in the protective aluminium oxide layer of the substrate. This problem can largely be overcome by measuring the integrated areas for the C1s and Al2p spectra. Equations 1 and 2 below can then be used to estimate i) the depth, d, of the film on the substrate; ii) the integrated area for the theoretical C1s spectrum of the sample assuming an infinitely thickk sampling depth; iii) the expected integrated area for a polymer layer d $\AA$ thick (via equation 3). The values obtained enable approximate elemental atomic ratios to be calcuated in the normal way.

$$IAl = I^{\infty}_{Al} \exp(-d/\lambda \cos\theta), \quad \text{where } \theta = \text{take off angle} \qquad (1)$$

$$IC1s = I^{\infty}_{Al,C1s} \exp(-d/\lambda \cos\theta) + I^{\infty}_{C1s,Polymer} (1 - \exp(-d/\lambda \cos\theta)) \qquad (2)$$

Now, (1) $\Rightarrow$ $IAl / I^{\infty}_{Al} = \exp(-d/\lambda \cos\theta) \Rightarrow d = \lambda \cos\theta \ln(IAl/I^{\infty}_{Al})$

Substituting into (2) for d gives $I^{\infty}_{C1s,polymer}$, which can in turn be substituted into (3) to give I'_{C1s}, the expected integrated area for a polymer layer d $\mathring{A}$ thick :

$$I'_{C1s} = IC1s \ (1 - \exp(-d/\lambda \cos\theta) \qquad (3)$$

NOTATION :

IAl	=	integral of Al2p signal in polymer spectrum
I^{∞}_{Al}	=	" " " " " Al substrate "
$IC1s$	=	" " C1s " " polymer " *
$I^{\infty}_{C1s,Polymer}$	=	" " " " " polymer " **
$I^{\infty}_{Al,C1s}$	=	" " " " " Al substrate "
I'_{C1s}	=	" " " " " polymer d $\mathring{A}$ thick

* i.e. the integral actually observed in the C1s spectrum

** i.e. the integral that would have been observed if the polymer sample had been infinitely thick with respect to the incident X-rays

d = total thickness of polymer in $\mathring{A}$

λ = mean free path (NB: different for each element)

REFERENCES :

1. H.R. Thomas. PhD Thesis. University of Durham. UK. (1973)

APPENDIX TWO

The sensitivity factor of element X, relative to carbon C, can be calculated from the formula :

$$\frac{X}{C} = \frac{\sigma_x^*}{\sigma_c^*} \frac{KE^{1.5}}{KE^{1.5}}$$

where

σ^* is the corrected photoionisation cross section and KE is the kinetic energy of the photoelectron.

σ^* can be calculated from

$$\sigma^* = \sigma / 4\pi [1 - \beta /2(3/2\cos^2 \theta - 1/2)]$$

σ = photoionisation cross section

β = an asymmetry parameter of the core level

θ = the angle between photon source and analyser (the "take off" angle).

Both σ and β have tabulated values which can be found in :

J.Electron.Spec.Related Phenom., 8, 129 (1976)

ibid 8, 389 (1976)

APPENDIX THREE

The Board of Studies in Chemistry requires that each postgraduate research thesis contains an appendix listing :

(A) All research colloquia, seminars and lectures arranged by the Department of Chemistry and by Durham University Chemical Society during the period of the author's residence as a postgraduate student;

(B) All research conferences attended and papers presented by the author during the period when research for the thesis was carried out;

(C) Details of the postgraduate induction course.

UNIVERSITY OF DURHAM

Board of Studies in Chemistry

COLLOQUIA, LECTURES AND SEMINARS GIVEN BY INVITED SPEAKERS 1ST OCTOBER 1985 TO 30TH JUNE 1986

BARNARD, Dr.C.J.F. (Johnson Matthey Group Research) 20th February 1986
Platinum Anti-Cancer Drug Development - Serendipity to Science

BROWN. Dr. J.M. (University of Oxford) 12th March 1986
Chelate Control in Homogeneous Catalysis

CLARK, Dr. B.A.J. (Research Division, Kodak Ltd.) 28th November 1985
Chemistry and Principles of Colour Photography

CLARK, Dr. J.H. (University of York) 29th January 1986
Novel Fluoride Ion Reagents

DAVIES, Dr. S.G. (University of Oxford) 14th November 1985
Chirality Control and Molecular Recognition

Dewing, Dr. J. (U.M.I.S.T.) 24th October 1985
Zeolites - Small Holes, Big Opportunities

Ertl, Prof. G. (University of Munich) 7th November 1985
Heterogeneous Catalysis

Grigg, Prof. R. (Queen's University, Belfast) 13th February 1986
Thermal Generation of 1,3-Dipoles

HARRIS, Prof. R.K. (University of Durham) 27th February 1986
The Magic of Solid State NMR

HATHWAY, Dr. D. (University of Durham) 5th March 1986)
Herbicide Selectivity

Iddon, Dr. B. (University of Salford) 6th March 1986
The Magic of Chemistry (A Demonstration Lecture)

JACK, Prof. K.H., F.R.S. (University of Newcastle) 21st November 1985
Chemistry of Si-Al-O-N Engineering Ceramics

Langridge-Smith, Dr. P.R.R. (University of Edinburgh) 14th May 1986
Naked Metal Clusters - Synthesis, Characterisation and Chemistry

Lewis, Prof. Sir Jack, F.R.S. (University of Cambridge) 23rd Jan 1986
Some More Recent Aspects in the Cluster Chemistry of Ruthenium and Osmium Carbonyls

Ludman, Dr. C.J. (University of Durham) 17th October 1985
Some Thermochemical Aspects of Explosions (A Demonstration Lecture)

MacBride, Dr. J.A.H. (Sunderland Polytechnic) 20th November 1985
A Heterocyclic Tour on a Distorted Tricycle Biphenylene

O'DONNEL, Prof. M.J. (Indiana-Purdue University) 5th November 1985
New Methodology for the Synthesis of Amino Acids

Phillips, Dr. N.J. (University of Technology, Loughborough) 30 Jan 86
Laser Holography

Procter, Prof.G. (University of Salford) 19th February 1986
Approaches to the Synthesis of Some Natural Products

Schmutzler, Prof. R. (University of Braunschweig) 9th June 1986
Mixed Valence Diphosphorous Compounds

Schroder, Dr. M. (University of Edinburgh) 5th March 1986
Studies on Macrocyclic Complexes

Sheppard, Prof. N. (University of East Anglia) 15th January 1986
Vibrational and Spectroscopic Determinations of the Structure of Molecules Chemisorbed on Metal Surfaces

Tee, Prof. O.S. (Concordia University, Montreal) 12th February 1986
Bromination of Phenols

Till, Miss C. (University of Durham) 26th February 1986
ESCA and Optical Emission Studies of the Plasma Polymerisation of Perfluoroaromatics

Timms, Dr. P. (University of Bristol) 31st October 1985
Some Chemistry of Fireworks (A Demonstration Lecture)

Waddington, Prof. D.J. (University of York) 28th November 1985
Resources for the Chemistry Teacher

Wilde, Prof. R.E. (Texas technical University) 23rd June 1986
Molecular Dynamic Processes from Vibrational Bandshapes

Yarwood, Dr. J. (University of Durham) 12th February 1986
The Structure of Water in Liquid Crystals

UNIVERSITY OF DURHAM

Board of Studies in Chemistry

COLLOQUIA, LECTURES AND SEMINARS GIVEN BY INVITED SPEAKERS 1ST AUGUST 1986 TO 31ST JULY 1987

ALLEN, Prof. Sir G. (Unilever Research) Biotechnology and the Future of the Chemical Industry	13th November 1986
BARTSCH, Dr. R. (University of Sussex) Low Co-ordinated Phosphorus Compounds	6th May 1987
BLACKBURN, Dr. M. (University of Sheffield) Phosphonates as Analogues of Biological Phosphate Esters	27th May 1987
BORDWELL, Prof. F.G. (Northeastern University, U.S.A.) Carbon Anions, Radicals, Radical Anions and Radical Cations	9th March 1987
* CANNING, Dr. N.D.S. (University of Durham) Surface Adsorption Studies of Relevance to Heterogeneous Ammonia Synthesis	26th November 1986
CANNON, Dr. R.D. (University of East Anglia) Electron Transfer in Polynuclear Complexes	11th March 1987
CLEGG, Dr. W. (University of Newcastle-upon-Tyne) Carboxylate Complexes of Zinc; Charting a Structural Jungle	28th January 1987
DÖPP, Prof. D. (University of Duisburg) Cyclo-additions and Cyclo-reversions Involving Captodative Alkenes	5th November 1986
* DORFMÜLLER, Prof. T. (University of Bielefeld) Rotational Dynamics in Liquids and Polymers	8th December 1986
GOODGER, Dr. E.M. (Cranfield Institute of Technology) Alternative Fuels for Transport	12th March 1987
GREENWOOD, Prof. N.N. (University of Leeds) Glorious Gaffes in Chemistry	16th October 1986
HARMER, Dr. M. (I.C.I. Chemicals & Polymer Group) The Role of Organometallics in Advanced Materials	7th May 1987
HUBBERSTEY, Dr. P. (University of Nottingham) Demonstration Lecture on Various Aspects of Alkali Metal Chemistry	5th February 1987
HUDSON, Prof. R.F. (University of Kent) Aspects of Organophosphorus Chemistry	17th March 1987
* HUDSON, Prof. R.F. (University of Kent) Homolytic Rearrangements of Free Radical Stability	18th March 1987

*	OLAH, Prof. G.A. (University of Southern California) New Aspects of Hydrocarbon Chemistry)	29th June, 1988
*	PALMER, Dr. F. (University of Nottingham) Luminescence (Demonstration Lecture)	21st January 1988
	PINES, Prof. A. (University of California, Berkeley, U.S.A.) Some Magnetic Moments	28th April 1988
	RICHARDSON, Dr. R. (University of Bristol) X-Ray Diffraction from Spread Monolayers	27th April 1988
	ROBERTS, Mrs. E. (SATRO Officer for Sunderland) Talk - Durham Chemistry Teachers' Centre - "Links Between Industry and Schools"	13th April 1988
	ROBINSON, Dr. J.A. (University of Southampton) Aspects of Antibiotic Biosynthesis	27th April 1988
*	ROSE van Mrs. S. (Geological Museum) Chemistry of Volcanoes	29th October 1987
	SAMMES, Prof. P.G. (Smith, Kline and French) Chemical Aspects of Drug Development	19th December 1987
	SEEBACH, Prof. D. (E.T.H. Zurich) From Synthetic Methods to Mechanistic Insight	12th November 1987
	SODEAU, Dr. J. (University of East Anglia) Durham Chemistry Teachers' Centre Lecture: "Spray Cans, Smog and Society"	11th May 1988
	SWART, Mr. R.M. (I.C.I.) The Interaction of Chemicals with Lipid Bilayers	16th December 1987
	TURNER, Prof. J.J. (University of Nottingham) Catching Organometallic Intermediates	11th February 1988
*	UNDERHILL, Prof. A. (University of Bangor) Molecular Electronics	25th February 1988
	WILLIAMS, Dr. D.H. (University of Cambridge) Molecular Recognition	26th November 1987
*	WINTER, Dr. M.J. (University of Sheffield) Pyrotechnics (Demonstration Lecture)	15th October 1987

UNIVERSITY OF DURHAM

Board of Studies in Chemistry

COLLOQUIA, LECTURES AND SEMINARS GIVEN BY INVITED SPEAKERS
1ST AUGUST 1987 to 31st JULY 1988

*	BIRCHALL, Prof. D. (I.C.I. Advanced Materials) Environmental Chemistry of Aluminium	25th April 1988
*	BORER, Dr. K. (University of Durham Industrial Research Labs.) The Brighton Bomb - A Forensic Science View	18th February 1988
	BOSSONS, L. (Durham Chemistry Teachers' Centre) GCSE Practical Assessment	16th March 1988
*	BUTLER, Dr. A.R. (University of St. Andrews) Chinese Alchemy	5th November 1987
*	CAIRNS-SMITH, Dr. A. (Glasgow University) Clay Minerals and the Origin of Life	28th January 1988
	DAVIDSON, Dr. J. (Herriot-Watt University) Metal Promoted Oligomerisation Reactions of Alkynes	November 1987
*	GRADUATE CHEMISTS (Northeast Polytechnics and Universities) R.S.C. Graduate Symposium	19th April 1988
	GRAHAM, Prof. W.A.G. (University of Alberta, Canada) Rhodium and Iridium Complexes in the Activation of Carbon-Hydrogen Bonds	3rd March 1988
*	GRAY, Prof. G.W. (University of Hull) Liquid Crystals and their Applications	22nd October 1987
	HARTSHORN, Prof. M.P. (University of Canterbury, New Zealand) Aspects of Ipso-Nitration	7th April 1988
*	HOWARD, Dr. J. (I.C.I. Wilton) Chemistry of Non-Equilibrium Processes	3rd December 1987
*	LUDMAN, Dr. C.J. (Durham University) Explosives	10th December 1987
*	McDONALD, Dr. W.A. (I.C.I. Wilton) Liquid Crystal Polymers	11th May 1988
	MAJORAL, Prof. J.-P. (Université Paul Sabatier) Stabilisation by Complexation of Short-Lived Phosphorus Species	8th June 1988
	MAPLETOFT, Mrs. M. (Durham Chemistry Teachers' Centre) Salters' Chemistry	4th November 1987
	NIETO DE CASTRO, Prof. C.A. (University of Lisbon and Imperial College) Transport Properties of Non-Polar Fluids	18th April 1988

*	JARMAN, Dr. M. (Institute of Cancer Research) The Design of Anti Cancer Drugs	19th February 1987
	KRESPAN, Dr. C. (E.I. Dupont de Nemours) Nickel(0) and Iron(0) as Reagents in Organofluorine Chemistry	26th June 1987
*	KROTO, Prof. H.W. (University of Sussex) Chemistry in Stars, between Stars and in the Laboratory	23rd October 1986
	LEY, Prof. S.V. (Imperial College) Fact and Fantasy in Organic Synthesis	5th March 1987
	MILLER, Dr. J. (Dupont Central Research, U.S.A.) Molecular Ferromagnets; Chemistry and Physical Properties	3rd December 1986
*	MILNE/CHRISTIE, Dr. A./Mr. S. (International Paints) Chemical Serendipity - A Real Life Case Study	20th November 1986
	NEWMAN, Dr. R. (University of Oxford) Change and Decay: A Carbon-13 CP/MAS NMR Study of Humification and Coalification Processes	4th March 1987
*	OTTEWILL, Prof. R.H. (University of Bristol) Colloid Science a Challenging Subject	22nd January 1987
	PASYNKIEWICZ, Prof. S. (Technical University, Warsaw) Thermal Decomposition of Methyl Copper and its Reactions with Trialkylaluminium	11th May 1987
	ROBERTS, Prof. S.M. (University of Exeter) Synthesis of Novel Antiviral Agents	24th June 1987
*	RODGERS, Dr. P.J. (I.C.I. Billingham) Industrial Polymers from Bacteria	12th February 1987
	SCROWSTON, Dr. R.M. (University of Hull) From Myth and Magic to Modern Medicine	6th November 1986
	SHEPHERD, Dr. T. (University of Durham) Pteridine Natural Products; Synthesis and Use in Chemotherapy	11th February 1987
	THOMSON, Prof. A. (University of East Anglia) Metalloproteins and Magnetooptics	4th February 1987
	WILLIAMS, Prof. R.L. (Metropolitan Police Forensic Science) Science and Crime	27th November 1987
	WONG, Prof. E.H. (University of New Hampshire, U.S.A.) Coordination Chemistry of P-O-P Ligands	29th October 1986
*	WONG, Prof. E.H. (University of New Hampshire, U.S.A.) Symmetrical Shapes from Molecules to Art and Nature	17th February 1987

(C) First Year Induction Course, October 1985

This course consisted of a series of one hour lectures on the services available in the department.

1. Departmental Organisation
2. Safety Matters
3. Electrical Appliances and Infra-red Spectroscopy
4. Chromatography and Microanalysis
5. Atomic Absorptiometry and Inorganic Analysis
6. Library Facilities
7. Mass Spectroscopy
8. Nuclear magnetic resonance Spectrometry
9. Glassblowing Techniques